Radio Resource Management Techniques for Industrial IoT in 5G-and-Beyond Networks

A thesis submitted in partial fulfillment of the
requirements of University of Greenwich
for the Degree of Doctor of Philosophy

IDAYAT O. SANUSI

June 2023

DECLARATION

I certify that the work contained in this thesis, or any part of it, has not been accepted in substance for any previous degree awarded to me or any other person, and is not currently being submitted for any other degree other than that of the Doctor of Philosophy which has been studied at the University of Greenwich, London UK.

I also declare that the work contained in this thesis is a result of my own investigations, except where otherwise identified and acknowledged by references. I further declare that no aspect of the contents of this thesis are the outcome of any form of research misconduct.

I declare any personal, sensitive or confidential information/data has been removed or participants have been anonymised. I further declare that where any questionnaires, survey answers or other qualitative responses of participants are recorded/included in the appendices, all personal information has been removed or anonymised. Where University forms (such as those from the Research Ethics Committee) have been included in appendices, all handwritten/scanned signatures have been removed.

Student Name: Idayat O. Sanusi

Student Signature:

Date: June 2023

First Supervisor: Dr. Karim M. Nasr

First Supervisor's Signature:

Date: June 2023

ACKNOWLEDGEMENTS

Firstly, I thank the Lord my God without whom I can do nothing.

My immense gratitude to the University of Greenwich for giving me the opportunity to undertake this research work by granting me the Engineering Vice-Chancellor Scholarship and additional financial support I received following the coronavirus pandemic, in particular. This research would not have been possible without the support and contributions of my supervisors. I would like to thank Dr. Karim M. Nasr, my first supervisor and Prof. Alan Reed, my second supervisor, for their helpful comments, feedback, patience, and guidance since the commencement of this programme. Many thanks to Prof. Klaus Moessner and Prof. Peter Kyberd for supporting my work. Thanks are due to Prof. James Gao and Dr. Anna Romanova for their valuable comments and feedback during the MPhil to PhD transfer viva. I would like to thank my good friend, Babatunde Giwa for his encouragement all the way, always providing me with valuable information to support my progress.

I would like to extend my gratitude to the support group in Church for the encouragement, prayers and kind words. My appreciation to my parents, siblings, and in-laws for regularly checking up on me, encouraging and praying for me. My deep gratitude to my husband for all the sleep deprivation and stress we had to go through to try to maintain a life-work balance. I wouldn't have come this far without his support.

DEDICATION

This thesis is dedicated to my Lord and Saviour, Jesus Christ. To you be all the glory. I dedicate this work also, to my dear and beloved husband, Sunday Falolu, for your selfless sacrifices, my adorable daughter and son, Heavenly and Nathaniel, for your 'contributions' to my thesis. I love you all without measure.

ABSTRACT

Fifth Generation (5G) and beyond wireless technologies are expected to support Quality of Service/Experience (QoS/QoE) requirements of new and emerging Internet of Things (IoT) applications and services. Smart manufacturing is one of the target verticals for 5G-and-beyond networks. Device-to-Device (D2D) communication is a key technology to facilitate Ultra-Reliable Low-Latency Communication (URLLC). Efficient Radio Resource Management (RRM) techniques are necessary to address the challenges posed by interference. The main objective of the research work reported in this thesis is the development of new RRM techniques for D2D communication in wireless industrial setting meeting QoS/QoE requirements of end-users in cellular networks and its deployment in Factories of the Future (FoF). The algorithms and techniques developed to address RRM challenges are a combination of centralised techniques such as mathematical optimisation and distributed approaches such as matching theory and machine learning.

The key contributions of this research work are the development of new RRM techniques optimising spectrum utilisation, in terms of energy efficiency and throughput performance. The first part of the thesis focuses on developing spectrum sharing schemes for D2D communication in cellular and Multi-tier Heterogeneous Networks (HetNet), resulting in new spectrum and energy-efficient solutions. The second part of the thesis focuses on ensuring reliable communication for the deployment of D2D communication in industrial settings. A new matching technique was developed to optimise matching between D2D links and cellular resources. A new stateless reinforcement learning scheme is also presented, to ensure a low-dimension state-action mapping with the latency and reliability specifications of the D2D users and minimum QoS of the cellular users. A comparative analysis of the results in terms of trade-offs between factors including performance, signalling overheads and complexity shows that the developed distributed RRM techniques outperform centralised methods for the studied industrial scenarios.

CONTENTS

LIST OF TABLES

LIST OF FIGURES

LIST OF ABBREVIATIONS AND MATHEMATICAL SYMBOLS

Acronyms

3G	Third Generation
3GPP	Third Generation Partnership Project
4G	Fourth Generation
5G	Fifth Generation
5G NR	Fifth Generation New Radio
5G PPP	Fifth Generation Public Partnership Project
6G	Sixth Generation
AI	Artificial Intelligence
AP	Access Point
AR	Augmented Reality
AWGN	Additive White Gaussian Noise
BB	Broadband
BLER	Block Error Rate
BS	Base Station
BS-A	Base Station-Assisted
CA	Carrier Aggregation
CAPEX	Capital Expenditure
CF-mMIMO	Cell-Free Multiple-In Multiple-Out
cMTC	Critical Machine-Type Communication
CPS	Cyber-Physical Systems
CSI	Channel State Information
CSRA	Cooperative Spectrum Resource Allocation
CUEs	Cellular User Equipment
D2D	Device-to-Device
DA	Deferred Acceptance
dB	Decibels
DL	Downlink
DNN	Deep Neural Network
DRL	Deep Reinforcement Learning
DUEs	Device-to-Device User Equipment
E2E	End-to-End
EB	Exabyte
EE	Energy Efficiency
eMBB	Enhanced Mobile Broadband
eNB	Evolved Node B
FBS	Femtocell Base Station
FDD	Frequency Division Duplexing
FoF	Factory-of-the-Future
FUE	Femtocell User Equipment
GS	Gale-Shapley
HetNet	Heterogeneous Network
HD	High Definition
HMM	Hidden Markov Model
HTC	Human-Type Communication
IEEE	Institute of Electrical Electronics Engineers
IoE	Internet of Everything

IIoT	Industrial Internet of Things
IoT	Internet of Things
IoTDs	Internet of Things Devices
ISA	Interference-Aware Spectrum Allocation
KKT	Karush-Kuhn-Tucker
KPI	Key Performance Indicator
LAN	Local Area Network
LTE	Long Term Evolution
LTE-A	Long Term Evolution-Advanced
M2M	Machine-to-Machine
MBS	Macro Base Station
Mbps	Megabits per second
MDP	Markov Decision Process
MHz	MegaHertz
MIMO	Multiple Input Multiple Output
MINLP	Mixed Integer Non-Linear Programming
ML	Machine Learning
mMTC	Massive Machine-Type Communication
MNO	Mobile Network Operators
MTC	Machine-Type Communication
MTCD	Machine-Type Communication Device
NFV	Network FunctionVirtualisation
No-UDU	No Underlay Users
NOMA	Non-Orthogonal Multiple Access
OAM	Orbital Angular Momentum
OFDM	Orthogonal Frequency Division Multiplexing
OFDMA	Orthogonal Frequency Division Multiple Access
OPEX	Operating Expenditure
P-DA	Priced-Deferred Acceptance
PER	Packet Error Ratio
PLC	Programmable Logic Controller
PRB	Physical Resource Block
PRR	Power-Rate Reduction Ratio
QoE	Quality of Experience
QoS	Quality of Service
RB	Resource Block
RLBM	Reinforcement Learning Based Matching
RRH	Remote Radio Head
RRM	Radio Resource Management
SDN	Software Defined Network
SE	Spectrum Efficiency
SINR	Signal-to-Interference-plus-noise ratio
SIR	Signal-to-Interference Ratio
SM-MIMO	Spatial Modulation- Multiple-In Multiple-Output
SMP	Stable Marriage Problem
SOM	Self Organising Map
SON	Self Organising Network
TDD	Time Frequency Duplex
THz	TeraHertz

TPC	Fixed-Target-SIR-Tracking Power Control
TTI	Transmission Time Interval
UC	Use Case
UDN	Ultra-Dense Network
UE	User Equipment
uHPC	Ultra-High Precision Communication
UL	Uplink
uMBB	Ultra-Mobile Broadband
UMTS	Universal Mobile Telecommunication System
URLLC	Ultra-Reliable Low-Latency Communication
UWI	Ubiquitous Wireless Intelligence
V2I	Vehicle-to-Infrastructures
VNO	Virtual Network Operator
V2V	Vehicle-to-Vehicle
VR	Virtual Reality

Mathematical Symbols

$\boldsymbol{a^t}$	Action taken by an agent at time slot $\boldsymbol{t}$
$\boldsymbol{A}$	Set of actions of DUE $\boldsymbol{d_j} \in \boldsymbol{D}$
$\boldsymbol{B}$	Base station
$\mathbf{B}_{\boldsymbol{d_j}}(\boldsymbol{t})$	Total packet transmitted by DUE $\boldsymbol{d_j}$ at time slot $\boldsymbol{t}$.
$\boldsymbol{C}$	Set of CUEs
$\boldsymbol{C}^{\mathbb{E}}$	Union of the set of all eligible CUEs
$\boldsymbol{D}$	Set of DUEs
$\boldsymbol{D}_{+}$	Set of DUEs under P-DA with CUE partners having utilities higher than matched partners
$\boldsymbol{D}_{-}$	Set of DUEs under P-DA with CUE partners with having lower than the matched partners in DA
$\mathbf{DA}$	Deferred Acceptance
$\boldsymbol{D}_{\boldsymbol{DA}}$	Set of DUEs under P-DA with CUE partners identical to the matching in DA
$\boldsymbol{D}^{\mathbb{E}}$	Union of the set of admissible DUEs
$\boldsymbol{D}_{\boldsymbol{m}}$	Number of admitted DUEs
$\mathbf{D}_{\boldsymbol{u}}$	Total number of admitted underlay (sharing) users,
$\mathbf{EE}_{\boldsymbol{D}}$	Total energy efficiency of the DUEs
$\mathbf{EE}_{\boldsymbol{d_j}}^{\mathbf{opt}}$	Optimal energy efficiency
$\boldsymbol{F}$	Number of FUEs
$\boldsymbol{G_k}$	Pathloss constant
$\boldsymbol{h_{q,r}}$	Channel gain between node $\boldsymbol{q}$ and $\boldsymbol{r}$
$\boldsymbol{H}$	Set of FBS
$\mathbf{I}_{\boldsymbol{B},\mathbf{max}}^{\boldsymbol{i}}$	Interference limit to guarantee the received SINR at the BS on the channel of CUE $\boldsymbol{c_i}$
$\boldsymbol{K}$	Set of PRBs
$\boldsymbol{l_{d_j}}$	Transmission latency
$\boldsymbol{l_{d_j,\mathbf{max}}}$	Latency budget
$\boldsymbol{L}$	Set of FUEs
$\mathbf{L}_{\boldsymbol{d_j}}$	Number of packets
$\mathbf{L}'_{\boldsymbol{d_j}}$	**N**umber of packets delivered within the latency bound
$\boldsymbol{L_{q,r}}$	Euclidean distance between terminal $\boldsymbol{q}$ and $\boldsymbol{r}$
$\boldsymbol{M}$	Number of DUEs
$\boldsymbol{N}$	Number of CUEs
$\boldsymbol{p_R}$	Outage probability
$\boldsymbol{p_{R_0}}$	Maximum tolerable outage probability
$\boldsymbol{P}$	Number of FBS
$\mathbf{P}_{\boldsymbol{c_i}}$	Transmit power of CUE $\boldsymbol{c_i} \in \boldsymbol{C}$
$\mathbf{P}_{\boldsymbol{c_i},\mathbf{max}}$	Maximum transmit power for a CUE $\boldsymbol{c_i}$
$\boldsymbol{P_C}$	Set of feasible transmit power for and CUE $\boldsymbol{c_i}$
$\mathbf{P}_{\boldsymbol{d_j},\mathbf{max}}$	Maximum transmit power for DUE link $\boldsymbol{d_j}$
$\mathbf{P}_{\boldsymbol{d_j}}$	Transmit power of DUE $\boldsymbol{d_j} \in \boldsymbol{D}$
$\mathbf{P}_{\boldsymbol{d_j},\mathbf{min}}$	Minimum transmit power for DUE to guarantee its target SINR
$\mathbf{P}_{\boldsymbol{d_j}}^{\mathbf{opt}}$	Transmit power that maximises the energy efficiency of DUE $\boldsymbol{d_j}$

$\mathbf{P}^{*}_{d_j,\mathbf{max}}$	Transmit power of DUE $\boldsymbol{d_j}$ for which its data rate is maximum
$\boldsymbol{P_D}$	Set of feasible transmit power for DUE $\boldsymbol{d_j}$
$\mathbf{P}_{f_k}$	Transmit power of FUE $\boldsymbol{f_k} \in \boldsymbol{F}$
$\mathbf{P}_{f_k,\mathbf{min}}$	Minimum transmit power for FUE to guarantee its target SINR
$\boldsymbol{P_F}$	Set of feasible transmit power for and FUE $\boldsymbol{f_k}$
$\boldsymbol{PL}$	Preference list
$\boldsymbol{P(S)}$	State transition probability function
$\boldsymbol{P_{s,s'}}$	Transition probability from state $\boldsymbol{s}$ to state $\boldsymbol{s'}$
$\boldsymbol{q_c}$	Quota of resource $\boldsymbol{c}$
$\boldsymbol{q_d}$	Quota of user $\boldsymbol{d}$
$\boldsymbol{Q^i_{d_j}}$	$\boldsymbol{Q}$-value of $\boldsymbol{j}$th DUE on $\boldsymbol{i}$th cellular channel
$\boldsymbol{Q^j_{c_i}}$	$\boldsymbol{Q}$-value of the $\boldsymbol{i}$th CUE for action taken by the $\boldsymbol{j}$th DUE
$\boldsymbol{r(a^t)}$	Immediate reward for selecting $\boldsymbol{a}$ at time slot $\boldsymbol{t}$
$\boldsymbol{r_{c_i}(a^t)}$	Reward of the $\boldsymbol{i}$th CUE for selecting $\boldsymbol{a}$ at time slot $\boldsymbol{t}$
$\boldsymbol{r_{d_j}(a^t)}$	Reward of the $\boldsymbol{j}$th DUE for selecting $\boldsymbol{a}$ at time slot $\boldsymbol{t}$
$\mathbf{R}^{*}_{d_j,\mathbf{max}}$	Data rate of DUE $\boldsymbol{d_j}$ from $\mathbf{P}^{*}_{d_j,\mathbf{max}}$
$\mathbf{R}_{d_j,\mathbf{min}}$	Data rate of DUE $\boldsymbol{d_j}$ for transmitting with $\mathbf{P}_{d_j,\mathbf{min}}$
$\boldsymbol{R^c_{d_j}}$	Set of CUEs that $\boldsymbol{d_j}$ can share resources with
$\boldsymbol{R^d_{c_i}}$	Set of reuse (or admissible) DUEs for CUE $\boldsymbol{c_i}$
$\boldsymbol{s^t}$	State of an agent at time slot $\boldsymbol{t}$
$\boldsymbol{S^i_{d_j}(t)}$	State observed by DUE $\boldsymbol{d_j} \in \boldsymbol{D}$, on RB $\boldsymbol{k_i}$ at time slot $\boldsymbol{t}$
$\boldsymbol{S_u}$	System utility
$\mathbf{T}_{c_i,d_j}$	**S**um rate **of** DUE $\boldsymbol{d_j} \in \boldsymbol{D}^{\mathbb{E}}$ **and** $\boldsymbol{c_i} \in \boldsymbol{C}^{\mathbb{E}}$
$\mathbf{T}^{k}_{c_i}(t)$	CUE throughput on channel $\boldsymbol{k}$ at time slot $\boldsymbol{t}$
$\mathbf{T}^{k}_{d_j}(t)$	DUE throughput on channel $\boldsymbol{k}$ at time slot $\boldsymbol{t}$
$\mathbf{T}_C$	Total throughput of the CUEs
$\mathbf{T}_G$	System throughput gain
$\mathbf{T}_R$	Total system throughput
$\boldsymbol{U}$	Utility function
$\boldsymbol{U_B(\pi)}$	Total revenue generated by the BS
$\boldsymbol{U^{d_j}_{c_i}}$	Utility function of CUE $\boldsymbol{c_i}$ from sharing its subchannel with DUE $\boldsymbol{d_j}$
$\boldsymbol{U^{c_i}_{d_j}}$	Utility function of DUE $\boldsymbol{d_j}$ from sharing its subchannel with CUE $\boldsymbol{c_i}$
$\boldsymbol{U_M}$	Set of unmatched CUEs
$\boldsymbol{V^{\pi}(s)}$	Expected return if an agent is in this state $\boldsymbol{s^t = s}$ at time $\boldsymbol{t}$, under a policy $\boldsymbol{\pi}$
$\boldsymbol{V^{*}(s)}$	Optimised value function under the optimised policy $\boldsymbol{\pi^{*}}$
$\boldsymbol{W_i}$	Bandwidth of the resource block
$\boldsymbol{x}$	Input variable in supervised learning
$\boldsymbol{y}$	Output variable in supervised learning
$\boldsymbol{X}$	Set of men in SMP
$\boldsymbol{Y}$	Set of women in SMP
$\succ$	Preference relation

Greek-letter notations

$\boldsymbol{\Gamma_{c_i,\min}}$	Minimum SINR requirement for CUE $\boldsymbol{c_i}$
$\boldsymbol{\Gamma_{d_j,\min}}$	Minimum SINR requirement for DUE link $\boldsymbol{d_j}$
$\boldsymbol{\Gamma_{f_k,\min}}$	Minimum SINR requirement for FUE $\boldsymbol{f_k}$
$\boldsymbol{\lambda_j^i}$	Channel reuse indicator for CUE $\boldsymbol{c_i}$ and DUE $\boldsymbol{d_j}$
$\boldsymbol{\lambda_k^i}$	Channel reuse indicator CUE $\boldsymbol{c_i}$ and FUE $\boldsymbol{f_k}$
$\boldsymbol{\lambda_k^j}$	Channel reuse indicator CUE $\boldsymbol{c_i}$, DUE $\boldsymbol{d_j}$ and FUE $\boldsymbol{f_k}$
$\boldsymbol{\chi_{q,r}}$	Shadowing slow fading gain
$\boldsymbol{\gamma_{q,r}}$	Small-scale fading gain due to multipath propagation
$\boldsymbol{\pi}$	Policy used to select an action based on the current evaluation of the $\boldsymbol{Q}$-value at each time slot
$\boldsymbol{\pi^*}$	Optimal policy
$\boldsymbol{\pi_{c_i}}$	Price charged per connection for the CUEs.
$\boldsymbol{\pi_{d_j}}$	Price charged per connection for the DUEs
$\boldsymbol{\pi_{\mathcal{L}}}$	Rate loss price
$\boldsymbol{\varepsilon}$	Exploration rate
$\boldsymbol{\tau}$	Rate loss
$\boldsymbol{\psi}$	Price per unit rate
$\boldsymbol{\eta}$	Discount factor
$\boldsymbol{\sigma}$	Learning rate
$\boldsymbol{\sigma_D}$	Difference of the reduction ratios $\boldsymbol{\sigma_P}$ and $\boldsymbol{\sigma_R}$
$\boldsymbol{\sigma_N^2}$	Noise spectral density
$\boldsymbol{\sigma_P}$	Power reduction ratio
$\boldsymbol{\sigma_R}$	Rate reduction ratio
$\boldsymbol{\xi_{d_j}}$	**P**robability of packet latency exceeding a predefined latency bound, $\boldsymbol{l_{d_j,\max}}$
$\boldsymbol{\mu}$	Matching game output

Mathematical operators and symbols:

$\mathbf{argmax}(.)$	Arguments of the maxima. It is an operation that finds the argument that returns the maximum value from the input function
$\boldsymbol{f}(.)$	Function of the input
$\boldsymbol{F_\gamma}(.)$	Cumulative distribution Function
$\boldsymbol{f_\gamma}(.)$	Probability distribution Function
$\lvert\boldsymbol{\mu}(.)\rvert$	Cardinality of the outcome
$\mathbf{Pr}(.)$	Probability of the input
$\mathbf{max}(.)$	Maximise the input
$\mathbf{max}\,\boldsymbol{PL}(.)$	Highest-ranked element
$\mathbf{O}(.)$	Complexity

Chapter 1

Introduction

The motivation and justification for the research scope of this thesis are presented in this chapter. Research questions, aims and objectives of the work reported in this thesis are also discussed.

1.1 Background and Motivation

Machine-Type Communication (MTC) usually refers to direct communication between smart objects exclusive of human intervention. Internet of Things (IoT) is a paradigm evolving from wide-scale MTC, which incorporates the inter-operation of physical and virtual units/systems to manage interactions among heterogeneous smart devices via the Internet. With the emergence of IoT, objects and devices that are not expected to be conventionally connected to the Internet will be enabled to send, receive and process data. This has been made possible by the rapid advancements and innovations in sensors, radio frequency technologies and emerging wireless networks. Smart devices possess the ability to autonomously learn and apply knowledge to make resource management decisions. The physical environment where smart devices interact through a continuous network is called a smart environment [1].

There are three major application categories or use cases for 5G-and-beyond networks: enhanced Mobile Broadband (eMBB), massive MTC (mMTC) and critical MTC (cMTC). Enhanced mobile broadband comprises applications with high bandwidth/data rate demands. Massive MTC applications include smart homes or smart agriculture, and typically involve a large number of low-cost smart devices with QoS requirements related to extended coverage and energy efficiency. Critical MTC applications, on the other hand, require real-time communication between smart devices such as in remote surgery, smart manufacturing, autonomous car, road traffic management etc [2].

Current wireless communication technologies have limitations in supporting the above-mentioned use cases in terms of performance, managing heterogeneity, security, and trust, leveraging Internet technologies, flexible networks, and service management. It is expected that 5G-and-beyond wireless technologies will enable diverse new and emerging IoT use cases that existing wireless technologies are unable to support. While 5G offers substantial advances

by introducing better QoS provisioning relative to the previous generations of wireless networks, the sixth generation of cellular communication (6G) is expected to deliver a fully automated and smart environment [3].

Industry 4.0 and the emerging Industry 5.0 are considered new paradigms to optimally exploit the potential enhancements covered by 6G. Industry 4.0 also known as smart industry or Industrial IoT (IIoT), is an industrial technological revolution that integrates Cyber-Physical Systems (CPS), Artificial Intelligence (AI) and IoT to transform manufacturing and production processes. Smart industry relies on massive Machine-To-Machine (M2M) communication, which involves interaction between sensors, machines, robots, and wearable devices. While Industry 4.0 prioritises process automation, thereby reducing human involvement in the manufacturing process, Industry 5.0 is conceptualised to exploit the creativity of human experts to collaborate with intelligent machines [4]. The Fifth-Generation Infrastructure Public-Private Partnership (5G PPP) identified the manufacturing industry as one of the most demanding use cases with respect to ultra-low latency, ultra-high availability, and reliable indoor coverage in metalised industrial environments. MTC for automation processes in factory environments is considered one of the most important use cases for 5G-and-beyond networks [5].

While legacy cellular networks are primarily designed for Human-Type Communication (HTC), they are expected to support the MTC at a reduced cost of implementation. Therefore, cellular networks need to be modified to accommodate MTC due to new requirements [6]. The service requirements for MTC in Long Term Evolution-Advanced (LTE-A) were first proposed in [7], but did not draw the distinction between the MTC Devices (MTCDs) and mainstream Cellular User Equipment (CUEs) for HTC.

In contrast to HTC,

i. MTC is expected to support large numbers of smart devices, predominantly with small data sizes, which aggregate into a massive amount of data from parallel transmissions of a large number of MTCDs.
ii. The uplink periodic reporting packets in MTC, account for the higher proportion of the total traffic while the downlink consists of occasional query and control information.
iii. The majority of the MTCDs are required to have a battery life that will last up to a minimum of ten years without replacement. In addition, it will feature heterogeneous devices with diverse QoS requirements [8].

Generally, smart devices are physically resource-constrained in terms of power, processing capabilities, memory, and the availability of radio spectrum [9]. The global mobile data traffic is forecast to increase to 670 Exabytes (EB) per month by 2025, which is an increase of 250% from the projection made in 2020. This unprecedented increase in data traffic is a result of the rapid growth in the number of smart wireless devices and bandwidth-intensive applications and services (e.g., online video streaming, gaming, etc.). MTCs will constitute approximately 50% (~14.7 billion devices) of globally connected devices by 2023, in addition to the traffic generated from smartphone connections [8]. This forecast shows that the rapid growth in the number of smart wireless devices will put pressure on radio spectrum resources that are already considered scarce and expensive. Fig. 1.1. represents an estimated exponential growth of global mobile connectivity [10].

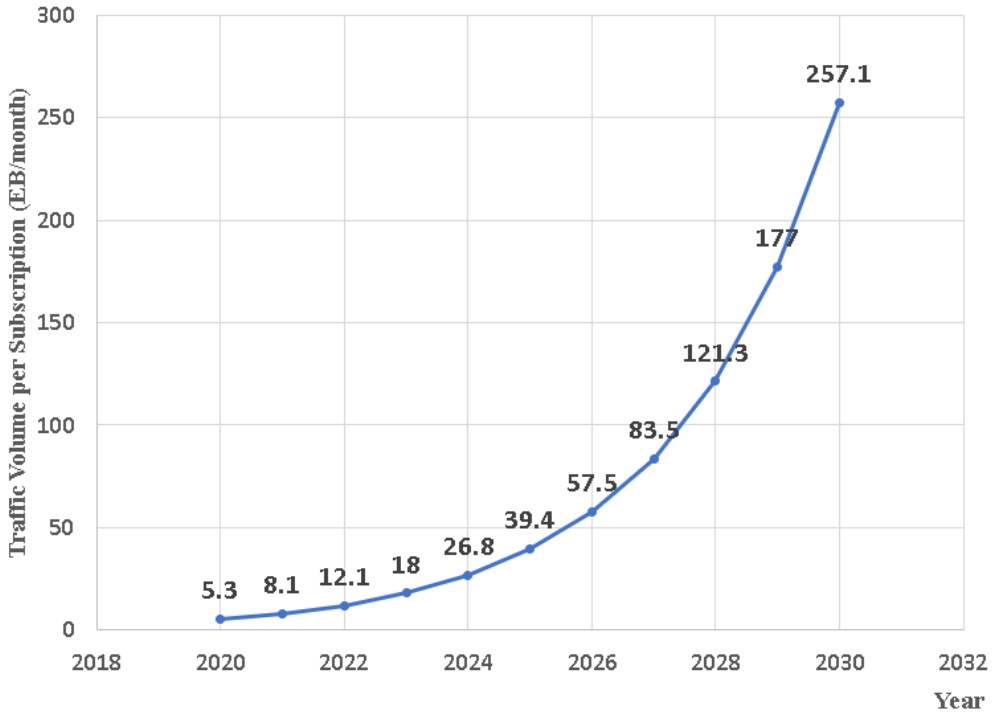

Fig. 1.1. The predicted growth of global mobile connectivity for 2020-2030 [10].

The increased processing power of Internet of Things Devices (IoTDs) will result in a rise in energy consumption which will have a significant impact on battery life. Furthermore, increased data rates from massive connections of IoTDs will lead to a rise in overall network energy consumption, thus posing a major design challenge for wireless IoT based systems [11]. The global energy consumption of Internet devices is predicted to grow by 46% between 2013

and 2025, if there are no improvements in energy usage [12]. Consequently, Mobile Network Operators (MNO) with existing cellular technologies are faced with the challenges posed by these developments. A global survey of telecommunication engineers has ranked spectrum availability the highest among obstacles to the success of 5G [13].

MTCDs can be deployed in licensed spectrum bands by reusing the existing cellular infrastructures or the license-exempt (or unlicensed) bands. Licensed bands are known for guaranteed reliability, extensive range, and ability to provide access to a larger number of devices in comparison to the unlicensed spectrum bands. However, a service fee is usually charged by regulators. Moreover, the scarcity and cost of licensed bands will result in higher congestion and blocking as network traffic grows. The performance of the regular HTC can be significantly degraded if congestion or system overload occurs. Congestion can arise as a result of concurrent uplink data transmissions or concurrent attempts to connect to the network by a large number of MTCDs. Cellular networks are mainly designed to manage HTC, in which uplink traffic is usually less than the downlink traffic, whereas MTC generates more traffic in the uplink than in downlink [14].

Ultra-Reliable Low-Latency Communication (URLLC) traffic is characterised by sporadic and small packet sizes typically 10-20 bytes [15], end-to-end latency typically in the order of a few milliseconds (ms) and a packet loss probability of at least 99.999%, which can only be presently achieved by wired solutions, as current wireless technologies, cellular and non-cellular, have limitations in meeting strict target QoS requirements [16]. Device-to-Device (D2D) communication has the potential to achieve reduced latency and improved reliability, because it allows devices to communicate directly without traversing the network infrastructure. Therefore, D2D is considered one of the key enabling technologies of 5G-and-beyond wireless systems [17].

In terms of spectrum usage, a D2D user either transmits exclusively via a dedicated channel or shares a channel with a cellular user, thus, addressing the challenges of insufficiency and under-utilisation of spectrum resources. D2D-type communication can be used to create massive MTC connections for future wireless industrial networks in factories of the future (FoF) and next-generation smart manufacturing, also known as Industry 4.0/5.0. Integrating D2D communication within an IoT environment will facilitate meeting the stringent QoS requirements of the target use cases [18].

Cellular service providers are able to mitigate problems such as poor indoor coverage and low data rates at the edge of the cell, by allowing users to connect to the cellular network, via a femtocell or small cell. Cell-edge users are users located at the edge of the cell, i.e., they are far away from the base station. They commonly experience low Signal-to-Interference-Plus-Noise Ratio (SINR), which results in a low date rate [19]. A femtocell is a small low-power cellular base station that connects the mainstream mobile devices to a network operator [20]. The integration of femtocells into a larger network, called a macrocell, forms a multi-tier Heterogeneous Network (HetNet). This structure has the potential of increasing the network capacity but will also increase the demand for spectrum resources. Spectrum sharing among the macrocell and femtocells may result in cross-tier interference. The introduction of D2D communication in a multi-tier network can, increase the overall network throughput, however, interference will become more complex when D2D and femtocell users have to reuse the macro-cell user resources.

Power control plays a crucial role in interference management and meeting the data rate demand of different users [21]. Therefore, advanced RRM using power control is necessary. This can be achieved by using intelligent algorithms to efficiently allocate limited power and radio resources and manage the impact of interference to an acceptable level, such that the QoS requirements of all users are simultaneously satisfied. Limitations in terms of radio resource availability and energy consumption are key issues to be considered in addressing RRM challenges to achieve URLLC requirements for smart manufacturing [22].

1.2 Main RRM Approaches

There are two main approaches to RRM, namely: centralised and distributed. In centralised RRM, the resource allocation policies are centrally controlled and coordinated by a Base Station (BS) or Access Point (AP), whereas distributed RRM is user terminal-centric. Owing to the large-scale nature of some smart environments, such as in manufacturing, a centralised RRM solution may not be always viable or practical due to the computation cost, increased signalling overheads and complexity. Effective spectrum and energy management in a heterogeneous environment, as in the case of wireless IoT, require a self-organising approach that is scalable, while maintaining target QoS/QoE metrics for the intended users or applications. A distributed RRM implementation is device-centric, making it possible to realise

a Self-Organising Network (SON) and supporting autonomy, which is an inherent feature of smart environments [23].

Centralised approaches often adopt general mathematical optimisation techniques and may not be efficient in an ultra-dense network of devices having strict latency requirements. Some game theoretic based methodologies may be used to achieve distributed RRM solutions [24]. There are, however, some limitations that make a game theory solution inadequate for large-scale network deployment, such as in a smart factory. These limitations include the complexity associated with modelling utility functions, slow convergence to equilibrium and high overheads [25]. Matching theory [26] has been able to address these challenges by providing a structure that facilitates decentralised resource allocation with reduced overheads and complexity. Machine learning [27], which was originally designed and developed for systems to learn and make decisions that will yield better performance for a given task, should be explored to tackle RRM challenges in next-generation networks. A distributed solution is better suited to support device-centred learning. With a machine learning-based RRM solution, wireless network entities can learn from their environment and make autonomous decisions to determine their optimal resource allocation, which is able to adapt to the dynamics of the network and satisfy strict QoS requirements [28]. It is considered that Machine Learning (ML) and Artificial Intelligence (AI) are pivotal to the realisation of the visions for 5G and beyond networks [11].

1.3 Main Research Aim

As set out in the previous section, there are challenges that should be addressed for the realisation of the optimal deployment of D2D communication in 5G-and-beyond networks in general, and for wireless Industrial IoT (IIoT) in particular. The research work presented in this thesis aims at addressing some of the issues and presenting solutions specifically targetting D2D wireless communication for smart manufacturing. It focuses on investigating and developing new RRM techniques achieving energy efficiency and optimised spectrum utilisation, while maintaining target QoS/QoE metrics for intended users and services. Furthermore, recommendations for the target verticals and use cases will be provided.

1.4 Research Questions

In connection to addressing the main issues related to the research aim set out above, a number of inter-related research questions are investigated, namely:

1. What is the current state-of-the-art in RRM for D2D communication and its applications to Industrial IoT?
2. How will the diverse and conflicting QoS/QoE requirements/metrics of wireless Industrial IoT be met with newly developed RRM schemes?
3. How will the newly developed RRM algorithms compare with other conventional methods in terms of KPIs and QoS metrics?

1.5 Research Objectives

This research work investigates new RRM frameworks including centralised optimisation, matching theory, and machine learning techniques to address some of the underlying challenges of next-generation wireless communication networks. The target vertical/domain of applications is D2D communication in cellular networks and its deployment in Factories-of-the-Future (FoF), which is enabled by Industrial (IIoT). IIoT is characterised by traffic that demands guaranteed delivery within extremely very time-sensitive intervals, with a reliability requirement of over 99.9999% and latency of less than 0.5ms for certain use cases. This is stricter than most Critical IoT applications, making IIoT one of the most demanding verticals in terms of ultra-reliable, low-latency communication (URLLC). The focus of this work is to develop novel algorithms and evaluate their performance for different use cases. The main issues to be considered are:

1. Spectrum sharing and interference mitigation for D2D-enabled cellular networks.
2. Resource allocation for URLLC targetting wireless industrial scenarios.

This research work contributed to the H2020 CLEAR5G project [29], which aims to investigate and demonstrate some of the key enablers necessary to support MTC in 5G networks, particularly in FoF environments.

1.6 Main Contributions and Progress beyond State-of-the-Art

The main contributions of this research work are focused on developing new RRM techniques for improving resource utilisation, while maintaining the QoS demands for a D2D-enabled cellular network in a wireless industrial environment.

1. Resource allocation for channel assignment and power control in a system with differentiated QoS for CUEs and D2D User Equipment (DUEs), is presented in Chapter 3. A Power-Rate Reduction Ratio (PRR) scheme is designed to address the multiple-

objective optimisation problem by maximising the energy efficiency of the DUEs, while satisfying the QoS of the cellular users. This scheme is compared to a method that adopts Fixed-Target-SINR Tracking Power Control (TPC). Numerical results show that the TPC algorithm provides a good CUE throughput performance and DUE power savings, whereas the PRR scheme generates a higher overall system utility which better realises the system's objectives.

2. Spectrum Sharing for D2D deployment in a multi-tier HetNet, in which the DUEs and Femtocell User Equipment (FUEs) are to share the same cellular resources, is presented in Chapter 4. A heuristic centralised Interference-Aware Spectrum Sharing Algorithm (ISA) is presented to solve the spectrum sharing problem, resulting in a resource-efficient allocation with throughput maximisation for the connected users. Results from numerical simulations demonstrate that the presented scheme achieves higher network throughput compared to a scenario where the active devices transmit at peak power, and where the CUEs have exclusive channel use.

3. In Chapter 5, resource allocation for reliable D2D communication in a wireless industrial scenario is investigated. A novel matching theory-based technique, denoted as Priced-Deferred Acceptance (P-DA) algorithm, is presented to improve resource utilisation. The scheme uses incentive-based stability to match D2D users to cellular resources and optimise the reuse gain. The performance of the P-DA algorithm is compared to the traditional Deferred Acceptance (DA), centralised optimisation and random algorithms. Numerical simulations show that the P-DA scheme outperforms the other algorithms for optimisation of spectrum utilisation in wireless industrial scenarios where MTCs are expected to support large numbers of sensors/devices.

4. A distributed stateless reinforcement learning technique, denoted as Reinforcement Learning Based Matching (RLBM) algorithm, is presented in Chapter 6 to solve spectrum-sharing and resource allocation problem, while considering the latency and reliability requirements in an industrial setting. The $\boldsymbol{Q}$-value function is formulated using action-reward only, making the state transition irrelevant but, nevertheless capturing the QoS requirements of the DUEs. As such, the challenges caused by traditional problem of large state-action mapping are mitigated, resulting in reduced complexity and signalling overheads. Also, $\boldsymbol{Q}$-tables for the CUEs are maintained and updated for the actions of the DUEs so that the satisfaction and preferences of the

cellular users are considered during resource allocation. This scheme is different from conventional techniques, where the QoS of the cellular users is modelled in the state space or reward function and the BS reports the QoS measurement of the CUE to the DUE at each time slot. The RLBM scheme is compared to a semi-distributed scheme, denoted as Base Station-Assisted (BS-A), where the DUEs upload their Q-tables to the BS for centralised channel allocation. Simulation results show that RLBM is more viable for massive device deployments such as in FoF, achieving good throughput performance at lower signalling overhead and complexity compared to other schemes, if device autonomy and stability are important system requirements.

1.7 Dissemination of Results

This research work resulted in the following technical papers and presentation:

Journal papers

1. I. O. Sanusi and K. M. Nasr, "Channel Selection in D2D Wireless Industrial Applications- A Reinforcement Learning Approach," IEEE Transactions on Network Management and Service (Submitted)

2. I. O. Sanusi and K. M. Nasr, "Base Station-Assisted Reinforcement learning for Resource Allocation in Wireless Industrial Environments," International Journal on Advances in Telecommunications, Vol. 15, no. 3&4, Dec. 2022.

3. I. O. Sanusi, K. M. Nasr and K. Moessner, "Radio Resource Management Approaches for Reliable Device-to-Device (D2D) Communication in Wireless Industrial Applications," IEEE Transactions of Cognitive Communication and Networking, Vol.7, Issue 3, pp. 905-916, Oct. 2020.

Conference papers

4. I. O. Sanusi and K. M. Nasr, "A Machine Learning Approach for Resource Allocation in Wireless Industrial Environments," in Proc. of the Eighteenth Advanced International Conference on Telecommunications (AICT), pp. 18-23, Jun. 2022.

5. I. O. Sanusi, K. M. Nasr and K. Moessner, "A Priced-Deferred Acceptance (P-DA) Technique for D2D Communication in Factories of the Future," in Proc. of Cognitive Radio-Oriented Wireless Networks (CROWNCOM), Springer Cham, pp.102-111, Mar. 2021.

6. I. O. Sanusi, K. M. Nasr and K. Moessner, "Resource Allocation for a Reliable D2D Enabled Cellular Network in Factories of the Future," in Proc. of IEEE European Conference on Networks and Communications (EUCNC), pp. 83-89, Jun. 2020.

7. I. O. Sanusi, K. M. Nasr and K. Moessner, "Device-to-Device Communication (D2D) Spectrum Sharing Scheme for Wireless Industrial Networks," in Proc. of IEEE European Conference on Networks and Communications (EUCNC), pp. 353-357, Jun. 2019.

8. I. O. Sanusi, K. M. Nasr and K. Moessner, "Channel Assignment and Power Control for D2D-Enabled Cellular Networks," in Proc. of IEEE International Conference on Computing, Electronics and Communication (iCCECE), pp. 225-228, Aug. 2019.
9. I. O. Sanusi and K. M. Nasr, "Resource Management Techniques in Smart Environments," Third Medway Engineering Conference, University of Greenwich, Medway Campus, Jun. 2018.

Presentation

10. I. O. Sanusi, "Radio Resource Management for Wireless Industrial Applications," PGCon Edinburgh Postgraduate Conference, John McIntyre Conference Centre, University of Edinburgh, Oct. 2019.

1.8 Organisation of the Thesis

The thesis is organised as follows:

In Chapter 2, a literature review focusing on the state-of-art in IoT use cases, D2D communication and wireless factory automation is presented, together with the performance requirements of smart manufacturing. RRM challenges and associated approaches and techniques are critically surveyed.

In Chapter 3, a spectrum sharing scheme for D2D communication in a cellular network is presented. The problem is formulated as a multi-objective optimisation problem, which is solved using a low-complexity centralised heuristic algorithm.

In Chapter 4, a centralised algorithm is designed to address the resource allocation problem for D2D and femtocell users co-existing with cellular users in a multi-tier HetNet.

In Chapter 5, resource allocation for a D2D-enabled cellular network, targetting smart factory settings is presented. The aim is to maximise the overall system throughput comprising cellular users and D2D links with reliability constraints. A matching technique, which uses an incentive-based stability to optimise spectrum sharing is developed.

Reinforcement learning based RRM techniques for channel selection, targetting the deployment of D2D links in a wireless URLLC industrial environment, are presented in Chapter 6. The presented techniques adopt stateless learning without limiting the performance requirements of the users, in order to reduce the learning complexity.

The conclusions resulting from the research work carried out in this thesis are presented in Chapter 7. These include a summary of the contributions, recommendations, dissemination of results and potential directions for future research work.

Chapter 2

A Critical Review of Application Requirements and RRM Techniques in Wireless IoT Networks

In this chapter, a review of the state-of-the-art is presented, as identified by the published literature in the field of study. Initially, an overview of use cases for IoT in 5G-and-beyond networks is presented and discussed, with a specific focus on D2D communication and its deployments in smart industrial scenarios and highlighting the key enabling technologies. The RRM challenges faced in achieving the required QoS in smart manufacturing are discussed. The relevant techniques and main approaches to RRM are also overviewed. Finally, the chapter concludes with a summary of the main outcomes and implications of this literature survey as they relate to the research work reported in this thesis.

2.1 Internet of Things Use cases in 5G-and-Beyond Networks

The main 5G use cases include enhanced Mobile Broadband (eMBB), massive MTC (mMTC) and critical MTC (cMTC) [30,31]. These services have widely diverse QoS/QoE requirements and can be allowed to coexist within the same network architecture through the concept of network slicing [32].

a) Enhanced Mobile Broadband (eMBB)

eMBB has a high bandwidth requirement such as in High Definition (HD) video, Virtual Reality (VR), Augmented Reality (AR), on-body sensors etc. It supports connections with high peak data rates (approximately 10Gbps and with a bandwidth of several hundreds of MHz), as well as moderate rates for cell-edge users and moderate latency (a few milliseconds). eMBB is characterised by large data packets and regular traffic over an extended time interval. Thus, devices with eMBB traffic usually use dedicated radio resources. An eMBB service focuses on maximising data rate, while guaranteeing reliability ranging from low to average, with a Packet Error Rate (PER) of the order of 10^{-3} [33].

b) Massive Machine-Type Communication (mMTC)

Massive MTC is characterised by a vast number of IoT/MTC devices, which are only intermittently active and transmit few data packets at a relatively low data rate in the uplink. Only a random set of the large number of mMTC devices connected to a particular BS may be active at any given instant. Thus, it is practical to provide random access in spectrum sharing rather than pre-assigning dedicated radio resources to each device. The number of active sets of mMTC devices is a random variable, with a mean value that estimates the mMTC data traffic arrival rate (average number of data traffic per unit time). The design aim of mMTC is to maximise the arrival rate that can be supported in a given resource block [33]. The PER value of an mMTC transmission is typically low, for example, of the order of 10^{-1}.

c) Critical Machine-Type Communication (cMTC)

Critical MTC, also known as URLLC often requires real-time communication between smart devices. It supports relatively low transmission rate (typically 100kps) with strict demand for high reliability (typically 99.999%), extremely low delay (typically 0.25-0.3 ms/packet) and with a PER typically lower than 10^{-5}. URLLC transmissions are also sporadic, but the set of potential URLLC transmitters is much smaller than for mMTC and are usually event-driven. Critical MTC requires random access with a short Transmission Time Interval (TTI) to avoid waste of resources due to the periodic traffic [34-36].

In 6G, URLLC, eMBB, and mMTC) will be extended to other areas, which are Ultra-High Precision Communication (uHPC), Ultra-Broadband (uMBB), Ultra-Massive Machine-Type Communication (uMTC), respectively. uHPC provides higher reliability, lower latency, more precision in synchronicity compared 5G URLLC. uMBB have higher data rate requirements than 5G eMBB use case scenarios and uMTC supports ultra-high connection density compared to in 5G use case scenarios. A comparison of the different wireless generations [10, 37-40], using some Key Performance Indicators (KPIs), is shown in Table 2.1.

Table 2.1: Comparison of some KPIs of different wireless generations [10, 37-40],

	3G	**4G**	**5G**	**6G**
Year of Introduction	1998	2008	2018	2030
Wireless Standard or Technology	Universal Mobile Telecommunication Systems (UMTs)	Long Term Evolution (LTE)	5G New Radio (NR)	Ubiquitous Wireless Intelligence (UWI)
Example of use cases	MBB	MBB	eMBB, URLLC, mMTC	uMBB, uHPC, uMTC
Peak data rate	30Mbps	100Mbps	10Gbps	1Tbps
Experienced data rate	2Mbps	10Mbps	0.1Gbps	1Gbps
Frequency	800-2000MHz	Below 6GHz	Up to 300GHz	Up to 3THz
Latency	200ms	100ms	10ms	1ms
Mobility support	up to 300km/h	up to 350km/h	up to 500km/h	up to 1000km/h
Reliability	>99.9%	>99.99%	>99.999%	>99.9999%
Connection density	10^4Devices/km	10^5Devices/km^2	10^6Devices/km^2	10^7Devices/km^2
Area traffic capacity	100kb/s/m^2	0.1Mb/s/m^2	10Mb/s/m^2	10Gb/s/m^2
Examples of Applications	Voice, data, Video call	Voice, data, video call, High-Definition TV, Mobile TV	Voice, data, video call, Mobile TV, Smart city, Vehicle-to-Everything (V2X), Virtual Reality (VR)	Digital sensing and reality, autonomous driving, Tactile haptic Internet, Space travel, Internet of Bio-Nano Things, Internet of Everything (IoE), Augmented Reality (AR)
Technologies	Wideband Code Division Multiple Access (WCDMA), CDMA-2000	Orthogonal Frequency-Division Multiplexing (OFDM), Orthogonal Frequency-Division Multiple Access (OFDMA) Multiple- Input Multiple-Output (MIMO), Carrier Aggregation (CA), D2D	mm-Wave communication, Non-Orthogonal Multiple Access (NOMA), Massive MIMO, Software defined Network (SDN), Network Function Virtualisation (NFV), Network slicing, Edge computing, Virtual Network Operator (VNO)	Tera-Hertz (THz) communication, Spatial Modulation MIMO (SM-MIMO), Orbital Angular Momentum (OAM) multiplexing, Blockchain-based spectrum sharing, Quantum communication, AI, ML

2.2 Wireless Factory Automation (Wireless Industrial IoT)

Smart industry, also known as smart factory, Industry 4.0 or Industrial IoT (IIoT), is an industrial, technological development that integrates cyber-physical systems (CPS), artificial intelligence (AI) and IoT to transform manufacturing and production processes through automation [41]. While Industry 4.0 is still being adopted by businesses, Industry 5.0 has emerged recently. The concept of Industry 4.0 focuses on connectivity through cyber-physical systems. Industry 5.0, while aligned with objectives of Industry 4.0, addresses the interaction between "humans and machines," otherwise known as robots or cobots [42,43].

One of the key aspects of factory automation is real-time control of machines and systems. Wireless factory automation has gained much attention in recent times. This can be attributed to its merits in terms of low installation and maintenance costs with flexibility and scalability compared to wired networks, in addition to its suitability to meet the requirements of FoF. Factory automation can provide new opportunities and prospects for manufacturing and enhance the efficiency of production and increase productivity. Smart factories rely on MTCs. This involves interaction between sensors, machines, robots, and wearable devices. Fig. 2.1 depicts a graphical illustration of a typical smart factory [44]. The industrial evolution [45], highlighting the key technological development at each phase is shown in Table. 2.2. The principal challenges for the deployment of industrial wireless networks are the stringent performance requirements in terms of very low end-to-end latency and high reliability with low power consumption for data acquisition and control [46].

2.2.1 Wireless Technologies used in Industrial Environments

The most common existing wireless standards used for communication in factory automation include Zigbee, WirelessHART, ISA100.11a and IEEE 802.11x [47]. These technologies are deployed in the license-exempt bands which are subjected to co-channel interference and congestion as the number of devices increases, as well as security and privacy issues, thus limiting their QoS/QoE guarantees. Cellular technologies, on the other hand, offer long-range connectivity and provide access to a larger number of devices, and are also recognised for their reliability [48].

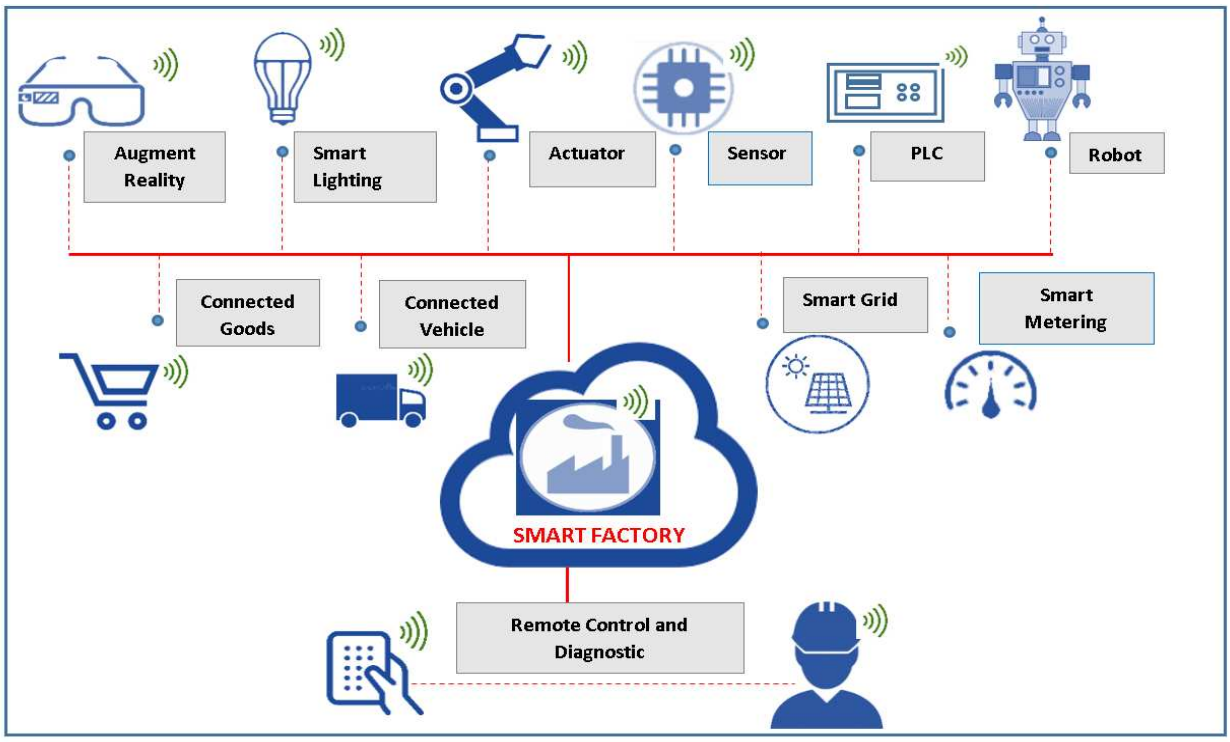

Fig. 2.1. An illustration of Industry 4.0 [44]

Table 2.2: Different Eras of the Industrial Revolution [45]

Technology	Industry 1.0	Industry 2.0	Industry 3.0	Industry 4.0	Industry 5.0
Key feature	Mechanisation	Electrification	Automation	Cyber-physical systems	Collaborative robots (Cobots)
Characteristics	Mechanical weaving looms, steam power etc.	Production lines, mass production using electrical energy	Electronics and information technology for automation	Intelligent production integrated with Internet of Things, machine learning and artificial intelligence	Mass customization and cyber-physical cognitive systems
Year	1784	1870	1969	Today	Within the present decade

The current technologies, both cellular and cell-free architectures, have limitations in terms of capabilities in handling performance requirements (e.g., low-latency and high reliability) for FoF [5]. 5G-and-beyond technologies are expected to provide performance improvements to

enable applications and services that cannot be supported by existing wireless networks or standards.

2.2.2 D2D Communication for Wireless Industrial Applications in 5G-and-Beyond Networks

Device-to-Device communication (D2D) is considered as a promising solution for URLLC use cases, especially for proximity communication. MTC within the factory is an example of URLLC [49]. Factory automation typically involves a closed loop that comprises sensors and actuators (e.g., a robot and a Programmable Logic Controller (PLC)). Fig. 2.2. illustrates D2D communication in a typical smart factory. The sensor sends its measured data to the PLC, which then instructs the actuator to implement a certain action [50]. These devices have the potential for direct D2D communication because they usually operate in proximity to each other. Integrating D2D into future industrial wireless networks and next-generation manufacturing can support the creation of mMTCs [51]. With D2D, proximal devices can bypass the network infrastructure and communicate directly. D2D communication aims to provide three main types of gains, namely, proximity, hop and reuse gain. Proximity gain is achieved through short-range direct communication of D2D links which results in reduced delay and a lower power consumption, improved reliability, and data rates. Hop gain is where a D2D link uses a single hop as opposed to the conventional cellular transmission which uses both uplink and downlink resources, thus contributing to reducing the end-to-end latency. Reuse gain is achieved by the simultaneous use of channels by D2D links and cellular links, thus enhancing spectrum efficiency and increasing network capacity and traffic offload [52]. Considering the limitations of the current wireless solutions, D2D communication is a key enabler to satisfying URLLC requirements for factory automation [53].

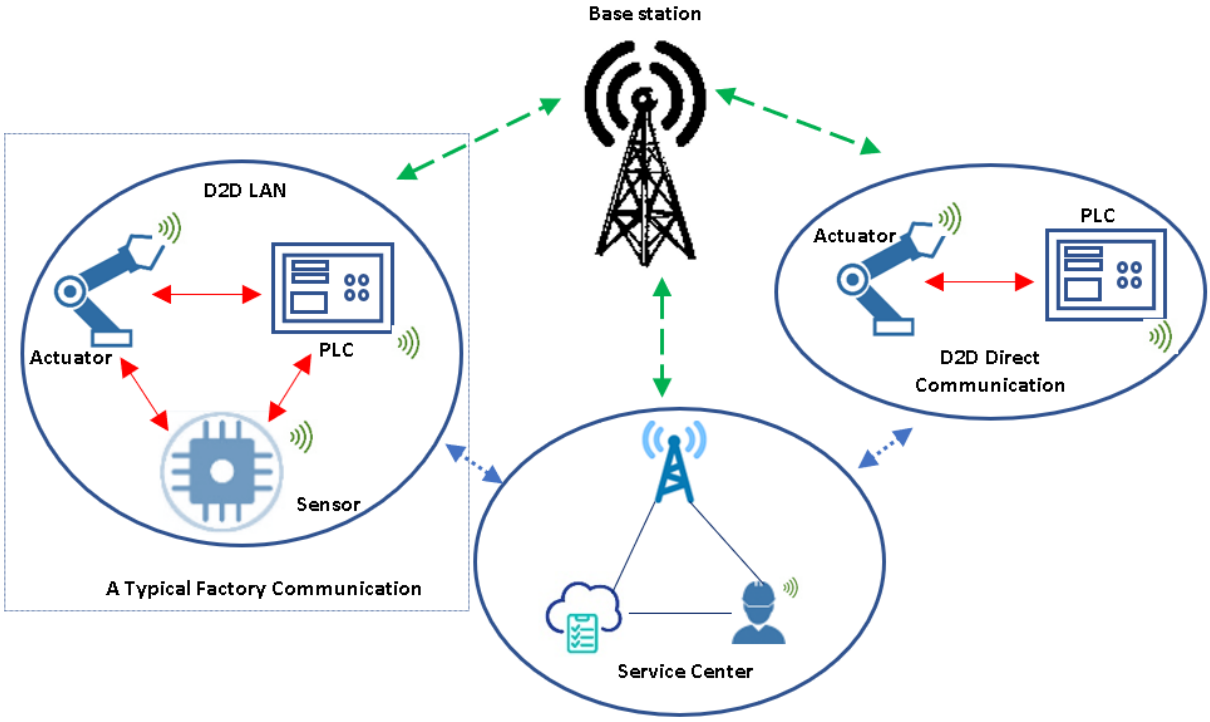

Fig. 2.2. D2D communication in smart factory [46]

D2D communication can take place in the cellular licensed spectrum bands (called in-band communication) or in the unlicensed spectrum bands (or out-band communication [54]). D2D communication links deployed in the licensed spectrum bands have gained much attention because of their reliability in terms of QoS guarantees that can be attained relative to the unlicensed bands which are unregulated and uncoordinated [55]. Spectrum access in a licensed band by D2D links can either be via shared channels with cellular users (referred to as shared mode, also called underlay) or via exclusive use of dedicated channels (referred to as dedicated mode, also called overlay). Due to the high cost associated with a license fee and scarcity of dedicated radio resources, spectrum sharing is now receiving increased interest [56]. Furthermore, spectrum efficiency in 5G-and-beyond systems will depend on developing sharing techniques to offload the already congested network and expand capacity. While resource-sharing tends to improve spectrum utilisation, the main challenge is how to address co-channel interference. As a result, new spectrum sharing schemes are essential to satisfy the target QoS/QoE of coexisting users. The use of dedicated channels by D2D links, on the other hand, may lead to an under-utilisation of limited spectrum resources, but interference between D2D users and cellular users is avoided because of orthogonal channel assignment. Orthogonal channels are channels that are sufficiently distant from each other such that interference can be avoided [57].

2.2.3 Performance Requirements in a Wireless Smart Manufacturing Environment

To measure the efficiency of connectivity solutions of the current wireless communication technologies for diverse use cases and applications, the operational requirements and metrics needed for the deployment of these services should be considered. 5GPPP identified five manufacturing Use Cases (UC) to describe these requirements [5] as presented in Table 2.3. These requirements encompass both performance and design requirements for the various use cases. Latency, reliability, and data rates are further elaborated and investigated in this research work as they critical QoS metrics for efficient radio resource management for Industrial IoT (IIoT) applications. These metrics are interdependent and impact the overall performance of IIoT systems.

Table 2.3: Communication requirements for different smart manufacturing use cases [5]

		Latency	Reliability	Bandwidth	Coverage	Security	Heterogeneity	Autonomy
UC1	Time-critical process optimisation	Very low	Very high	Low to high	Indoor	Critical	Important	Less Critical
UC2	Non-time critical optimisation	Less stringent	High	Low to high	Indoor + On site outdoor	Critical	Important	Critical
UC3	Remote control	Less stringent	High	Low to high	Wide area	Critical	Important	Less Critical
UC4	Inter-/Intra-Enterprise Communication	Very low to less stringent	High	Low to high	Wide area (On site/outdoor)	Critical	Important	Less Critical
UC5	Less stringent	Less stringent	Low	Low to high	Wide area	Important	Important	Critical

a) Latency

Latency is expressed in terms of end-to-end delay perceived by the user [58]. End-to-End (E2E) latency includes queuing delay, propagation delay, transmission, and re-transmission (if allowed) delay and processing delay [59]. Critical MTC has hard latency requirements which vary from one URLLC application to the other. Typical values of E2E delay for motion control in factory automation are down to 1ms, or less depending on the application [60] A shorter frame structure for an LTE system with a duration of 1ms transmission time interval (TTI) was proposed in [61] to reduce transmission delay. Direct communication via Device-to-Device (D2D) communication can also reduce transmission delay [62].

b) Reliability and Availability

Reliability can be described as the successful or guaranteed packet delivery within the latency bound and typically expressed as a target maximum Block Error Rate (BLER) or Packet Error Ratio (PER) depending on the layer of the communication protocol stack [16]. Factory automation is characterised by a reliability of at least 99.999% or PER not higher than 10^{-5} [63]. Reliability and availability are terms often used interchangeably for cMTC, but, are generally often referred to as "reliability". Reliability is related to short-term communication quality and is impacted by multipath fading and rapidly changing interference in a dynamic environment. Multipath fading is a characteristic of a wireless channel which occurs when signals reach a receiver via more than one path. This leads to variations in their signal strengths and phases, which may result in signal distortion [64,65]. Availability is usually defined in terms of geographic service coverage. It is the long-term service quality of the end-users and is impacted by path loss, shadowing and other slowly varying channel characteristics [66]. Reliable wireless communication requires a higher immunity to interference and environmental clutter. Reliability against factors such as bandwidth, latency budget, interference power level, are discussed in more detail in [15,22,67].

c) Data rate

Various use case families in the manufacturing industry are characterised by applications with diverse data rate requirements ranging from low to high. For example, some sensors may communicate (measurements, control commands and signalling) at a low bit rate (typically 100kbps [68]), but with ultra-high reliability and low latency, whereas AR, VR, vision-controlled robot arms or mobile robots may require high-bandwidth communication [5]. Typical packet sizes for video-operated remote control are up to 250kbytes [69]

2.2.4 RRM challenges in achieving QoS requirements for smart manufacturing

Factory automation is considered one of the most demanding 5G-and-beyond use cases, as some of its applications have stringent latency requirements typically of few milliseconds [60]. To achieve the QoS demands for D2D-enabled factory automation, the main challenges to address include interference management, power consumption, heterogeneity and self-organisation and autonomy. These issues are discussed as follows:

a) Spectrum and interference management

Achieving ultra-reliability and low latency pose challenges in terms of bandwidth requirements. The work in [22] studied the transmission bandwidth needed to enable URLLC for factory automation and found that the system bandwidth depends on the number of connected user equipment and the behaviour of their traffic. The scarcity of radio resources and the limitations on the available system bandwidth makes spectrum sharing a necessity for D2D implementation of MTC for factory automation [67]. RRM schemes need to be efficiently designed for interference management and coordination, while guaranteeing tight URLLC demands. Channel reuse among active devices in the same cell will generate interference which degrades system performance. Interference management is crucial to ensure efficient utilisation of available. Interference coordination is particularly challenging in deployment scenarios where DUEs share cellular resources. Spectrum and interference management is an important concern in sixth-generation (6G) networks that needs addressing.

Ningombam et al, developed a model to determine the minimum number of channels for real-time traffic scheduling for a given local cell while coordinating the interference to achieve high reliability and low-latency communication in a factory automation use case [70]. A reliable real-time scheduling assignment was obtained using a heuristic algorithm with near-optimal results. However, power management was not considered, which is pivotal to interference control and enhancing the quality of the solution. The effect of the increased interference due to high user density on data rates and packet latency for smart industrial environments was investigated in [63]. Multi-connectivity, multi-hop and D2D communication were highlighted as possible means to improve availability in the presence of interference and channel clutter. In [71], a Stackelberg game was used to model the interactions between D2D and cellular users to study interference management problems, with D2D links reusing multiple cellular channels. The eNodeB (eNB), as the leader in the game, sets the price for channel reuse by the D2D links so that the interference generated by the D2D users to the cellular communication is lower than a predefined threshold. Thus, the D2D users can regulate their transmit powers over the channels to maximise their data transmission rates. Price relates to a monetary payment made by the users for spectrum access [71], or cost of interference generated by a user to the BS, as in [72]. Results from [71] show that the throughput of D2D communication was improved for multiple channels compared to a single-channel reuse. However, the stability of the algorithm applies only to the D2D users. In [73], a heuristic algorithm was applied to obtain the optimal

D2D links with the potential of extending the network capacity and improving the spectrum efficiency by considering the outage probability of cellular communication and the D2D links. Their proposed method minimised the interference from D2D communication while the QoS of the D2D users are guaranteed. In [74], the Poisson Point Process (PPP), which is a model used to generate time series of discrete, stochastic events [75], was used to model the distribution of the network entities in order to study the effect of interference on network communication. Matching theory was then, used to assign cellular resources to the D2D links while mitigating the impact of interference. The authors assumed that the transmit power of the user equipment is fixed, hence, the impact of power control on the proposed solution was not considered. A joint mode selection and power control scheme was used in [76] to realise interference management. Specifically, power control was used to dynamically regulate the interference-limited area, therefore, managing interference and satisfying the minimum QoS requirements of the users. The proposed solution was able to achieve an improved sum data rate, particularly, for high-density systems. However, resource allocation, which could provide practical value for QoS gain improvement was not considered.

b) Power Consumption and Energy Efficiency

Low power consumption is a major target as most smart devices are battery-powered expected to operate for few years before replacement. Power consumption increases with range as data is transmitted from one smart device to the other. Smart devices are energy-constrained and mostly battery-powered, requiring frequent charging. Even with the use of 'green' sources (*e.g.,* solar, wind) and energy harvesting, energy demands are still challenging.

Power control and allocation play a crucial role in interference mitigation and achieving the desired data rate. New RRM mechanisms that will ensure communication in industrial IoT in an energy-efficient manner are necessary. Power control is used to regulate the transmit power of users in order to ensure the desired transmission rate is guaranteed. In 5G-and-beyond systems, the introduction of D2D communication into legacy cellular communication for shared spectrum access, makes power control significant in resource allocation. This is because of the potential of power control to manage intra-cell interference and to limit the power consumption of short-range communication, therefore, prolonging the battery lifetime of the user terminal. In [77], a power allocation method was used to achieve optimal power assignment, where the D2D transmitters use minimum power, while guaranteeing system

throughput maximisation. The link quality of the cellular and D2D users is estimated using stochastic geometry. Results from the proposed approach showed significant system sum-rate improvement compared to fixed power and random power allocation. However, since the objective is to maximise the overall system throughput, transmit power resources may be available which could possibly further increase the system throughput [21]. That is, the transmit power of users can be increased to achieve a higher system throughput given the predefined power limit is not exceeded. The power allocation problem was addressed in [78] with an iterative procedure to maximise the sum data rates of the cellular and D2D communication considering a multicell scenario. The power optimisation problem was solved by jointly considering multiple reuses of the cellular resource blocks by the D2D users, while keeping the adjacent cell interference below a predefined threshold. Semasinghe et al, proposed a power allocation technique based on the Nash bargaining solution and Nash competitive game [79]. The resource allocation problem was first reformulated as a convex optimisation before obtaining a solution. The Karush-Kuhn-Tucker (KKT) condition was applied and a closed-form solution for Nash Equilibrium was obtained. Results show that cooperation among the D2D users helped them to achieve a higher data rate. A double-layer resource and power allocation scheme were designed in [80] for D2D energy efficiency maximisation. Fractional programming was used to transform the non-convex optimisation problem into a subtractive form, then the power control problem was solved iteratively. The results of the proposed approach showed an improved energy efficiency compared to other considered power control schemes.

c) Self-organisation

Self-organisation is a core element envisioned to meet the needs of dense wireless networks. The large-scale nature of IoT environments necessitates a shift towards RRM approaches that support learning and can be implemented in a decentralised manner. This will reduce centralised processing and signalling overheads at the BS. Smart devices and networks are expected to learn from their immediate environment and adapt accordingly, while making autonomous, independent decisions for performance optimisation. Self-organisation is the inter-operation of self-configuration, self-optimisation, and self-healing to achieve performance optimisation, maintenance, monitoring and learning with minimal human intervention [81]. RRM techniques with learning capabilities are therefore necessary. Self-organisation is presently considered a key concept to introduce intelligence and autonomy,

reduced complexity, cost of operation and network management and improve the reliability of RRM design. Self-organisation requires RRM decisions to be based on local information [82], which is usually facilitated by a distributed RRM scheme. Autonomy is identified as one of the high-level communication requirements smart manufacturing use cases defined by 5GPPP [5].

d) Heterogeneity

Smart factories are characterised by heterogeneity. Different device types with different service requirements in terms of energy consumption, cognitive abilities and resource demands are expected. A resource management framework that captures diverse device types and QoS requirements is necessary to ensure seamless, ubiquitous, and interoperable connectivity [5].

e) Scalability

Future expansion of the network requires that demands of new users, applications and services are met when introduced to an existing system, without compromising the QoS of existing users. A scalable RRM scheme with bounded computation complexity is, therefore, needed for future growth [25]. For scalable deployment of D2D communication for MTC in cellular networks, traffic balancing needs to be considered in the design of RRM schemes to ensure distributed spectrum usage as the number of users rises.

2.3 The Main Radio Resource Management (RRM) Approaches

The major RRM issues to be addressed have been outlined and discussed in the previous section. The approaches to tackle these challenges are reviewed in this section. There are two main approaches to RRM, namely: centralised and distributed. In centralised RRM, a central controller coordinates and controls the resource allocation policies, whereas distributed RRM is user terminal-centric.

a) Centralised RRM

In the centralised approach, the network has a single central controller e.g., BS or AP, that coordinates and controls the resource allocation policies [83]. This central entity obtains information such as channel quality and resource requirements from the user equipment (UE). Based on the information obtained, the central entity allocates the required amount of radio resources to each UE. With the global network information, the RRM problem can be formulated as an optimisation problem where the QoS (or performance) requirements of users

are the constraints. Nevertheless, these optimisation problems are often complex and hard to be solved directly. Consequently, several methods have been presented in the literature where the problem is broken into multiple steps to obtain a local optimal or sub-optimal solution. The centralised approach may provide globally optimal or near optimal resource allocation for cellular networks, but often results in increased signalling overheads and increased complexity [84]. Therefore, it has been suggested that centralised schemes may not be viable for high-density networks [85]. Most RRM schemes are implemented in a centralised manner where the D2D users have to report local Channel State Information (CSI) to the BS for centralised decision-making. Centralised resource allocation is challenging for D2D-enabled cellular networks because a large number of devices will be required to report their CSI to the BS. The CSI feedback and update rate greatly increase the signalling overheads. Therefore, there is a paradigm shift towards distributed resource management which has the potential to mitigate these issues.

b) Distributed RRM

The distributed RRM approaches are mainly terminal-centric. In distributed RRM, the UE is capable of making decisions with reference to resource utilisation based on local information. This enables a reduction in network complexity, signalling and computation load, particularly in heterogeneous environments, hence it does not require a central entity. Autonomous decision-making entails integrating cognition, such as environmental sensing and learning capabilities, into the UEs [86]. With a distributed learning approach, cellular systems can learn from their wireless environment and make decisions to determine the optimal resource allocation. A distributed RRM scheme is favourable because of its low implementation complexity and signalling overheads and is more feasible for high-density networks. Since IoT environments are characterised by some level of intelligence, a distributed RRM mechanism that supports self-organisation and autonomy would be required. However, optimal resource allocation among the UEs may be difficult to achieve [85]. In a distributed approach, it is assumed that UEs are selfish, which means that their primary objective is to maximise their individual utility functions, which may not necessarily optimise the overall system performance. Selfishness and rationality are characteristic features of distributed and intelligent users, as the output of a centralised resource allocation may not be in the interest of some UEs. Another drawback of the distributed approach is message passing among the devices which tends to increase signalling overheads across the whole network [87].

c) Hybrid RRM

Although both centralised and distributed approaches have their merits and drawbacks, trade-offs can be achieved. The trade-off between performance and signalling overhead for both centralised and distributed resource allocation remains an open research question that need investigating. Such RRM schemes are said to be "hybrid". A hybrid scheme combines centralised and distributed approaches in allocating resources among UEs. For example, the central unit performs global RRM functions, such as the gathering of channel state and traffic information, while UEs are responsible for local RRM functions, such as packet scheduling. Such schemes could be well suited for moderately dense networks. The large-scale nature of IoT environments, such as in a smart factory, poses a limitation on a purely centralised approach because a large amount of information exchange is often incurred leading to increased complexity, and signalling overheads [88]. On the other hand, a distributed approach may just be able to achieve a near-optimal solution [89].

2.4 Discussion of some Relevant RRM Techniques

RRM techniques can rely on centralised or distributed approaches as described above. Different methodologies can be used to realise an RRM framework depending on the system under consideration. Mathematical optimisation [90], matching theory [91, 92] and machine learning [93, 94] are the major tools investigated and considered in this thesis.

a) Mathematical Optimisation

Mathematical optimisation involves techniques used for the minimisation or maximisation of a utility function with a given set of constraints. The goal of optimisation is to determine the best possible value from some available sets of alternatives. Common optimisation methods applied in resource allocation include combinatorial optimisation, heuristics, nonlinear programming and integer programming [95]. Mathematical optimisation techniques have been used for overall network throughput or data rate maximisation [96], energy efficiency [97] and delay optimisation [98]. A heuristic centralised scheme for maximising the sum rate of cellular users was proposed in [90]. This was achieved by transforming the reliability and latency requirements of vehicle-to-vehicle communication (V2V) into computable optimisation constraints. A minimum vehicle-to-infrastructure (V2I) capacity maximisation framework was designed in [99], to improve the overall throughput. A joint mode selection, power and spectrum allocation scheme was proposed in [100] with the aim of maximising the total sum

rates for varying network load. Mathematical optimisation schemes as in [90,99,100] often adopt centralised approaches and require large information exchange which renders it unfeasible for ultra-dense networks due high signalling overheads incurred. Mathematical optimisation techniques will be developed and used a baseline for comparing the performance of the newly developed schemes reported in thesis.

b) Matching Theory

Matching theory is a sub-category of game theory having the capability to provide low-complexity distributed and self-organised solutions to resource allocation problems. Matching theory is a model traditionally applied in mathematics and economics to provide tractable solutions to the assignment problem of matching players in distinct sets. As such, matching theory has emerged as a promising method for resource allocation in wireless networks because it can overcome some of the limitations of traditional game theory such as high information exchange and complexity, slow convergence to equilibrium, and the notion of one-sided stability which may be impractical where there are distinct sets of players with diverse objectives; and optimisation which is characterised by the high cost of information acquisition/gathering. Some of the advantages of matching theory include [101]:

i. Suitability to represent interactions between heterogeneous entities with diverse classes, goals and information.
ii. Ability to define 'preferences' related to heterogeneous QoS requirements.
iii. Suitability to provide stable and optimal solutions with respect to different system objectives.
iv. Tractable and self-organising algorithmic implementation.

The Stable Marriage Problem (SMP) is a popular illustrative example of a matching model. A stable assignment can be achieved by the Deferred Acceptance (DA) algorithm (also known as the Gale Shapley (GS) algorithm). The basic elements, terms and definitions of matching problems are as follows:

i. **Players:** The matching problem is defined by two distinct sets of players. The sets of players here are the decision-makers. The matching output $\boldsymbol{\mu}$ assigns the players (resource $\boldsymbol{c} \in \boldsymbol{C}$) in one set to the players (user $\boldsymbol{d} \in \boldsymbol{D}$) of the other set.

ii. **Quota:** This defines the maximum number of players with which each player can be matched. Denote $\boldsymbol{q_c}$ and $\boldsymbol{q_d}$ as the quota of resource $\boldsymbol{c}$ and user $\boldsymbol{d}$, respectively, such that $|\boldsymbol{\mu(c)}| \leq \boldsymbol{q_c}$ and $|\boldsymbol{\mu(d)}| \leq \boldsymbol{q_d}$.

iii. **Utility function:** This defines the value each player attributes to the players of the other set. For certain assignment problem, the utility function $\boldsymbol{U}$ evaluates specific QoS of the network. $\boldsymbol{U_d^c}$ denotes the utility function of player $\boldsymbol{d}$ from being matched to $\boldsymbol{c}$.

iv. **Preference relation:** A preference relation $\succ$ is a complete, reflexive, and transitive binary relation between the players of sets $\boldsymbol{C}$ and $\boldsymbol{D}$. A player ($\boldsymbol{d} \in \boldsymbol{D}$) builds its preference relation over player in set $\boldsymbol{C}$ by ranking them according to the utility generated (based on local information). Let $\succ_{\boldsymbol{d}}$ denote the preference relation of player $\boldsymbol{d}$ over set $\boldsymbol{C}$, then $\boldsymbol{c_1} \succ_{\boldsymbol{d}} \boldsymbol{c_2}$ if and only if $\boldsymbol{U_d^{c_1}} > \boldsymbol{U_d^{c_2}}$. The notation $\boldsymbol{c_1} \succ_{\boldsymbol{d}} \boldsymbol{c_2}$ implies that the player $\boldsymbol{d} \in \boldsymbol{D}$ prefers $\boldsymbol{c_1}$ to $\boldsymbol{c_2}$.

v. **Matching game solution:** The game solution is the output of the matching and defined as function $\boldsymbol{\mu}: \boldsymbol{C} \rightarrow \boldsymbol{D}$ such that (i) $\forall \boldsymbol{c} \in \boldsymbol{C}$, $\boldsymbol{\mu(c)} \in \boldsymbol{D}$ and $|\boldsymbol{\mu(c)}| \leq \boldsymbol{q_c}$ (ii) $\forall \boldsymbol{d} \in \boldsymbol{D}$, $\boldsymbol{\mu(d)} \in \boldsymbol{C}$ and $|\boldsymbol{\mu(d)}| \leq \boldsymbol{q_d}$, and (iii) $\boldsymbol{c} \in \boldsymbol{\mu(d)}$ if and only if $\boldsymbol{d} \in \boldsymbol{\mu(c)}$.

vi. **Matching output stability:** A matching output $\boldsymbol{\mu}$ is a set of matched pair of players from two distinct sets $\boldsymbol{C}$ and $\boldsymbol{D}$. It is stable if and only if there exist no blocking pair $(\boldsymbol{c}, \boldsymbol{d})$, where $\boldsymbol{c} \in \boldsymbol{C}$, $\boldsymbol{d} \in \boldsymbol{D}$, such that $\boldsymbol{c} \succ_{\boldsymbol{d}} \boldsymbol{\mu(d)}$ and $\boldsymbol{d} \succ_{\boldsymbol{c}} \boldsymbol{\mu(c)}$, where $\boldsymbol{\mu(c)}$ and $\boldsymbol{\mu(d)}$ represent, respectively, the current assigned partner of $\boldsymbol{c}$ and $\boldsymbol{d}$.

The conventional matching game is classified according to the value of the quota. In one-to-one matching, the quota of each player is one (i.e., the players can be matched to a maximum of one member of the opposite set). For many-to-one matching, at least one player can be matched to multiple members of the opposite set, while players in the other set have their quotas set to one. In many-to-many matching, players from the two sets can be matched to multiple players. The DA algorithm is an efficient algorithm often used to solve the many-to-one and one-to-one matching problem [102], with the existence of at least one stable matching. The DA algorithm has been widely applied and adapted to achieve stable matchings for other models and applications.

In the context of wireless communication, the players $\boldsymbol{c} \in \boldsymbol{C}, \boldsymbol{d} \in \boldsymbol{D}$ (i.e., the user equipment (UE) and base station in the considered cases) can define their utility function $\boldsymbol{U}$ based on the local information they possess for other players [101]. The primary goal of the matching for wireless RRM is to provide an optimal assignment of users and resources (e.g., spectrum channels, power levels) while considering the network constraints. Matching theory can provide a framework that allows IoT devices and entities to make some form of interdependent choices and the DA algorithm can achieve a distributed resource allocation solution.

Matching theory can also be categorised into three classes to characterise RRM in wireless networks namely: Class I-canonical matching, Class II-matching with externalities and Class III-matching with dynamics [101]. Class I type is the reference class in which the preference of a player depends exclusively on the information available to the player and its potential matched partners. In Class II, there are interdependencies between the preferences of the players (i.e., the preference of a player depends on the information to the player and matching of other players). For the Class III type, the preference of a player is time-varying and must be considered in the matching solution.

Information exchange during a matching routine can be implemented in a distributive, semi-distributive or centralised manner. This implies that some processes are carried out based on the local information acquired by the players; some may partially involve the participation of the BS, while for others, the operations take place entirely at BS, which acts as the matchmaker as in [103]. In this case, the estimated CSI at the receiver of the D2D link will need to be reported to the BS, for building the preference profiles of the D2D links. Prior to the execution of the matching subroutine, the preference profiles of the players need to be formed, which can be set up through the local acquisition of channel state information by each player. For example, in SMP, a set of $\boldsymbol{X}$ men and a set of $\boldsymbol{Y}$ women are the players or agents in the game. Each player in $\boldsymbol{X}$ will build a preference list from $\boldsymbol{Y}$. Similarly, each player in $\boldsymbol{Y}$ will construct a preference list over players in $\boldsymbol{X}$ that they find acceptable. After obtaining the information, the players will order the players of other sets according to preference based on a certain QoS criteria, in increasing or decreasing order. The players do not need to have a knowledge of the preferences of the other players. Therefore, the preference profile of each player can be established, and the DA algorithm can be executed in a distributed manner without requiring a central controller or coordination [101].

The matching phase involves proposing and accepting/rejecting operations. A proposal is sent through a communication signal from one player type in a set $\boldsymbol{X}$ to the other type of player in a set $\boldsymbol{Y}$ (the one that receives the proposal). The player that receives the proposal sends a communication signal with accept and reject overheads to the ones accepted and rejected respectively, taking into account the set quota, while giving consideration to its most preferred or highest-ranked member of set $\boldsymbol{X}$. The matching matrices are then updated. The rejected players of set $\boldsymbol{X}$ will start to initiate new proposals to the next most preferred member of set $\boldsymbol{Y}$ in its preference list depending on whether there are still players in the preference list that has not been proposed to before. The iteration will continue until no further proposals are made and members of set $\boldsymbol{Y}$ are matched to $\boldsymbol{X}$. The exchange of proposals during the matching incurs additional signalling overheads. A matching is stable if no pair of $\boldsymbol{x} \in \boldsymbol{X}$ and $\boldsymbol{y} \in \boldsymbol{Y}$ have an incentive to leave their current partners and be matched to each other.

Matching game algorithms have been applied to address resource allocation problems in D2D-based networks. In [104], the DA algorithm was used to associate D2D pairs to cellular resources and introduced the concept of 'cheating' to allow further improvements for D2D pairs. A proximity-based matching game was developed in [105] to maximise the system rate but did not consider the actual channel condition. A constrained-DA algorithm was proposed in [106] to assign pre-allocated macrocell users subchannels to multiple D2D users and Remote Radio Head (RRH) users for channel reuse. It was demonstrated through numerical simulations that the proposed scheme improved the overall system throughput compared to the conventional DA. This shows that the framework of the DA algorithm can be modified for a resource allocation problem to obtain an enhanced system performance. In [107], the DA algorithm was adopted to match the remote resource heads (RRHs) to cellular users then applied a resource exchange policy that conforms with the Kaldor-Hicks principles to improve system throughput. An alteration in resource allocation is said to be Kaldor-Hicks efficient when it produces more gains than losses (i.e., those who are made better off could theoretically, compensate those who are made worse off). A decentralised spectrum allocation scheme was proposed in [108], to maximise the D2D sum-rate in a downlink but only focused on protecting the cellular users from interference posed by the D2D transmitter. The interference from the BS to the D2D receivers were not considered, hence no QoS guarantee for the D2D communication.

The DA algorithm is often used to solve the SMP in matching theory for equally sized sets of elements. From the viewpoint of spectrum reuse and resource allocation for D2D communication within cellular networks, the DA algorithm may not give an optimal solution when there are variations in the sizes of the sets of players (devices and cellular users in this case) and the preference lists. This research work further develops and extends the DA technique to address these shortcomings will be presented Chapter 5.

c) Machine Learning (ML)

The densification of future wireless networks requires the implementation of increased intelligence in network functions. This can be achieved by Self-Organising Networks (SON) to reduce the Capital Expenditure (CAPEX) and Operating Expenditure (OPEX) as well as complexity and simplify network management [109]. Machine Learning (ML) comprises a set of promising tools to perform predictions, support learning and decision-making of smart devices. Thus, ML algorithms should possess the necessary "intelligence" to realise a SON [110]. ML techniques are currently investigated to study intelligent spectrum selection and interference mitigation for radio entities by learning from experience in a dynamic environment [81].

By learning, smart devices can dynamically adapt to the environment, manage their limited resources, and satisfy strict QoS requirements [23]. Machine learning was originally designed and developed for computers to learn and make decisions that will yield better performance for a given task without being explicitly programmed [111]. With a machine learning-based RRM solution, wireless network entities such as the UEs, can learn from their environment and make autonomous decisions to determine their optimal resource allocation which is adaptable to the dynamics of the network. ML and AL are pivotal to the realisation of 6G wireless networks [27,112].

There are three main categories of ML depending on how learning is performed, namely supervised, unsupervised and reinforcement learning [113,114]. Supervised learning algorithms require learning from training data sets. The input data is labelled before it is used to train and test the model. After training, a relationship between the input and output data is established and used to categorise new and unknown data. Data labelling is the process of identifying raw data by adding attributes to it so that the ML model can learn from it. For input variable ($\boldsymbol{x}$) and output variable ($\boldsymbol{y}$), the supervised ML algorithm learns the mapping function

from the input to the output, $\boldsymbol{y} = \boldsymbol{f}(\boldsymbol{x})$. The objective is to approximate the mapping function efficiently and to determine a model such that with new and unknown input data fed into the learned model, the output for that data can be predicted. Supervised learning algorithms include linear regression, random forest, and support vector machine [115].

Unsupervised learning algorithms require a given set of raw, unlabelled input data to be trained by identifying patterns and trends in the raw set of data. The objective of unsupervised learning is to model the underlying framework or distribution in the given data to learn about the data and correctly deduce the output without a trainer. Common unsupervised learning algorithms applied in SON are K-means, Self-Organising Maps (SOM) and anomaly detectors [113].

Reinforcement learning is a machine learning technique in which an agent learns through interactions with its environment by trial and error using the feedback from its actions and experiences. The agent learns from the consequences of its action rather than by being trained. Differently from supervised learning, where the feedback to the agents are correct sets of actions for carrying out a given task, reinforcement learning uses rewards and penalties as signals for good and bad actions respectively.

Unsupervised learning and reinforcement learning differ in terms of their objectives. The goal of unsupervised learning is to deduce the similarities and dissimilarities between data sets, whereas reinforcement learning aims to find a suitable model that would maximise the accumulated reward of the agent. Comparing the three major categories of ML, reinforcement learning is therefore, well-suited to support decision making in 5G-and-beyond networks with uncertainties, for example, in the case of distributed resource allocation with partial information of network conditions.

For this reason, only reinforcement learning is investigated and further developed in Chapter 6. One of the most common reinforcement learning algorithms is $\boldsymbol{Q}$-Learning, which is developed further in this thesis. Others include multi-arm bandit games and Markov Decision Process (MDP). Fig. 2.3., illustrates the basic components of reinforcement learning.

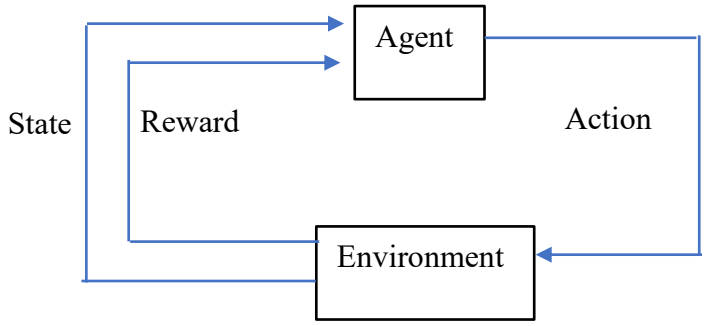

Fig. 2.3. Block diagram illustrating a reinforcement learning system [116]

The basic elements of such a system are described below.

i. **Environment:** This is the physical surrounding where the agent operates. It defines the states and sets of actions an agent can take.

ii. **Agent:** This is the entity that senses and explores the environment.

iii. **State:** This is the current status of the agent reported by the environment after each action taken by the agent.

iv. **Reward function:** This is the feedback from the environment that provides the assessment of the current state and gives reward or punishment based on the outcome of the previous action taken by the agent.

v. **Value function:** This evaluates the future reward that an agent would receive for the action taken in a certain state.

$\boldsymbol{Q}$-learning is a model-free reinforcement learning technique in which an agent learns the optimal policy to adopt by interacting with the environment. It is formulated as a four-tuple $(\boldsymbol{S}, \boldsymbol{A}, \boldsymbol{P}, \boldsymbol{R})$ where $\boldsymbol{S}$ represents a finite set of states, $\boldsymbol{s^t} \in S$, $\boldsymbol{A}$ is the finite set of agent discrete actions , $\boldsymbol{a^t} \in \boldsymbol{A}$, $\boldsymbol{P}: \boldsymbol{S} \times \boldsymbol{A} \rightarrow \boldsymbol{P}(\boldsymbol{S})$ is the state transition probability function that defines the probability of the next states $\boldsymbol{s^{t+1}}$ if the agent is at state $\boldsymbol{s^t}$ and takes action $\boldsymbol{a^t}$, $\boldsymbol{r^t}: \boldsymbol{S} \times \boldsymbol{A} \rightarrow \boldsymbol{R}(\boldsymbol{s^t}, \boldsymbol{a^t}, \boldsymbol{s^{t+1}})$ is the reward function that acts as feedback from the environment based on action taken at state $\boldsymbol{s^t}$ and informs the agent of next action to take as it transitions to the next state $\boldsymbol{s^{t+1}}$ and reward $\boldsymbol{r^t}$.

At each discrete time step $\boldsymbol{t}$, the agent interacts with the environment and senses the current state $\boldsymbol{s^t} \in \boldsymbol{S}$ and takes an action $\boldsymbol{a^t} \in \boldsymbol{A}$ according to a policy $\boldsymbol{\pi}$, which is a function that maps

state to action defined as $\boldsymbol{\pi : S \rightarrow A}$, and receives an observation which includes a reward $\boldsymbol{r^t}$. The environment transitions to a new state $\boldsymbol{s^{t+1}}$ and reward $\boldsymbol{r^{t+1}}$corresponding to the transition $(\boldsymbol{s^t, a^t, s^{t+1}})$. The process is repeated until the optimal policy $\boldsymbol{\pi^*}$ is obtained. The objective of an agent in reinforcement learning is to determine the optimal policy $\boldsymbol{\pi^*}$ that maximises the total expected reward. For a policy $\boldsymbol{\pi}$, the state-value or value of a state $\boldsymbol{s}$, $\boldsymbol{V^{\pi}(s)}$, is the expected return if an agent is in this state at time $\boldsymbol{t}$, $\boldsymbol{s^t = s}$ and given as:

$$\boldsymbol{V^{\pi}(s)}=\mathbb{E}\left\{\sum_{\boldsymbol{k=1}}^{\infty} \boldsymbol{\eta^k r^{t+k+1} \mid s^t = s}\right\} \tag{2.1}$$

where $\boldsymbol{0 \leq \eta \leq 1}$ is a discount factor, $\mathbb{E}\{.\}$ denotes the expectation operation and $\boldsymbol{V^{\pi}(s)}$ represents the expected discounted reward. Through learning repeatedly, an optimal action $\boldsymbol{a^* \in A}$ can be obtained by maximising a cumulative measurement of rewards over time. To build an optimal policy, the agent is faced with the trade-off notion of exploring new states (exploration) versus maximising the reward of current known action (exploitation) [116]. According to Bellman optimality criterion [117], there is at least one optimal strategy $\boldsymbol{\pi^*}$ such that:

$$\boldsymbol{V^*(s)} = \boldsymbol{V^{\pi^*}(s)}=\max_{\boldsymbol{a \in A}}\left\{\boldsymbol{R(s,a)} + \boldsymbol{\eta} \sum_{\boldsymbol{s' \in S}} \boldsymbol{P_{s,s'}(a)\, V^*(s')}\right\} \tag{2.2}$$

where **max(.)** is an operation to maximise the input, $\boldsymbol{V^*(s)}$ is the optimised value function under the optimised policy $\boldsymbol{\pi^*}$, $\boldsymbol{R(s,a)}$ is the expectation of $\boldsymbol{r(s,a)}$ and $\boldsymbol{P_{s,s'}}$ is transition probability from state $\boldsymbol{s}$ to state $\boldsymbol{s'}$. The expression $\sum_{\boldsymbol{s' \in S}} \boldsymbol{P_{s,s'}(a)\, V^*(s')}$ is the expected return of the next state $\boldsymbol{s'}$. The optimised policy can be obtained from $\boldsymbol{V^{\pi^*}(s)}$ as:

$$\boldsymbol{\pi^*(s)} = \operatorname*{\mathbf{argmax}}_{\boldsymbol{a \in A}}\left\{\boldsymbol{R(s,a)} + \boldsymbol{\eta} \sum_{\boldsymbol{s' \in S}} \boldsymbol{P_{s,s'}(a)\, V^*(s')}\right\} \tag{2.3}$$

where **argmax(.)** is an operation that finds the argument that returns the maximum value from the input function. The $\boldsymbol{Q}$-value (or action-value function) is the expected reward of taking action $\boldsymbol{a}$ in state $\boldsymbol{s}$ using policy $\boldsymbol{\pi}$:

$$\boldsymbol{Q^{\pi}(s,a)} = \boldsymbol{R(s,a)} + \boldsymbol{\eta} \sum_{\boldsymbol{s' \in S}} \boldsymbol{P_{s,s'}(a)\, Q(s',a)} \tag{2.4}$$

The optimal policy $\boldsymbol{Q^*(s,a) \equiv Q^{\pi^*}(s,a)}, \ \boldsymbol{\forall s, a}$

Then,

$$\boldsymbol{V^*(s)} = \max_{\boldsymbol{a \in A}}\{\, \boldsymbol{Q^*(s,a)}\} \tag{2.5}$$

With $\boldsymbol{Q}$-learning, the agent tries to learn the optimal policy $\boldsymbol{\pi}^*$ without prior knowledge of the dynamics of the environment. The $\boldsymbol{Q}$-learning algorithm adjusts $\boldsymbol{Q}$-values according to the update rule as described in equation (2.6) where $\boldsymbol{\sigma} \in [\mathbf{0}, \mathbf{1}]$ is the learning rate. $\boldsymbol{Q^{t+1}(s^t, a^t)} = \boldsymbol{Q^t(s^t, a^t)} + \boldsymbol{\sigma}\left[\boldsymbol{r^{t+1}} + \boldsymbol{\eta}\max_{\boldsymbol{a'}} \boldsymbol{Q^t(s^{t+1}, a^{t+1})} - \boldsymbol{Q^t(s^t, a^t)}\right]$ **if** $\boldsymbol{s = s^t,\ \ a = a^t}$

(2.6a)

which may also be written as:

$$\boldsymbol{Q(s, a) = Q(s, a) + \sigma\left[r(s, a) + \eta \max_{a'} Q(s', a') - Q(s, a)\right]} \tag{2.6b}$$

In wireless communication scenarios, the agents are the network entities, such as the CUEs, DUEs and the BS. The actions $\boldsymbol{a^t}$ could be the selection of transmit power levels and/or resource blocks. The reward $\boldsymbol{r^t}$ is often formulated to reflect some QoS performance metrics such as throughput or SINR. The agents keep a $\boldsymbol{Q}$-table with states $\boldsymbol{s^t}$ and actions $\boldsymbol{a^t}$, in which the $\boldsymbol{Q}$-values are updated iteratively according to (2.6) and an optimal value is chosen based on the $\boldsymbol{Q}$-values after training.

$\boldsymbol{Q}$-learning is associated with the problem of the 'curse of dimensionality', which is the exponential growth of the state-action space when the number of states and actions increases (sufficiently large), leading to slow convergence. Additionally, the memory requirement for the $\boldsymbol{Q}$-table for every agent, state and action may limit its adaptability to practical scenarios [118]. Deep Reinforcement Learning (DRL), which is an ML technique that combines reinforcement learning and deep learning, is used to address these issues by using Deep Neural Networks (DNNs) to approximate the tables [119]. However, the practicality of DRL is argued to suffer from high complexity and infeasible amount of data required to learn [120,121] and therefore, is not investigated further in this research work.

Reinforcement learning techniques have been widely investigated to study intelligent power level and spectrum channel allocations for D2D-enabled cellular networks. In [82], a stochastic non-cooperative game is used to formulate the interactions among the D2D users. A finite-state Markov Decision Process (MDP) is used to model the game dynamics and a $\boldsymbol{Q}$-learning method is derived for channel selection in the multiagent environment. Rather than relying on the global knowledge of the strategies of other players, each DUE estimated their beliefs about the strategy of other players. A proof of convergence of the approach to a mixed-strategy Nash

Equilibrium was presented. However, the stability achieved is one-sided as the learning environment consists of one 'type' of agents i.e., only DUEs, which may not be feasible when considering resource allocation between two disjointed sets of agents (CUEs and DUEs) with diverse goals. Moreover, the protection of cellular users from the interference generated by D2D users was not considered in the cellular reuse scenario of [82]. In [87], a framework was proposed that involves cooperation between the D2D users and sharing of all historical information (states, actions, and policies) in a centralised training which, consequently, will increase processing workload at the base station and the amount of signalling overheads due to information gathering. In [87,116,122], the reward function was designed to capture the QoS metric of the cellular users in a centralised $\boldsymbol{Q}$-learning approach, which leads to increased signalling overheads as well.

The afore-mentioned works focused on the operations of D2D communication and did not consider the preferences and satisfaction of cellular users and furthermore, the achieved stability that may be achieved is single -sided as the multi-agent environment comprises only one set of agents i.e., DUEs. Meanwhile, the issues of rationality and selfishness of intelligent nodes may cause instability in practical scenarios where the D2D and cellular users have conflicting objectives, and the final resource allocation solution may not be in the interest of some cellular users.

Matching stability is an important concept in intelligent radio resource allocation which refers to robustness to deviations that can benefit resource owners (i.e., the cellular users) and the users (i.e., the D2D links). For instance, a CUE and a DUE might decide to leave their current partners and be matched to each other because they prefer each other to current partners (i.e., they are both better off being matched together compared to being with their current partners). Such unstable matchings may lead to undesirable network operations if it is large-scale [104]. Designing an RRM scheme that balances the trade-off between performance, complexity and signalling overheads as well as guaranteeing stability, is an open research question. It is the aim of this research work to address some of these challenges.

2.5 Summary of Main Findings from Literature Review and Implications for Research Work

In this chapter, the state-of-the art in D2D communication and its applications to wireless industrial settings was discussed. The major RRM issues that need to be addressed to achieve

optimal QoS requirements for the deployment in D2D communication and its applications to FoF, were identified. The critical survey of the main approaches to RRM, highlighting their advantages and disadvantages, their suitability for different use cases and outcomes of previous related works, was presented. Below is the summary of the main findings of the above critical literature review.

1. Massive connections of IoT/smart devices and sensors such as in mMTC, pose some challenges in the design and deployment of future industrial wireless networks. These challenges include limited spectrum resources and power consumption issues.
2. D2D communication deployed into a wireless smart factory environment can be used to create mMTC. D2D communication is considered a promising technology to address the challenges of spectrum insufficiency and under-utilisation, as well as improve performance requirements such as latency and reliability.
3. Spectrum access with D2D links coexisting with cellular users may result in co-channel interference which may cause performance degradation. New intelligent RRM techniques are required to ensure that the QoS requirements for all intended users are met.
4. RRM approaches are broadly classified into two major categories: centralised and distributed. Mathematical optimisation is an example of the centralised approach. Distributed approaches, on the other hand, includes matching theory, which is a game theoretic approach and machine learning techniques.
5. The centralised scheme may provide a global-optimal solution, but generally incurs large signalling overheads and high complexity due to the global acquisition of information of network entities by a central controller. Consequently, there is a shift towards distributed RRM solutions, especially when a large number of links and devices are present. Furthermore, self-organisation is envisaged to be an integral component of 5G-and-beyond networks, and a distributed solution is key to achieving self-organisation and autonomy.
6. From the study of different RRM techniques, the following knowledge gaps were identified in the application of matching theory (a subset of game theory) and machine learning (specifically reinforcement learning) respectively to address RRM issues and challenges for D2D enabled wireless industrial networks.
    i. The DA algorithm is often used to solve the SMP in matching theory for ‘equally sized sets’ of players, where every member of one set ranks the members of the

other set. However, from the perspective of spectrum sharing for D2D communication links in a cellular network, the DA algorithm may not result in an optimal solution when there are variations in the size of the sets of players (CUEs and DUEs in the case under consideration) and the preference lists.

ii. The preference and satisfaction of cellular users in the learning environment were seldomly considered. In reality, D2D and cellular users may have conflicting objectives and the final resource allocation solution may not be in the interest of some cellular users, thereby potentially causing instability in an SON system.

The solutions to many RRM optimisation problems are often non-convex. Non-convex optimisation problems are non-linear programming problems where the objectives or constraints are non-convex. Such problems may have multiple feasible solution regions and multiple locally optimal points within each region [123]. They are usually complex, intractable and unscalable. In addition, optimal resource allocation often utilises full CSI of all active links and involves a large amount of information exchange and updates in a dynamic environment. This poses significant challenges due to the corresponding large overheads that will be generated. Consequently, new RRM techniques are needed with a good trade-off between performance and applicability, and a good balance between conflicting requirements.

2.6 Chapter Conclusions

Based on the above, the research reported in this thesis focusses on the development of new RRM techniques targetting D2D in wireless industrial scenarios, while mitigating the identified gaps, using the following main approaches.

i. Mathematical optimisation (centralised approach, also used as a baseline for comparison)
ii. Matching theory (distributed approach)
iii. Machine learning (distributed approach)

The developed techniques presented in Chapters 3, 4, 5 and 6 were compared to conventional methods using key performance metrics to determine the approach that offers the most efficient solution for the considered target scenarios. The following research points are investigated:

1. Spectrum Sharing for D2D-Enabled Communication in Cellular Networks

As stated above, D2D is a promising technology for performance improvements for 5G-and-beyond networks. However, interference and spectrum management are key challenges that need to be addressed, particularly for resource-sharing scenarios, to satisfy the QoS/QoE requirements of the intended users. Therefore, the focus of this use case is to investigate the resource-sharing for D2D communication in cellular networks. Two scenarios are considered:

i. Energy-efficient D2D communication with cellular throughput maximisation (Chapter 3).
ii. Interference-aware resource allocation in a multi-tier HetNet with D2D links (Chapter 4).

2. Resource Allocation for D2D URLLC in Cellular Networks for Smart Wireless Environment

A typical application relating to this use case is a factory located within the coverage of a cellular network comprising of traditional cellular users and devices (sensors/actuators) as D2D users, aiming to reuse resources of the cellular users. The following techniques are developed and presented.

i. Joint admission and power control for a reliable D2D communication (Chapter 5).
ii. Autonomous channel selection using a learning-based approach for URLLC (Chapter 6).

Chapter 3
Energy-Efficient D2D Communication with Cellular Throughput Maximisation

As discussed in Chapter 2, energy and spectrum efficiency are major concerns for the deployment of 5G and beyond networks. Future networks will feature devices characterised by diverse QoS requirements. An example is the coexistence of high-data rate cellular services, such as high-definition video applications together D2D communication between factory sensors with low data rates and high-power saving requirements (in the case of frequent packet exchange for reduced latency).

Power control plays a crucial role in interference management and meeting the data rate demand of different users. Some of the works reported in the literature [105,108] focus on achieving higher Signal-to-Interference-Plus-Noise-Ratio (SINR) and in turn, higher data rates for users, even if a higher than needed SINR value has no practical effect on the QoS (e.g., low data rate applications such as voice) [124]. As opposed to QoS maximisation, the objective of achieving the minimum satisfactory QoS levels can provide several benefits such as [125]:

i. Reduced power consumption;
ii. Tighter fixed data rate service compliance;
iii. A good performance perception of QoE by users, as users are often insensitive to small changes in the level of QoS, thus, making allowance for power savings;
iv. Cost-effective solutions.

A Fixed-Target-SIR-Tracking Power Control (TPC) was proposed in [126] to allow each user to track its own predefined SIRs with the minimum possible transmit power. In [127], an extended-distributed TPC was adopted for joint power control and mode selection where a DUE selects its communication mode and adjusts it transmit power level such that the QoS of users are satisfied. However, there was no constraint on the transmit power of individual users.

In the following, an energy-efficient D2D communication scheme in a cellular network is presented, where CUEs and DUEs share Resource Blocks (RB) such that the QoS constraints of all users are satisfied. In this scenario, the CUEs have high data rate demands with the objective of throughput maximisation, whereas the DUEs aim at energy-efficiency

maximisation through power control. The resource allocation problem is formulated as a multi-objective Mixed-Integer Non-linear Programming (MINLP) optimisation problem which cannot be solved directly. To solve this optimisation problem, two heuristic algorithms with reduced computation complexity are developed and presented in the following sections. A Power-Rate Reduction Ratio (PRR) scheme is designed to maximise the energy-efficiency of the DUEs while guaranteeing the QoS requirement of the CUEs. This method is compared to the approach in which the DUEs adopt the TPC scheme to transmit at power levels sufficient to attain a satisfactory QoS.

3.1 System Model

The uplink transmission of a D2D-enabled cellular network with a BS, $\boldsymbol{N}$ CUEs and $\boldsymbol{M}$ DUEs is considered. Fig. 3.1 is an illustration of D2D communication in a cellular network. Resource sharing between CUEs and DUEs will cause co-channel interference from the D2D transmitter to the BS and from the CUE to the D2D receiver. The QoS requirements of the CUEs and DUEs must be satisfied before they can share the same channel. The CUEs, denoted by set $\boldsymbol{C} = \{\boldsymbol{c_1}, \boldsymbol{c_2}, \dots, \boldsymbol{c_N}\}$, have a high data rate demand and require a minimum SINR to guarantee their target data rates. The DUEs, denoted by set $\boldsymbol{D} = \{\boldsymbol{d_1}, \boldsymbol{d_2}, \dots, \boldsymbol{d_M}\}$, aim at achieving a high Energy-Efficiency (EE) through power control. D2D pairing is implemented during the proximal device discovery phase, which is out of the scope of this research work. Therefore, it is assumed that the D2D links have already been established. The total resource block in the uplink period is divided into $\boldsymbol{N}$ sub-channels denoted by set $\boldsymbol{K} = \{\boldsymbol{k_1}, \boldsymbol{k_2}, \dots, \boldsymbol{k_N}\}$ which is allocated to the CUEs.

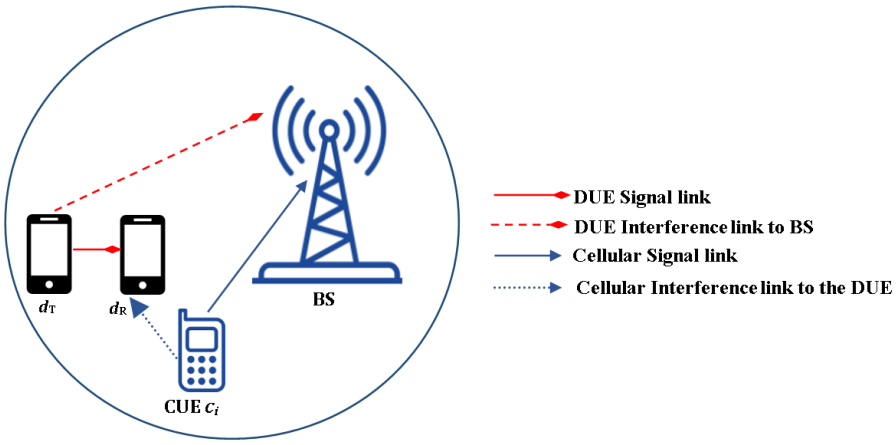

Fig. 3.1 An illustration of D2D communication in a cellular network

To reduce co-channel interference in a resource sharing scheme, a DUE can re-use the sub-channel of only one CUE and a CUE sub-channel can be re-used by one DUE. The BS or evolved NodeB (eNB) is assumed to have full instantaneous CSIs of all the users. The channel gain of the signal link, $\boldsymbol{h_{c,B}}$, between CUE $\boldsymbol{c_i}$ and the BS can be expressed as follows:

$$\boldsymbol{h_{c,B}} = \boldsymbol{G_k \chi_{c,B} L_{c,B}^{-\alpha_k}} \tag{3.1}$$

The channel gain is composed of pathloss with exponent $\boldsymbol{\alpha_k}$ and shadowing, which has a slow fading gain $\boldsymbol{\chi_{c,B}}$ with a log-normal distribution [128]. $\boldsymbol{L_{c,B}}$ is the distance from CUE $\boldsymbol{c_i}$ to the BS B and $\boldsymbol{G_k}$ denotes the pathloss constant, which depends on the frequency and antenna gains [65]. The channel gain of the interference link between CUE $\boldsymbol{c_i}$ and DUE receiver $\boldsymbol{d_R}$ is denoted by $\boldsymbol{h_{c,d_R}}$, between DUE transmitter $\boldsymbol{d_T}$ and the BS B by $\boldsymbol{h_{d_T,B}}$. The channel gain of the DUE link $\boldsymbol{d_j}$ and signal link between CUE $\boldsymbol{c_i}$ and the BS is denoted by $\boldsymbol{h_{d_T,d_R}}$ and $\boldsymbol{h_{c,B}}$ respectively. $\boldsymbol{\sigma_N^2}$ is the variance of the Additive White Gaussian Noise (AWGN) at the receiver. $\boldsymbol{\lambda_j^i} \in \{0,1\}$ is the resource-sharing index between the CUE and the DUE. $\boldsymbol{\lambda_j^i}$=1 if DUE $\boldsymbol{d_j}$ is assigned to CUE $\boldsymbol{c_i}$ subchannel and $\boldsymbol{\lambda_j^i}$= 0 otherwise. $\mathbf{P}_{\boldsymbol{c_i}}$ and $\mathbf{P}_{\boldsymbol{d_j}}$ denotes the transmit powers of the CUE $\boldsymbol{c_i}$ and DUE $\boldsymbol{d_j}$ respectively. The received SINR at the CUE receiver, and at the DUE receiver is denoted by $\boldsymbol{\Gamma_{c_i}}$ and $\boldsymbol{\Gamma_{d_j}}$ respectively and given by (3.2) and (3.3).

$$\boldsymbol{\Gamma_{c_i}} = \frac{\mathbf{P}_{\boldsymbol{c_i}} \boldsymbol{h_{c,B}}}{\boldsymbol{\lambda_j^i} \mathbf{P}_{\boldsymbol{d_j}} \boldsymbol{h_{d_T,B}} + \boldsymbol{\sigma_N^2}} \tag{3.2}$$

$$\boldsymbol{\Gamma_{d_j}} = \frac{\mathbf{P}_{\boldsymbol{d_j}} \boldsymbol{h_{d_T,d_R}}}{\boldsymbol{\lambda_j^i} \mathbf{P}_{\boldsymbol{c_i}} \boldsymbol{h_{c,d_R}} + \boldsymbol{\sigma_N^2}} \tag{3.3}$$

The total throughput of the CUEs is given as:

$$\mathbf{T_C} = \sum_{\boldsymbol{c_i} \in \boldsymbol{C}} \mathbf{W_i} \log_2\left(\mathbf{1} + \boldsymbol{\Gamma_{c_i}}\right) \tag{3.4}$$

The total EE (in b/s/Hz/W) of the DUEs is the ratio of the total DUE spectrum efficiency to the total power of the DUEs, and given by:

$$\mathbf{EE_D} = \sum\nolimits_{\boldsymbol{d_j} \in \boldsymbol{D}} \boldsymbol{\lambda_j^i} \left[\frac{\log_2(\mathbf{1} + \boldsymbol{\Gamma_{d_j}})}{\mathbf{P}_{\boldsymbol{d_j}}} \right] \tag{3.5}$$

The expression $\mathbf{log_2}\left(\mathbf{1}+\mathbf{\Gamma}_{\boldsymbol{d_j}}\right)$ is the spectrum efficiency (in b/s/Hz) of DUE $\boldsymbol{d_j} \in \boldsymbol{D}$ or the data rate normalised by the bandwidth $\mathbf{W_i}$ [129].

The resource allocation optimisation problem can be formulated as follows:

$$\mathbf{max}\ \mathbf{T_C} \tag{3.6}$$
$$\mathbf{max}\ \mathbf{EE_D}$$

subject to

$$\mathbf{\Gamma}_{\boldsymbol{c_i}} \geq \mathbf{\Gamma}_{\boldsymbol{c_i},\mathbf{min}} \quad \forall\, \boldsymbol{c_i} \in \boldsymbol{C} \tag{3.6a}$$
$$\mathbf{\Gamma}_{\boldsymbol{d_j}} \geq \mathbf{\Gamma}_{\boldsymbol{d_j},\mathbf{min}} \quad \forall\, \boldsymbol{d_j} \in \boldsymbol{D} \tag{3.6b}$$
$$\textstyle\sum_{\boldsymbol{c_i}\in\boldsymbol{C}} \boldsymbol{\lambda_j^i} \leq \mathbf{1} \quad \forall\, \boldsymbol{d_j} \in \boldsymbol{D} \tag{3.6c}$$
$$\textstyle\sum_{\boldsymbol{d_j}\in\boldsymbol{C}} \boldsymbol{\lambda_j^i} \leq \mathbf{1} \quad \forall\, \boldsymbol{c_i} \in \boldsymbol{C} \tag{3.6d}$$
$$\mathbf{P}_{\boldsymbol{c_i}} \leq \mathbf{P}_{\boldsymbol{c_i},\mathbf{max}} \quad \forall\, \boldsymbol{c_i} \in \boldsymbol{C} \tag{3.6e}$$
$$\mathbf{P}_{\boldsymbol{d_j}} \leq \mathbf{P}_{\boldsymbol{d_j},\mathbf{max}} \quad \forall\, \boldsymbol{d_j} \in \boldsymbol{D} \tag{3.6f}$$

The optimisation goal is to maximise the throughput of the CUEs and the EE of the DUEs. Constraints (3.6a) and (3.6b) set the SINR for CUEs and DUEs, respectively. $\mathbf{\Gamma}_{\boldsymbol{c_i},\mathbf{min}}$ and $\mathbf{\Gamma}_{\boldsymbol{d_j},\mathbf{min}}$ denote the minimum acceptable SINR for a CUE and DUE link respectively. Constraints (3.6c) - (3.6d) indicate channel association between a CUE and a DUE. With constraints (3.6e) and (3.6f), the maximum CUE transmit power is $\mathbf{P}_{\boldsymbol{c_i},\mathbf{max}}$, while $\mathbf{P}_{\boldsymbol{d_j},\mathbf{max}}$ is the maximum transmit power for DUE. The multi-objective optimisation problem is an MINLP which is a non-deterministic Polynomial (NP)-hard and cannot be solved directly.

To reduce the computation complexity, the problem is solved by setting the objective function to the maximisation of the QoS of 'one type' of user (e.g., CUEs) while maintaining QoS of the 'other type' of user (e.g., DUEs) as constraints and vice-versa. A heuristic channel assignment and power control algorithm is then developed to address the resulting optimisation problem.

In resource-sharing mode, the DUE transmitter $\boldsymbol{d_T}$ will interfere with the BS, while the CUE will interfere with the DUE receiver $\boldsymbol{d_R}$. To meet the QoS requirements as stated in (3.6), the minimum SINR for all the links must be satisfied. Since the objective of the CUEs is to maximise data rates, the transmit power is fixed to the maximum allowable value, $\mathbf{P}_{\boldsymbol{c_i},\mathbf{max}}$, while the transmit powers of the DUEs are controlled to achieve energy efficiency. Two

heuristic centralised algorithms are developed to address this problem. The first approach aims to maximise the CUE throughput while guaranteeing the QoS of the DUEs. The second approach aims to maximise the DUE energy efficiency, while satisfying the minimum performance requirement of the CUEs. The approach that provides better system utility, which is defined in terms of the CUE throughput, DUE EE and the number of admitted DUEs, is evaluated.

3.2 Fixed-Target SINR Tracking Power Control (TPC) for Cellular Throughput Maximisation

In this TPC approach, a DUE sets its power by tracking its SINR to meet a predefined minimum. With the CUE $\boldsymbol{c_i}$ transmit power set as $\mathbf{P}_{\boldsymbol{c_i},\mathbf{max}}$, the optimisation problem in (3.6) can be reformulated as (3.7). The optimisation problem (3.7) is set to maximise the CUE data rate, while attaining the minimum required SINR for the DUEs. With the TPC approach, the DUE $\boldsymbol{d_j}$ computes the transmit power $\mathbf{P}_{\boldsymbol{d_j},\mathbf{min}}$, defined in (3.8), on the subchannel of the CUE $\boldsymbol{c_i}$ that achieves $\boldsymbol{\Gamma}_{\boldsymbol{d_j},\mathbf{min}}$. $\mathbf{P}_{\boldsymbol{d_j},\mathbf{min}}$ is the minimum transmit power for DUE $\boldsymbol{d_j}$ to guarantee its target SINR; which implies CUE $\boldsymbol{c_i}$ can attain the highest possible throughput with $\mathbf{P}_{\boldsymbol{c_i},\mathbf{max}}$. The SINR value of CUE $\boldsymbol{c_i}$ resulting from sharing its resource DUE $\boldsymbol{d_j}$ can determined from equation (3.9).

$$\mathbf{max}\ \mathbf{T_C} = \sum_{\boldsymbol{c_i}\in\boldsymbol{C}} \mathbf{W_i}\ \mathbf{log_2}\left(\mathbf{1}+\boldsymbol{\Gamma}_{\boldsymbol{c_i}}\right) \tag{3.7}$$

subject to

$$\boldsymbol{\Gamma}_{\boldsymbol{c_i}} \geq \boldsymbol{\Gamma}_{\boldsymbol{c_i},\mathbf{min}} \qquad \forall\, \boldsymbol{c_i} \in \boldsymbol{C} \tag{3.7a}$$
$$\boldsymbol{\Gamma}_{\boldsymbol{d_j}} = \boldsymbol{\Gamma}_{\boldsymbol{d_j},\mathbf{min}} \qquad \forall\, \boldsymbol{d_j} \in \boldsymbol{D} \tag{3.7b}$$
$$\sum_{\boldsymbol{c_i}\in\boldsymbol{C}} \boldsymbol{\lambda_j^i} \leq \mathbf{1} \qquad \forall\, \boldsymbol{d_j} \in \boldsymbol{D} \tag{3.7c}$$
$$\sum_{\boldsymbol{d_j}\in\boldsymbol{C}} \boldsymbol{\lambda_j^i} \leq \mathbf{1} \qquad \forall\, \boldsymbol{c_i} \in \boldsymbol{C} \tag{3.7d}$$
$$\mathbf{P}_{\boldsymbol{c_i}} = \mathbf{P}_{\boldsymbol{c_i},\mathbf{max}} \qquad \forall\, \boldsymbol{c_i} \in \boldsymbol{C} \tag{3.7e}$$
$$\mathbf{P}_{\boldsymbol{d_j}} \leq \mathbf{P}_{\boldsymbol{d_j},\mathbf{max}} \qquad \forall\, \boldsymbol{d_j} \in \boldsymbol{D} \tag{3.7f}$$

$$\mathbf{P}_{\boldsymbol{d_j},\mathbf{min}} = \mathbf{min}\left\{ \frac{\boldsymbol{\Gamma}_{\boldsymbol{d_j},\mathbf{min}}\left(\mathbf{P}_{\boldsymbol{c_i},\mathbf{max}}\, \boldsymbol{h}_{\boldsymbol{c},\boldsymbol{d_R}} + \boldsymbol{\sigma}_{\boldsymbol{N}}^{\mathbf{2}}\right)}{\boldsymbol{h}_{\boldsymbol{d_T},\boldsymbol{d_R}}},\ \mathbf{P}_{\boldsymbol{d_j},\mathbf{max}} \right\} \tag{3.8}$$

$$\boldsymbol{\Gamma}_{\boldsymbol{c_i}}^{*} = \frac{\mathbf{P}_{\boldsymbol{c_i},\mathbf{max}}\, \boldsymbol{h}_{\boldsymbol{c},\boldsymbol{B}}}{\mathbf{P}_{\boldsymbol{d_j},\mathbf{min}} \boldsymbol{h}_{\boldsymbol{d_T},\boldsymbol{B}} + \boldsymbol{\sigma}_{\boldsymbol{N}}^{\mathbf{2}}} \tag{3.9}$$

DUE $\boldsymbol{d_j}$ is a potential reuse partner for CUE $\boldsymbol{c_i}$ if $\boldsymbol{\Gamma^*_{c_i}} \geq \boldsymbol{\Gamma_{c_i,\min}}$. For CUEs with more than one potential re-use partners, the optimal re-use partner for CUE $\boldsymbol{c_i}$ is the DUE $\boldsymbol{d_j^*}$ that maximises CUE's rate as follows:

$$\boldsymbol{d_j^*} = \underset{\boldsymbol{d_j} \in \boldsymbol{R^d_{c_i}}}{\mathbf{argmax}} \left(\mathbf{W}_i \mathbf{log_2}\left(\mathbf{1} + \boldsymbol{\Gamma^*_{c_i}}\right)\right) \tag{3.10}$$

where $\boldsymbol{R^d_{c_i}}$ is the set of potential DUE reuse partners for CUE $\boldsymbol{c_i}$. The TPC resource allocation scheme is set out in Algorithm 3.1.

Algorithm 3.1. The TPC Algorithm

1: Input $\boldsymbol{C}$ and $\boldsymbol{D}$ as sets of CUEs and DUEs respectively. $\mathbf{P}_{\boldsymbol{c_i},\mathbf{max}}$ and $\mathbf{P}_{\boldsymbol{d_j},\mathbf{max}}$ are the maximum transmit powers of the CUEs and DUEs. The CUEs are pre-allocated a channel each, the DUEs are waiting to be assigned a CUE subchannel;
2: for $\boldsymbol{c_i} \in \boldsymbol{C}$ $1 \leq \boldsymbol{i} \leq \boldsymbol{N}$ do
3: Set up $\boldsymbol{R^d_{c_i}}$ as set of potential CUE reuse partners for $\boldsymbol{d_j}$;
4: for $\boldsymbol{d_j} \in \boldsymbol{D}$ do
5: compute $\mathbf{P}_{\boldsymbol{d_j},\mathbf{min}}$ according to (3.8)
if $\boldsymbol{\Gamma_{d_j}} \geq \boldsymbol{\Gamma_{d_j,\min}}$ then
6: compute $\boldsymbol{\Gamma^*_c}$ with $\mathbf{P}_{\boldsymbol{d_j},\mathbf{min}}$ according to (3.9)
7: if $\boldsymbol{\Gamma^*_c} \geq \boldsymbol{\Gamma_{c_i,\min}}$ then
8: $\boldsymbol{R^d_{c_i}} = \boldsymbol{R^d_{c_i}} + \boldsymbol{d_j}$
9: end if
10: end if
11: end for
12: if $\boldsymbol{R^d_{c_i}} \neq \emptyset$ then
13: obtain optimal re-use partner $\boldsymbol{d_j^*}$, for $\boldsymbol{c_i}$ according to (3.10);
14: $\boldsymbol{D} = \boldsymbol{D} - \boldsymbol{d_j^*}$;
15: end if
16: end for

3.3 Power-Rate Reduction Ratio (PRR) Scheme for D2D Energy Efficiency Maximisation

The TPC scheme discussed in the previous section can achieve throughput maximisation for the CUEs and a high-power saving for the DUEs, but EE for the DUEs may not be optimal. This is because transmitting at $\mathbf{P}_{\boldsymbol{d_j},\mathbf{min}}$ (minimum power of DUE $\boldsymbol{d_j}$ to guarantee its QoS) only satisfies the best effort throughput for the DUEs. The disadvantage of this approach is that additional transmit power resources that may be used to achieve a higher rate and perhaps a better energy efficiency are unused and made redundant.

To address this, a PRR scheme is presented, which aims to maximise the EE of DUE while guaranteeing the minimum QoS of the CUE. Therefore, the optimisation problem in (3.6) is reformulated as (3.11). The transmit power of the CUE is set to $\mathbf{P}_{c_i,\max}$ to optimise the achieved rate of the CUE (i.e., ensure the CUEs achieve the highest throughput possible) while maximising the EE of the DUEs.

$$\max \mathbf{EE}_{D} = \sum_{d_j \in D} \boldsymbol{\lambda}_j^i \left[\frac{\log_2\left(1+\Gamma_{d_j}\right)}{\mathrm{P}_{d_j}} \right] \tag{3.11}$$

subject to

$$\boldsymbol{\Gamma}_{c_i} \geq \boldsymbol{\Gamma}_{c_i,\min} \qquad \forall\, \boldsymbol{c_i} \in \boldsymbol{C} \tag{3.11a}$$
$$\boldsymbol{\Gamma}_{d_j} \geq \boldsymbol{\Gamma}_{d_j,\min} \qquad \forall\, \boldsymbol{d_j} \in \boldsymbol{D} \tag{3.11b}$$
$$\sum_{c_i \in C} \boldsymbol{\lambda}_j^i \leq 1 \qquad \forall\, \boldsymbol{d_j} \in \boldsymbol{D} \tag{3.11c}$$
$$\sum_{d_j \in C} \boldsymbol{\lambda}_j^i \leq 1 \qquad \forall\, \boldsymbol{c_i} \in \boldsymbol{C} \tag{3.11d}$$
$$\mathbf{P}_{c_i} = \mathbf{P}_{c_i,\max} \qquad \forall\, \boldsymbol{c_i} \in \boldsymbol{C} \tag{3.11e}$$
$$\mathbf{P}_{d_j} \leq \mathbf{P}_{d_j,\max} \qquad \forall\, \boldsymbol{d_j} \in \boldsymbol{D} \tag{3.11f}$$

The TPC scheme is adopted to obtain $\mathbf{P}_{d_j,\min}$, as in (3.8) and $\mathbf{R}_{d_j,\min}$ is the achieved data rate of DUE $\boldsymbol{d_j}$ for transmitting with $\mathbf{P}_{d_j,\min}$ and expressed in (3.12).

$$\mathbf{R}_{d_j,\min} = \mathbf{W}_i \log_2 \left(1 + \frac{\mathrm{P}_{d_j,\min} h_{d_T,d_R}}{\mathrm{P}_{c_i,\max} h_{c,d_R} + \sigma_N^2} \right) \tag{3.12}$$

Next, the transmit power of DUE $\boldsymbol{d_j}$ for which its data rate is maximum, while satisfying the QoS of the DUE and CUE, is obtained from the optimisation problem in (3.13).

$$\mathbf{P}^*_{d_j,\max} = \underset{\left\{\mathrm{P}_{d_j,\min} \leq \mathrm{P}_{d_j} \leq \mathrm{P}_{d_j,\max}\right\}}{\mathbf{argmax}} \left[\mathbf{W}_i \log_2 \left(1 + \frac{\mathrm{P}_{d_j} h_{d_T,d_R}}{\mathrm{P}_{c_i,\max} h_{c,d_R} + \sigma_N^2} \right) \right] \tag{3.13}$$

subject to

$$\boldsymbol{\Gamma}_{c_i} \geq \boldsymbol{\Gamma}_{c_i,\min} \tag{3.13a}$$
$$\boldsymbol{\Gamma}_{d_j} \geq \boldsymbol{\Gamma}_{d_j,\min} \tag{3.13b}$$

The data rate of DUE $\boldsymbol{d_j}$ from $\mathbf{P}^*_{d_j,\max}$ is given in (3.14)

$$\mathbf{R}^*_{d_j,\max} = \mathbf{W}_i \log_2 \left(1 + \frac{\mathrm{P}^*_{d_j,\max} h_{d_T,d_R}}{\mathrm{P}_{c_i,\max} h_{c,d_R} + \sigma_N^2} \right) \tag{3.14}$$

Therefore, the feasible power bound of the DUE that satisfies the minimum QoS of CUE $\boldsymbol{c_i} \in \boldsymbol{C}$ and DUE $\boldsymbol{d_j} \in \boldsymbol{D}$ is $\mathbf{P}_{d_j,\min} \leq \mathbf{P}_{d_j} \leq \mathbf{P}^*_{d_j,\max}$, while $\mathbf{P}_{c_i} = \mathbf{P}_{c_i,\max}$. From (3.5), intuitively, a high $\log_2 \left(1 + \frac{\mathrm{P}_{d_j} h_{d_T,d_R}}{\mathrm{P}_{c_i,\max} h_{c,d_R} + \sigma_N^2} \right)$ and low $\mathbf{P}_{d_j}$ means a high $\mathbf{EE}_D$. An optimal transmit power

$\mathbf{P}_{d_j}^{\mathbf{opt}}$ is desired, for which the reduction ratio from $\mathbf{P}_{d_j,\mathbf{max}}^{*}$ to $\mathbf{P}_{d_j}$ is higher than the reduction ratio of the corresponding data rate from $\mathbf{R}_{d_j,\mathbf{max}}^{*}$ to $\mathbf{R}_{d_j}$. $\mathbf{P}_{d_j}^{\mathbf{opt}}$power that maximises the energy efficiency of DUE $\boldsymbol{d_j}$ and given in (3.15).

$$\mathbf{P}_{d_j}^{\mathbf{opt}} = \underset{\left\{\mathbf{P}_{d_j,\mathbf{min}} \le \mathbf{P}_{d_j} \le \mathbf{P}_{d_j,\mathbf{max}}^{*}\right\}}{\mathbf{argmax}} \left[\frac{\mathbf{P}_{d_j,\mathbf{max}}^{*} - \mathbf{P}_{d_j}}{\mathbf{P}_{d_j,\mathbf{max}}^{*}} - \frac{\mathbf{R}_{d_j,\mathbf{max}}^{*} - \mathbf{R}_{d_j}}{\mathbf{R}_{d_j,\mathbf{max}}^{*}}\right] \tag{3.15}$$

where

$$\mathbf{R}_{d_j} = \mathbf{W_i}\mathbf{log_2}\left(\mathbf{1} + \frac{\mathbf{P}_{d_j} g_{d_T,d_R}}{\mathbf{P}_{c_i,\mathbf{max}} h_{c_i,d_R} + \sigma_N^2}\right) \tag{3.16}$$

Equation (3.15) implies that $\mathbf{P}_{d_j}^{\mathbf{opt}}$ will have the least corresponding impact on $\mathbf{R}_{d_j,\mathbf{max}}^{*}$ when DUE transmit power is reduced from $\mathbf{P}_{d_j,\mathbf{max}}^{*}$. Denote $\mathbf{EE}_{d_j}^{*}$ as the EE of $\boldsymbol{d_j}$ for power level $\mathbf{P}_{d_j,\mathbf{max}}^{*}$ and $\mathbf{EE}_{d_j}^{\mathbf{opt}}$ be the optimal EE for reducing $\mathbf{P}_{d_j,\mathbf{max}}^{*}$ to $\mathbf{P}_{d_j}^{\mathbf{opt}}$, it follows that:

$$\mathbf{EE}_{d_j}^{*} = \boldsymbol{f}\left(\mathbf{P}_{d_j,\mathbf{max}}^{*}\right) \triangleq \frac{\mathbf{log_2}\left(1 + \frac{\mathbf{P}_{d_j,\mathbf{max}}^{*} h_{d_T,d_R}}{\mathbf{P}_{c_i,\mathbf{max}} h_{c,d_R} + \sigma_N^2}\right)}{\mathbf{P}_{d_j,\mathbf{max}}^{*}} = \frac{\mathbf{R}_{d_j,\mathbf{max}}^{*} / \mathbf{W_i}}{\mathbf{P}_{d_j,\mathbf{max}}^{*}} \tag{3.17}$$

$$\mathbf{EE}_{d_j}^{\mathbf{opt}} = \boldsymbol{f}\left(\mathbf{P}_{d_j}^{\mathbf{opt}}\right) \triangleq \frac{\mathbf{log_2}\left(1 + \frac{\mathbf{P}_{d_j}^{\mathbf{opt}} h_{d_T,d_R}}{\mathbf{P}_{c_i,\mathbf{max}} h_{c,d_R} + \sigma_N^2}\right)}{\mathbf{P}_{d_j}^{\mathbf{opt}}} = \frac{\mathbf{R}_{d_j}^{*} / \mathbf{W_i}}{\mathbf{P}_{d_j}^{\mathbf{opt}}} \tag{3.18}$$

The reduction ratios are given by:

$$\boldsymbol{\sigma_P} = \frac{\mathbf{P}_{d_j,\mathbf{max}}^{*} - \mathbf{P}_{d_j}^{\mathbf{opt}}}{\mathbf{P}_{d_j,\mathbf{max}}^{*}} \tag{3.19a}$$

$$\boldsymbol{\sigma_R} = \frac{\mathbf{R}_{d_j,\mathbf{max}}^{*} - \mathbf{R}_{d_j}^{*}}{\mathbf{R}_{d_j,\mathbf{max}}^{*}} \tag{3.19b}$$

For $\mathbf{P}_{d_j}^{\mathbf{opt}}$ to be the optimal EE, $\boldsymbol{\sigma_P} > \boldsymbol{\sigma_R}$ as in (3.15). Denote $\boldsymbol{\sigma_D}$ as difference of the reduction ratios given by:

$$\boldsymbol{\sigma_D} = \boldsymbol{\sigma_P} - \boldsymbol{\sigma_R} \tag{3.20}$$

$$\mathbf{EE}_{d_j}^{\mathbf{opt}} = \frac{\mathbf{R}_{d_j}^{*} / \mathbf{W_i}}{\mathbf{P}_{d_j}^{\mathbf{opt}}} = \frac{\frac{\mathbf{R}_{d_j,\mathbf{max}}^{*}}{\mathbf{W_i}}(\mathbf{1} - \boldsymbol{\sigma_R})}{\mathbf{P}_{d_j,\mathbf{max}}^{*}(\mathbf{1} - \boldsymbol{\sigma_P})} = \mathbf{EE}_{d_j}^{*}\left(\frac{\mathbf{1} - \boldsymbol{\sigma_P} + \boldsymbol{\sigma_D}}{\mathbf{1} - \boldsymbol{\sigma_P}}\right) \tag{3.21}$$

$$\mathbf{EE}_{d_j}^{\mathbf{opt}} = \mathbf{EE}_{d_j}^{*}(\mathbf{1} + \boldsymbol{\sigma_D}) \tag{3.22}$$

Therefore, if the transmit power of DUE $\boldsymbol{d_j} \in \boldsymbol{D}$ is reduced from $\mathbf{P}_{d_j,\mathbf{max}}^{*}$ to $\mathbf{P}_{d_j}^{\mathbf{opt}}$ (i.e., reduced by $\frac{\mathbf{1}}{\mathbf{1}-(\boldsymbol{\sigma_D}+\boldsymbol{\sigma_R})}$, the EE is increased by (1+$\boldsymbol{\sigma_D}$).

Algorithm 3.2 presents the PRR scheme in detail.

Algorithm 3.2 The PRR Algorithm

Input $\boldsymbol{C}$ and $\boldsymbol{D}$ as sets of CUEs and DUEs respectively. $\mathbf{P}_{c_i,\mathbf{max}}$ and $\mathbf{P}_{d_j,\mathbf{max}}$ are the maximum transmit powers of the CUEs and DUEs. The CUEs are pre-allocated a channel each, the DUEs are waiting to be assigned a CUE subchannel;
for $\boldsymbol{c_i} \in \boldsymbol{C}$ $1 \leq \boldsymbol{i} \leq \boldsymbol{N}$ do
    Set up $\boldsymbol{R}_{c_i}^{\boldsymbol{d}}$ as set of potential DUE $\boldsymbol{d_j}$reuse partner for $\boldsymbol{c_i}$;
    for $\boldsymbol{d_j} \in \boldsymbol{D}$ do
        compute $\mathbf{P}_{d_j,\mathbf{min}}$ according to (3.8)
        if $\boldsymbol{\Gamma}_{d_j} \geq \boldsymbol{\Gamma}_{d_j,\mathbf{min}}$ then
            compute $\boldsymbol{\Gamma}_{c}^{*}$ with $\mathbf{P}_{d_j,\mathbf{min}}$ according to (3.9)
            if $\boldsymbol{\Gamma}_{c}^{*} \geq \boldsymbol{\Gamma}_{c_i,\mathbf{min}}$ then
                compute $\mathbf{R}_{d_j,\mathbf{min}}$ according to (3.12)
                compute $\mathbf{P}_{d_j,\mathbf{max}}^{*}$ and $\mathbf{R}_{d_j,\mathbf{max}}^{*}$ according (3.13) and (3.14) respectively
                compute $\mathbf{P}_{d_j}^{*}$ according to (3.15)
                $\boldsymbol{R}_{c_i}^{\boldsymbol{d}} = \boldsymbol{R}_{c_i}^{\boldsymbol{d}} + \boldsymbol{d_j}$
            end if
        end if
    end for
    if $\boldsymbol{R}_{c_i}^{\boldsymbol{d}} \neq \emptyset$ then
        obtain optimal re-use partner for $\boldsymbol{c_i}$, $\boldsymbol{d_j^*} = \underset{\boldsymbol{d_j} \in \boldsymbol{R}_{c_i}^{\boldsymbol{d}}}{\mathbf{argmax}} \left[\mathbf{W}_i \log_2 \left(1 + \frac{\mathbf{P}_{c_i,\mathbf{max}} h_{c,B}}{\mathbf{P}_{d_j}^{*} h_{d_T,B} + \sigma_N^2} \right) \right]$
        $\boldsymbol{D} = \boldsymbol{D} - \boldsymbol{d_j^*}$;
    end if
end for

3.4 Simulation Case Study and Analysis

In this section, example simulations are presented to validate the presented algorithms. The uplink of a single-cell network is considered, with a radius of 400m. The CUEs and DUEs are randomly distributed within the coverage of the BS. The main simulation parameters are shown in Table 3.1 and as guided by LTE-A and 5G-NR standards.

To evaluate the performances of the TPC and PRR schemes, the results are compared to a scheme, Pmax, where the active UEs transmit at maximum power i.e., no power optimisation was adopted. The same power values are used for the CUEs and DUEs, i.e., $\mathbf{P}_{c_i,\mathbf{max}} = \mathbf{P}_{d_j,\mathbf{max}}$ to demonstrate the effect of power control. The number of DUE $\boldsymbol{M} = \mathbf{20}$ and $\boldsymbol{N}$ is varied from $\mathbf{25}\%$ to $\mathbf{100}\%$ of $\boldsymbol{M}$. Firstly, the performances of the three schemes are compared in terms of the number of admitted DUEs, $\boldsymbol{D_m}$, which is the number of DUEs that have been assigned to share or reuse CUE channels such that the QoS of the CUE-DUE match is not violated.

Table 3.1: Main simulation parameters for the TPC and PRR algorithms [127,129-131]

Parameter	Value
Carrier frequency, $\boldsymbol{f_c}$	$\mathbf{2GHz}$
RB bandwidth, $\mathbf{W_i}$	$\mathbf{180\ kHz}$
Maximum CUE transmit power, $\mathbf{P}_{c_i,\mathbf{max}}$	$\mathbf{23dBm}$
Maximum DUE transmit power, $\mathbf{P}_{d_j,\mathbf{max}}$	$\mathbf{23dBm}$
Maximum D2D distance, $\boldsymbol{L}_{d_T,d_R}$	50m
CUE SINR Threshold, $\boldsymbol{\Gamma}_{c_i,\mathbf{min}}$	20 dB
DUE SINR Threshold, $\boldsymbol{\Gamma}_{d_j,\mathbf{min}}$	20 dB
Noise power density	$-\mathbf{174}\frac{\mathbf{dBm}}{\mathbf{Hz}}$
UE-UE Pathloss	$\mathbf{28.03 + 40log10(d[m])}$ dB
BS-UE Pathloss	$\mathbf{15.3 + 37.6log10(d[m])}$ dB
BS-UE Shadowing standard deviation	$\mathbf{8}$dB
UE-UE Shadowing standard deviation	$\mathbf{6}$dB

It can be concluded from Fig. 3.2 that the number of admitted DUEs increases with $\boldsymbol{N}$ because more CUE-DUE partnerships are established as more $\boldsymbol{N}$ is introduced into the system. The Pmax method shows the least number of admitted DUEs $\boldsymbol{D_m}$, as expected. This is because the active UEs are transmitting at maximum powers and no power control is implemented to mitigate interference when the QoS requirements of the CUEs/DUEs are not met. The TPC method performed slightly better than the PRR method particularly at $\boldsymbol{N} > \mathbf{15}$, showing up to

$\mathbf{6.67}\%$ higher in $\boldsymbol{D_m}$. This can be attributed to the fact that the DUEs only aim to achieve their minimum target SINR and transmit at the lowest possible powers.

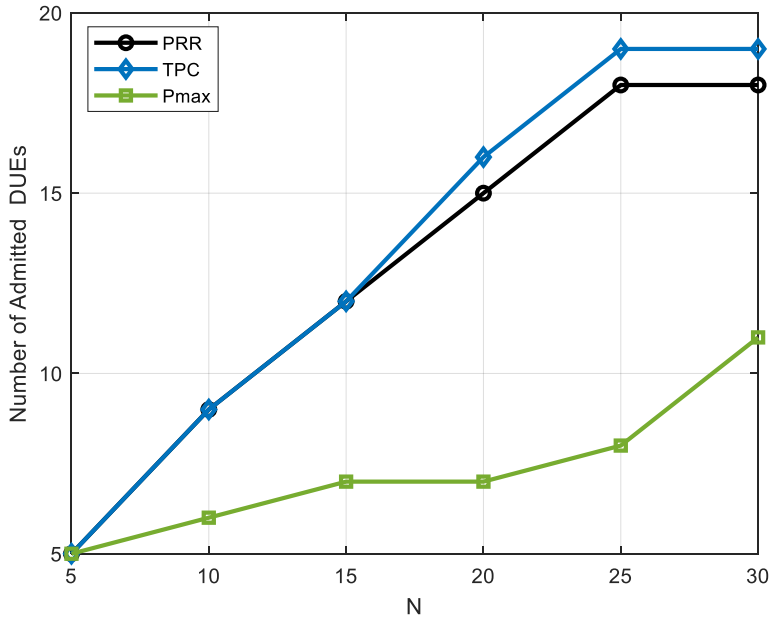

Fig. 3.2. The number of admitted DUEs, $\boldsymbol{D_m}$ varying the number of CUEs, $\boldsymbol{N}$ in the network where $\boldsymbol{M = 20}$, $\mathbf{P}_{c_i,\mathbf{max}} = \mathbf{P}_{c_i,\mathbf{max}} = \mathbf{23dBm}$

A plot of the total CUE throughput is shown in Fig. 3.3. Expectedly, the throughput of the CUEs $\mathbf{T_C}$, increases with $\boldsymbol{N}$ for all considered algorithms. The Pmax scheme has the worst performance because no optimisation is implemented. Since the active UEs are transmitting at their maximum powers, the effect of interference is higher compared to other approaches. TPC shows the best CUE throughput performance with up to $\mathbf{18.57}\%$ higher throughput than PRR. This is because the impact of interference generated by the DUEs to CUEs is low; the DUEs transmit at powers sufficient just to achieve $\boldsymbol{\Gamma_{d_j,\mathbf{min}}}$. Therefore, a CUE can attain a high throughput, while a DUE can simultaneously achieve a low power consumption for a CUE-DUE pairing, which may not be necessarily optimal in terms of energy efficiency for the DUE as can be seen in Fig. 3.5.

The total power consumption by the DUEs is shown in Fig. 3.4. The Pmax scheme shows the highest power as expected. The PRR algorithm shows the least power consumption with up to $\mathbf{49.39}\%$ reduction transmit power compared to the TPC scheme. This is because the PRR scheme tries to optimise power relative to the achieved rate which results in different matchings by the PRR and TPC algorithms.

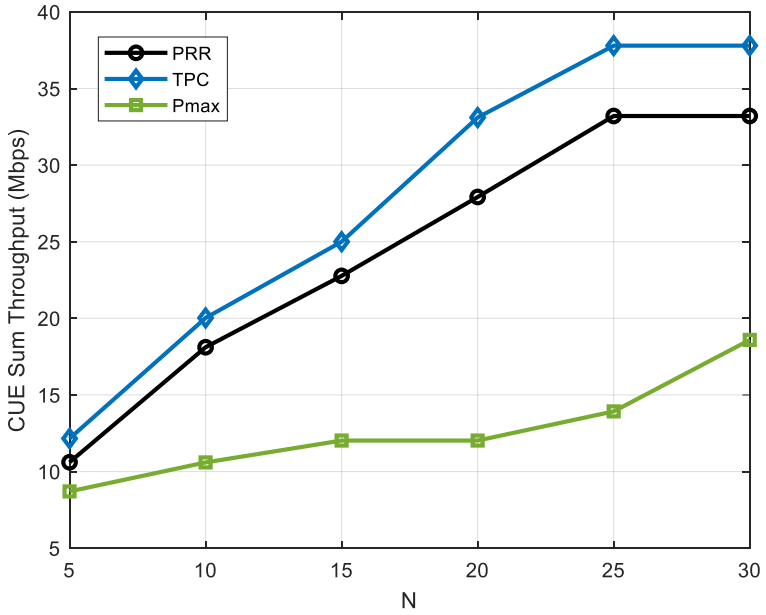

Fig. 3.3. Sum-throughput of the cellular users with respect to the number of CUEs, $\boldsymbol{N}$ in the network where $\boldsymbol{M = 20}$

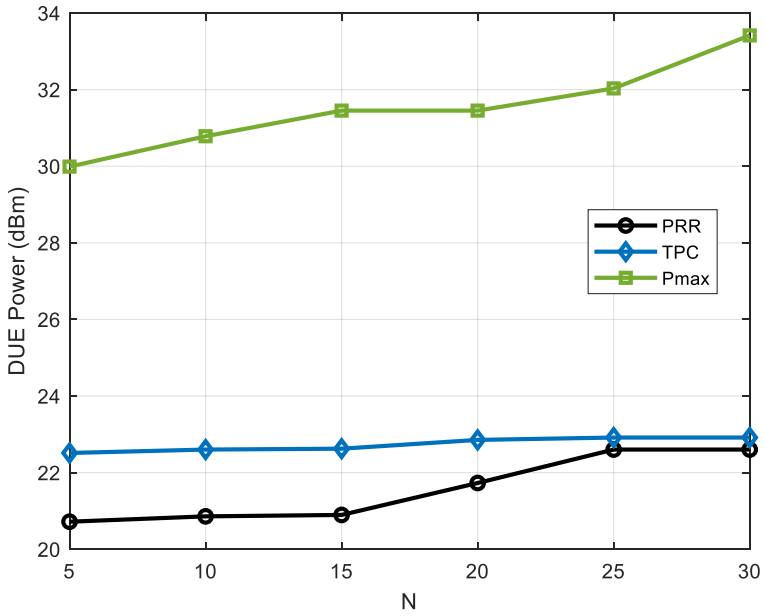

Fig. 3.4. Total power consumed by the DUE with respect to the number of CUEs, $\boldsymbol{N}$ in the network where $\boldsymbol{M = 20}$

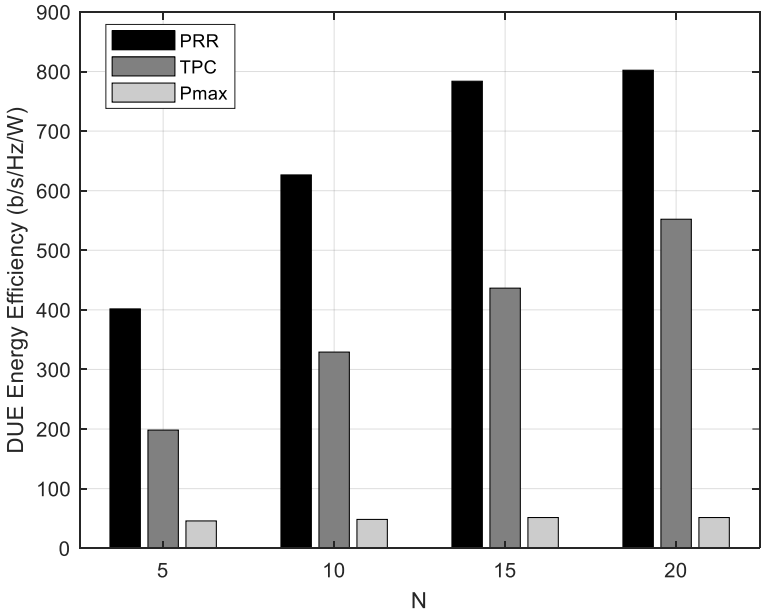

Fig. 3.5. Energy efficiency of admitted DUEs, $\boldsymbol{D_m}$ varying the number of CUEs, $\boldsymbol{N}$ in the network where $\boldsymbol{M = 20}$

The EE of the DUEs is shown in Fig. 3.5. The Pmax scheme performed worst, as there is no EE optimisation objective in the resource allocation. The PRR technique shows up to $\boldsymbol{102.62\%}$ improvement in EE at $\boldsymbol{N = 5}$ in particular, compared to the TPC approach. This is because the PRR algorithm targets a DUE transmit power $\mathbf{P}_{\boldsymbol{d_j}}$ that results in where the power reduction ratio is higher than the corresponding rate reduction ratio.

The objective function of the TPC algorithm is centred on CUE throughput maximisation, while guaranteeing the QoS constraints of the DUEs, whereas the objective function of the PRR scheme is focused on maximising the EE of the DUEs, while satisfying the QoS requirements of the CUEs. The best method is determined by evaluating a system utility metric $\boldsymbol{S_u}$, which is a unitless metric and defined as the weighted sum of the total CUE throughput, DUE energy efficiency and the number of admitted DUEs. The min-max scaling [132] is used to normalise the parameters of the system utility expressed as:

$$\boldsymbol{S_u}=\mathbf{T_C} + \boldsymbol{EE_D} + \boldsymbol{D_m} \tag{3.17}$$

As seen in Fig. 3.6., the system utility of the PRR technique shows resulting in a better satisfaction of the system objectives compared to TPC and Pmax. The Pmax scheme, where no

power optimisation is done shows a consistent worst performance for all the considered metrics and expectedly, in terms of system utility.

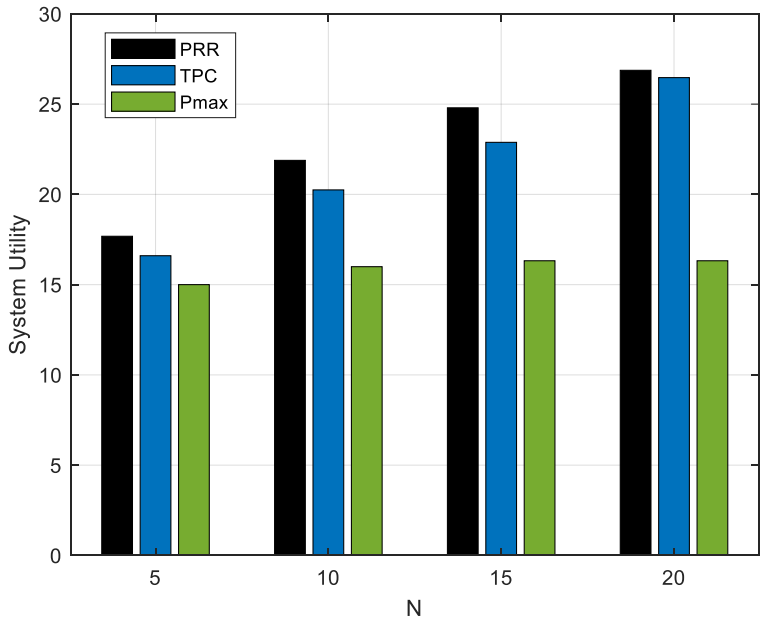

Fig. 3.6. System utility with respect to the number of CUEs, $\boldsymbol{N}$ in the network and where $\boldsymbol{M = 20}$

3.5 Chapter Conclusions

Resource-efficient algorithms were presented for the coexistence of D2D users with cellular user in a single-cell scenario. The joint optimisation of CUE throughput and DUE energy efficiency was considered. A fixed-target SINR TPC scheme was presented that allows a DUE to select a CUE subchannel for resource-sharing if the DUE target SINR is achieved, while satisfying the QoS of the CUE. The TPC algorithm is able to achieve high CUE throughput and a high-power saving for the DUE which may not be necessarily energy-efficient because the DUE transmits with the minimum possible power. To address this, the PRR scheme was presented, where a DUE selects a power level with a higher reduction ratio compared to the corresponding reduction ratio of the data rate. The simulation results show the PRR algorithm offers a better system utility compared to the TPC and Pmax schemes. The PRR and TPC adopt a separate optimisation approach in which system objectives are optimised independently, producing low-complexity solutions. Joint optimisation of the resource allocation problem could be a promising way to extend this work. While this approach may offer a more optimal solution as it considers the interactions between system objectives and variables, it could also be more complex and computationally demanding.

Chapter 4

Interference-Aware Resource Allocation in Multi-Tier Heterogeneous Networks (HetNet)

Resource allocation for a D2D-enabled cellular network with diverse QoS requirements, where the CUEs and DUEs have conflicting objectives, was considered in Chapter 3. In this chapter, resource allocation of D2D users in a multi-tier Heterogeneous Network (HetNet) where D2D and femtocells users are to share cellular resources, is investigated.

Cellular service providers are able to mitigate problems such as poor indoor coverage and low data rates at edge of the cell, by allowing users to connect to the cellular network, via a femtocell, which is a small cell base station [20]. The integration of femtocells into a larger network, called a macrocell, forms a two-tier Heterogeneous Network (HetNet) [116].

This structure has the potential of increasing the network capacity but will also increase the demand for spectrum resources. Furthermore, co-channel use among the macro-cell and femto-cells may result in cross-tier interference. The introduction of D2D communication in such a multi-tier network can increase the overall network throughput, however, interference becomes more challenging when D2D and femtocell users have to reuse the macro-cell resources. Therefore, efficient interference management is crucial, in order to satisfy the QoS/QoE demands of users for D2D-enabled multi-tier HetNet. In this chapter, an interference aware resource-efficient allocation scheme is developed and presented to solve the optimisation problem of maximising network throughput with the constraints of guaranteeing the minimum QoS requirements of all users.

4.1 System Model

The uplink of a typical D2D-enabled multi-tier HetNet is considered as illustrated in Fig. 4.1. The network comprises D2D communication, and a set of femtocell base stations (FBS) denoted by a set $\boldsymbol{H} = \{\boldsymbol{h_1}, \boldsymbol{h_2}, \dots, \boldsymbol{h_P}\}$ deployed under the coverage of a macro-cell base station (MBS). The set of $\boldsymbol{N}$ CUEs is denoted by $\boldsymbol{C} = \{\boldsymbol{c_1}, \dots, \boldsymbol{c_i}, \dots, \boldsymbol{c_N}\}$, the set of $\boldsymbol{M}$ DUEs is denoted by $\boldsymbol{D} = \{\boldsymbol{d_1}, \dots, \boldsymbol{d_j}, \dots, \boldsymbol{d_M}\}$ and the set of $\boldsymbol{L}$ FUEs denoted by $\boldsymbol{F} = \{\boldsymbol{f_1}, \dots, \boldsymbol{f_k}, \dots, \boldsymbol{f_L}\}$. The DUEs and FUEs are to coexists and reuse the same cellular uplink, allowing for a maximum of three

users per channel. It is assumed that the CSI of the communication links are available at the MBS.

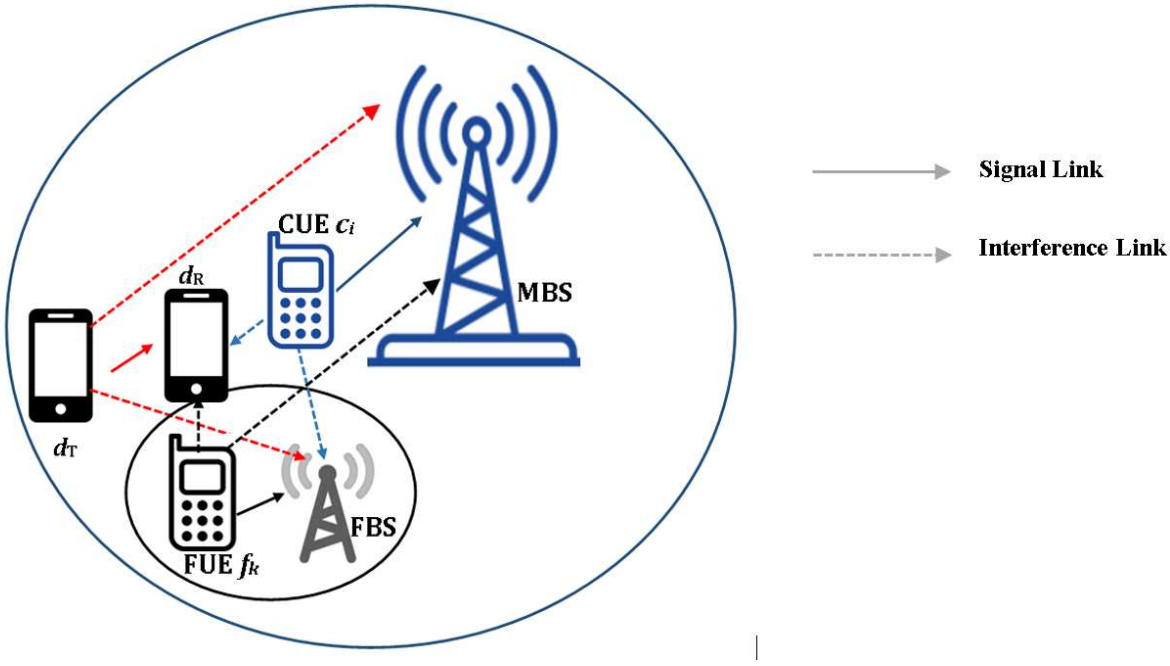

Fig. 4.1. An illustration of a D2D-enabled cellular two-tier HetNet

The channel gain is due to pathloss and shadowing as presented in Chapter 3. The signal channel gain from CUE $\boldsymbol{c_i}$ to the MBS, from DUE transmitter $\boldsymbol{d_T}$ to its receiver $\boldsymbol{d_R}$, from FUE transmitter $\boldsymbol{f_T}$ to FUE receiver $\boldsymbol{f_R}$ (i.e., the FBS) is represented by $\boldsymbol{h_{c,B}}$, $\boldsymbol{h_{d_T,d_R}}$, and $\boldsymbol{h_{f_T,f_R}}$, respectively. The interference caused to the Macro Base Station (MBS) is generated by the DUE transmitter $\boldsymbol{d_T}$ and FUE transmitter $\boldsymbol{f_T}$, and the interference gains of the links is signified by $\boldsymbol{h_{d_T,B}}$ and $\boldsymbol{h_{f_T,B}}$, respectively.

Let $\boldsymbol{h_{c,d_R}}$ and $\boldsymbol{h_{f_T,d_R}}$ represent the interference gains of the links from the CUE $\boldsymbol{c_i}$ and the FUE transmitter to the DUE receiver, respectively. The interference gains of the links from the CUE $\boldsymbol{c_i}$ and the DUE transmitter to FUE receiver are denoted by $\boldsymbol{h_{c,f_R}}$ and $\boldsymbol{h_{d_T,f_R}}$, respectively. CUEs, DUEs and FUEs are considered to be using the same on the same channel. The received SINR of the CUE $\boldsymbol{c_i}$, DUE $\boldsymbol{d_j}$ and FUE $\boldsymbol{f_k}$ are denoted by $\boldsymbol{\Gamma_{c_i}}$, $\boldsymbol{\Gamma_{d_j}}$ and $\boldsymbol{\Gamma_{f_k}}$, respectively and are given by (4.1).

$$\boldsymbol{\Gamma_{c_i}} = \frac{\mathbf{P}_{c_i} h_{c,B}}{\sum_{d_j \in D} \boldsymbol{\lambda}_j^i \mathbf{P}_{d_j} h_{d_T,B} + \sum_{f_k \in F} \boldsymbol{\lambda}_k^i \mathbf{P}_{f_k} h_{f_T,B} + \boldsymbol{\sigma}_N^2} \tag{4.1a}$$

$$\boldsymbol{\Gamma_{d_j}} = \frac{\mathbf{P}_{d_j} h_{d_T,d_R}}{\sum_{c_i \in C} \boldsymbol{\lambda}_j^i \mathbf{P}_{c_i} h_{c,d_R} + \sum_{f_k \in F} \boldsymbol{\lambda}_k^j \mathbf{P}_{f_k} h_{f_T,d_R} + \boldsymbol{\sigma}_N^2} \tag{4.1b}$$

$$\boldsymbol{\Gamma_{f_k}} = \frac{\mathbf{P}_{f_k} h_{f_T,f_R}}{\sum_{c_i \in C} \boldsymbol{\lambda}_k^i \mathbf{P}_{c_i} h_{c,f_R} + \sum_{d_j \in D} \boldsymbol{\lambda}_k^j \mathbf{P}_{d_j} h_{d_T,f_R} + \boldsymbol{\sigma}_N^2} \tag{4.1c}$$

where $\mathbf{P}_{c_i}$, $\mathbf{P}_{d_j}$, and $\mathbf{P}_{f_k}$ denote the transmit powers of the CUE $\boldsymbol{c_i}$, DUE $\boldsymbol{d_j}$ and FUE $\boldsymbol{f_k}$, respectively. The variance of the Additive White Gaussian Noise (AWGN) at the receiver is denoted by $\boldsymbol{\sigma_N^2}$. $\boldsymbol{\lambda_j^i = 1}$ when DUE $\boldsymbol{d_j}$ shares the channel of CUE $\boldsymbol{c_i}$, otherwise 0. $\boldsymbol{\lambda_k^i = 1}$ when FUE $\boldsymbol{f_k}$ shares the channel of CUE $\boldsymbol{c_i}$, otherwise 0. $\boldsymbol{\lambda_k^j = 1}$ when DUE $\boldsymbol{d_j}$ and FUE $\boldsymbol{f_k}$ share the channel of CUE $\boldsymbol{c_i}$, otherwise 0.

Resource-sharing between a DUE and FUE using the same CUE channel will result in mutual interference among devices. The system objective is to maximise the total throughput with maximum transmit power and SINR threshold constraints. It is assumed that each CUE channel cannot be reused by more than one underlay (sharing) user in the same category. Using the Shannon Capacity formula [133], the objective function and constraints for the optimisation problem are expressed as follows:

$$\begin{aligned}\mathbf{max}\, \mathbf{T_R} = \mathbf{W}_i \Big[&\textstyle\sum_{c_i \in C} \mathbf{log_2}\big(\mathbf{1} + \boldsymbol{\Gamma}_{c_i}\big) + \sum_{d_j \in D} \big(\boldsymbol{\lambda}_j^i + \boldsymbol{\lambda}_k^j\big) \mathbf{log_2}\Big(\mathbf{1} + \boldsymbol{\Gamma}_{d_j}\Big) + \\ &\textstyle\sum_{f_k \in F} \big(\boldsymbol{\lambda}_k^i + \boldsymbol{\lambda}_k^j\big) \mathbf{log_2}\big(\mathbf{1} + \boldsymbol{\Gamma}_{f_k}\big)\Big] \end{aligned} \tag{4.2}$$

with

$$\boldsymbol{\Gamma}_{c_i} \geq \boldsymbol{\Gamma}_{c_i,\mathbf{min}} \quad \forall\, \boldsymbol{c_i} \in \boldsymbol{C} \tag{4.2a}$$
$$\boldsymbol{\Gamma}_{d_j} \geq \boldsymbol{\Gamma}_{d_j,\mathbf{min}} \quad \forall\, \boldsymbol{d_j} \in \boldsymbol{D} \tag{4.2b}$$
$$\boldsymbol{\Gamma}_{f_k} \geq \boldsymbol{\Gamma}_{f_k,\mathbf{min}} \quad \forall\, \boldsymbol{f_k} \in \boldsymbol{F} \tag{4.2c}$$
$$\textstyle\sum_{c_i \in C} \big(\boldsymbol{\lambda}_j^i + \boldsymbol{\lambda}_k^j\big) \leq \mathbf{1} \quad \forall\, \boldsymbol{d_j} \in \boldsymbol{D} \tag{4.2d}$$
$$\textstyle\sum_{c_i \in C} \big(\boldsymbol{\lambda}_k^i + \boldsymbol{\lambda}_k^j\big) \leq \mathbf{1} \quad \forall\, \boldsymbol{f_k} \in \boldsymbol{F} \tag{4.2e}$$
$$\mathbf{P}_{c_i} \leq \mathbf{P}_{c_i,\mathbf{max}} \quad \forall\, \boldsymbol{c_i} \in \boldsymbol{C} \tag{4.2f}$$
$$\mathbf{P}_{d_j} \leq \mathbf{P}_{d_j,\mathbf{max}} \quad \forall\, \boldsymbol{d_j} \in \boldsymbol{D} \tag{4.2g}$$
$$\mathbf{P}_{f_k} \leq \mathbf{P}_{f_k,\mathbf{max}} \quad \forall\, \boldsymbol{f_k} \in \boldsymbol{F} \tag{4.2h}$$

Constraints (4.2a)- (4.2c) represent the minimum QoS requirements with $\boldsymbol{\Gamma}_{c_i,\mathbf{min}}$, $\boldsymbol{\Gamma}_{d_j,\mathbf{min}}$ and $\boldsymbol{\Gamma}_{f_k,\mathbf{min}}$, denoting the SINR thresholds of the CUEs, DUEs and FUEs, respectively. Constraints (4.2d) - (4.2e) represent the channel associations of the UEs. Constraints (4.2f) - (4.2h) is to

ensure the transmit powers of the UEs do not exceed the limit. The optimisation problem in (4.2) is a MINLP, which is NP-hard and cannot be solved directly. To reduce the computation complexity, the problem is decomposed into sub-problems and a centralised heuristic interference-aware algorithm is developed to solve the problem in phases as described in the following sections.

4.2 Interference-Aware Spectrum Management (ISA) Scheme

In this ISA scheme, interference management is through power allocation. Firstly, the maximum allowable interference from the combined reuse of a channel CUE $\boldsymbol{c_i}$ with a DUE $\boldsymbol{d_j}$ and FUE $\boldsymbol{f_k}$ is obtained. From (4.1a) and constraint (4.2a), the interference limit to guarantee the received SINR at the BS on the channel of CUE $\boldsymbol{c_i}$ is denoted by $\mathbf{I}^{\boldsymbol{i}}_{\boldsymbol{B},\mathbf{max}}$ and given as:

$$\mathbf{I}^{\boldsymbol{i}}_{\boldsymbol{B},\mathbf{max}} = \frac{\mathbf{P}_{\boldsymbol{c_i}} \boldsymbol{h_{c,B}}}{\boldsymbol{\Gamma}_{\boldsymbol{c_i},\mathbf{min}}} - \boldsymbol{\sigma}^{\mathbf{2}}_{\boldsymbol{N}} \qquad \forall\, \boldsymbol{c_i} \in \boldsymbol{C} \tag{4.3}$$

With priority given to the CUEs, $\mathbf{P}_{\boldsymbol{c_i}} = \mathbf{P}_{\boldsymbol{c_i},\mathbf{max}},\ \forall\, \boldsymbol{c_i} \in \boldsymbol{C}$. Assuming that $\boldsymbol{\sigma}^{\mathbf{2}}_{\boldsymbol{N}}$ is neglected, the minimum transmit power of DUE $\boldsymbol{d_j}$ and FUE $\boldsymbol{f_k}$ is given by (4.4a) and (4.4b).

$$\mathbf{P}_{\boldsymbol{d_j},\mathbf{min}} = \mathbf{min}\left\{\mathbf{P}_{\boldsymbol{d_j},\mathbf{max}},\ \ \boldsymbol{\Gamma}_{\boldsymbol{d_j},\mathbf{min}}\left[\mathbf{P}_{\boldsymbol{c_i},\mathbf{max}}\left(\frac{\boldsymbol{h_{c,d_R}}}{\boldsymbol{h_{d_T,d_R}}}\right) + \mathbf{P}_{\boldsymbol{f_k},\mathbf{max}}\left(\frac{\boldsymbol{h_{f_T,d_R}}}{\boldsymbol{h_{d_T,d_R}}}\right)\right]\right\} \tag{4.4a}$$

$$\mathbf{P}_{\boldsymbol{f_k},\mathbf{min}} = \mathbf{min}\left\{\mathbf{P}_{\boldsymbol{f_k},\mathbf{max}},\ \ \boldsymbol{\Gamma}_{\boldsymbol{f_k},\mathbf{min}}\left[\mathbf{P}_{\boldsymbol{c_i},\mathbf{max}}\left(\frac{\boldsymbol{h_{c,f_R}}}{\boldsymbol{h_{f_T,f_R}}}\right) + \mathbf{P}_{\boldsymbol{d_j},\mathbf{max}}\left(\frac{\boldsymbol{h_{d_T,f_R}}}{\boldsymbol{h_{f_T,f_R}}}\right)\right]\right\} \tag{4.4b}$$

$\mathbf{P}^{\boldsymbol{c}}_{\boldsymbol{d_j},\mathbf{max}}$ and $\mathbf{P}^{\boldsymbol{c}}_{\boldsymbol{f_k},\mathbf{max}}$ are the upper bounds of the transmit powers of DUE $\boldsymbol{d_j}$ and FUE $\boldsymbol{f_k}$ respectively, to guarantee the SINR of CUE $\boldsymbol{c_i}$, $\boldsymbol{\Gamma}_{\boldsymbol{c_i},\mathbf{min}}$. Similarly, and $\mathbf{P}^{\boldsymbol{d}}_{\boldsymbol{f_k},\mathbf{max}}$ is the limit of the transmit power of FUE $\boldsymbol{f_k}$ to guarantee the SINR of DUE $\boldsymbol{d_j}$, $\boldsymbol{\Gamma}_{\boldsymbol{d_j},\mathbf{min}}$, while $\mathbf{P}^{\boldsymbol{f}}_{\boldsymbol{d_j},\mathbf{max}}$ is the upper bound of the transmit power of DUE $\boldsymbol{d_j}$ to guarantee the SINR of FUE $\boldsymbol{f_k}$, $\boldsymbol{\Gamma}_{\boldsymbol{f_k},\mathbf{min}}$. Equations in (4.5) are set to the maximum transmit power to eliminate infeasible transmit powers. For example, if $\mathbf{P}^{\boldsymbol{c}}_{\boldsymbol{d_j},\mathbf{max}} \leq \mathbf{0}$, DUE $\boldsymbol{d_j}$ cannot transmit (i.e., $\mathbf{P}_{\boldsymbol{d_j}}$ is invalid), hence $\boldsymbol{\lambda}^{\boldsymbol{j}}_{\boldsymbol{k}} = \mathbf{0}$, since the QoS of DUE $\boldsymbol{d_j}$ cannot be satisfied. This may happen if there is a high interference gain from the FUE transmitter $\boldsymbol{f_T}$ to the MBS, therefore, $\mathbf{P}^{\boldsymbol{c}}_{\boldsymbol{d_j},\mathbf{max}} = \mathbf{P}_{\boldsymbol{d_j},\mathbf{max}}$.

$$\mathbf{P}^{c}_{d_j,\max} = \begin{cases} \mathbf{P}_{c_i,\max}\left(\dfrac{\boldsymbol{h}_{c,B}}{\boldsymbol{h}_{d_T,B}}\right) - \mathbf{P}_{f_k,\max}\left(\dfrac{\boldsymbol{h}_{f_T,B}}{\boldsymbol{h}_{d_T,B}}\right), & \dfrac{\mathbf{P}_{c_i,\max}}{\boldsymbol{\Gamma}_{c_i,\min}}\left(\dfrac{\boldsymbol{h}_{c,B}}{\boldsymbol{h}_{d_T,B}}\right) > \mathbf{P}_{f_k,\max}\left(\dfrac{\boldsymbol{h}_{f_T,B}}{\boldsymbol{h}_{d_T,B}}\right) \\ \mathbf{P}_{d_j,\max}, & \dfrac{\mathbf{P}_{c_i,\max}}{\boldsymbol{\Gamma}_{c_i,\min}}\left(\dfrac{\boldsymbol{h}_{c,B}}{\boldsymbol{h}_{d_T,B}}\right) \leq \mathbf{P}_{f_k,\max}\left(\dfrac{\boldsymbol{h}_{f_T,B}}{\boldsymbol{h}_{d_T,B}}\right) \end{cases} \tag{4.5a}$$

$$\mathbf{P}^{c}_{f_k,\max} = \begin{cases} \dfrac{\mathbf{P}_{c_i,\max}}{\boldsymbol{\Gamma}_{c_i,\min}}\left(\dfrac{\boldsymbol{h}_{c,B}}{\boldsymbol{h}_{f_T,B}}\right) - \mathbf{P}_{d_j,\max}\left(\dfrac{\boldsymbol{h}_{d_T,B}}{\boldsymbol{h}_{f_T,B}}\right), & \dfrac{\mathbf{P}_{c_i,\max}}{\boldsymbol{\Gamma}_{c_i,\min}}\left(\dfrac{\boldsymbol{h}_{c,B}}{\boldsymbol{h}_{f_T,B}}\right) > \mathbf{P}_{d_j,\max}\left(\dfrac{\boldsymbol{h}_{d_T,B}}{\boldsymbol{h}_{f_T,B}}\right) \\ \mathbf{P}_{f_k,\max}, & \dfrac{\mathbf{P}_{c_i,\max}}{\boldsymbol{\Gamma}_{c_i,\min}}\left(\dfrac{\boldsymbol{h}_{c,B}}{\boldsymbol{h}_{f_T,B}}\right) \leq \mathbf{P}_{d_j,\max}\left(\dfrac{\boldsymbol{h}_{d_T,B}}{\boldsymbol{h}_{f_T,B}}\right) \end{cases} \tag{4.5b}$$

$$\mathbf{P}^{f}_{d_j,\max} = \begin{cases} \dfrac{\mathbf{P}_{f_k,\max}}{\boldsymbol{\Gamma}_{f_k,\min}}\left(\dfrac{\boldsymbol{h}_{f_T,f_R}}{\boldsymbol{h}_{d_T,f_R}}\right) - \mathbf{P}_{c_i,\max}\left(\dfrac{\boldsymbol{h}_{c,f_R}}{\boldsymbol{h}_{d_T,f_R}}\right), & \dfrac{\mathbf{P}_{f_k,\max}}{\boldsymbol{\Gamma}_{f_k,\min}}\left(\dfrac{\boldsymbol{h}_{f_T,f_R}}{\boldsymbol{h}_{d_T,f_R}}\right) > \mathbf{P}_{c_i,\max}\left(\dfrac{\boldsymbol{h}_{c,f_R}}{\boldsymbol{h}_{d_T,f_R}}\right) \\ \mathbf{P}_{d_j,\max}, & \dfrac{\mathbf{P}_{f_k,\max}}{\boldsymbol{\Gamma}_{f_k,\min}}\left(\dfrac{\boldsymbol{h}_{f_T,f_R}}{\boldsymbol{h}_{d_T,f_R}}\right) \leq \mathbf{P}_{c_i,\max}\left(\dfrac{\boldsymbol{h}_{c,f_R}}{\boldsymbol{h}_{d_T,f_R}}\right) \end{cases} \tag{4.5c}$$

$$\mathbf{P}^{d}_{f_k,\max} = \begin{cases} \dfrac{\mathbf{P}_{d_j,\max}}{\boldsymbol{\Gamma}_{d_j,\min}}\left(\dfrac{\boldsymbol{h}_{d_T,d_R}}{\boldsymbol{h}_{f_T,d_R}}\right) - \mathbf{P}_{c_i,\max}\left(\dfrac{\boldsymbol{h}_{c,d_R}}{\boldsymbol{h}_{f_T,d_R}}\right), & \dfrac{\mathbf{P}_{d_j,\max}}{\boldsymbol{\Gamma}_{d_j,\min}}\left(\dfrac{\boldsymbol{h}_{d_T,d_R}}{\boldsymbol{h}_{f_T,d_R}}\right) > \mathbf{P}_{c_i,\max}\left(\dfrac{\boldsymbol{h}_{c,d_R}}{\boldsymbol{h}_{f_T,d_R}}\right) \\ \mathbf{P}_{f_k,\max}, & \dfrac{\mathbf{P}_{d_j,\max}}{\boldsymbol{\Gamma}_{d_j,\min}}\left(\dfrac{\boldsymbol{h}_{d_T,d_R}}{\boldsymbol{h}_{f_T,d_R}}\right) \leq \mathbf{P}_{c_i,\max}\left(\dfrac{\boldsymbol{h}_{c,d_R}}{\boldsymbol{h}_{f_T,d_R}}\right) \end{cases} \tag{4.5d}$$

The set of feasible transmit power for DUE $\boldsymbol{d_j}$ and FUE $\boldsymbol{f_k}$ are given by (4.6)

$$\boldsymbol{P_D} = \left\{\mathbf{P}_{d_j,\min}, \mathbf{min}\left(\mathbf{P}^{c}_{d_j,\max}, \mathbf{P}_{d_j,\max}\right), \mathbf{min}\left(\mathbf{x_1}\mathbf{P}^{f}_{d_j,\max}, \mathbf{P}_{d_j,\max}\right), \mathbf{P}_{d_j,\max}\right\} \quad \forall\, \boldsymbol{d_j} \in \boldsymbol{D} \tag{4.6a}$$

$$\boldsymbol{P_F} = \left\{\mathbf{P}_{f_k,\min}, \mathbf{min}\left(\mathbf{P}^{c}_{f_k,\max}, \mathbf{P}_{f_k,\max}\right), \mathbf{min}\left(\mathbf{x_2}\mathbf{P}^{d}_{f_k,\max}, \mathbf{P}_{f_k,\max}\right), \mathbf{P}_{f_k,\max}\right\} \quad \forall\, \boldsymbol{f_k} \in \boldsymbol{F} \tag{4.6b}$$

where $\mathbf{x_1}$ and $\mathbf{x_2}$ are used to set $\mathbf{P}^{f}_{d_j,\max}$ and $\mathbf{P}^{d}_{f_k,\max}$ in (4.6), respectively, for channel associations $\boldsymbol{\lambda^i_j}$, $\boldsymbol{\lambda^i_k}$ and $\boldsymbol{\lambda^j_k}$, $\forall\, \boldsymbol{c_i} \in \boldsymbol{C}$. For $\boldsymbol{\lambda^i_j}$, $\boldsymbol{P_F} = \emptyset$, whereas $\boldsymbol{P_D} = \emptyset$ for $\boldsymbol{\lambda^i_k}$. The values for $\mathbf{x_1}$ and $\mathbf{x_2}$ are given in (4.7).

$$\begin{cases} \boldsymbol{\lambda^j_k}, & \mathbf{x_1} = \mathbf{x_2} = \mathbf{1} \\ \boldsymbol{\lambda^i_j}, & \mathbf{x_1} = \dfrac{\mathbf{P}_{d_j,\max}}{\mathbf{P}^{f}_{d_j,\max}} \\ \boldsymbol{\lambda^i_k}, & \mathbf{x_2} = \dfrac{\mathbf{P}_{f_k,\max}}{\mathbf{P}^{j}_{f_k,\max}} \end{cases} \tag{4.7}$$

The ISA scheme is presented to solve the resource allocation problem by jointly considering the power allocation and channel assignment in two phases, ISA-I and ISA-II. First, ISA-I is used to determine $\boldsymbol{\lambda_k^j}$, then the optimal power allocation for DUE $\boldsymbol{d_j}$ and FUE $\boldsymbol{f_k}$ reusing the $\boldsymbol{i}$th CUE channel is evaluated. Next, the optimal CUE-DUE-FUE resource-sharing partners are determined. The underlay users (i.e., DUEs and FUEs) unassigned from ISA-I, because the minimum QoS constraints for them to coexist on a cellular channel are not satisfied, are assigned to unmatched cellular resources in ISA-II. This is to determine $\boldsymbol{\lambda_j^i}$ (CUE-DUE assignments) and $\boldsymbol{\lambda_k^i}$ (CUE-FUE assignments). The two phases of the algorithm are presented in Algorithms 4.1 and 4.2.

Algorithm 4.1. ISA Phase I

Phase I: To determine $\sum_{c_i \in \mathbf{C}} \sum_{d_j \in \mathbf{D}} \sum_{f_k \in \mathbf{D}} \boldsymbol{\lambda}_k^j$

1: Input $\boldsymbol{C}$, $\boldsymbol{D}$ and $\boldsymbol{F}$; $\mathbf{P}_{c_i,\max}$, $\mathbf{P}_{d_j,\max}$, and $\mathbf{P}_{f_k,\max}$; $\boldsymbol{\Gamma}_{c_i,\min}$, $\boldsymbol{\Gamma}_{d_j,\min}$ and $\boldsymbol{\Gamma}_{f_k,\min}$

2: Initialisation: $\mathbf{x_1} = \mathbf{x_2} = \mathbf{1}$

3: for $\boldsymbol{c_i} \in \boldsymbol{C}$ $1 \leq \boldsymbol{i} \leq \boldsymbol{N}$ do

4: Compute $\mathbf{I}_{B,\max}^{i}$

5: for $\boldsymbol{d_j} \in \boldsymbol{D}$ $\mathbf{1} \leq \boldsymbol{i} \leq \boldsymbol{M}$ do

6: $\boldsymbol{F_1} = \emptyset$

7: for $\boldsymbol{f_k} \in \boldsymbol{F}$ $\mathbf{1} \leq \boldsymbol{i} \leq \boldsymbol{F}$ do

8: $\boldsymbol{P_{\bar{D}}} = \boldsymbol{f_{A_1}}\left(\mathbf{P}_{d_j}\right) \triangleq \mathbf{P}_{d_j} \boldsymbol{h_{d_T,B}} \; < \; \mathbf{I}_{B,\max}^{i}, \forall \mathbf{P}_{d_j} \in \mathbf{P}_D$

9: if $\boldsymbol{P_{\bar{D}}} \neq \emptyset$ then

10: Compute $\boldsymbol{f_{A_2}}\left(\mathbf{P}_{d_j}\right) \triangleq \mathbf{I}_{B,\Delta}^{i} = \mathbf{I}_{B,\max}^{i} - \boldsymbol{f_{A_1}}\left(\mathbf{P}_{d_j}\right), \forall \mathbf{P}_{d_j} \in \boldsymbol{P_{\bar{D}}}$

11: Compute $\boldsymbol{f_B}(\mathbf{P}_{f_k}) \triangleq \mathbf{P}_{f_k} \boldsymbol{h_{f_T,B}}$

12: $\boldsymbol{P_{DF}} = \left\{\left(\mathbf{P}_{d_j}, \mathbf{P}_{f_k}\right)_1, \ldots, \left(\mathbf{P}_{d_j}, \mathbf{P}_{f_k}\right)_{|\boldsymbol{P_{DF}}|}\right\} \triangleq \boldsymbol{f_B}(\mathbf{P}_{f_k}) - \boldsymbol{f_{A_2}}\left(\mathbf{P}_{d_j}\right) \leq \mathbf{0}, \forall \mathbf{P}_{f_k} \in \boldsymbol{P_F}$

13: if $\boldsymbol{P_{DF}} \neq \emptyset$ then

14: $$\boldsymbol{P_{DF}^*} = \left\{\left(\mathbf{P}_{d_j}^*, \mathbf{P}_{f_k}^*\right)_1, \ldots, \left(\mathbf{P}_{d_j}^*, \mathbf{P}_{f_k}^*\right)_{|\boldsymbol{P_{DF}^*}|}\right\}$$
$$\triangleq \begin{cases} \boldsymbol{f_{D_1}}\left(\mathbf{P}_{d_j}, \mathbf{P}_{f_k}\right) \triangleq \frac{\mathbf{P}_{c_i,\max} h_{c,B}}{\mathbf{P}_{d_j} h_{d_T,B} + \mathbf{P}_{f_k} h_{f_T,B} + \sigma_N^2} \geq \boldsymbol{\Gamma}_{c_i,\min} \\ \boldsymbol{f_{D_2}}\left(\mathbf{P}_{d_j}, \mathbf{P}_{f_k}\right) \triangleq \frac{\mathbf{P}_{d_j} h_{d_T,d_R}}{\mathbf{P}_{c_i,\max} h_{c,d_R} + \mathbf{P}_{f_k} h_{f_T,d_R} + \sigma_N^2} \geq \boldsymbol{\Gamma}_{d_j,\min} \\ \boldsymbol{f_{D_3}}\left(\mathbf{P}_{d_j}, \mathbf{P}_{f_k}\right) \triangleq \frac{\mathbf{P}_{f_k} h_{f_T,f_R}}{\mathbf{P}_{c_i,\max} h_{c,f_R} + \mathbf{P}_{d_j} h_{d_T,f_R} + \sigma_N^2} \geq \boldsymbol{\Gamma}_{f_k,\min} \\ \forall \left(\mathbf{P}_{d_j}, \mathbf{P}_{f_k}\right) \in \boldsymbol{P_{DF}} \end{cases}$$

15: if $\boldsymbol{P_{DF}^*} \neq \emptyset$ then

$$\left(\mathbf{P}_{d_j}^*, \mathbf{P}_{f_k}^*\right) = \underset{\left(\mathbf{P}_{d_j}, \mathbf{P}_{f_k}\right) \in \boldsymbol{P_{DF}^*}}{\mathbf{argmax}} \; \mathbf{W}_i \left[\mathbf{log_2}\left(\mathbf{1} + \boldsymbol{f_{D_1}}\left(\mathbf{P}_{d_j}, \mathbf{P}_{f_k}\right)\right) + \mathbf{log_2}\left(1 + \boldsymbol{f_{D_2}}\left(\mathbf{P}_{d_j}, \mathbf{P}_{f_k}\right)\right) + \mathbf{log_2}\left(\mathbf{1} + \boldsymbol{f_{D_3}}\left(\mathbf{P}_{d_j}, \mathbf{P}_{f_k}\right)\right)\right]$$

16: $\boldsymbol{F_1} = \boldsymbol{F_1} + \boldsymbol{f_k}$

17: end if

18: end if

19: end if

20: end for

21: $\boldsymbol{R_{d_j}^{F_1}} = \left\{(\boldsymbol{d_j}, \boldsymbol{f_k})_1, \ldots, (\boldsymbol{d_j}, \boldsymbol{f_k})_{|\boldsymbol{F_1}|}\right\}$

22: end for

23: $\boldsymbol{R_{DF}^*} = \left\{\boldsymbol{\pi}_{d_1}^{\mathbf{F_1}}, \ldots, \boldsymbol{\pi}_{d_j}^{\mathbf{F_1}}, \ldots, \boldsymbol{\pi}_{\pi_{DF}^*}^{\mathbf{F_1}}\right\}$

24: Obtain optimal re-use partner for $\boldsymbol{c_i}$, $(\boldsymbol{d_j^*}, \boldsymbol{f_k^*}) = \underset{(\boldsymbol{d_j}, \boldsymbol{f_k}) \in \boldsymbol{R_{DF}^*}}{\mathbf{argmax}} \; \mathbf{W}_i \left[\mathbf{log_2}\left(\mathbf{1} + \frac{\mathbf{P}_{c_i,\max} h_{c,B}}{\mathbf{P}_{d_j}^* h_{d_T,B} + \mathbf{P}_{f_k}^* h_{f_T,B} + \sigma_N^2}\right) + \mathbf{log_2}\left(1 + \frac{\mathbf{P}_{d_j}^* h_{d_T,d_R}}{\mathbf{P}_{c_i,\max} h_{c,d_R} + \mathbf{P}_{f_k}^* h_{f_T,d_R} + \sigma_N^2}\right) + \mathbf{log_2}\left(1 + \frac{\mathbf{P}_{f_k}^* h_{f_T,f_R}}{\mathbf{P}_{c_i,\max} h_{c,f_R} + \mathbf{P}_{d_j}^* h_{d_T,f_R} + \sigma_N^2}\right)\right]$

25: $\boldsymbol{F} = \boldsymbol{F} - \boldsymbol{f_k^*}$; $\boldsymbol{D} = \boldsymbol{D} - \boldsymbol{d_j^*}$; $\boldsymbol{C} = \boldsymbol{C} - \boldsymbol{c_i}$;

26: end for

Algorithm 4.2. ISA Phase II

Phase II: To determine $\sum_{c_i \in \mathbf{C}} \sum_{d_j \in \mathbf{D}} \sum_{f_k \in \mathbf{D}} (\boldsymbol{\lambda}_j^i + \boldsymbol{\lambda}_k^i)$

1: Input $\boldsymbol{C}$, $\boldsymbol{D}$ and $\boldsymbol{F}$ from Algorithm 4.1.

2: if $\boldsymbol{C} \neq \emptyset$ then

3: Initialisation $\mathbf{x_1} = \frac{\mathrm{P}_{d_j,\max}}{\mathrm{P}^f_{d_j,\max}}$, $\mathbf{x_2} = \frac{\mathrm{P}_{f_k,\max}}{\mathrm{P}^j_{f_k,\max}}$

4: for $\boldsymbol{c_i} \in \boldsymbol{C}$ $1 \leq \boldsymbol{i} \leq |\boldsymbol{C}|$ do

5: Compute $\mathbf{I}^i_{B,\max}$

6: Set up $\boldsymbol{R}^{\boldsymbol{d}}_{\boldsymbol{c_i}}(\boldsymbol{R}^{\boldsymbol{f}}_{\boldsymbol{c_i}})$ as set of potential DUE $\boldsymbol{d_j}$ (FUE $\boldsymbol{f_k}$) reuse partner for $\boldsymbol{c_i}$;

7: for $\boldsymbol{d_j} \in \boldsymbol{D}$ $1 \leq \boldsymbol{j} \leq |\boldsymbol{D}|$ do

8: $\boldsymbol{P_F} = \emptyset$;

9: $\boldsymbol{P_{\bar{D}}} = \boldsymbol{f_{A_1}}\left(\mathrm{P}_{d_j}\right) \triangleq \mathrm{P}_{d_j} \boldsymbol{h_{d_T,B}} < \mathbf{I}^i_{B,\max}, \forall \mathrm{P}_{d_j} \in \boldsymbol{P_D}$

10: if $\boldsymbol{P_{\bar{D}}} \neq \emptyset$ then

11: $$\boldsymbol{P^*_D} = \left\{\mathrm{P}_{d_j}, \ldots, \mathrm{P}_{d_{|P^*_D|}}\right\} \triangleq \begin{cases} \boldsymbol{f_{D_1}}\left(\mathrm{P}_{d_j}\right) \triangleq \frac{\mathrm{P}_{c_i,\max} h_{c,B}}{\mathrm{P}_{d_j} h_{d_T,B} + \sigma_N^2} \geq \boldsymbol{\Gamma_{c_i,\min}} \\ \boldsymbol{f_{D_2}}\left(\mathrm{P}_{d_j}\right) \triangleq \frac{\mathrm{P}_{d_j} h_{d_T,d_R}}{\mathrm{P}_{c_i,\max} h_{c,d_R} + \sigma_N^2} \geq \boldsymbol{\Gamma_{d_j,\min}} \\ \forall \mathrm{P}_{d_j} \in \boldsymbol{P_{\bar{D}}} \end{cases}$$

12: if $\boldsymbol{P^*_D} \neq \emptyset$ then

13: $$\mathrm{P}^*_{d_j} = \underset{\mathrm{P}_{d_j} \in P^*_D}{\mathbf{argmax}} \mathbf{W}_i \left[\log_2\left(1 + \boldsymbol{f_{D_1}}\left(\mathrm{P}_{d_j}\right)\right) + \log_2\left(1 + \boldsymbol{f_{D_2}}\left(\mathrm{P}_{d_j}\right)\right)\right]$$

14: $\boldsymbol{R^d_{c_i}} = \boldsymbol{R^d_{c_i}} + \boldsymbol{d_j}$

15: end if

16: end if

17: end for

18: for $\boldsymbol{f_k} \in \boldsymbol{F}$ $1 \leq \boldsymbol{k} \leq |\boldsymbol{F}|$ do

19: $\boldsymbol{P_D} = \emptyset$;

20: $\boldsymbol{P_{\bar{F}}} = \boldsymbol{f_{A_2}}(\mathrm{P}_{f_k}) \triangleq \mathrm{P}_{f_k} \boldsymbol{h_{f_T,B}} < \mathbf{I}^i_{B,\max}, \forall \mathrm{P}_{f_k} \in \mathrm{P}_F$

21: if $\boldsymbol{P_{\bar{F}}} \neq \emptyset$ then

22: $$\boldsymbol{P^*_F} = \left\{\mathrm{P}_{f_k}, \ldots, \mathrm{P}_{f_{|P^*_F|}}\right\} \triangleq \begin{cases} \boldsymbol{f_{D_3}}(\mathrm{P}_{f_k}) \triangleq \frac{\mathrm{P}_{c_i,\max} h_{c,B}}{\mathrm{P}_{f_k} h_{f_T,B} + \sigma_N^2} \geq \boldsymbol{\Gamma_{c_i,\min}} \\ \boldsymbol{f_{D_4}}(\mathrm{P}_{f_k}) \triangleq \frac{\mathrm{P}_{f_k} h_{f_T,f_R}}{\mathrm{P}_{c_i,\max} h_{c,f_R} + \sigma_N^2} \geq \boldsymbol{\Gamma_{f_k,\min}} \\ \forall \mathrm{P}_{f_k} \in \boldsymbol{P_{\bar{F}}} \end{cases}$$

23: if $\boldsymbol{P^*_F} \neq \emptyset$ then

24: $$\mathrm{P}^*_{f_k} = \underset{\mathrm{P}_{f_k} \in P^*_F}{\mathbf{argmax}} \mathbf{W}_i \left[\log_2\left(1 + \boldsymbol{f_{D_3}}(\mathrm{P}_{f_k})\right) + \log_2\left(1 + \boldsymbol{f_{D_4}}(\mathrm{P}_{f_k})\right)\right]$$

25: $\boldsymbol{R^f_{c_i}} = \boldsymbol{R^f_{c_i}} + \boldsymbol{f_k}$

end if

26: end if

27: end for

28: $\boldsymbol{R^{DF}_{c_i}} = \{\boldsymbol{R^d_{c_i}} + \boldsymbol{R^f_{c_i}}\} \triangleq \{\boldsymbol{R_h}, \ldots, \boldsymbol{R_H}\}$ $\boldsymbol{h} = \mathbf{1}, \mathbf{2}, .. \boldsymbol{H}$, $\boldsymbol{H} = |\boldsymbol{R^{DF}_{c_i}}|$

29: $$\boldsymbol{h^*} \triangleq \boldsymbol{d^*_j}(\boldsymbol{f^*_k}) = \underset{\boldsymbol{h} \in \boldsymbol{R^{DF}_{c_i}}}{\mathbf{argmax}} \mathbf{W}_i \left[\log_2\left(1 + \frac{\mathrm{P}_{c_i,\max} h_{c,B}}{\mathrm{P}^*_{d_j} h_{d_T,B}\left(\mathrm{P}^*_{f_k} h_{f_T,B}\right) + \sigma_N^2}\right) + \log_2\left(1 + \frac{\mathrm{P}^*_{d_j} h_{d_T,d_R}\left(\mathrm{P}^*_{f_k} h_{f_T,f_R}\right)}{\mathrm{P}_{c_i,\max} h_{c,d_R}\left(\mathrm{P}_{c_i,\max} h_{c,f_R}\right) + \sigma_N^2}\right)\right]$$

30: $$\boldsymbol{h^*} = \begin{cases} \boldsymbol{d^*_j}, \ \boldsymbol{D} = \boldsymbol{D} - \boldsymbol{d^*_j} \\ \boldsymbol{f^*_k}, \ \boldsymbol{F} = \boldsymbol{F} - \boldsymbol{f^*_k} \end{cases}$$

31: end for

32: end if

Table 4.1: Main simulation parameters for the ISA Algorithm [130,131]

Parameter	Value
Carrier frequency, $\boldsymbol{f_c}$	$\mathbf{2GHz}$
RB bandwidth	$\mathbf{180\ kHz}$
FBS radius	$\mathbf{50m}$
Maximum CUE transmit power, $\mathbf{P}_{\boldsymbol{c_i},\mathbf{max}}$	$\mathbf{23dBm}$
Maximum DUE transmit power, $\mathbf{P}_{\boldsymbol{d_j},\mathbf{max}}$	$\mathbf{23dBm}$
Maximum FUE transmit power, $\mathbf{P}_{\boldsymbol{f_k},\mathbf{max}}$	$\mathbf{10dBm}$
MaximumD2D distance, $\boldsymbol{L_{d_T,d_R}}$	$\mathbf{50m}$
CUE SINR Threshold, $\boldsymbol{\Gamma}_{\boldsymbol{c_i},\mathbf{min}}$	$\mathbf{20\ dB}$
DUE SINR Threshold, $\boldsymbol{\Gamma}_{\boldsymbol{d_j},\mathbf{min}}$	$\mathbf{20\ dB}$
FUE SINR Threshold, $\boldsymbol{\Gamma}_{\boldsymbol{f_k},\mathbf{min}}$	$\mathbf{20\ dB}$
Noise power density	$\mathbf{-174dBm/Hz}$
BS-UE Pathloss model	$\mathbf{28.03 + 40log10(d[m])}$ dB
UE-UE Pathloss model	$\mathbf{15.3 + 37.6log10(d[m])}$ dB

4.3 Simulation Case Study and Analysis

The performance of the ISA scheme presented above is verified by considering the uplink of a two-tier HetNet with FBSs underlaying cellular system and the MBS positioned at the center with radius of 400m. There are $\boldsymbol{P}$ FBSs of 50m radius with $\boldsymbol{L}$ FUEs, $\boldsymbol{M}$ DUEs and $\boldsymbol{N}$ CUEs randomly distributed within the coverage of the MBS. The main simulation parameters are summarised in Table 4.1 guided by 4G and 5G standards.

The presented ISA scheme is evaluated in terms of overall network throughput since this is aim of the optimisation problem. The system throughput gain and the total number of admitted underlay (sharing) users are also determined to assess the impact of spectrum sharing on expanding network capacity. The scheme is compared to ISA-Pmax, where the all the active CUEs, DUEs and FUEs transmit at peak power (i.e., no power control is implemented). ISA-Pmax is implemented using Algorithm 4.1 and 4.2 with $\mathbf{P}_{\boldsymbol{c_i}}$, $\mathbf{P}_{\boldsymbol{d_j}}$, and $\mathbf{P}_{\boldsymbol{f_k}}$ set to $\mathbf{P}_{\boldsymbol{c_i},\mathbf{max}}$, $\mathbf{P}_{\boldsymbol{d_j},\mathbf{max}}$ and $\mathbf{P}_{\boldsymbol{f_k},\mathbf{max}}$, respectively. A scenario where there is no underlay or sharing users (No-UDU) is also considered. There is no impact of interference on the cellular users in this scenario since there is no spectrum sharing.

The total number of admitted underlay users, $\mathbf{D}_{\boldsymbol{u}}=\sum_{\boldsymbol{c_i}\in\mathbf{C}}\sum_{\boldsymbol{d_j}\in\mathbf{D}}\sum_{\boldsymbol{f_k}\in\mathbf{F}}(\boldsymbol{\lambda_k^j}+\boldsymbol{\lambda_j^i}+\boldsymbol{\lambda_k^i})$ with $\boldsymbol{M}=\mathbf{20}, \boldsymbol{L}=\mathbf{20}$ and varying $\boldsymbol{N}$, for the ISA and ISA-Pmax schemes, is shown in Fig. 4.2. It can be

seen that $\mathbf{D}_u$ increases with N for both methods, with ISA showing up to 80% higher number of accessed DUEs compared to ISA-Pmax at $N = 14$. This is due to the fact that power is not optimised in ISA-Pmax, which may have increased the potential resource-sharing partners for the CUEs. The number of admitted underlay or sharing users $\mathbf{D}_u$, are limited since the UEs are transmitting at maximum power.

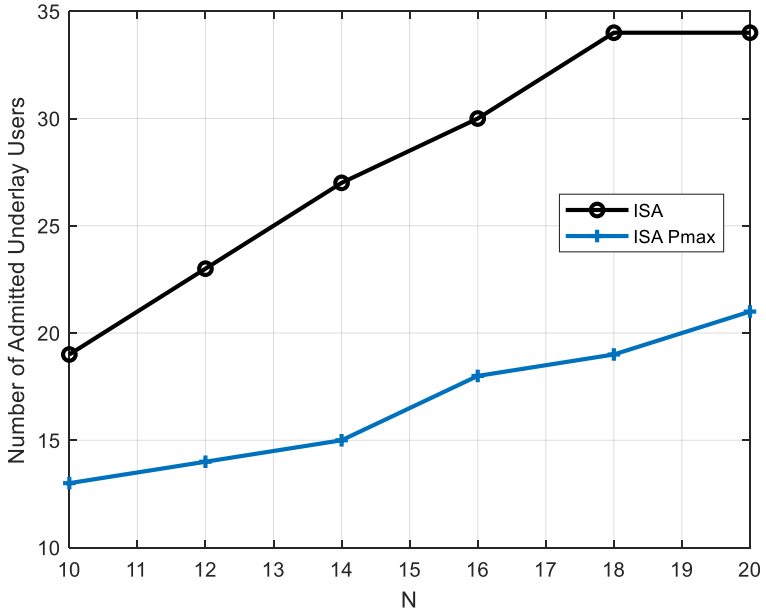

Fig. 4.2. The number of admitted underlay users, D_u varying the number of CUEs, N in the network where $L = M = 20$

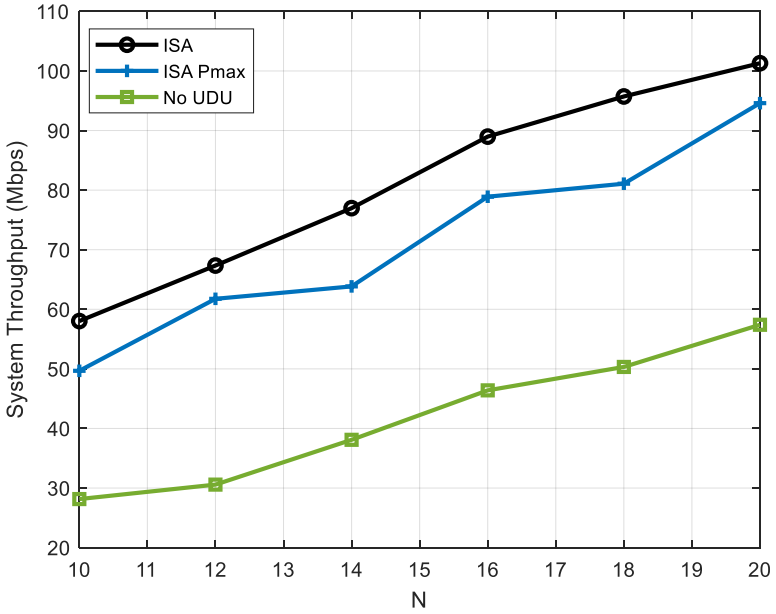

Fig. 4.3. System throughput, T_R for different number of CUEs, N in the network where $L = M = 20$

The effect of varying $\boldsymbol{N}$ on the performance of the system throughput, $\mathbf{T}_{\boldsymbol{R}}$, is shown in Fig. 4.3. It can be seen from the figure that $\mathbf{T}_{\boldsymbol{R}}$ increases with $\boldsymbol{N}$ for the three algorithms. The ISA scheme performed best, showing up to 25.27% and 67.57% higher system throughput compared to ISA-Pmax and No-UDU schemes, respectively, particularly at $\boldsymbol{N} = \mathbf{14}$. This can be attributed to the higher re-use gain of the ISA scheme as a result of spectrum-sharing.

The system throughput gain is shown in Fig. 4.4. The system throughput gain $\mathbf{T}_{\boldsymbol{G}}$ is the increase in the overall network throughput due to spectrum sharing [134] and is evaluated using (4.9).

$$\begin{aligned}\mathbf{T}_{\boldsymbol{G}} = \mathbf{W}_i \sum_{c_i \in C} \log_2\left(1 + \frac{\mathbf{P}_{c_i,\max}\, \boldsymbol{h}_{c,B}}{\mathbf{P}^*_{d_j} \boldsymbol{h}_{d_T,B} + \mathbf{P}^*_{f_k} \boldsymbol{h}_{f_T,B} + \boldsymbol{\sigma}^2_N}\right) \\ + \mathbf{W}_i \sum_{d_j \in D} \log_2\left(\frac{\mathbf{P}^*_{d_j} \boldsymbol{h}_{d_T,d_R}}{\mathbf{P}_{c_i,\max}\, \boldsymbol{h}_{c,d_R} + \mathbf{P}^*_{f_k} \boldsymbol{h}_{f_T,d_R} + \boldsymbol{\sigma}^2_N}\right) \\ + \mathbf{W}_i \sum_{f_k \in F} \log_2\left(\frac{\mathbf{P}^*_{f_k} \boldsymbol{h}_{f_T,f_R}}{\mathbf{P}_{c_i,\max} \boldsymbol{h}_{c,f_R} + \mathbf{P}^*_{d_j} \boldsymbol{h}_{d_T,f_R} + \boldsymbol{\sigma}^2_N}\right) \\ - \mathbf{W}_i \sum_{c_i \in C} \log_2\left(1 + \frac{\mathbf{P}_{c_i,\max}\, \boldsymbol{h}_{c,B}}{\boldsymbol{\sigma}^2_N}\right)\end{aligned} \tag{4.9}$$

It can be seen that $\mathbf{T}_{\boldsymbol{G}}$ increases with $\boldsymbol{N}$. The ISA shows up to 51.26% higher throughput gain in comparison to ISA-Pmax. This can be due to the impact of the power optimisation which translates to an increase in $\mathbf{D}_{\boldsymbol{u}}$ and $\mathbf{T}_{\boldsymbol{G}}$.

The impact of the DUE distance on the system throughput performance is shown in Fig. 4.5. It can be seen that the system throughput decreases as the DUE distance increases for the considered scenario. This is because increasing the DUE distance decreases the channel gain. Therefore, a higher transmit power is required for the DUE minimum SINR to be satisfied.

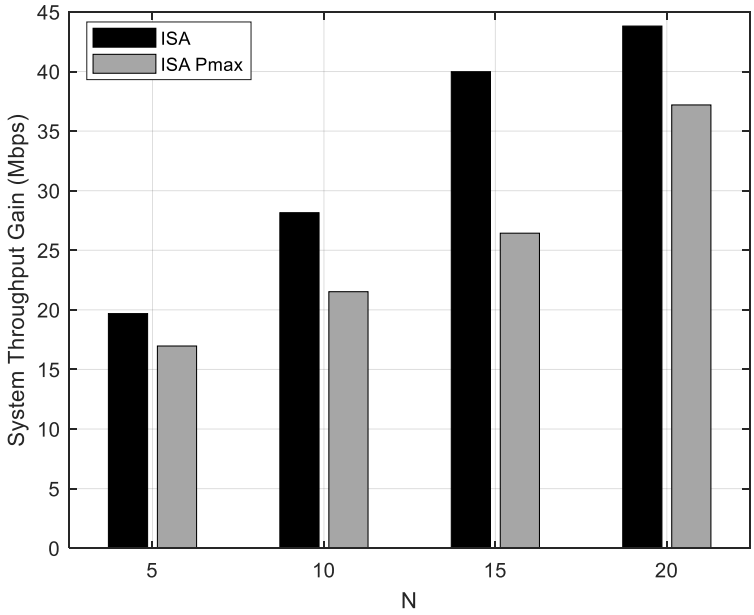

Fig. 4.4. System throughput gain, $\boldsymbol{T_G}$ for different number of CUEs, $\boldsymbol{N}$ in the network where $\boldsymbol{L = M = 20}$

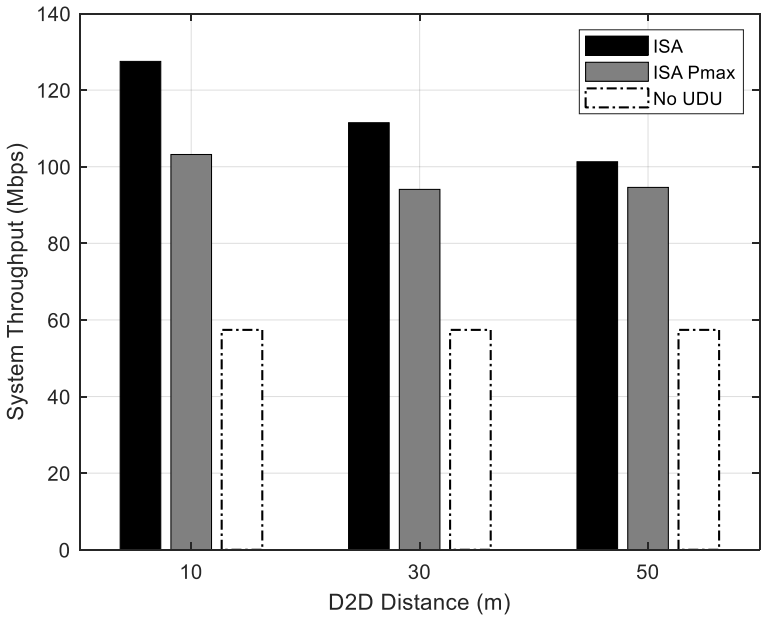

Fig. 4.5. Effect of varying the DUE link distance on the system throughput $\boldsymbol{T_R}$,where $\boldsymbol{L = M = N = 20}$

4.4 Chapter Conclusions

An interference-aware spectrum allocation scheme denoted as ISA, is developed for system throughput maximisation in a two-tier HetNet D2D-enabled cellular network. The network comprises D2D users and femtocell users as underlay to the cellular network. ISA is a heuristic

joint power and channel allocation algorithm presented to solve resource optimisation problem. The objective of the ISA scheme to ensure tolerable interference level among users sharing a channel and the minimum SINR for each user is achieved. The presented solution is compared to schemes with no power control (ISA-Pmax) and with no underlay users (No-UDU). Numerical results show that the presented ISA scheme is resource-efficient, with 25.27% and 65.57% higher throughput compared to Pmax and No-UDU, respectively.

Chapter 5

Joint Power Control and Spectrum Allocation for a Reliable D2D Communication in an Industrial Wireless Environment

In the previous two chapters, interference, and spectrum management, were considered for D2D communication in cellular and multi-tier HetNet. The resource allocation problem was addressed using centralised approaches where the CSI of the links is available at the BS. Current and next-generation wireless networks are ultra-dense and will be deployed in environments with rapidly varying network conditions. The centralised approach requires global information gathering which incurs high signalling overheads resulting from information exchange (which in turn increases the latency in the system), as well as increased computation and complexity as the number of users increase.

To address the aforementioned challenges, a distributed approach, which can capture fast-changing network conditions becomes necessary. Centralised approaches may achieve better performances in comparison to the distributed approaches [100]. However, centralised schemes suffer from higher signalling overheads due to the global acquisition of channel information.

For a distributed approach, it is assumed that UEs are 'selfish', which means that their primary objective is to maximise their individual utility functions. The output of a centralised resource allocation approach may not be in the interest of some UEs. Selfishness and rationality are characteristic features of distributed and intelligent users. Matching theory and machine learning are inherently distributive and can support self-organising resource allocation solutions [26,27]. The distributed approach is device or user-centric. The UEs are capable of making resource management decisions based on local information and partially relying on a centralised controller. The UEs can measure their received SINR values based on locally.

Distributed approaches such as matching theory will be investigated and developed below, because of their scalability and due to their inherent characteristics of self-organisation in high-density deployments such as in FoF. The use case scenario of interest is a scenario with high

reliability and moderate latency, as in the case of non-time critical quality control and sensor data capturing on the factory floor [5] will be considered.

A system consisting of DUEs, which are industrial devices enabled for direct D2D communication and CUEs, is considered. The D2D links are to share channel resources with the cellular users given that the target QoS requirements are satisfied for all users. The CUE and DUE links are characterised by minimum SINR requirements to guarantee their target data rates. Additionally, the DUEs have minimum reliability requirements which are ensured by maintaining the outage probability below a certain threshold. The resource allocation problem is first formulated using a centralised optimisation approach, namely, MINLP which is complex and cannot be solved directly.

A distributed approach is then introduced based on the Stable Marriage Problem (SMP) game theoretic framework. To guarantee the minimum SINR requirement, co-channel interference of the CUEs and DUEs is mitigated based on the distance between the signal link and interfering link so that those users resulting in large interference are avoided. The minimum distance metric was used in [135,136] to determine potential CUE-DUE partners. However, the reuse candidates were obtained before allocating the optimal transmit power, thus possibly missing some potential reuse candidates.

To increase the feasibility of obtaining potential sets of CUE-DUE pairs, the set of power pairs that satisfies the distance metric for potential reuse partners are first obtained. Subsequently, the set of power pairs that guarantees the reliability requirement of the DUEs are then obtained. The optimal power allocation that maximises the sum throughput of all users is finally identified.

5.1 System Model

The uplink of a typical D2D-enabled cellular network for an industrial factory scenario is considered as illustrated in Fig. 5.1. The network is composed of $\boldsymbol{N}$ CUEs and $\boldsymbol{M}$ DUEs deployed randomly. The DUEs are sensors/actuators which are enabled for direct D2D communication and are deployed along the production lines or fixed on the robots. The UEs are considered to be static or quasi-static. $\boldsymbol{C} = \{\boldsymbol{c_1}, \dots, \boldsymbol{c_i}, \dots \boldsymbol{c_N}\}$ denotes the set of CUEs with minimum SINR threshold values to guarantee the data rate requirements. The DUEs are URLLC links denoted by the set $\boldsymbol{D} = \{\boldsymbol{d_1}, \dots, \boldsymbol{d_j}, \dots \boldsymbol{d_M}\}$ with minimum SINR and reliability

requirements. The reliability constraint is guaranteed by controlling the outage probability through setting the received SINR to a minimum target value.

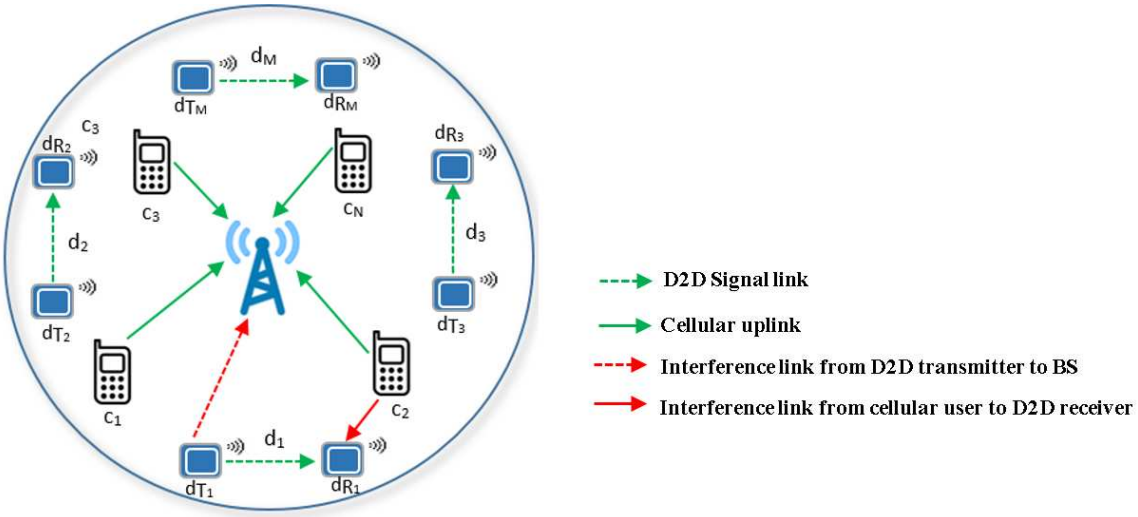

Fig. 5.1. An illustration of D2D communication in the factory underlaying a cellular network

The network is served by a set of orthogonal Physical Resource Blocks (PRBs) following the OFDMA structure, as defined in the 4G and 5G standards. These channels are pre-assigned to the CUEs but can be reused by the DUE links once the minimum QoS requirements of CUEs and DUEs are jointly satisfied. Interference generated by DUE transmitters in the uplink resource-sharing mode only affects the base station. The channel gains for the different links can be expressed as follows:

$$\begin{cases} \boldsymbol{h_{c,B}} = \boldsymbol{G_1}\boldsymbol{\gamma_{c,B}}\boldsymbol{\chi_{c,B}}\boldsymbol{L_{c,B}^{-\alpha_1}} \triangleq \boldsymbol{\zeta_{c,B}}\boldsymbol{L_{c,B}^{-\alpha_1}} \\ \boldsymbol{h_{d_T,B}} = \boldsymbol{G_2}\boldsymbol{\gamma_{d_T,B}}\boldsymbol{\chi_{d_T,B}}\boldsymbol{L_{d_T,B}^{-\alpha_2}} \triangleq \boldsymbol{\zeta_{d_T,B}}\boldsymbol{L_{d_T,B}^{-\alpha_2}} \\ \boldsymbol{h_{d_T,d_R}} = \boldsymbol{G_3}\boldsymbol{\gamma_{d_T,d_R}}\boldsymbol{\chi_{d_T,d_R}}\boldsymbol{L_{d_T,d_R}^{-\alpha_3}} \triangleq \boldsymbol{\zeta_{d_T,d_R}}\boldsymbol{L_{d_T,d_R}^{-\alpha_3}} \\ \boldsymbol{h_{c,d_R}} = \boldsymbol{G_4}\boldsymbol{\gamma_{c,d_R}}\boldsymbol{\chi_{c,d_R}}\boldsymbol{L_{c,d_R}^{-\alpha_4}} \triangleq \boldsymbol{\zeta_{c,d_R}}\boldsymbol{L_{c,d_R}^{-\alpha_4}} \end{cases} \quad (5.1)$$

where $\boldsymbol{h_{c,B}}$, is the channel gain from CUE $\boldsymbol{c_i}$ to the BS. The channel gain from DUE link $\boldsymbol{d_j}$ of transmitter $\boldsymbol{d_T}$ to the receiver $\boldsymbol{d_R}$ is $\boldsymbol{h_{d_T,d_R}}$, the channel gain of the interference link from $\boldsymbol{d_T}$ to the BS is $\boldsymbol{h_{d_T,B}}$ and from CUE $\boldsymbol{c_i}$ to DUE $\boldsymbol{d_j}$ receiver is $\boldsymbol{h_{c,d_R}}$. Rayleigh fading channel is considered with a small-scale fading gain $\boldsymbol{\gamma_{q,r}}$ and assumed to have an exponential distribution with unit mean [137]. The large-scale fading is composed of pathloss with exponent $\boldsymbol{\alpha_k}$ and shadowing, which has a slow fading gain $\boldsymbol{\chi_{q,r}}$ with a log-normal distribution. $\boldsymbol{G_k}$ is the pathloss constant which is depends on antenna gains and frequency [40]. $\boldsymbol{L_{q,r}}$ is the distance from

terminal $\boldsymbol{q}$ to terminal $\boldsymbol{r}$. The received SINR at the BS from CUE $\boldsymbol{c_i}$ and at the DUE $\boldsymbol{d_j}$ receiver $\boldsymbol{d_R}$ are denoted by $\boldsymbol{\Gamma_{c_i}}$ and $\boldsymbol{\Gamma_{d_j}}$ respectively, and given as follows:

$$\boldsymbol{\Gamma_{c_i}} = \frac{\mathbf{P}_{c_i} h_{c,B}}{\sigma_N^2 + \sum_{d_j \in D} \lambda_j^i \mathbf{P}_{d_j} h_{d_T,B}} \tag{5.2}$$

$$\boldsymbol{\Gamma_{d_j}} = \frac{\mathbf{P}_{d_j} h_{d_T,d_R}}{\sigma_N^2 + \sum_{c_i \in C} \lambda_j^i \mathbf{P}_{c_i} h_{c,d_R}} \tag{5.3}$$

where $\mathbf{P}_{c_i}$ and $\mathbf{P}_{d_j}$ are the transmit powers of CUE $\boldsymbol{c_i}$ and DUE $\boldsymbol{d_j}$ respectively, $\boldsymbol{\sigma_N^2}$ is the variance of additive white Gaussian noise of each channel. $\boldsymbol{\lambda_j^i} \in \{\mathbf{0}, \mathbf{1}\}$ is the resource reuse indicator, $\boldsymbol{\lambda_j^i} = \mathbf{1}$ if DUE $\boldsymbol{d_j}$ reuses CUE $\boldsymbol{c_i}$ subchannel and otherwise is 0. The reliability of DUE $\boldsymbol{d_j}$ is expressed in terms of the maximum tolerable outage probability, $\boldsymbol{p_{R_0}}$. The outage probability constraint, $\boldsymbol{p_R}$, is given in (5.4) where $\mathbf{Pr}(.)$ denotes the probability of the input and $\boldsymbol{\Gamma_{d_j,\min}}$ is the minimum target SINR for $\boldsymbol{d_j}$.

$$\boldsymbol{p_R} = \mathbf{P\,r}\left(\boldsymbol{\Gamma_{d_j}} \leq \boldsymbol{\Gamma_{d_j,\min}}\right) \leq \boldsymbol{p_{R_0}} \tag{5.4}$$

The optimisation objective is to maximise the overall system throughput $\mathbf{T_R}$ and formulated as follows:

$$\max_{\lambda_j^i, P_{c_i}, P_{c_j}} \mathbf{T_R} = \boldsymbol{W_i}\left(\sum_{c_i \in C}\left(\mathbf{log_2}\left(\mathbf{1} + \boldsymbol{\Gamma_{c_i}}\right) + \sum_{d_j \in D^{\mathbb{E}}} \boldsymbol{\lambda_j^i}\, \mathbf{log_2}\left(\mathbf{1} + \boldsymbol{\Gamma_{d_j}}\right)\right)\right) \tag{5.5}$$

subject to

$$\boldsymbol{\Gamma_{c_i}} \geq \boldsymbol{\Gamma_{c_i,\min}} \quad \forall\, \boldsymbol{c_i} \in \boldsymbol{C} \tag{5.5a}$$
$$\boldsymbol{\Gamma_{d_j}} \geq \boldsymbol{\Gamma_{d_j,\min}} \quad \forall\, \boldsymbol{d_j} \in \boldsymbol{D}^{\mathbb{E}} \tag{5.5b}$$
$$\boldsymbol{\lambda_j^i p_R} \leq \boldsymbol{p_{R_0}} \quad \forall\, \boldsymbol{d_j} \in \boldsymbol{D}^{\mathbb{E}} \tag{5.5c}$$
$$\mathbf{P}_{c_i} \leq \mathbf{P}_{c_i,\max} \quad \forall\, \boldsymbol{c_i} \in \boldsymbol{C} \tag{5.5d}$$
$$\mathbf{P}_{d_j} \leq \mathbf{P}_{d_j,\max} \quad \forall\, \boldsymbol{d_j} \in \boldsymbol{D}^{\mathbb{E}} \tag{5.5e}$$
$$\sum_{c_i \in C} \boldsymbol{\lambda_j^i} \leq \mathbf{1} \quad \forall\, \boldsymbol{d_j} \in \boldsymbol{D}^{\mathbb{E}} \tag{5.5f}$$
$$\sum_{d_j \in D^{\mathbb{E}}} \boldsymbol{\lambda_j^i} \leq \mathbf{1} \quad \forall\, \boldsymbol{c_i} \in \boldsymbol{C} \tag{5.5g}$$

where $\boldsymbol{W_i}$ is the bandwidth, $\boldsymbol{D}^{\mathbb{E}}$ ($\boldsymbol{D}^{\mathbb{E}} \subseteq \boldsymbol{D}$) denotes the set of admissible DUEs, $\boldsymbol{\Gamma_{c_i,\min}}$ is the minimum SINR for $\boldsymbol{c_i}$. $\mathbf{P}_{c_i,\max}$ and $\mathbf{P}_{d_j,\max}$ denote the maximum transmit powers of $\boldsymbol{c_i}$ and $\boldsymbol{d_j}$, respectively. Constraints 5.5(a) and 5.5(b) are the minimum SINR requirements for $\boldsymbol{c_i}$ and $\boldsymbol{d_j}$, respectively. Constraints 5.5(c) is the outage requirement for a valid matching between $\boldsymbol{c_i}$ and $\boldsymbol{d_j}$. Constraints 5.5(d) and 5.5(e) are to guarantee that the transmit of powers of $\boldsymbol{c_i}$ and $\boldsymbol{d_j}$ lie

within the acceptable limits. Constraints 5.5(f) and 5.5(g) ensure a one-to-one assignment between CUEs and DUEs.

The optimisation problem in (5.5) is an MINLP which is NP-hard. Direct solution to this problem is difficult to obtain. The problem is therefore solved by decomposing it into simpler sub-problems as described in the following section. In the first step, the admission and power control are jointly solved to determine whether $\boldsymbol{c_i}$ and $\boldsymbol{d_j}$ are potential resource-sharing partners. The optimal power allocation that maximises the sum throughput is then obtained. Subsequently, the matching (channel assignment) is identified to find the optimal reuse partner.

5.2 Joint Power and Admission Control (JPAC)

The optimisation problem in (5.5) is solved by first determining whether a DUE is admissible by a CUE. For a DUE $\boldsymbol{d_j}$ to share resources with a CUE $\boldsymbol{c_i}$, constraints 5.5(a) to 5.5(e) must be satisfied. Relaxing the channel assignment constraints (5.5f) and (5.5g), the following is obtained:

$$\boldsymbol{\Gamma_{c_i}} = \frac{\mathbf{P}_{c_i}\zeta_{c,B}L_{c,B}^{-\alpha_1}}{\sigma_N^2 + \mathbf{P}_{d_j}\zeta_{d_T,B}L_{d_T,B}^{-\alpha_2}} \geq \boldsymbol{\Gamma_{c_i,\min}} \tag{5.6a}$$

$$\boldsymbol{\Gamma_{d_j}} = \frac{\mathbf{P}_{d_j}\zeta_{d_T,d_R}L_{d_T,d_R}^{-\alpha_3}}{\sigma_N^2 + \mathbf{P}_{c_i}\zeta_{c,d_R}L_{c,d_R}^{-\alpha_4}} \geq \boldsymbol{\Gamma_{d_j,\min}} \tag{5.6b}$$

$$\boldsymbol{p_R} = \mathbf{P}\,\mathbf{r}\left(\boldsymbol{\Gamma_{d_j}} \leq \boldsymbol{\Gamma_{d_j,\min}}\right) \leq \boldsymbol{p_{R_0}} \tag{5.6c}$$

$$\mathbf{P}_{c_i} \leq \mathbf{P}_{c_i,\max},\ \mathbf{P}_{d_j} \leq \mathbf{P}_{d_j,\max} \tag{5.6d}$$

Equations 5.6(a) and 5.6(b) indicate that the received SINR at the BS and at $\boldsymbol{d_R}$ has to be greater than minimum target threshold values. Considering the relative distances between all participating devices and BS:

$$\begin{cases} \boldsymbol{L_{d_T,B} \geq \Delta_1 \left(L_{c,B}\right)^{\frac{\alpha_1}{\alpha_2}}} \\ \boldsymbol{L_{c,d_R} \geq \Delta_2 \left(L_{d_T,d_R}\right)^{\frac{\alpha_3}{\alpha_4}}} \end{cases} \tag{5.7}$$

where

$$\begin{cases} \boldsymbol{\Delta_1} = \left(\dfrac{\mathbf{P}_{d_j}\Gamma_{c_i,\min}\zeta_{d_T,B}}{\mathbf{P}_{c_i}\zeta_{c,B} - \sigma_N^2\Gamma_{c_i,\min}\left(L_{c,B}\right)^{\alpha_1}}\right)^{\frac{1}{\alpha_2}} \\ \boldsymbol{\Delta_2} = \left(\dfrac{\Gamma_{d_j,\min}\left[\mathbf{P}_{c_i}\zeta_{c,d_R} + \sigma_N^2\left(L_{c,d_R}\right)^{\alpha_3}\right]}{\mathbf{P}_{d_j}\zeta_{d_T,d_R}}\right)^{\frac{1}{\alpha_4}} \end{cases}$$

Setting $\boldsymbol{\alpha_1 = \alpha_2}$ and $\boldsymbol{\alpha_3 = \alpha_4}$, (5.7) becomes:

$$\begin{cases} \boldsymbol{L_{d_T,B} \geq \Delta_1 L_{c,B}} \\ \boldsymbol{L_{c,d_R} \geq \Delta_2 L_{d_T,d_R}} \end{cases} \tag{5.8}$$

From (5.8) it can be inferred that the distance of the interfering link should be greater than the distance of the intended signal link. Therefore, to mitigate interference and guarantee the minimum SINR requirements of $\boldsymbol{c_i}$ and $\boldsymbol{d_j}$, the relative distance between DUE $\boldsymbol{d_j}$ transmitter $\boldsymbol{d_T}$ and the BS should be greater than the distance between the CUE $\boldsymbol{c_i}$ and the BS by $\boldsymbol{\Delta_1}$. Similarly, the distance from CUE $\boldsymbol{c_i}$ to the DUE $\boldsymbol{d_j}$ receiver should be greater than the distance of the DUE link by $\boldsymbol{\Delta_2}$. Next, the power allocations for which (5.8) is valid is determined. The power pair extrema values that can be allocated to $\boldsymbol{c_i}$ and $\boldsymbol{d_j}$ while satisfying (5.7) are given in (5.9). For $\boldsymbol{\Gamma_{c_i,\min}}$ to be satisfied, the minimum transmit power of $\boldsymbol{d_j}$ are expressed in 5.9(a) and 5.9(b). Similarly, for the SINR threshold $\boldsymbol{\Gamma_{d_j,\min}}$ to be guaranteed, the minimum transmit power of $\boldsymbol{d_j}$ and the maximum transmit power $\boldsymbol{c_i}$ are expressed in 5.9(c) and 5.9(d).

$$\mathbf{P}_{\boldsymbol{c_i},\min} = \frac{\Gamma_{c_i,\min}\left(\sigma_N^2 + h_{d_T,B}\mathbf{P}_{d_j,\max}\right)}{h_{c,B}} \tag{5.9a}$$

$$\mathbf{P}^{c}_{\boldsymbol{d_j},\max} = \frac{h_{c,B}\mathbf{P}_{c_i,\max} - \sigma_N^2\Gamma_{c_i,\min}}{h_{d_T,B}\Gamma_{c_i,\min}} \tag{5.9b}$$

$$\mathbf{P}_{\boldsymbol{d_j},\min} = \frac{\Gamma_{d_j,\min}\left(\sigma_N^2 + h_{c,d_R}\mathbf{P}_{c_i,\max}\right)}{h_{d_T d_R}} \tag{5.9c}$$

$$\mathbf{P}^{d}_{\boldsymbol{c_i},\max} = \frac{h_{d_T d_R}\mathbf{P}_{d_j,\max} - \sigma_N^2\Gamma_{d_j,\min}}{h_{c,d_R}\Gamma_{d_j,\min}} \tag{5.9d}$$

$\boldsymbol{P_C}$ and $\boldsymbol{P_D}$ denote the set of transmit extrema power for $\boldsymbol{c_i}$ and $\boldsymbol{d_j}$, respectively.

$$\boldsymbol{P_C} = \left\{\mathbf{P}_{\boldsymbol{c_i},\max},\ \mathbf{P}^{d}_{\boldsymbol{c_i},\max}, \mathbf{P}_{\boldsymbol{c_i},\min}\right\} \tag{5.10a}$$

$$\boldsymbol{P_D} = \left\{\mathbf{P}_{\boldsymbol{d_j},\max},\ \mathbf{P}^{c}_{\boldsymbol{d_j},\max}, \mathbf{P}_{\boldsymbol{d_j},\min}\right\} \tag{5.10b}$$

The possible set of power pairs for $\boldsymbol{c_i}$ and $\boldsymbol{d_j}$ to share the same sub-channel is the Cartesian product of $\boldsymbol{P_C}$ and $\boldsymbol{P_D}$ and expressed in (5.11) as:

$$\boldsymbol{P_{CD}} = \boldsymbol{P_C} \times \boldsymbol{P_D} \triangleq \left\{\left(\mathbf{P}_{\boldsymbol{c_i},\max}, \mathbf{P}_{\boldsymbol{d_j},\max}\right), \left(\mathbf{P}_{\boldsymbol{c_i},\max}, \mathbf{P}^{c}_{\boldsymbol{d_j},\max}\right), \ldots, \left(\mathbf{P}_{\boldsymbol{c_i},\min}, \mathbf{P}_{\boldsymbol{d_j},\min}\right)\right\} \tag{5.11}$$

The invalid power pairs are eliminated from $\boldsymbol{P_{CD}}$. A power pair is invalid if any of the transmit powers in the pair exceed $\mathbf{P}_{\boldsymbol{c_i},\max}$, $\mathbf{P}_{\boldsymbol{d_j},\max}$. This is due to the dependence of the transmit powers

in (5.10) on the channel conditions. For example, a high interference and a low signal channel gain, the transmit power will tend to rise to compensate for the poor channel condition in order to meet the minimum SINR requirement [124].

Let $\boldsymbol{P}_{\boldsymbol{CD}}^{\sim}$ denote the set of invalid power pairs, $\boldsymbol{P}_{\boldsymbol{CD}}^{\sim} \subset \boldsymbol{P}_{\boldsymbol{CD}}$: $\forall \left(\mathbf{P}_{c_i}, \mathbf{P}_{d_j}\right) \in \boldsymbol{P}_{\boldsymbol{CD}}, \mathbf{P}_{c_i} > \mathbf{P}_{c_i,\max}$ or $\mathbf{P}_{d_j} > \mathbf{P}_{d_j,\max}$ or both and $\boldsymbol{P}_{\boldsymbol{CD}}^{-}$ denote the set of valid power pairs.

$$\boldsymbol{P}_{\boldsymbol{CD}}^{-} = \boldsymbol{P}_{\boldsymbol{CD}} - \boldsymbol{P}_{\boldsymbol{CD}}^{\sim} \triangleq \left\{ \left(\boldsymbol{P}_{c_i,}^{-}\, \boldsymbol{P}_{d_j,}^{-}\right)_{\mathbf{1}}, \ldots, \left(\boldsymbol{P}_{c_i,}^{-}\, \boldsymbol{P}_{d_j,}^{-}\right)_{|\boldsymbol{P}_{\boldsymbol{CD}}^{-}|.} \right\} \tag{5.12}$$

Having obtained the set of valid power pairs, the set of power pairs for which the minimum SINR threshold values for $\boldsymbol{c_i}$ and $\boldsymbol{d_j}$ are guaranteed is determined as described in Lemma 1.

Lemma 1. Denoting $\boldsymbol{f_1}\left(\mathbf{P}_{c_i}, \mathbf{P}_{d_j}\right) \triangleq \boldsymbol{\Delta_1}\left(\boldsymbol{L}_{c,B}\right)^{\frac{\alpha_1}{\alpha_2}}$ and $\boldsymbol{f_2}\left(\mathbf{P}_{c_i}, \mathbf{P}_{d_j}\right) \triangleq \boldsymbol{\Delta_2}\left(\boldsymbol{L}_{d_T,d_R}\right)^{\frac{\alpha_3}{\alpha_4}}$, $\boldsymbol{P}_{\boldsymbol{CD}}^{\prime}$ is the set of power pairs for which the minimum SINR of $\boldsymbol{c_i}$ and $\boldsymbol{d_j}$ are satisfied.

$$\boldsymbol{P}_{\boldsymbol{CD}}^{\prime} \triangleq \left\{ \left(\boldsymbol{P}_{c_i,}^{\prime}\, \boldsymbol{P}_{d_j,}^{\prime}\right)_{\mathbf{1}}, \ldots, \left(\boldsymbol{P}_{c_i,}^{\prime}\, \boldsymbol{P}_{d_j,}^{\prime}\right)_{|\boldsymbol{P}_{\boldsymbol{CD}}^{\prime}|.} \right\} = \begin{cases} \boldsymbol{L}_{d_T,B} \geq \boldsymbol{f_1}\left(\mathbf{P}_{c_i}, \mathbf{P}_{d_j}\right) \\ \boldsymbol{L}_{c,d_R} \geq \boldsymbol{f_2}\left(\mathbf{P}_{c_i}, \mathbf{P}_{d_j}\right) \\ \forall \left(\mathbf{P}_{c_i}, \mathbf{P}_{d_j}\right) \in \boldsymbol{P}_{\boldsymbol{CD}}^{-} \end{cases} \tag{5.13}$$

The reliability constraint 5.6(c) is next evaluated. Reliability is expressed in terms of the outage probability. The outage probability of DUE $\boldsymbol{d_j}$ is defined as the probability that the received SINR $\boldsymbol{\Gamma}_{\boldsymbol{d_j}}$, falls below the minimum SINR, $\boldsymbol{\Gamma}_{\boldsymbol{d_j,\min}}$ and expressed as [138]. The reliability requirement is to

$$\mathbf{Pr}\left(\boldsymbol{\Gamma}_{\boldsymbol{d_j}} \leq \boldsymbol{\Gamma}_{\boldsymbol{d_j,\min}}\right) = \int_{\mathbf{0}}^{\boldsymbol{\Gamma}_{\boldsymbol{d_j,\min}}} \boldsymbol{f}_{\boldsymbol{\gamma}}\left(\boldsymbol{\Gamma}_{\boldsymbol{d_j}}\right) \boldsymbol{d\Gamma}_{\boldsymbol{d_j}} = \boldsymbol{F}_{\boldsymbol{\gamma}}(\boldsymbol{\Gamma}_{\boldsymbol{d_j,\min}}) \tag{5.14}$$

where $\boldsymbol{f}_{\boldsymbol{\gamma}}(.)$ and $\boldsymbol{F}_{\boldsymbol{\gamma}}(.)$ denote the Probability Distribution Function (PDF) and Cumulative Distribution Function (CDF), respectively. A closed form expression of the outage probability of DUE $\boldsymbol{d_j}$ conditioned on the selected CUE $\boldsymbol{c_i}$ is defined as [99]:

$$\boldsymbol{p_R} = \mathbf{Pr}\left(\boldsymbol{\Gamma}_{\boldsymbol{d_j}} \leq \boldsymbol{\Gamma}_{\boldsymbol{d_j,\min}}\right) = \mathbf{1} - \frac{\mathbf{P}_{d_j} \boldsymbol{g}_{d_T,d_R} \exp\left(-\frac{\boldsymbol{\Gamma}_{d_j,\min}\sigma_N^2}{\mathbf{P}_{d_j} \boldsymbol{g}_{d_T,d_R}}\right)}{\mathbf{P}_{d_j} \boldsymbol{g}_{d_T,d_R} + \boldsymbol{\Gamma}_{d_j,\min} \mathbf{P}_{c_i} \boldsymbol{g}_{c,,d_R}} \leq \boldsymbol{p}_{\boldsymbol{R_0}} \tag{5.15}$$

where $\boldsymbol{g}_{\boldsymbol{d_T,d_R}} = \boldsymbol{G_3} \boldsymbol{\chi}_{\boldsymbol{d_T,d_R}} \boldsymbol{L}_{\boldsymbol{d_T,d_R}}^{-\boldsymbol{\alpha_3}}$ and $\boldsymbol{g}_{\boldsymbol{c,d_R}} = \boldsymbol{G_4} \boldsymbol{\chi}_{\boldsymbol{c,d_R}} \boldsymbol{L}_{\boldsymbol{c,d_R}}^{-\boldsymbol{\alpha_4}}$. It is assumed that $\boldsymbol{\gamma}_{\boldsymbol{c,B}}$ and $\boldsymbol{\gamma}_{\boldsymbol{d_T,d_R}}$ are Independent and Identically Distributed (I.I.D) exponential random variables.

Having obtained the set of power pairs, $\boldsymbol{P'_{CD}}$, for which the minimum SINR of $\boldsymbol{c_i}$ and $\boldsymbol{d_j}$ is satisfied in (5.13), the solution to the reliability constraint of $\boldsymbol{d_j}$ is expressed using the following Lemma.

Lemma 2. Denoting $\boldsymbol{f_3}\left(\mathbf{P}_{c_i}, \mathbf{P}_{d_j}\right) \triangleq \boldsymbol{p_R}$, the set of power pairs, $\boldsymbol{P^R_{CD}}$ that satisfies the minimum outage probability of $\boldsymbol{d_j}$, for a pairing between $\boldsymbol{c_i}$ and $\boldsymbol{d_j}$ with minimum SINR requirement can be expressed as:

$$\boldsymbol{P^R_{CD}} \triangleq \left\{\left(\boldsymbol{P^R_{c_i,}}\, \boldsymbol{P^R_{d_j,}}\right)_1, \ldots, \left(\boldsymbol{P^R_{c_i,}}\, \boldsymbol{P^R_{d_j,}}\right)_{|\boldsymbol{P^R_{CD}}|}\right\} = \begin{cases} \boldsymbol{f_3}\left(\mathbf{P}_{c_i}, \mathbf{P}_{d_j}\right) \leq \boldsymbol{p_{R_0}} \\ \forall \left(\mathbf{P}_{c_i}, \mathbf{P}_{d_j}\right) \in \boldsymbol{P'_{CD}} \end{cases} \tag{5.16}$$

The minimum QoS of $\boldsymbol{c_i}$ and $\boldsymbol{d_j}$ can be satisfied from (5.16) and expressed using Lemma 3.

Lemma 3. CUE $\boldsymbol{c_i}$ and DUE $\boldsymbol{d_j}$ are potential resource-sharing partners if $\boldsymbol{P^R_{CD}} \neq \emptyset$.

Having addressed the admission and power control to satisfy the minimum QoS requirement for a pairing between $\boldsymbol{c_i}$ and $\boldsymbol{d_j}$, then the optimal transmit power pair for CUE $\boldsymbol{c_i}$ and DUE $\boldsymbol{d_j}$ that maximise the sum throughput is evaluated. This can be expressed as follows:

$$(\mathbf{P}^*_{c_i,}\, \mathbf{P}^*_{d_j}) = \mathbf{arg}\max_{\mathbf{P}_{c_i}, \mathbf{P}_{d_j}} [\boldsymbol{W_i}(\mathbf{log_2}(\mathbf{1} + \boldsymbol{\Gamma}_{c_i}) + \mathbf{log_2}\left(\mathbf{1} + \boldsymbol{\Gamma}_{d_j}\right))] \tag{5.17}$$

subject to (5.6a) – (5.6d)

The optimisation problem in (5.17) aims at finding the power pairs within the set $\boldsymbol{P^R_{CD}}$, that maximise the sum throughput of $\boldsymbol{c_i}$ and $\boldsymbol{d_j}$ and expressed in the following Lemma.

Lemma 4. Denoting $\boldsymbol{f_4}(\mathbf{P}_{c_i}, \mathbf{P}_{d_j}) \triangleq \boldsymbol{W_i}(\mathbf{log_2}(\mathbf{1} + \boldsymbol{\Gamma}_{c_i}) + \mathbf{log_2}\left(\mathbf{1} + \boldsymbol{\Gamma}_{d_j}\right))$, the optimal power pair $(\boldsymbol{P^*_{c_i,}}\, \boldsymbol{P^*_{d_j}})$ in (5.17) is:

$$(\boldsymbol{P^*_{c_i,}}\, \boldsymbol{P^*_{d_j}}) = \mathbf{arg}\max_{(\mathbf{P}_{c_i}, \mathbf{P}_{d_j}) \in \boldsymbol{P^R_{CD}}} \boldsymbol{f_4}\left(\mathbf{P}_{c_i}, \mathbf{P}_{d_j}\right) \tag{5.18}$$

From the above Lemma, it is shown that for a pair $(\boldsymbol{P^*_{c_i,}}\, \boldsymbol{P^*_{d_j}})$, either the CUE or DUE has to transmit at peak power to maximise the sum throughput as will be also demonstrated in the example simulation results.

To identify the resource-sharing pairs satisfying minimum QoS requirements and the optimal power allocations to maximise sum throughput, let $\boldsymbol{R^d_{c_i}}$ be the set of reuse (or admissible) DUEs for CUE $\boldsymbol{c_i}$ and $\boldsymbol{R^c_{d_j}}$ be the set of CUEs that $\boldsymbol{d_j}$ can share resources with. CUEs (DUEs) with

$\boldsymbol{R}_{c_i}^{d} \neq \emptyset$ ($\boldsymbol{R}_{d_j}^{c} \neq \emptyset$) is referred to as eligible CUEs (admissible DUEs). The set of all admissible DUEs, $\boldsymbol{D}^{\mathbb{E}} = \{ \boldsymbol{R}_{c_1}^{d} \cup \boldsymbol{R}_{c_i}^{d} \cup \ldots \cup \boldsymbol{R}_{c_N}^{d}\} \triangleq \{\boldsymbol{d_1}, \ldots, \boldsymbol{d_j}, \ldots, \boldsymbol{d_m}\}$ where $\boldsymbol{m} = |\boldsymbol{D}^{\mathbb{E}}|$ whereas the set of all eligible CUEs, $\boldsymbol{C}^{\mathbb{E}} = \{ \boldsymbol{R}_{d_1}^{c} \cup \boldsymbol{R}_{d_2}^{c} \cup \ldots \cup \boldsymbol{R}_{d_M}^{c}\} \triangleq \{\boldsymbol{c_1}, \ldots, \boldsymbol{c_i}, \ldots, \boldsymbol{c_n}\}$ where $\boldsymbol{n} = |\boldsymbol{C}^{\mathbb{E}}|$, with $|\,.\,|$ indicating the cardinality of the set.

The Joint Power and Admission Control Algorithm (JPAC) to determine the set of eligible CUEs and admissible DUEs with guaranteed minimum QoS requirements, is described in Algorithm 5.1.

Algorithm 5.1 The JPAC Algorithm

1: Input: $\boldsymbol{C}$, $\boldsymbol{D}$, $\boldsymbol{\Gamma}_{c_i,\mathbf{min}}$, $\boldsymbol{\Gamma}_{d_j,\mathbf{min}}$, $\mathbf{P}_{c_i,\mathbf{max}}$ and $\mathbf{P}_{d_j,\mathbf{max}}$
2: Set up the set of admissible DUEs for $\boldsymbol{c_i}$, $\boldsymbol{R}_{c_i}^{d}$, $\boldsymbol{R}_{c_i}^{d} = \emptyset$, $\forall\, \boldsymbol{c_i} \in \boldsymbol{C}$
3: Set up the set of eligible CUEs for $\boldsymbol{d_j}$, $\boldsymbol{R}_{d_j}^{c}$, $\boldsymbol{R}_{d_j}^{c} = \emptyset$, $\forall\, \boldsymbol{d_j} \in \boldsymbol{D}$
4: for $\boldsymbol{c_i} \in \boldsymbol{C}$ $\quad \boldsymbol{1 \leq i \leq N}$ do
5: for $\boldsymbol{d_j} \in \boldsymbol{D}$ $\quad \boldsymbol{1 \leq j \leq M}$ do
6: compute valid set of power pair $\boldsymbol{P}_{\boldsymbol{CD}}^{-}$ as in (5.12)
7: compute set of power pair $\boldsymbol{P}_{\boldsymbol{CD}}'$, for which $\boldsymbol{\Gamma}_{c_i,\mathbf{min}}$ and $\boldsymbol{\Gamma}_{d_j,\mathbf{min}}$ is satisfied as in (5.13)
8: if $\boldsymbol{P}_{\boldsymbol{CD}}' \neq \emptyset$ then
9: compute set of power pair $\boldsymbol{P}_{\boldsymbol{CD}}^{\boldsymbol{R}}$ for which $\boldsymbol{p_R}$ is satisfied as in (5.16)
10: if $\boldsymbol{P}_{\boldsymbol{CD}}^{\boldsymbol{R}} \neq \emptyset$ then
11: $\boldsymbol{d_j}$ is a reuse candidate for $\boldsymbol{c_i}$
12: $\boldsymbol{R}_{c_i}^{d} = \boldsymbol{R}_{c_i}^{d} + \boldsymbol{d_j}$
13: $\boldsymbol{R}_{d_j}^{c} = \boldsymbol{R}_{d_j}^{c} + \boldsymbol{c_i}$
14: compute optimal power allocation $(\boldsymbol{P}_{c_i}^{*}, \boldsymbol{P}_{d_j}^{*})$ as in (5.18)
15: end if
16: end if
17: end for
21: end for
22: $\boldsymbol{C}^{\mathbb{E}} = \{ \boldsymbol{R}_{d_1}^{c} \cup \boldsymbol{R}_{d_2}^{c} \cup \ldots \cup \boldsymbol{R}_{d_M}^{c}\}$
23: $\boldsymbol{D}^{\mathbb{E}} = \{ \boldsymbol{R}_{c_1}^{d} \cup \boldsymbol{R}_{c_i}^{d} \cup \ldots \cup \boldsymbol{R}_{c_N}^{d}\}$
24: Output $\boldsymbol{C}^{\mathbb{E}}$, $\boldsymbol{D}^{\mathbb{E}}$, $\boldsymbol{R}_{c_i}^{d}$ $\forall\, \boldsymbol{c_i} \in \boldsymbol{C}^{\mathbb{E}}$, $\boldsymbol{R}_{d_j}^{c}$ $\forall\, \boldsymbol{d_j} \in \boldsymbol{D}^{\mathbb{E}}$ and $(\boldsymbol{P}_{c_i}^{*}, \boldsymbol{P}_{d_j}^{*})$ for potential $(\boldsymbol{c_i}, \boldsymbol{d_j})$ pairing

5.3 Matching between CUEs and DUEs

Having obtained the sets of eligible CUEs and admissible DUEs, the aim is to find the optimal reuse partner for the CUEs $\forall\, \boldsymbol{c_i} \in \boldsymbol{C}$ with multiple reuse candidates. The optimal resource sharing partner for CUE $\boldsymbol{c_i}$ is DUE $\boldsymbol{d_j}$ that achieves the highest sum rate. When DUE $\boldsymbol{d_j} \in \boldsymbol{D}^{\mathbb{E}}$ reuses the resource of $\boldsymbol{c_i} \in \boldsymbol{C}^{\mathbb{E}}$, the sum rate of the two users is expressed as:

$$\mathbf{T}_{c_i,d_j} = \boldsymbol{W_i}\left(\mathbf{log_2}\left[1+\frac{\boldsymbol{P^*_{c_i}h_{c,B}}}{\boldsymbol{\sigma_N^2 + P^*_{d_j}h_{d_T,B}}}\right] + \mathbf{log_2}\left[1+\frac{\boldsymbol{P^*_{d_j}h_{d_T,d_R}}}{\boldsymbol{\sigma_N^2 + P^*_{c_i}h_{c,d_R}}}\right]\right) \tag{5.19}$$

where $(\boldsymbol{P^*_{c_i,}}\ \boldsymbol{P^*_{d_j}})$ is optimal power as obtained in Lemma 4. Thus, the optimal partner of $\boldsymbol{c_i}$ when there are multiple DUEs is given as:

$$\boldsymbol{d_j^*} = \max_{\boldsymbol{d_j} \in \boldsymbol{R^d_{c_i}}} \mathbf{T}_{c_i,d_j} \tag{5.20}$$

For multiple DUEs and CUEs, the resource allocation procedure becomes complicated as different CUEs can have the same optimal partners and may have varying size of $\boldsymbol{R^d_{c_i}}$. The resource allocation problem can be formulated as:

$$\max_{\boldsymbol{c_i} \in \boldsymbol{C}^{\mathbb{E}}, \boldsymbol{d_j} \in \boldsymbol{D}^{\mathbb{E}}} \boldsymbol{\lambda_j^i}\mathbf{T}_{c_i,d_j} \tag{5.21}$$

such that

$$\textstyle\sum_{\boldsymbol{d_j} \in \boldsymbol{D}^{\mathbb{E}}} \boldsymbol{\lambda_j^i} \leq \mathbf{1} \tag{5.21a}$$

$$\textstyle\sum_{\boldsymbol{c_i} \in \boldsymbol{C}^{\mathbb{E}}} \boldsymbol{\lambda_j^i} \leq \mathbf{1} \tag{5.21b}$$

To solve the assignment problem in (5.21), matching theory techniques, namely, Deferred Acceptance (DA) and Priced Deferred Acceptance (P-DA) are presented, in the following section.

5.4 Matching Theory – The Stable Marriage Problem

The Stable Marriage Problem (SMP) is a category of matching theory or matching game. The resource allocation problem in (5.5) is modelled using the framework of the SMP. The players in the game are a set of eligible CUEs $\boldsymbol{C}^{\mathbb{E}}$ and a set of admissible DUEs $\boldsymbol{D}^{\mathbb{E}}$ (obtained from Algorithm 5.1), with preference profiles that allow them to build their preference list of potential partners. The output of the game is the matching of a CUE channel to a DUE. The definition of matching is given as follows [139]:

Definition 1: A matching $\boldsymbol{\mu}$ between eligible DUEs and eligible CUEs is a function that maps the set of $\boldsymbol{D}^{\mathbb{E}}$ DUEs to set of $\boldsymbol{C}^{\mathbb{E}}$ CUEs such that:

1. $\boldsymbol{\mu}(\boldsymbol{d_j}) \in \boldsymbol{C}^{\mathbb{E}} \cup \{\emptyset\}$ and $|\boldsymbol{\mu}(\boldsymbol{d_j})| \in \{\mathbf{0}, \mathbf{1}\}$
2. $\boldsymbol{\mu}(\boldsymbol{c_i}) \in \boldsymbol{D}^{\mathbb{E}} \cup \{\emptyset\}$ and $|\boldsymbol{\mu}(\boldsymbol{c_i})| \in \{\mathbf{0}, \mathbf{1}\}$

where $\boldsymbol{\mu}(\boldsymbol{d_j}) = \{\boldsymbol{c_i}\} \Leftrightarrow \boldsymbol{\mu}(\boldsymbol{c_i}) = \{\boldsymbol{d_j}\}$, $\forall \boldsymbol{d_j} \in \boldsymbol{D}^{\mathbb{E}}$, $\forall \boldsymbol{c_i} \in \boldsymbol{C}^{\mathbb{E}}$ and $|\boldsymbol{\mu}(.)|$ indicates the cardinality of the outcome. Definition 1 states that $\boldsymbol{\mu}$ is a one-to-one matching which implies one eligible DUE can reuse only one eligible CUE subchannel and an eligible CUE can share its resource with only one eligible DUE to satisfy (5.21). $\boldsymbol{\mu}(\boldsymbol{c_i}), \boldsymbol{\mu}(\boldsymbol{d_j}) = \emptyset$ implies there is no resource-sharing between an eligible CUE and eligible DUE. For any DUE $\boldsymbol{d_j} \in \boldsymbol{D}^{\mathbb{E}}$ and $\boldsymbol{c_i} \in \boldsymbol{C}^{\mathbb{E}}$ such that $\boldsymbol{c_i} \in \boldsymbol{\mu}(\boldsymbol{d_j})$, $\boldsymbol{c_i}$ and $\boldsymbol{d_j}$ prefers to be matched to each other than being unmatched.

Utility Function and Preference Profile

The utility $\boldsymbol{c_i} \in \boldsymbol{C}^{\mathbb{E}}$ obtains from sharing its subchannel with DUEs $\boldsymbol{d_j} \in \boldsymbol{R}_{\boldsymbol{c_i}}^{\boldsymbol{d}}$ is the CUE's throughput and defined as:

$$\boldsymbol{U}_{\boldsymbol{c_i}}^{\boldsymbol{d_j}} = \boldsymbol{W_i} \log_2 \left(1 + \frac{\boldsymbol{P}_{\boldsymbol{c_i}}^{*} \boldsymbol{h}_{\boldsymbol{c},\boldsymbol{B}}}{\boldsymbol{\sigma}_{\boldsymbol{N}}^2 + \boldsymbol{P}_{\boldsymbol{d_j}}^{*} \boldsymbol{h}_{\boldsymbol{d_T},\boldsymbol{B}}}\right) \tag{5.22}$$

while the utility of any eligible DUE $\boldsymbol{d_j} \in \boldsymbol{D}^{\mathbb{E}}$ obtains from reusing subchannel of CUE $\boldsymbol{c_i} \in \boldsymbol{R}_{\boldsymbol{d_j}}^{\boldsymbol{c}}$ is the DUE's throughput when matched to the CUE and defined as:

$$\boldsymbol{U}_{\boldsymbol{d_j}}^{\boldsymbol{c_i}} = \boldsymbol{W_i} \log_2 \left(1 + \frac{\boldsymbol{P}_{\boldsymbol{d_j}}^{*} \boldsymbol{h}_{\boldsymbol{d_T},\boldsymbol{d_R}}}{\boldsymbol{\sigma}_{\boldsymbol{N}}^2 + \boldsymbol{P}_{\boldsymbol{c_i}}^{*} \boldsymbol{h}_{\boldsymbol{c},\boldsymbol{d_R}}}\right) \tag{5.23}$$

Definition 2: A preference relation $\succ$ is a complete, reflexive and transitive binary relation between the set of CUE $\boldsymbol{c_i} \in \boldsymbol{C}^{\mathbb{E}}$ and DUE $\boldsymbol{d_j} \in \boldsymbol{D}^{\mathbb{E}}$. $\forall \boldsymbol{c_i} \in \boldsymbol{C}^{\mathbb{E}}$ define a strict preference relation $\succ_{\boldsymbol{c}}$ over a set of DUEs $\boldsymbol{R}_{\boldsymbol{c_i}}^{\boldsymbol{d}} \subseteq \boldsymbol{D}^{\mathbb{E}}$ such that any two DUEs $\boldsymbol{d_1}, \boldsymbol{d_2} \in \boldsymbol{R}_{\boldsymbol{c_i}}^{\boldsymbol{d}}$, $\boldsymbol{d_1} \neq \boldsymbol{d_2}$,

$$\boldsymbol{d_1} \succ_{\boldsymbol{c_i}} \boldsymbol{d_2} \Leftrightarrow \boldsymbol{U}_{\boldsymbol{c_i}}^{\boldsymbol{d_1}} > \boldsymbol{U}_{\boldsymbol{c_i}}^{\boldsymbol{d_2}} \tag{5.24}$$

This implies that $\boldsymbol{c_i}$ prefers $\boldsymbol{d_1}$ to $\boldsymbol{d_2}$. $\forall \boldsymbol{d_j} \in \boldsymbol{D}^{\mathbb{E}}$, a strict preference relation $\succ_{\boldsymbol{d}}$ is defined over a set of CUEs $\boldsymbol{R}_{\boldsymbol{d_j}}^{\boldsymbol{c}} \subseteq$ such that any two CUEs $\boldsymbol{c_1}, \boldsymbol{c_2} \in \boldsymbol{R}_{\boldsymbol{d_j}}^{\boldsymbol{c}}$ $\boldsymbol{c_1} \neq \boldsymbol{c_2}$,

$$\boldsymbol{c_1} \succ_{\boldsymbol{d_j}} \boldsymbol{c_2} \Leftrightarrow \boldsymbol{U}_{\boldsymbol{d_j}}^{\boldsymbol{c_1}} > \boldsymbol{U}_{\boldsymbol{d_j}}^{\boldsymbol{c_2}} \tag{5.25}$$

This implies that $\boldsymbol{d_j}$ prefers $\boldsymbol{c_1}$ and $\boldsymbol{c_2}$.

With the preference relation, $\forall \boldsymbol{c_i} \in \boldsymbol{C}^{\mathbb{E}}$ and $\forall \boldsymbol{d_j} \in \boldsymbol{D}^{\mathbb{E}}$ can build their preference list $\boldsymbol{PL}_{\boldsymbol{c_i}}$ and $\boldsymbol{PL}_{\boldsymbol{d_j}}$ by ranking $\boldsymbol{R}_{\boldsymbol{c_i}}^{\boldsymbol{d}}$ and $\boldsymbol{R}_{\boldsymbol{d_j}}^{\boldsymbol{c}}$, respectively, giving priority to the ones that provides higher

utility. The solution to the game is a match $\boldsymbol{\mu}$ defined on the set $\boldsymbol{C}^{\mathbb{E}}$ and $\boldsymbol{D}^{\mathbb{E}}$ that assigns a DUE to a CUE.

Definition 3: A matching $\boldsymbol{\mu}$ is stable if there does not exist any pair of CUEs $\boldsymbol{c_i}, \boldsymbol{c_i'} \in \boldsymbol{C}^{\mathbb{E}}$ assigned respectively to DUEs $\boldsymbol{d_j'}, \boldsymbol{d_j} \in \boldsymbol{D}^{\mathbb{E}}$, although $\boldsymbol{c_i}$ prefers $\boldsymbol{d_j}$ to $\boldsymbol{d_j'}$ i.e., $\boldsymbol{d_j} \succ_{\boldsymbol{c_i}} \boldsymbol{d_j'}$ and $\boldsymbol{d_j}$ prefers $\boldsymbol{c_i}$ to $\boldsymbol{c_i'}$ i.e., $\boldsymbol{c_i} \succ_{\boldsymbol{d_j}} \boldsymbol{c_i'}$. $(\boldsymbol{c_i}, \boldsymbol{d_j})$ are said to be blocking pairs.

5.4.1 Deferred Acceptance (DA)

In a standard SMP, there are two disjoint finite sets ($\boldsymbol{X}$ men and $\boldsymbol{Y}$ women) equal in size. In DA, each member of the set ranks the members of the other set. Each $\boldsymbol{x} \in \boldsymbol{X}$ proposes to $\boldsymbol{y} \in \boldsymbol{Y}$ its preference list, starting with the most preferred $\boldsymbol{y}$ and ceases when a proposal is considered, but continues if a proposal is rejected. When $\boldsymbol{y}$ receives a proposal, it is rejected if there is a more preferable proposal, and otherwise agreed to be held for consideration. The algorithm terminates when no $\boldsymbol{x}$ needs to propose [102,104].

When $|\boldsymbol{X}| = |\boldsymbol{Y}|$, with all member of $\boldsymbol{Y}$ is acceptable to $\boldsymbol{x} \in \boldsymbol{X}$, $\forall \boldsymbol{x} \in \boldsymbol{X}$ and all members of $\boldsymbol{X}$ is acceptable to $\boldsymbol{y} \in \boldsymbol{Y}$, $\forall \boldsymbol{y} \in \boldsymbol{Y}$, then the cardinality of the output of the matching is $|\boldsymbol{X}| = |\boldsymbol{Y}|$, i.e., each member of $\boldsymbol{X}$ will be matched to a member $\boldsymbol{Y}$ and vice versa. If $|\boldsymbol{X}| \neq |\boldsymbol{Y}|$, there will be an incomplete preference list and some player(s) will remain unmatched or matched to themselves i.e., $\mu(\boldsymbol{x}) = \boldsymbol{x}$, $\mu(\boldsymbol{y}) = \boldsymbol{y}$. For $|\boldsymbol{X}| < |\boldsymbol{Y}|$, there are $|\boldsymbol{X}|$ matchings i.e., all members of $\boldsymbol{X}$ are matched and $|\boldsymbol{Y} - \boldsymbol{X}|$ are unmatched, given that all members of $\boldsymbol{Y}$ is acceptable to $\boldsymbol{x} \in \boldsymbol{X}$, $\forall \boldsymbol{x} \in \boldsymbol{X}$ and all members of $\boldsymbol{X}$ is acceptable by $\boldsymbol{y} \in \boldsymbol{Y}$, $\forall \boldsymbol{y} \in \boldsymbol{Y}$. For $|\boldsymbol{X}| > |\boldsymbol{Y}|$, there are $|\boldsymbol{Y}|$ matchings i.e., all members of $\boldsymbol{Y}$ are matched and $|\boldsymbol{X} - \boldsymbol{Y}|$ are unmatched, given that all members of $\boldsymbol{Y}$ is acceptable by $\boldsymbol{x} \in \boldsymbol{X}$, $\forall \boldsymbol{x} \in \boldsymbol{X}$ and all members of $\boldsymbol{X}$ is acceptable to $\boldsymbol{y} \in \boldsymbol{Y}$, $\forall \boldsymbol{y} \in \boldsymbol{Y}$. For a scenario where $|\boldsymbol{X}| \neq |\boldsymbol{Y}|$ and there are variations in the sizes of the preference lists of each agent i.e., where some or all members of $\boldsymbol{X}$ are not acceptable to $\forall \boldsymbol{y} \in \boldsymbol{Y}$ and vice versa, the number of matchings will vary. This can occur, for example, if a DUE $\boldsymbol{d_j} \in \boldsymbol{D}$ is not in the preference list of a CUE $\boldsymbol{c_i} \in \boldsymbol{C}$ because resource sharing will violate the QoS requirements. In such scenarios, applying DA might not achieve the optimal matching because the sizes of the sets and the length of the preference lists of each of the player are unequal. Acceptability is defined as the inclusion of a player $\boldsymbol{x} \in \boldsymbol{X}$ in the preference list of $\boldsymbol{y} \in \boldsymbol{Y}$ because it satisfies its requirements and vice versa. The CUEs are assumed to be $\boldsymbol{X}$ and DUEs to be $\boldsymbol{Y}$. The sizes of sets in the problem under consideration depends on $\boldsymbol{n} = |\boldsymbol{C}^{\mathbb{E}}|$ and $\boldsymbol{m} =$

$|\boldsymbol{D}^{\mathbb{E}}|$. Moreover, $\forall \boldsymbol{c_i} \in \boldsymbol{C}^{\mathbb{E}}$ ($\forall \boldsymbol{d_j} \in \boldsymbol{D}^{\mathbb{E}}$), only the members of $\boldsymbol{R}_{\boldsymbol{c_i}}^{\boldsymbol{d}}$ $\left(\boldsymbol{R}_{\boldsymbol{d_j}}^{\boldsymbol{c}}\right)$ is ranked and not set $\boldsymbol{D}$ (set $\boldsymbol{C}$) to construct its preference list.

Definition 4: For $\boldsymbol{n} \neq \boldsymbol{m}$, $\exists \boldsymbol{c_i} \in \boldsymbol{C}^{\mathbb{E}}$ for which $\left|\boldsymbol{PL}_{\boldsymbol{c_i}}\right| = \mathbf{1} = \{\boldsymbol{d_j}\}$ and $\boldsymbol{c_i} \neq \max \boldsymbol{PL}_{\boldsymbol{d_j}}$, then $\boldsymbol{\mu}(\boldsymbol{c_i}) = \emptyset$. This states that if there exist a CUE $\boldsymbol{c_i} \in \boldsymbol{H_c}$, with only one potential DUE partner $\boldsymbol{d_j}$ in its preference list and $\boldsymbol{c_i}$ is not the highest ranked (most preferred) by $\boldsymbol{d_j}$ then $\boldsymbol{c_i}$ will certainly be unmatched at the output $\boldsymbol{\mu}$. Therefore, the output of the matching may not be optimal from a resource sharing point of view using the DA approach, as some eligible CUE(s) might not be matched. To overcome this challenge and maximise number of eligible CUEs sharing their channels, 'Priced' Deferred Acceptance (P-DA) algorithm is presented.

5.4.2 Priced-Deferred Acceptance (P-DA)

It is assumed that each connected UE is charged with fees corresponding to the achieved data rate. Let $\boldsymbol{\pi}_{\boldsymbol{c_i}}$ and $\boldsymbol{\pi}_{\boldsymbol{d_j}}$ represent the price charged per connection for the CUEs and DUEs respectively.

$$\begin{cases} \boldsymbol{\pi}_{\boldsymbol{c_i}} = \boldsymbol{\psi W_i} \log_2(\mathbf{1} + \boldsymbol{\Gamma}_{\boldsymbol{c_i}}) \\ \boldsymbol{\pi}_{\boldsymbol{d_j}} = \boldsymbol{\psi W_i} \log_2(\mathbf{1} + \boldsymbol{\Gamma}_{\boldsymbol{d_j}}) \end{cases} \tag{5.26}$$

where $\boldsymbol{\psi}$ is the price per unit rate and assumed to be uniform for all the UEs. Therefore, the total revenue generated by the BS is given by (5.27).

$$\boldsymbol{U_B}(\boldsymbol{\pi}) = \sum_{\boldsymbol{c_i} \in \boldsymbol{C}} \boldsymbol{\pi}_{\boldsymbol{c_i}} + \sum_{\boldsymbol{d_j} \in \boldsymbol{D}^{\mathbb{E}}} \boldsymbol{\pi}_{\boldsymbol{d_j}} \tag{5.27}$$

with $\mathbf{1} \leq \boldsymbol{i} \leq \boldsymbol{N}$ and $\mathbf{1} \leq \boldsymbol{j} \leq \boldsymbol{D_m}$, where $\boldsymbol{D_m}$ is the number of admitted DUEs. To increase the number of CUE-DUE pairing and the number of admitted DUEs (or reuse gain), $\boldsymbol{d_j} \in \boldsymbol{D}^{\mathbb{E}}$ considers the size of the preference list $\boldsymbol{PL}_{\boldsymbol{c_i}}$, of $\forall \boldsymbol{c_i} \in \boldsymbol{C}^{\mathbb{E}}$ that proposes at each iteration round and gives priority to the most preferred CUE with the least size of $\boldsymbol{PL}_{\boldsymbol{c_i}}$. This is because CUEs with larger sizes of $\boldsymbol{PL}_{\boldsymbol{c_i}}$ will have more DUEs to propose to after being rejected in a previous round of proposals and vice versa. In particular, at iteration $\boldsymbol{k}$, $\forall \boldsymbol{d_j} \in \boldsymbol{D}^{\mathbb{E}}$ will consider the proposal of the most preferred CUE with least size of preference list at iteration $\boldsymbol{k} + \mathbf{1}$, $\left|\boldsymbol{PL}_{\boldsymbol{c_i}}{}^{(\boldsymbol{k}+\mathbf{1})}\right|$, defined in (5.28).

$$\left|\boldsymbol{PL}_{\boldsymbol{c_i}}{}^{(\boldsymbol{k}+\mathbf{1})}\right| \triangleq \left|\boldsymbol{PL}_{\boldsymbol{c_i}}{}^{(\boldsymbol{k}-\mathbf{1})}\right| - \boldsymbol{d}_{\boldsymbol{j}}^{(\boldsymbol{k})} \tag{5.28}$$

Definition 5: For $\boldsymbol{c_i},\ \mathbf{c}_i',\ \mathbf{c}_i'' \in \boldsymbol{C}^{\mathbb{E}},\ \boldsymbol{c_i} \neq \mathbf{c}_i' \neq \mathbf{c}_i''$, that proposes to $\boldsymbol{d_j}$ such that $\boldsymbol{U}_{\boldsymbol{d_j}}^{\mathbf{c}_i'} > \boldsymbol{U}_{\boldsymbol{d_j}}^{\boldsymbol{c_i}} > \boldsymbol{U}_{\boldsymbol{d_j}}^{\mathbf{c}_i''}$, $\left|\boldsymbol{PL}_{\mathbf{c}_i'}\right| > \left|\boldsymbol{PL}_{\boldsymbol{c_i}}\right|, \left|\boldsymbol{PL}_{\mathbf{c}_i''}\right|$ and $\left|\boldsymbol{PL}_{\boldsymbol{c_i}}\right| = \left|\boldsymbol{PL}_{\mathbf{c}_i''}\right|$, $\mathbf{c}_i'$ is the most preferred CUE, while $\boldsymbol{c_i}$ is the most preferred CUE with the least size of preference list, then $\boldsymbol{d_j}$ will consider the proposal of $\boldsymbol{c_i}$ and reject the rest. However, $(\mathbf{c}_i', \boldsymbol{d_j})$ will form a blocking pair at the matching output $\boldsymbol{\mu}$, if $\mathbf{c}_i'$ is the highest ranked CUE that proposes to $\boldsymbol{d_j}$ when the algorithm terminates.

To ensure stability, a monetised incentive-based mechanism to balance the utility loss of $\boldsymbol{d_j}$ is presented. Since utility is in terms of the achieved rate, $\boldsymbol{d_j}$ will demand from the BS, a reduction in its price which is equivalent to its rate loss from being paired with $\boldsymbol{c_i}$ rather than $\mathbf{c}_i'$, else $\boldsymbol{d_j}$ will deviate from the matching.

$\mathbf{T}_{\boldsymbol{d_j}}[\boldsymbol{c_i}]$ and $\mathbf{T}_{\boldsymbol{d_j}}[\mathbf{c}_i']$ denotes the achieved rate from $(\boldsymbol{c_i}\ \boldsymbol{d_j})$ and $(\mathbf{c}_i'\ \boldsymbol{d_j})$ pairing, respectively. The rate loss of $\boldsymbol{d_j}$ is given in (5.29).

$$\boldsymbol{\tau} = \mathbf{T}_{\boldsymbol{d_j}}[\mathbf{c}_i'] - \mathbf{T}_{\boldsymbol{d_j}}[\boldsymbol{c_i}] \tag{5.29}$$

where

$$\boldsymbol{\tau} = \begin{cases} \mathbf{0}, & \boldsymbol{c_i} = \mathbf{c}_i' \\ \mathbf{T}_{\boldsymbol{d_j}}[\mathbf{c}_i'] \leq \boldsymbol{\tau} < \mathbf{T}_{\boldsymbol{d_j}}[\boldsymbol{c_i}], & \textbf{otherwise} \end{cases}$$

The price of the rate loss is given as follows:

$$\boldsymbol{\pi_{\mathcal{L}}} = \boldsymbol{\psi}\ \boldsymbol{\tau} \tag{5.30}$$

The new rate price for $\boldsymbol{d_j}$ for $(\boldsymbol{c_i}\ \boldsymbol{d_j})$ pairing for that balances its rate loss and new revenue for the BS is expressed in (5.31) and (5.32) respectively.

$$\boldsymbol{\pi}_{\boldsymbol{d_j}}^{*} = \boldsymbol{\pi}_{\boldsymbol{d_j}} - \boldsymbol{\pi_{\mathcal{L}}} \tag{5.31}$$

$$\boldsymbol{U}_{\boldsymbol{B}}^{*}(\boldsymbol{\pi}) = \sum_{\boldsymbol{c_i} \in \boldsymbol{C}} \boldsymbol{\pi}_{\boldsymbol{c_i}} + \sum_{\boldsymbol{d_j} \in \boldsymbol{D}^{\mathbb{E}}} \boldsymbol{\pi}_{\boldsymbol{d_j}}^{*} \tag{5.32}$$

The characteristics of the output of the P-DA matching with respect to DA matching in the CUE-DUE pairings are described. In what follows, let $\boldsymbol{c_i}$ denote the most preferred CUE and $\mathbf{c}_i'$ as the most preferred CUE with least preference list at iteration $\boldsymbol{k}$. Let $\boldsymbol{D_M}$ be set of admitted DUE, where $\boldsymbol{D_m} = |\boldsymbol{D_M}|$. $\boldsymbol{D_M}$ is characterised by subsets of DUEs denoted by $\boldsymbol{D_{DA}}$, $\boldsymbol{D}_{-}$ and $\boldsymbol{D}_{+}$. Let $\mathbf{c}_i^{*}$ be the matched partner of $\boldsymbol{d_j}$ under P-DA and $\mathbf{c}_i^{-*}$ be the matched partner of $\boldsymbol{d_j}$

under DA. Without loss of generality, it is assumed that $\mathbf{c}_i^*$ is matched (or makes it final proposal) at iteration $\boldsymbol{k}$.

- $\boldsymbol{D_{DA}}$ is the set of DUEs under P-DA having CUE partners identical with the matching in DA: This implies $\boldsymbol{d_j} \in \boldsymbol{\mu}(\mathbf{c}_i^*) = \boldsymbol{d_j} \in \boldsymbol{\mu}(\mathbf{c}_i^{-*})$, hence $\boldsymbol{U}_{\mathbf{c}_i^*}^{\boldsymbol{d_j}} = \boldsymbol{U}_{\mathbf{c}_i^{-*}}^{\boldsymbol{d_j}}$. This happens if DUE $\boldsymbol{d_j}$ accepts $\mathbf{c}_i^*$ because $\mathbf{c}_i^* = \boldsymbol{c_i} = \mathbf{c}_i'$ under DA and $\mathbf{c}_i^{-*} = \mathbf{c}_i'$, thus $\mathbf{c}_i^* = \mathbf{c}_i^{-*}$.
- $\boldsymbol{D_-}$ is the set of DUEs under P-DA having CUE partners with utilities lower than the matched partners in DA: This implies $\boldsymbol{d_j} \in \boldsymbol{\mu}(\mathbf{c}_i^*)$ under P-DA will generate lower utility for $\boldsymbol{d_j}$ than $\boldsymbol{d_j} \in \boldsymbol{\mu}(\mathbf{c}_i^{-*})$ under DA, hence, $\boldsymbol{U}_{\mathbf{c}_i^*}^{\boldsymbol{d_j}} < \boldsymbol{U}_{\mathbf{c}_i^{-*}}^{\boldsymbol{d_j}}$. If CUE $\mathbf{c}_i^{-*} = \mathbf{c}_i'$, then DUE $\boldsymbol{d_j}$ will consider the proposal of $\mathbf{c}_i^{-*}$ under DA, and reject $\mathbf{c}_i^{-*}$ under P-DA if $\mathbf{c}_i^{-*} \neq \boldsymbol{c_i}$ and be matched to $\mathbf{c}_i^* = \boldsymbol{c_i}$, while the BS incentivises $\boldsymbol{d_j}$ with rate loss price, $\boldsymbol{\pi_{\mathcal{L}}}$ to remain matched to $\mathbf{c}_i^*$.
- $\boldsymbol{D_+}$ is the set of DUEs under P-DA having CUE partners with utilities higher than matched partners DA ($\boldsymbol{d_j} \in \boldsymbol{\mu}(\emptyset)$ in DA inclusive): This implies $\boldsymbol{d_j} \in \boldsymbol{\mu}(\mathbf{c}_i^*)$ under P-DA generate higher utility for $\boldsymbol{d_j}$ than $\boldsymbol{d_j} \in \boldsymbol{\mu}(\mathbf{c}_i^{-*})$ under DA, thus $\boldsymbol{U}_{\mathbf{c}_i^*}^{\boldsymbol{d_j}} > \boldsymbol{U}_{\mathbf{c}_i^{-*}}^{\boldsymbol{d_j}}$. This happens if $\mathbf{c}_i^{-*}$ has been held for consideration by $\boldsymbol{d_j}$ because $\mathbf{c}_i^{-*} = \boldsymbol{c_i}$, while $\mathbf{c}_i^*$ is rejected by a DUE $\boldsymbol{d_j'}$ under P-DA but $\mathbf{c}_i^{-*} = \mathbf{c}_i'$ under DA at some previous iteration $\boldsymbol{k - l}$. At iteration $\boldsymbol{k}$, $\boldsymbol{d_j}$ will be reject $\mathbf{c}_i^{-*}$ and be matched to $\mathbf{c}_i^* = \boldsymbol{c_i} = \mathbf{c}_i'$.

Based on the above analysis, the rate loss price, $\boldsymbol{\pi_l}$ paid by the BS as incentive to $\boldsymbol{d_j} \in \boldsymbol{D_-}$ is offset by the rate price gain due to rate increase by $\boldsymbol{d_j} \in \boldsymbol{D_+}$. The DA and P-DA algorithms are set out in Algorithms 5.2 and 5.3, respectively.

Algorithm 5.2 The DA Algorithm

1: Input $\boldsymbol{C}^{\mathbb{E}}$, $\boldsymbol{D}^{\mathbb{E}}$, $\boldsymbol{R}_{\boldsymbol{c}_i}^{\boldsymbol{d}}\ \forall\, \boldsymbol{c}_i \in \boldsymbol{C}^{\mathbb{E}}$, $\boldsymbol{R}_{\boldsymbol{d}_j}^{\boldsymbol{c}}\ \forall\, \boldsymbol{d}_j \in \boldsymbol{D}^{\mathbb{E}}$ and $(\boldsymbol{P}_{\boldsymbol{c}_i}^{*}, \boldsymbol{P}_{\boldsymbol{d}_j}^{*})$ for potential $(\boldsymbol{c}_i, \boldsymbol{d}_j)$ pairing from Algorithm 5.1.
2: Set up the preference list of eligible CUEs, $\boldsymbol{PL}_{\boldsymbol{c}_i}, \forall\, \boldsymbol{c}_i \in \boldsymbol{C}^{\mathbb{E}}$
3: Set up the preference list of admissible DUEs, $\boldsymbol{PL}_{\boldsymbol{d}_j}, \forall\, \boldsymbol{d}_j \in \boldsymbol{D}^{\mathbb{E}}$
4: Set up a list of unmatched $\boldsymbol{U_M} = \{\boldsymbol{c_i}: \forall \boldsymbol{c_i} \in \boldsymbol{C}^{\mathbb{E}}\}$
5: while $\boldsymbol{U_M} \neq \emptyset$ do
6: $\boldsymbol{c_i}$ proposes to its most preferred $\boldsymbol{d_j} \in \boldsymbol{D}^{\mathbb{E}}$ that it has not proposed to in its preference list, $\forall\, \boldsymbol{c_i} \in \boldsymbol{U_M}$;
7: if $\forall\, \boldsymbol{d_j} \in \boldsymbol{D}^{\mathbb{E}}$ that receives a proposal from $\boldsymbol{c_i} \in \boldsymbol{U_M}$, $\boldsymbol{c_i}$ is more preferred to its current match $\mathbf{c}_i'$ then
8: $\boldsymbol{d_j}$ accepts $\boldsymbol{c_i}$ and rejects $\mathbf{c}_i'$;
9: $\boldsymbol{U_M} = \boldsymbol{U_M} - \boldsymbol{c_i}$;
10: $\boldsymbol{U_M} = \boldsymbol{U_M} + \mathbf{c}_i'$;
11: else
12: $\boldsymbol{d_j}$ rejects $\boldsymbol{c_i}$ and remain matched to $\mathbf{c}_i'$;
13: end if
14: end while
15: output matching $\boldsymbol{\mu}$

Proposition 1: The matching $\boldsymbol{\mu}$ returned by the P-DA algorithm is stable.

Proof: The P-DA algorithm will converge to stable matching after finite number of iterations since $\boldsymbol{m}$ and $\boldsymbol{n}$ are finite. The stable matching for SMP under DA always exists [98]. Proposition 1 is proved by contraction. Assume that the P-DA algorithm produces a matching $\boldsymbol{\mu}$ with a blocking pair $(\boldsymbol{c_i}, \boldsymbol{d_j})$ then $\exists \boldsymbol{c_i'} \in \boldsymbol{\mu}(\boldsymbol{d_j})$: $\boldsymbol{c_i} \succ_{\boldsymbol{d_j}} \boldsymbol{c_i'}$ and $\boldsymbol{d_j} \succ_{\boldsymbol{c_i}} \boldsymbol{\mu}(\boldsymbol{c_i})$. Therefore, $\boldsymbol{c_i}$ must have proposed to $\boldsymbol{d_j}$. Since $\boldsymbol{c_i}$ has proposed and not matched to $\boldsymbol{d_j}$, it means that (i) $\boldsymbol{c_i}$ has been rejected because it not the most preferred CUE with the least preference list. Since $\boldsymbol{c_i}$ was rejected, $\boldsymbol{c_i'}$ will also be rejected as $\boldsymbol{c_i}$ is ranked higher than $\boldsymbol{c_i'}$. Hence, $\boldsymbol{c_i'} \notin \boldsymbol{\mu}(\boldsymbol{d_j})$, which contradicts the assumption or (ii) $\boldsymbol{c_i}$ is the most preferred CUE, but $\boldsymbol{d_j}$ is matched to $\boldsymbol{c_i'}$ because the rate price of $\boldsymbol{d_j}$ has been reduced by the rate loss ratio from being matched to $\boldsymbol{c_i}$. If $\boldsymbol{d_j}$ rejects $\boldsymbol{c_i'}$, then it is matched to $\boldsymbol{c_i}$ and stable by the DA algorithm and so a contradiction to the assumption.

5.5 The Centralised Optimisation Scheme

In the DA and P-DA algorithms, CUEs select their resource-sharing partners that optimise their individual utilities (throughput in this case). To evaluate the performance of the DA and P-DA

algorithms, a centralised optimisation solution for the problem in (5.21) to realise a baseline for comparison, is presented Algorithm 5.4.

Algorithm 5.3 The P-DA Algorithm

1: Input $\boldsymbol{C}^{\mathbb{E}}$, $\boldsymbol{D}^{\mathbb{E}}$, $\boldsymbol{R}_{\boldsymbol{c}_i}^{\boldsymbol{d}}\ \forall\, \boldsymbol{c}_i \in \boldsymbol{C}^{\mathbb{E}}$, $\boldsymbol{R}_{\boldsymbol{d}_j}^{\boldsymbol{c}} \forall\, \boldsymbol{d}_j \in \boldsymbol{D}^{\mathbb{E}}$ and $(\boldsymbol{P}_{\boldsymbol{c}_i}^{*}, \boldsymbol{P}_{\boldsymbol{d}_j}^{*})$ for potential $(\boldsymbol{c}_i, \boldsymbol{d}_j)$ pairing from Algorithm 5.1.
2: Set up the preference list of eligible CUEs, $\boldsymbol{PL}_{\boldsymbol{c}_i}, \forall\, \boldsymbol{c}_i \in \boldsymbol{C}^{\mathbb{E}}$
3: Set up the preference list of admissible DUEs, $\boldsymbol{PL}_{\boldsymbol{d}_j}, \forall\, \boldsymbol{d}_j \in \boldsymbol{D}^{\mathbb{E}}$
4: Set up a list of unmatched CUEs $\boldsymbol{U}_{\boldsymbol{M}} = \{\boldsymbol{c}_i : \forall \boldsymbol{c}_i \in \boldsymbol{C}^{\mathbb{E}}\}$
5: while $\boldsymbol{U}_{\boldsymbol{M}} \neq \emptyset$ do
6: $\boldsymbol{c}_i$ proposes and sends $\left|\boldsymbol{PL}_{\boldsymbol{c}_i}^{(\boldsymbol{k+1})}\right|$ to its most preferred $\boldsymbol{d}_j \in \boldsymbol{D}^{\mathbb{E}}$ that it has not proposed to in its preference list, $\forall\, \boldsymbol{c}_i \in \boldsymbol{U}_{\boldsymbol{M}}$
7: if $\forall\, \boldsymbol{d}_j \in \boldsymbol{D}^{\mathbb{E}}$ that receives a proposal from $\boldsymbol{c}_i \in \boldsymbol{U}_{\boldsymbol{M}}$, $\boldsymbol{c}_i$ is the more preferred CUE with the least preference list, $\left|\boldsymbol{PL}_{\boldsymbol{c}_i}^{(\boldsymbol{k+1})}\right|$, compared to its current match $\mathbf{c}_i''$ and $\mathbf{c}_i'$ is the most preferred CUE then
8: $\boldsymbol{d}_j$ accepts $\boldsymbol{c}_i$ and rejects $\mathbf{c}_i'$ and $\mathbf{c}_i''$;
9: $\boldsymbol{U}_{\boldsymbol{M}} = \boldsymbol{U}_{\boldsymbol{M}} - \boldsymbol{c}_i$;
10: $\boldsymbol{U}_{\boldsymbol{M}} = \boldsymbol{U}_{\boldsymbol{M}} + \mathbf{c}_i'$;
11: $\boldsymbol{U}_{\boldsymbol{M}} = \boldsymbol{U}_{\boldsymbol{M}} + \mathbf{c}_i''$;
12: $\boldsymbol{d}_j$ obtains its rate loss as in (5.29);
13: else
14: $\boldsymbol{d}_j$ rejects $\boldsymbol{c}_i$ and remain matched to $\mathbf{c}_i''$;
15: end if
16: end while
17: output matching $\boldsymbol{\mu}$

Algorithm 5.4 The Centralised Optimisation Scheme

1: Input $\boldsymbol{C}^{\mathbb{E}}$, $\boldsymbol{D}^{\mathbb{E}}$, $\boldsymbol{R}_{\boldsymbol{c}_i}^{\boldsymbol{d}}\ \forall\, \boldsymbol{c}_i \in \boldsymbol{C}^{\mathbb{E}}$, $\boldsymbol{R}_{\boldsymbol{d}_j}^{\boldsymbol{c}} \forall\, \boldsymbol{d}_j \in \boldsymbol{D}^{\mathbb{E}}$ and $(\boldsymbol{P}_{\boldsymbol{c}_i}^{*}, \boldsymbol{P}_{\boldsymbol{d}_j}^{*})$ for potential $(\boldsymbol{c}_i, \boldsymbol{d}_j)$ pairing from Algorithm 5.1.
2: Set up a set of unmatched CUEs, $\boldsymbol{U}_{\boldsymbol{M}} = \{\boldsymbol{c}_i : \forall \boldsymbol{c}_i \in \boldsymbol{C}^{\mathbb{E}}\}$
3: while $\boldsymbol{U}_{\boldsymbol{M}} \neq \emptyset$ do
4: Sort $\boldsymbol{U}_{\boldsymbol{M}}$ in ascending order of $\left|\boldsymbol{R}_{\boldsymbol{c}_i}^{\boldsymbol{d}}\right|$
5: Start with $\boldsymbol{c}_i \in \boldsymbol{C}^{\mathbb{E}}$ with least $\left|\boldsymbol{R}_{\boldsymbol{c}_i}^{\boldsymbol{d}}\right|$
6: if $\exists \boldsymbol{c}_i,\ \mathbf{c}_i' \in \boldsymbol{C}^{\mathbb{E}}, \boldsymbol{c}_i \neq \mathbf{c}_i' : \left|\boldsymbol{R}_{\boldsymbol{c}_i}^{\boldsymbol{d}}\right| = \left|\boldsymbol{R}_{\mathbf{c}_i'}^{\boldsymbol{d}}\right| = \mathbf{1}, \mathbf{T}_{\boldsymbol{c}_i,\boldsymbol{d}_j} > \mathbf{T}_{\mathbf{c}_i',\boldsymbol{d}_j}$ then
7: $\boldsymbol{U}_{\boldsymbol{M}} = \boldsymbol{U}_{\boldsymbol{M}} - \mathbf{c}_i'$
8: end if
9: $\boldsymbol{d}_j^{*} = \underset{\boldsymbol{d}_j \in \boldsymbol{R}_{\boldsymbol{c}_i}^{\boldsymbol{d}}}{\mathbf{argmax}}\, \mathbf{T}_{\boldsymbol{c}_i,\boldsymbol{d}_j}$
10: $\boldsymbol{U}_{\boldsymbol{M}} = \boldsymbol{U}_{\boldsymbol{M}} - \boldsymbol{c}_i$
11: $\boldsymbol{R}_{\boldsymbol{c}_i}^{\boldsymbol{d}} = \boldsymbol{R}_{\boldsymbol{c}_i}^{\boldsymbol{d}} - \boldsymbol{d}_j^{*}\ \ \forall\, \boldsymbol{c}_{-i} \in \boldsymbol{U}_{\boldsymbol{M}}$
12: end while
13: Output matching

5.6 Simulation Case Study and Performance Evaluation

Examples of simulations are carried out to validate and compare the presented algorithms. An industrial environment with a factory floor dimension of $\mathbf{300m \times 300m}$ is simulated. The BS has a $\mathbf{400m}$ cell radius, positioned at the center of the factory layout. $\boldsymbol{N}$ CUEs are randomly distributed within the cell coverage and the $\boldsymbol{M}$ DUEs or factory devices (i.e., sensors and/or actuators enabled for D2D communications links) are also randomly distributed within the factory floor.

For communication between the DUEs, the channel is modeled using the A1-Indoor scenario of the Winner II project [140]. This is a suitable representation of the factory environments where it is assumed the D2D links are usually in proximity, with little spatio-temporal dynamics and are static or quasi-static. The main simulation parameters [127] are summarised in Table 5.1 and the summary of the channel models for the CUE and DUE links are given in Table 5.2. The performance of the P-DA and DA algorithms are investigated and compared to the centralised approach and a random approach.

Table 5.1: Main simulation parameters for the JPAC, DA, P-DA and Centralised Algorithms

Parameter	Value
Carrier frequency, $\boldsymbol{f_c}$	$\mathbf{2GHz}$
System bandwidth	$\mathbf{10MHz}$
Number of resource blocks (RB), $\boldsymbol{K}$	$\mathbf{50}$
RB bandwidth	$\mathbf{180\ kHz}$
Maximum CUE transmit power, $\mathbf{P}_{\boldsymbol{c_i},\mathbf{max}}$	$\mathbf{23dBm}$
Maximum DUE transmit power, $\mathbf{P}_{\boldsymbol{d_j},\mathbf{max}}$	$\mathbf{23dBm}$
D2D distance, $\boldsymbol{L_{d_T,d_R}}$	$\mathbf{10m \leq L_{d_T,d_R} \leq 20m}$
CUE SINR Threshold, $\boldsymbol{\Gamma_{c_i,\mathbf{min}}}$	$\mathbf{7\ dB}$
DUE SINR Threshold, $\boldsymbol{\Gamma_{d_j,\mathbf{min}}}$	$\mathbf{3\ dB}$
Noise power density	$\mathbf{-174\ \frac{dBm}{Hz}}$
Number of CUEs, $\boldsymbol{N}$	$\mathbf{50}$
Number of DUEs, $\boldsymbol{M}$	$\mathbf{50}$
Reliability for DUE, $\boldsymbol{p_{R_0}}$	$\mathbf{10^{-5}}$

Table 5.2: Channel models for P-DA, DA and Centralised Algorithms [130,131,140]

Parameter	In-factory DUE link	UE-UE link	BS-UE link
Pathloss model	$\mathbf{36.8\log_{10}(d[km]) + 94.2 + 20\log_{10}\frac{f_c(MHz)}{5}}$ dB	$\mathbf{40\log_{10}(d[km]) + 49 + 30\log_{10} f_c(MHz)}$ dB	$\mathbf{37.6\log_{10}(d[km]) + 58.83 + 21\log_{10} f_c(MHz)}$ dB
Shadowing	**4dB**	**6dB**	**8dB**
Fast Fading	Rayleigh Fading	Rayleigh Fading	Rayleigh Fading

It is assumed that each CUE has been pre-allocated a sub-channel. Since the aim of the optimisation problem is system throughput maximisation for spectrum sharing scenarios, the metrics for evaluating the performance of the algorithms are the achieved throughput and number of admitted DUEs $\boldsymbol{D_m}$, which corresponds to the number of shared channels. The JPAC algorithm is used to determine the eligible CUEs and admissible DUEs, which are inputs to the centralised optimisation, DA and P-DA algorithms. The centralised approach is used as the reference or baseline algorithm for comparison with the other approaches.

Initially, the impact of varying the outage probability of the DUEs, $\boldsymbol{p_{R_0}}$, on the number of admissible DUEs, $\boldsymbol{n}$, is evaluated. As seen in Fig. 5.2., $\boldsymbol{n}$ gets larger as higher $\boldsymbol{p_{R_0}}$ is allowed. This can be attributed to the fact higher outage probabilities of the DUEs make them more tolerant of interference from the CUEs, thus enabling more CUEs to find potential partners for resource sharing.

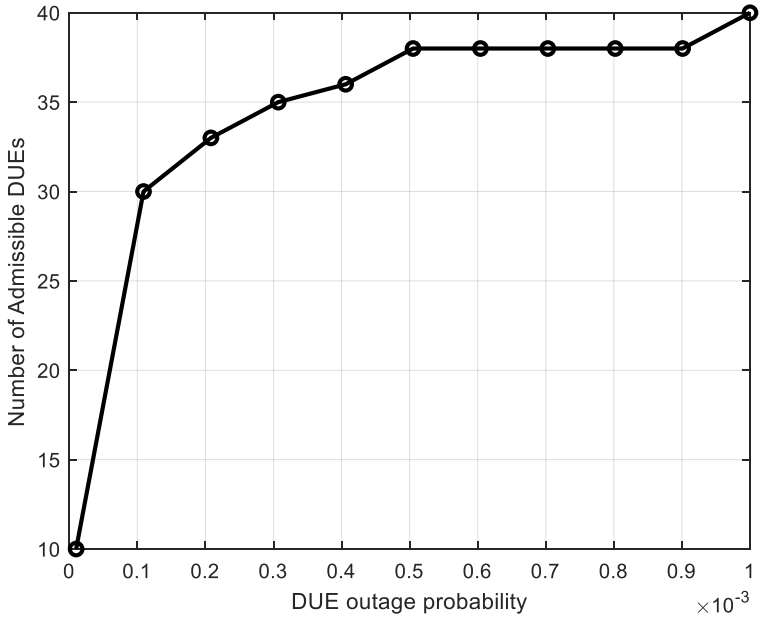

Fig. 5.2. The number of admissible DUEs, $\boldsymbol{n}$ varying the outage probability, $\boldsymbol{p_{R_0}}$, where $\boldsymbol{M = N = 50}$.

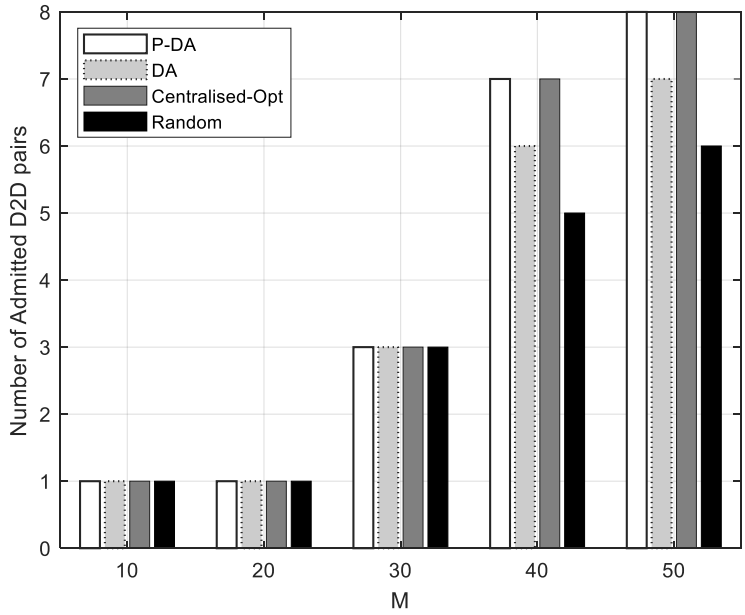

Fig. 5.3. The number of admitted DUEs, $\boldsymbol{D_m}$ varying the number of DUEs, $\boldsymbol{M}$ in the network where $\boldsymbol{N = 50}$, $\mathbf{P}_{c_i,\mathbf{max}} = \mathbf{23dBm}$

The number of admitted DUEs $\boldsymbol{D_m}$ is shown in Fig. 5.3., with $\boldsymbol{N = 50}$ and varying $\boldsymbol{M}$ from $\mathbf{10}\%$ to $\mathbf{100}\%$ of $\boldsymbol{N}$ (5 to 50). $\boldsymbol{D_m}$ remains constant when resource-sharing is not possible due to the violation of QoS requirements as illustrated at $\boldsymbol{M = 10}$ and $\boldsymbol{M = 20,}$ for all four algorithms. $\boldsymbol{D_m}$ increases as more valid pairings are established. Using DA or random allocation algorithms result in a lower performance. For the DA algorithm, $\forall \boldsymbol{c_i} \in \boldsymbol{H_c}$, will have $\boldsymbol{\mu(c_i)} = \emptyset$, resulting in a reduction of $\boldsymbol{D_m}$, while the random approach does not consider any optimisation objectives in the matching process, hence, resulting in a reduced performance. The P-DA algorithm performance is as good as the centralised algorithm because the length of the preference list is considered, and priority is given to CUEs with smaller preference lists at every round of the iteration process. The P-DA algorithm achieves $\mathbf{12}\%$ to $\mathbf{14}\%$ increase in $\boldsymbol{D_m}$ for $\boldsymbol{M > 30}$ in comparison to the DA and random algorithms. As more DUEs $\boldsymbol{M}$ are introduced to the system, when $\boldsymbol{D_m = N}$, the network reaches saturation and no DUE will be accessed.

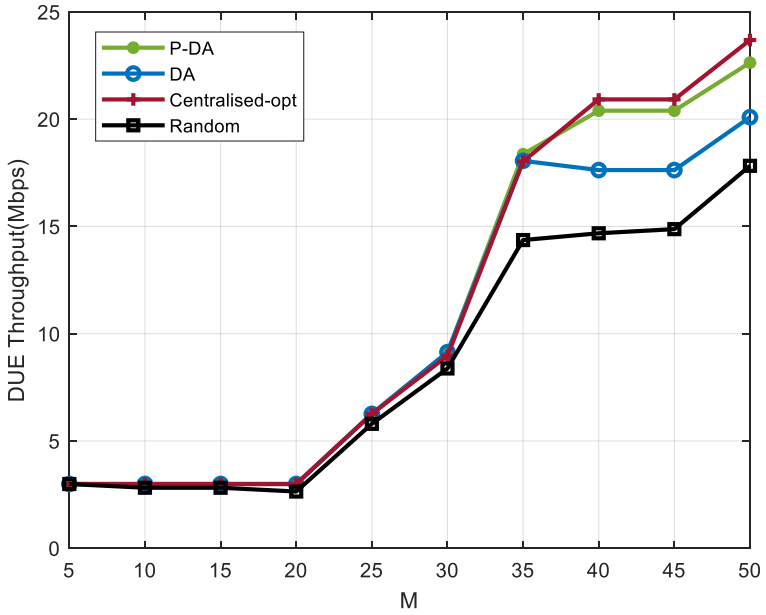

Fig. 5.4. The total DUE throughput with different number of DUEs, $\boldsymbol{M}$ in the network where $\boldsymbol{N = 50}$, $\mathbf{P}_{c_i,\mathbf{max}} = \mathbf{23dBm}$

The number of admitted DUEs $\boldsymbol{D_m}$, directly impacts the throughput performance. In Fig. 5.4., the total DUE throughput with respect to $\boldsymbol{M}$, is shown. Random allocation has the worst performance as expected followed by the DA algorithm. The performance of P-DA is comparable to the centralised approach. The P-DA algorithm achieves 13.57% and 28.02% higher throughput compared to DA and random approaches, respectively. The centralised approach achieves 15.74% and 29.8% higher DUE throughput compared to DA and random algorithm, respectively, at $\boldsymbol{M > 35}$.

In Fig. 5.5., it is shown that the overall system throughput performance increases with $\boldsymbol{M}$. The centralised approach is comparable to the P-DA scheme and outperforms the DA and random approaches. This is mainly because the matching is based on CUE-DUE assignments that provide higher system throughput rather than the satisfaction of individual utilities. The performance of P-DA and DA algorithms are close and significant difference are apparent as $\boldsymbol{M > 35}$, where the P-DA scheme shows an improved system throughput. The random approach has the worst performance as expected since no preference or utility maximisation is considered once the QoS criteria is satisfied.

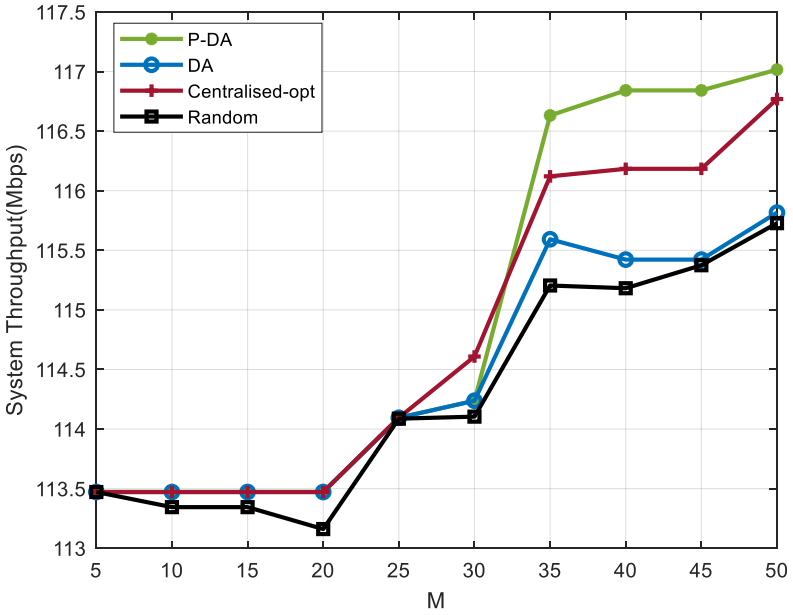

Fig. 5.5. System throughput with different number of DUEs, $\boldsymbol{M}$ in the network where $\boldsymbol{N = 50}$, $\mathbf{P}_{\boldsymbol{c_i},\mathbf{max}} = \mathbf{23dBm}$

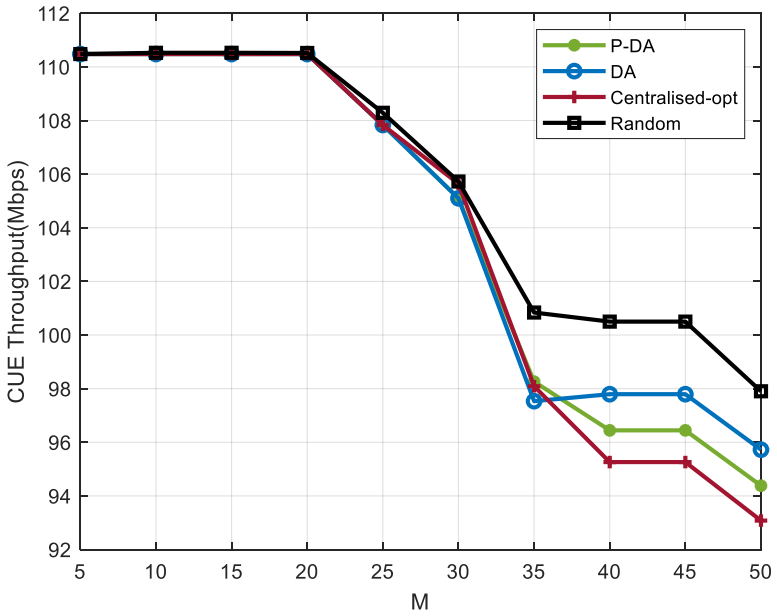

Fig. 5.6. Total CUE throughput with different number of DUEs, $\boldsymbol{M}$ in the network where $\boldsymbol{N = 50}$, $\mathbf{P}_{\boldsymbol{c_i},\mathbf{max}} = \mathbf{23dBm}$

The effects of increasing $\boldsymbol{M}$ on the quality of the CUE links is shown in Fig. 5.6. There is a reduction in the total CUE throughput as $\boldsymbol{M}$ increases as expected. Since CUEs have pre-

allocated sub-channels, the introduction of DUEs will cause the total CUE throughput to decrease as a result of the rate loss caused by interference generated by the DUEs, as $\boldsymbol{D_m}$ increases. This explains the lower performance of the centralised and the P-DA approaches compared to the random and DA approaches as $\boldsymbol{M \geq 35}$.

The performance of the four approaches is compared by investigating the effects of varying the maximum transmit power $\mathbf{P_{max}}$ on the number of admitted DUEs $\boldsymbol{D_m}$. It is concluded that $\boldsymbol{D_m}$ increases with $\mathbf{P_{max}}$ for all approaches as shown in Fig. 5.7. This is as a result of the increase in the $\left| \boldsymbol{R_{c_i}^d} \right|$ and $\left| \boldsymbol{R_{d_j}^c} \right|$ for certain CUEs and DUEs respectively. This translates to an increase in the number of eligible CUEs $\boldsymbol{n}$ and admissible DUEs $\boldsymbol{m}$, therefore increasing the potential of CUE-DUE pairings. It is observed that the optimal power allocation, $(\boldsymbol{P_{c_i}^*}, \boldsymbol{P_{d_j}^*})$, for a pairing $(\boldsymbol{c_i}, \boldsymbol{d_j})$ is increased by the same factor ($\mathbf{2}$dBm, for the studied scenario) as $\mathbf{P_{max}}$ increases (i.e., from $\mathbf{19}$dBm to $\mathbf{21}$dBm, $\mathbf{21}$dBm to $\mathbf{23}$dBm and so on). Again, random matching achieves the worst performance followed by the DA algorithm. The P-DA algorithm is as good as the centralised optimisation approach.

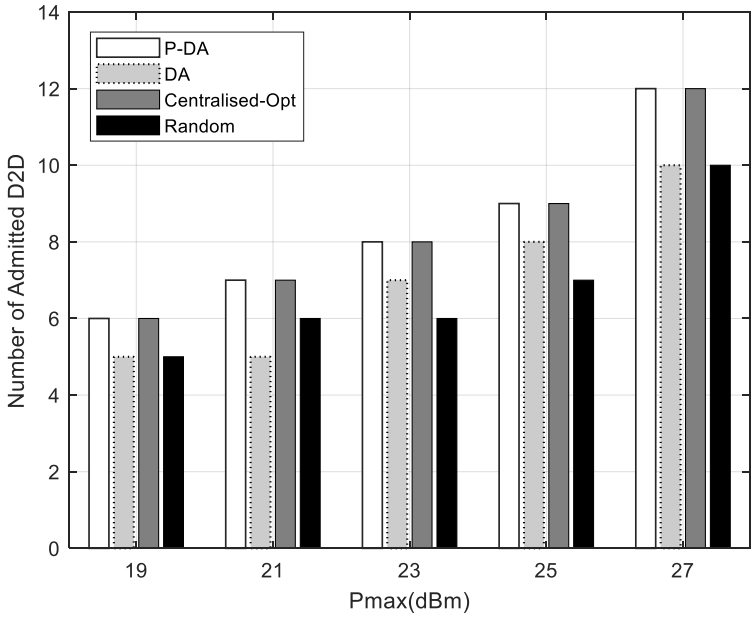

Fig. 5.7. The number of admitted DUEs, $\boldsymbol{D_m}$ versus maximum transmit power where $\boldsymbol{N = M = 50}$

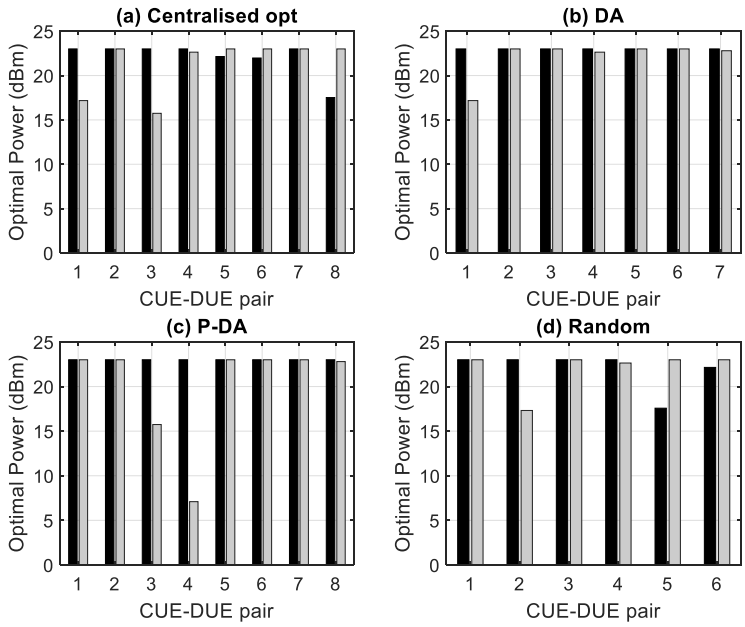

Fig. 5.8. Optimal transmit power ($\boldsymbol{P^*_{c_i,}}$ $\boldsymbol{P^*_{d_j}}$) for CUE-DUE pairing $\mathbf{P_{c_i,max}} = \mathbf{23dBm}$ and $\boldsymbol{N = M = 50}$

In Fig. 5.8., the optimal transmit power ($\boldsymbol{P^*_{c_i,}}$ $\boldsymbol{P^*_{d_j}}$), for a pairing ($\boldsymbol{c_i, d_j}$) is presented for all four algorithms with $\boldsymbol{N = M = 50}$. It is noted that in each case, at least one of the UEs is transmitting at peak power. This is consistent with [136], where it is shown that, at least one transmission power in the optimal power vector must be bounded by the maximum for system's throughput maximisation.

The total revenue generated for the four algorithms is compared and shown in Fig. 5.9. Revenue in this context, is the income generated by the service providers from the UE connection charges. Firstly, the impact of the rate loss price on the total revenue generated for P-DA is investigated, by comparing $\boldsymbol{U^*_B(\pi)}$ and $\boldsymbol{U_B(\pi)}$ for different number of DUE $\boldsymbol{D_m}$, as shown in Fig. 5.9(a). It is observed that the rate loss price $\boldsymbol{\pi_{\mathcal{L}}}$, used to incentivise the DUEs $\boldsymbol{d_j \in D_-}$ has a little effect on $\boldsymbol{U^*_B(\pi)}$ because it is compensated for rate price increase (or gain) by DUEs $\boldsymbol{d_j \in D_+}$. In particular, at $\boldsymbol{M \leq 30}$, $\boldsymbol{U^*_B(\pi) = U_B(\pi)}$ because the DUEs belong to $\boldsymbol{d_j \in D_{DA}}$, thus no incentives were given. At $\boldsymbol{M > 30}$, it is seen that $\boldsymbol{U^*_B(\pi)}$ is only 0.13% to 0.28% less than $\boldsymbol{U_B(\pi)}$ which is a good tradeoff to guarantee stability, improved DUE access rate and throughput. In Fig. 5.9(b), it is seen that the revenue is commensurate with the achieved system throughput (i.e., comparing with Fig. 5.5) for all four algorithms. The P-DA (with incentives) and centralised algorithms are comparable and achieve higher revenues compared to the DA

and random algorithms. This further shows that $\boldsymbol{\pi_{\mathcal{L}}}$ did not significantly affect the total BS revenue.

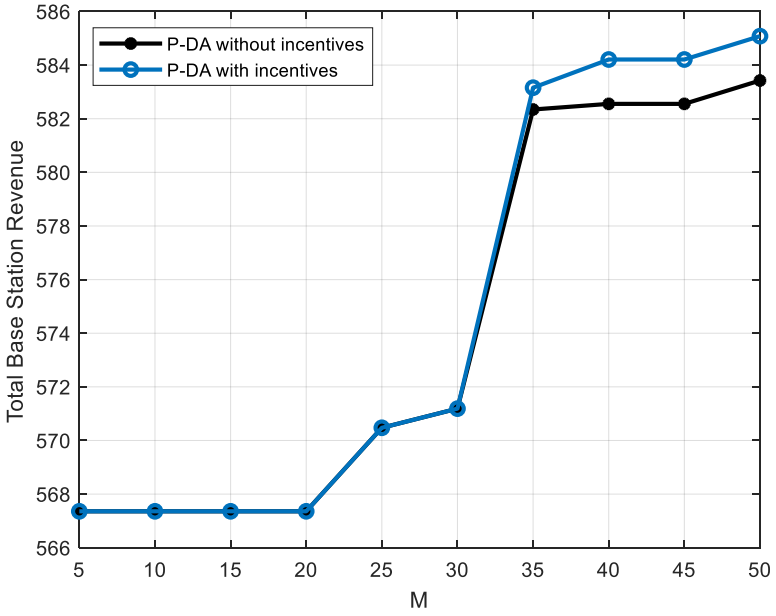

Fig. 5.9(a). Total base station revenue with different number of DUEs, $\boldsymbol{M}$,$\mathbf{P}_{c_i,\mathbf{max}} = \mathbf{23dBm}$, $\boldsymbol{N = 50}$, $\boldsymbol{\psi = 5 \times 10^{-6}}$ for the P-DA algorithm

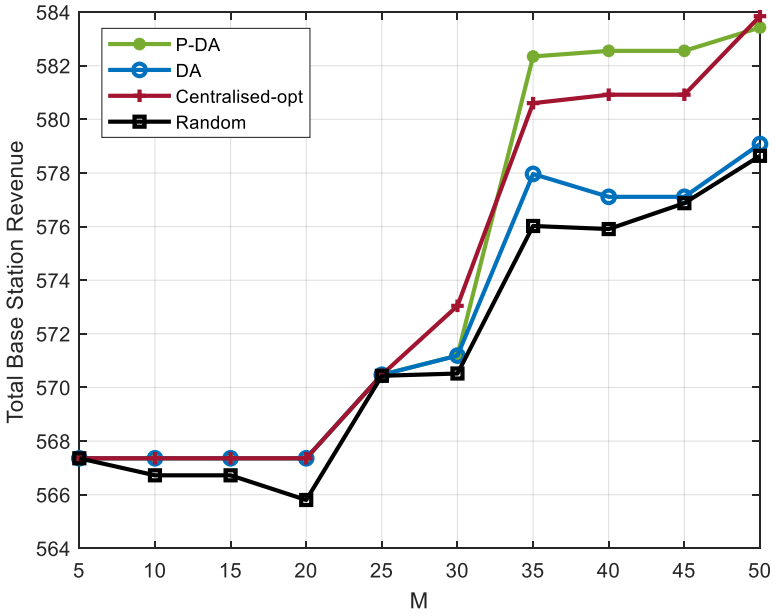

Fig. 5.9(b). Total base station revenue for different number of DUEs, $\boldsymbol{M}$,$\mathbf{P}_{c_i,\mathbf{max}} = \mathbf{23dBm}$, $\boldsymbol{N = 50}$, $\boldsymbol{\psi = 5 \times 10^{-6}}$ for the four algorithms

5.7 Chapter Conclusions

Resource allocation for a D2D-enabled cellular network targetting smart FoF was considered in this chapter. The aim was to maximise the overall system throughput comprising strict QoS requirements D2D links and cellular users in terms of reliability and target SINR, respectively. A matching theory technique, namely, a Priced-Deferred Acceptance (P-DA) algorithm which uses an incentive-based stability to optimise spectrum sharing was presented. Simulation results demonstrate that the P-DA algorithm is comparable in performance with the centralised optimisation approach and shows up to 13% and 28% improvement in throughput relative to the classical DA algorithm and the random matching method, respectively. Therefore, the P-DA scheme offers advantages for improved spectrum utilisation in wireless industrial applications where machine-type connections are expected to support large numbers of sensors/devices. These devices predominantly have small data sizes requirements, which may aggregate into a massive amount of data from concurrent transmissions.

Chapter 6

Autonomous Channel Selection for D2D Links in URLLC

Matching theory techniques for D2D communication with reliability requirements in a FoF, were developed in the previous chapter. In this chapter, channel selection in a D2D-enabled cellular network is considered, focusing on industrial wireless scenarios with latency and reliability QoS requirements. In particular, a time-critical use case with strict requirements on latency and reliability, such as in Augmented Reality (AR) application for maintenance and training [5], will be investigated. A scheme that exploits the advantages of reinforcement learning and matching theory is presented, to perform an autonomous and distributed resource allocation with a guaranteed stable assignment.

Recently, reinforcement learning is gaining a lot of attention because of its suitability in the decision-making process where prior information about the network is unknown. It is widely applicable for modelling dynamic wireless environments [141]. The absence of a central controller in a distributed scheme will result in a reduction in network complexity, signalling overheads and processing load, particularly in heterogeneous environments, making it more feasible for ultra-dense networks.

The approaches presented in this chapter adopt stateless learning, without limiting the performance requirements of the DUEs in order to reduce the learning complexity and the $\boldsymbol{Q}$-table dimension. $\boldsymbol{Q}$-table is lookup table that is used by an agent to store, update the Q-value after an episode and select the best action based on the Q-values**.** A $\boldsymbol{Q}$-table for the CUEs is also maintained and updated rather than having the BS report this information to the DUEs at each time slot. This makes it possible to satisfy not just the QoS of the CUEs but also their preferences, therefore achieving stability by using the DA algorithm for matching. A semi-distributed scheme is also presented where the DUEs upload their trained results to the BS for resource allocation. The performance of the presented approaches is verified using simulations and the results are compared with the centralised technique.

6.1 System Model and Problem Formulation

The coexistence of D2D and cellular communication within a cellular network for uplink resource-sharing in a wireless industrial setting is considered. There are $\boldsymbol{N}$ cellular users (CUEs) of a set $\boldsymbol{C} = \{\boldsymbol{c_1}, \dots, \boldsymbol{c_i}, \dots \boldsymbol{c_N}\}$ and $\boldsymbol{M}$ D2D users (DUEs) are industrial devices and represented by a set $\boldsymbol{D} = \{\boldsymbol{d_1}, \dots, \boldsymbol{d_j}, \dots \boldsymbol{d_M}\}$ deployed randomly within the BS coverage in a single cell network. The DUEs can autonomously select a resource block (RB) denoted by a set $\boldsymbol{K} = \{\boldsymbol{k_1}, \dots, \boldsymbol{k_i}, \dots \boldsymbol{k_N}\}$, from a pool of radio resources [142], which can overlap with that of the CUEs for the resource-sharing. The CUEs have minimum SINR requirement for data rate guarantee. The DUEs also have minimum SINR threshold to guarantee the rate constraints. In addition, the DUEs have reliability and latency requirements. The uplink transmission rate at the BS from $\boldsymbol{i}$th CUE and $\boldsymbol{j}$th DUE receiver $\boldsymbol{d_R}$ from its transmitter $\boldsymbol{d_T}$ over $\boldsymbol{i}$th sub-channel time slot $\boldsymbol{t}$ is given by (6.1) and (6.2), respectively.

$$\mathbf{T}_{c_i}^{k}(\boldsymbol{t}) = \boldsymbol{W_i} \log_2 \left(\mathbf{1} + \boldsymbol{\Gamma}_{c_i}(\boldsymbol{t})\right) \tag{6.1}$$

$$\mathbf{T}_{d_j}^{k}(\boldsymbol{t}) = \boldsymbol{W_i} \log_2 \left(\mathbf{1} + \boldsymbol{\Gamma}_{d_j}(\boldsymbol{t})\right) \tag{6.2}$$

where

$$\boldsymbol{\Gamma}_{c_i}(\boldsymbol{t}) = \frac{\mathbf{P}_{c_i} h_{c,B}(t)}{\sigma_N^2 + \sum_{d_j \in D} \boldsymbol{\lambda}_j^i(t) \mathbf{P}_{d_j} h_{d_T,B}(t)} \tag{6.3}$$

$$\boldsymbol{\Gamma}_{d_j}(\boldsymbol{t}) = \frac{\mathbf{P}_{d_j} h_{d_T,d_R}(t)}{\sigma_N^2 + \sum_{c_i \in C} \boldsymbol{\lambda}_j^i(t) \mathbf{P}_{c_i} h_{c,d_R}(t)} \tag{6.4}$$

$\boldsymbol{\Gamma}_{c_i}(\boldsymbol{t})$ and $\boldsymbol{\Gamma}_{d_j}(\boldsymbol{t})$ are the instantaneous received SINR at the BS and DUE transmitter from respectively. The transmit power of the CUEs and DUEs are represented by $\mathbf{P}_{c_i}$ and $\mathbf{P}_{d_j}$ respectively, $\boldsymbol{\lambda}_j^i(\boldsymbol{t})$ is channel selection indicator if DUE $\boldsymbol{d_j}$ chooses RB $\boldsymbol{i}$ at time slot $\boldsymbol{t}$, where $\boldsymbol{\lambda}_j^i = \mathbf{1}$ indicates $\boldsymbol{j}$th DUE uses $\boldsymbol{i}$th CUE sub-channel and $\boldsymbol{\lambda}_j^i = \mathbf{0}$ otherwise.

The channel gain form link $\boldsymbol{q}$ to $\boldsymbol{r}$ is given in (6.5).

$$\boldsymbol{h_{q,r=} G_k \gamma_{q,r} \chi_{q,r} L_{q,r}^{-\alpha_k}} \tag{6.5}$$

Similar to Chapter 3, Rayleigh fading is considered, with small-scale fading gain $\boldsymbol{\gamma_{q,r}}$ due to multipath propagation and assumed to have an exponential distribution with unit mean [137]. The large-scale fading comprises pathloss with exponent $\boldsymbol{\alpha_k}$ and shadowing which has a slow fading gain $\boldsymbol{\chi_{q,r}}$ with a log-normal distribution. $\boldsymbol{G_k}$ is the pathloss constant which is depends on antenna gains and frequency [65]. $\boldsymbol{L_{q,r}}$ is the distance from terminal $\boldsymbol{q}$ to terminal $\boldsymbol{r}$ [104]. The channel gain from DUE link $\boldsymbol{d_j}$ of transmitter $\boldsymbol{d_T}$ to the receiver $\boldsymbol{d_R}$ is $\boldsymbol{h_{d_T,d_R}}$, the channel gain of the interference link from $\boldsymbol{d_T}$ to the BS is $\boldsymbol{h_{d_T,B}}$ and from CUE $\boldsymbol{c_i}$ to DUE $\boldsymbol{d_j}$ receiver is $\boldsymbol{h_{c,d_R}}$ and $\boldsymbol{h_{c,B}}$, is the channel gain from CUE $\boldsymbol{c_i}$ to the BS.

The CSI in terms of $\boldsymbol{h_{d_T,d_R}}$ and $\boldsymbol{h_{c,d_R}}$ can be estimated at the receiver of the DUE $\boldsymbol{d_R}$ and made available at its transmitter $\boldsymbol{d_T}$ instantaneously. Similarly, $\boldsymbol{h_{c,B}}$ and $\boldsymbol{h_{d_T,B}}$ can be obtained at BS through local information since uplink transmission is considered. The cellular channel gains and interference gains of the DUEs on each RB can be estimated at the BS by local observation and the SINR of the CUEs can be determined. The variance of the additive white Gaussian noise (AWGN) is represented by $\boldsymbol{\sigma_N^2}$, $\boldsymbol{W_i}$ is the bandwidth of the resource blocks.

The reliability of a DUE link $\boldsymbol{d_j} \in \boldsymbol{D}$ is the successful or guaranteed packet delivery within the latency budget. For this work, reliability of $\boldsymbol{d_j} \in \boldsymbol{D}$, $\boldsymbol{\xi_{d_j}(t)}$, is defined as the probability of packet latency exceeding a predefined latency bound $\boldsymbol{l_{d_j,\max}}$, for channel $\boldsymbol{i}$ at slot $\boldsymbol{t}$ is less than a threshold [143]. Only the transmission latency is considered in this work. The system objective is to maximise the data rate of matched CUE and DUEs, while satisfying the QoS requirements in terms of latency constraints as formulated below.

$$\max_{\boldsymbol{\lambda_j^i}} \mathbf{T_R} = \boldsymbol{W_i}\left(\boldsymbol{\lambda_j^i}\left(\sum_{\boldsymbol{c_i}\in\boldsymbol{C}} \mathbf{log_2}\left(\mathbf{1}+\boldsymbol{\Gamma_{c_i}}\right) + \sum_{\boldsymbol{d_j}\in\boldsymbol{D}} \mathbf{log_2}\left(\mathbf{1}+\boldsymbol{\Gamma_{d_j}}\right)\right)\right) \tag{6.6}$$

subject to

$$\boldsymbol{\lambda_j^i}\boldsymbol{\Gamma_{c_i}} - \boldsymbol{\Gamma_{c_i,\min}} \geq \mathbf{0} \qquad \forall\, \boldsymbol{c_i} \in \boldsymbol{C} \tag{6.6a}$$

$$\mathbf{Pr}\left(\boldsymbol{l_{d_j}} > \boldsymbol{l_{d_j,\max}}\right) < \mathbf{1} - \boldsymbol{\xi_{d_j}^*} \qquad \forall\, \boldsymbol{d_j} \in \boldsymbol{D} \tag{6.6b}$$

$$\sum_{\boldsymbol{c_i}\in\boldsymbol{C}} \boldsymbol{\lambda_j^i} \leq \mathbf{1} \qquad \forall\, \boldsymbol{d_j} \in \boldsymbol{D} \tag{6.6c}$$

$$\sum_{\boldsymbol{d_j}\in\boldsymbol{D}} \boldsymbol{\lambda_j^i} \leq \mathbf{1} \qquad \forall\, \boldsymbol{c_i} \in \boldsymbol{C} \tag{6.6d}$$

Constraint (6.6a) is the minimum SINR condition to guarantee the data rate requirement of the CUEs. $\boldsymbol{\Gamma_{c_i,\min}}$ are as defined earlier. In (6.6b), $\boldsymbol{l_{d_j}}$ is the packet latency or time requirement for packet transmission for DUE $\boldsymbol{d_j}$. Constraint (6.6b) takes into account reliability and latency of each DUE. The expression captures the fact that the end-to-end latency should be less than

$\boldsymbol{l_{d_j,\max}}$ with a probability of at least $\mathbf{1}-\boldsymbol{\xi}^{*}_{\boldsymbol{d_j}}$. Constraints (6.6c) and (6.6d) are channel assignment conditions.

The reliability of the D2D links in (6.6c) is evaluated using an empirical estimation of number of packets transmitted from $\boldsymbol{d_T}$ to $\boldsymbol{d_R}$ whose latency is within the budget $\boldsymbol{l_{d_j,\max}}$ over the total number of packets sent to $\boldsymbol{d_R}$ at time slot $\boldsymbol{t}$, similar to [142].

$$\boldsymbol{\xi_{d_j}(t)} = \mathbf{1} - \mathbf{Pr}\left(\boldsymbol{l_{d_j}} > \boldsymbol{l_{d_j,\max}}\right) \approx \mathbf{1} - \frac{\mathbf{L}_{\boldsymbol{d_j}}(\boldsymbol{t})}{\mathbf{B}_{\boldsymbol{d_j}}(\boldsymbol{t})} \cong \frac{\mathbf{L}'_{\boldsymbol{d_j}}(\boldsymbol{t})}{\mathbf{B}_{\boldsymbol{d_j}}(\boldsymbol{t})} \tag{6.7}$$

where $\mathbf{L}_{\boldsymbol{d_j}}(\boldsymbol{t})$ is the number of packets for which $\boldsymbol{l_{d_j}} > \boldsymbol{l_{d_j,\max}}$ and $\mathbf{L}'_{\boldsymbol{d_j}}(\boldsymbol{t})$ is the number of packets transmitted with $\boldsymbol{l_{d_j}} \leq \boldsymbol{l_{d_j,\max}}$ (or number of packet delivered within the latency bound). $\mathbf{B}_{\boldsymbol{d_j}}(\boldsymbol{t})$ is total packet transmitted by DUE $\boldsymbol{d_j}$ at time slot $\boldsymbol{t}$. Reliability can also be measured in terms of the outage probability, which is the probability that the measured SINR is less than a predefined threshold. Using the closed expression of the outage probability of $\boldsymbol{j}$th DUE conditioned on the selected $\boldsymbol{i}$th channel at time slot $\boldsymbol{t}$, [95].

$$\boldsymbol{p_R(t)} = \mathbf{Pr}\left(\boldsymbol{\Gamma_{d_j}} \leq \boldsymbol{\Gamma_{d_j,\min}}\right) = \mathbf{1} - \frac{\mathbf{P}_{\boldsymbol{d_j}} h_{d_T,d_R} \exp\left(-\frac{\boldsymbol{\Gamma_{d_j,\min}}\sigma_N^2}{\mathbf{P}_{\boldsymbol{d_j}} h_{d_T,d_R}}\right)}{\mathbf{P}_{\boldsymbol{d_j}} h_{d_T,d_R} + \boldsymbol{\Gamma_{d_j,\min}} \mathbf{P}_{\boldsymbol{c_i}} h_{c_i,d_R}} \leq \boldsymbol{p_{R_0}} \tag{6.8}$$

where $\boldsymbol{p_R(t)}$ is the measured outage probability of DUE $\boldsymbol{d_j}$ at time slot $\boldsymbol{t}$ and $\boldsymbol{p_{R_0}}$ is the maximum tolerable outage probability of $\boldsymbol{d_j}$. Expressing reliability in terms of outage probability,

$$\boldsymbol{\xi_{d_j}(t)} = \mathbf{1} - \boldsymbol{p_R(t)} \tag{6.9}$$

Transmission latency is given as the ratio of packet size transmitted within latency bound to transmission rate [144]. Combining (6.7), (6.8) and (6.9), the transmission latency of $\boldsymbol{j}$th DUE on the $\boldsymbol{i}$th RB is formulated as:

$$\boldsymbol{l_{d_j}(t)} = \frac{\mathbf{L}'_{\boldsymbol{d_j}}(\boldsymbol{t})}{\boldsymbol{W_i} \mathbf{log_2}\left(\mathbf{1} + \boldsymbol{\Gamma_{d_j}(t)}\right)} \tag{6.10}$$

At each time slot $\boldsymbol{t}$, the resource allocation system has two tasks: I: Determining the SINR $\boldsymbol{\Gamma_{c_i}}$ that the $\boldsymbol{i}$th CUE should achieve to satisfy the minimum condition and the SINR $\boldsymbol{\Gamma_{d_j}}$ that the

$\boldsymbol{j}$th DUE should obtain in order to ensure minimum SINR and target reliability $\boldsymbol{\xi}^{*}_{\boldsymbol{d_j}}$ and II: Allocating RBs to $\boldsymbol{j}$th DUE so that $\mathbf{T}_{\boldsymbol{R}}$ is maximised.

The resource allocation problem for D2D communication in a cellular network is complex and a direct solution is not feasible. Firstly, a D2D resource allocation scheme, denoted as Reinforcement Learning-Based Matching (RLBM), is presented for a fully autonomous and distributed resource allocation. The second method presented is a Base Station Assisted (BS-A) technique, which is semi-distributed.

6.2 Stateless Reinforcement Learning for D2D Resource Allocation

The learning objectives of the agents is to maximise the throughput in a D2D-enabled cellular network. At each time slot $\boldsymbol{t}$, the DUE, observes a state $\boldsymbol{s^t}$ and takes an action $\boldsymbol{a^t}$ from the action space, (i.e., select an RB $\boldsymbol{k_i}$), according to the policy π. $\boldsymbol{Q}$-learning enables an agent to find the optimal policy that maximises its long term expected cumulative reward [116]. The $\boldsymbol{Q}$-value is updated as follows:

$$\boldsymbol{Q^{t+1}(s^t, a^t)} = \begin{cases} \boldsymbol{Q^t(s^t, a^t) + \sigma\left[r^t + \eta \max_{a'} Q^t(s^{t+1}, a^{t+1}) - Q^t(s^t, a^t)\right]} \\ \textbf{if } \boldsymbol{s = s^t,\ \ a = a^t} \\ \boldsymbol{Q^t(s^t, a^t)}\textbf{ , otherwise} \end{cases} \tag{6.11}$$

where $\boldsymbol{\sigma} \in [\mathbf{0}, \mathbf{1}]$ is the learning rate. Setting $\boldsymbol{\sigma}$ to 0 means that the Q-values are never updated, hence no learning has taken place; setting $\boldsymbol{\sigma}$ to a high value means that learning can occur quickly and $\mathbf{0} \leq \boldsymbol{\eta} \leq \mathbf{1}$ is the discount factor, used to balance immediate and future reward [145].

The state space, action space and rewards function in the learning environment are defined as follows:

i. State Space: The state observed by DUE $\boldsymbol{d_j} \in \boldsymbol{D}$, $\boldsymbol{S^i_{d_j}(t)}$, on RB $\boldsymbol{k_i}$ at time slot $\boldsymbol{t}$ is defined by three variables,

$$\boldsymbol{S^i_{d_j}(t)} = \begin{Bmatrix} \boldsymbol{S^i_{\Gamma_{d_j}}} \\ \boldsymbol{S^i_{\xi_{d_j}}} \\ \boldsymbol{S^i_{l_{d_j}}} \end{Bmatrix} \tag{6.12}$$

where $s \in S^i_{d_j} = \{0, 1\}$. $S^i_{\Gamma_{d_j}}(t)$ indicates the interference level measured by DUE $d_j \in D$ on RB k_i at time slot t and defined by

$$S^i_{\Gamma_{d_j}}(t) = \begin{cases} 1 & \Gamma_{d_j}(t) \geq \Gamma_{d_j,\min} \\ 0 & \text{otherwise} \end{cases} \quad (6.12a)$$

$S^i_{\xi_{d_j}}(t)$ indicates the level of reliability measured by DUE $d_j \in D$ on RB k_i at time slot t and defined by

$$S^i_{\xi_{d_j}}(t) = \begin{cases} 1 & \xi_{d_j}(t) \geq \xi^*_{d_j} \\ 0 & \text{otherwise} \end{cases} \quad (6.12b)$$

$S^i_{l_{d_j}}(t)$ indicates the packet transmission time measured by DUE $d_j \in D$ on RB k_i at time slot t and defined by:

$$S^i_{l_{d_j}}(t) = \begin{cases} 1 & l_{d_j}(t) \leq l_{d_j,\max} \\ 0 & \text{otherwise} \end{cases} \quad (6.12c)$$

Given this, there are eight possible states are defined in Table 6.1.

Table 6.1: State space for DUEs

$S^i_{\Gamma_{d_j}}$	$S^i_{\xi_{d_j}}$	$S^i_{l_{d_j}}$	$S^i_{d_j}$
0	0	0	0
0	0	1	0
0	1	0	0
0	1	1	0
1	0	0	0
1	0	1	0
1	1	0	0
1	1	1	1

To reduce the state-action dimension, a stateless learning is adopted. For the scenario under consideration, any action $a_i \in A$ taken by an agent will result in the end of an episode i.e., states 0 and 1 are terminal states, where $S^i_{d_j}(t) = 1$ is the goal state of the DUEs. A stateless Q-learning, therefore, can completely model the learning environment using action-reward only since there is state transition is not required. An agent can choose its action based solely on its Q-value and the updated Q-value of the chosen action is based on the current Q-value and the immediate return from selecting that action. The update function in (6.11) is re-formulated as follows:

$$\boldsymbol{Q^{t+1}(a^t)} = \begin{cases} \boldsymbol{Q^t(a^t) + \sigma[r(a^t) - Q^t(a^t)]}, \textbf{if } \boldsymbol{a = a^t} \\ \boldsymbol{Q^t(a^t)}, \qquad \textbf{otherwise} \end{cases} \tag{6.13}$$

where $\boldsymbol{r(a^t)}$ is the immediate reward of selecting $\boldsymbol{a}$. Comparing (6.11) i.e., (standard $\boldsymbol{Q}$-value update function) with (6.13), it can be seen that not only the state-action formation $(\boldsymbol{s, a})$, is not necessary but also the information of next state $\boldsymbol{s^{t+1}}$ is not required because the actions lead to the terminal state. This reduces the complexity of learning and the size of the $\boldsymbol{Q}$-table. Therefore, resulting in a $\boldsymbol{1 \times |N|}$ dimension $\boldsymbol{Q}$-table for $\boldsymbol{j}$th DUE. The $\boldsymbol{Q}$-table is defined in terms of the actions only and updated using the immediate reward.

To ensure the efficacy of the resource allocation the conventional CUEs need to be protected from the interference from the DUEs for the minimum SINR to be guaranteed. This has been addressed by including SINR of the CUE $\boldsymbol{\Gamma_{c_i}}$ in the state space or reward function modelling. In this way, the DUEs can obtain the information from the BS at time slot $\boldsymbol{t}$ as in [82,116, 122,146]; hence, the DUEs get a positive reward if the CUE SINR on the selected RB attains a value which is at least $\boldsymbol{\Gamma_{c_i,\min}}$ and a negative reward if below $\boldsymbol{\Gamma_{c_i,\min}}$. Rather than the BS reporting the CUE SINR $\boldsymbol{\Gamma_{c_i}}$ with the DUEs for every action $\boldsymbol{a^t}$ taken at each time slot, a scheme is adopted in which the BS keeps a $\boldsymbol{Q}$-table of the $\boldsymbol{i}$th CUE based on the actions on the DUEs. Therefore, the $\boldsymbol{Q}$-table for the $\boldsymbol{i}$th CUE is $\boldsymbol{1 \times |M|}$ considering a stateless $\boldsymbol{Q}$-learning formation.

ii. Action Space: The action space of DUE $\boldsymbol{d_j \in D}$ is a set of all actions denoted by $\boldsymbol{A = \{a_1^t, \dots, a_i^t, \dots a_N^t\}}$, where $\boldsymbol{a_i^t}$ as the action taken by $\boldsymbol{d_j \in D}$ at time slot $\boldsymbol{t}$ and defined as the selection of an RB $\boldsymbol{k_i}$.

iii. Action-Selection Strategy: There are a number of methods to select an action based on the current evaluation of the $\boldsymbol{Q}$-value at every time slot using a policy denoted by $\boldsymbol{\pi}$. These methods are used to balance exploration and exploitation [123]. Epsilon greedy ($\boldsymbol{\varepsilon}$-greedy) is one among other methods of choosing an optimal $\boldsymbol{Q}$-value and described as follows:

$$\boldsymbol{\pi} = \begin{cases} \boldsymbol{\underset{a \in A}{\operatorname{argmax}}\, Q(a)} & \textbf{probability } \boldsymbol{1 - \varepsilon} \textbf{ (exploitation)} \\ \textbf{Random action} & \textbf{probability } \boldsymbol{\varepsilon} \textbf{ (exploration)} \end{cases} \tag{6.14}$$

where $\boldsymbol{\varepsilon}$ is the exploration rate with $\boldsymbol{0 \leq \varepsilon \leq 1}$. The exploration rate is the probability that the agents will explore the environment rather than exploit it. $\boldsymbol{\varepsilon \to 1}$ results in greater exploration whereas $\boldsymbol{\varepsilon \to 0}$ means greater exploitation.

iv. Reward Function: The reward function is designed such that it relies only on local observations and can be implemented independently. The rewards of the $\boldsymbol{j}$th DUE and $\boldsymbol{i}$th CUE for taking an action $\boldsymbol{a_i^t}$ is expressed in terms of the achievable rate using the Shannon capacity formula. Thus, the reward is directly linked to the objective function of the optimisation problem. The reward function is given by (6.15).

$$\boldsymbol{r_{d_j}(a^t) = \begin{cases} \mathrm{T}_{d_j}^{k}(t) & \mathrm{S}_{d_j}^{i}(t) = 1 \\ 0, & \mathrm{S}_{d_j}^{i}(t) = 0 \end{cases}} \tag{6.15a}$$

$$\boldsymbol{r_{c_i}(a^t) = \begin{cases} \mathrm{T}_{c_i}^{k}(t) & \Gamma_{c_i} \geq \Gamma_{c_i,\min} \\ 0, & \text{otherwise} \end{cases}} \tag{6.15b}$$

Equation (6.15) shows that $\boldsymbol{j}$th DUE only gets a reward when all the state variables are 1 (i.e., the minimum QoS requirements are met), while $\boldsymbol{i}$th CUE gets a reward if its minimum SINR is satisfied at each time slot for the action taken by $\boldsymbol{j}$th DUE. From the reward function defined above, learning can be implemented independently in a decentralised manner such that each agent will maintain a local $\boldsymbol{Q}$-table. There is no information exchange related to other agents' actions or rewards and no cooperation is needed between the agents, which results in reduced signalling overheads and reduced complexity compared to a centralised $\boldsymbol{Q}$-learning approach. The Q-value of the $\boldsymbol{j}$th DUE for selecting $\boldsymbol{i}$th RB at time slot $\boldsymbol{t}$ is updated as follows:

$$\boldsymbol{Q_{d_j}^{i}(a^t) = \begin{cases} Q_{d_j}^{i}(a^t) + \sigma\left[r_{d_j}(a^t) - Q_{d_j}^{i}(a^t)\right], \text{if } a = a^t \\ Q_{d_j}^{i}(a^t), \quad \text{otherwise} \end{cases}} \tag{6.16a}$$

Similarly, the Q-value of the $\boldsymbol{i}$th CUE for action taken by the $\boldsymbol{j}$th DUE is updated as follows:

$$\boldsymbol{Q_{c_i}^{j}(a^t) = \begin{cases} Q_{c_i}^{j}(a^t) + \sigma\left[r_{c_i}(a^t) - Q_{c_i}^{j}(a^t)\right], \text{if } a = a^t \\ Q_{c_i}^{j}(a^t), \quad \text{otherwise} \end{cases}} \tag{6.16b}$$

From (6.16), it can be seen that after the training, the Q-table of the $\boldsymbol{j}$th DUE, $\boldsymbol{Q_{d_j}(a)}$, will return $\boldsymbol{Q_{d_j}^{i}(a) = 0}$ for its action on $\boldsymbol{i}$th RB that do not meet its QoS requirements. Similarly, the $\boldsymbol{Q}$-table of the $\boldsymbol{i}$th CUE, $\boldsymbol{Q_{c_i}(a)}$, will return $\boldsymbol{Q_{c_i}^{j}(a) = 0}$ for the action of $\boldsymbol{j}$th DUE on $\boldsymbol{i}$th RB that do not meet its QoS requirements.

6.2.1 Reinforcement Learning Based Matching (RLBM)

The goal of each DUE is to obtain its own preferred cellular channel without being affected by other DUEs. Therefore, the DUEs can learn their strategies independently, so their actions have no effect on each other. Creating $\boldsymbol{Q}$-tables for the CUEs make it compliant with the structure of the Stable Matching Problem (SMP). A Reinforcement Learning Based Matching (RLBM) is presented as shown in Algorithm 6.1. After the training of the agents is accomplished, the local $\boldsymbol{Q}$-tables are ordered to build their preference profiles. The matching phase is implemented using the DA algorithm [104], which converges to a stable output with DUEs sending proposals and CUEs accepting/rejecting proposals.

6.2.2 Base Station Assisted Reinforcement Learning (BS-A)

In the RLBM technique, the matching is implemented using the DA procedure, which is a decentralised scheme, to find a stable assignment between the CUEs and the DUEs with sub-optimal system throughput performance. Hence, the autonomy of the DUEs and the preferences of the UEs are considered in the resource allocation. However, the process of accepting/rejecting proposals involves messaging passing between UEs which will incur some amount signalling overheads.

A Base Station Assisted (BS-A) approach to optimise the achieved system throughput, is presented. For this method, after the training phase, each DUE loads its Q-value table, $\boldsymbol{Q}_{d_j}(\boldsymbol{a})$, to the BS for centralised matching. The BS will allocate a cellular RB to the D2D link that maximises the total Q-values (of the CUE and DUE) on the channel and there is no need for information exchange between the UEs to find a preferred candidate. The BS-A is given in Algorithm 6.2.

Algorithm 6.1 The RLBM Algorithm

1: Initialise the action-value function for the DUEs

$\left[\boldsymbol{Q_{d_j}(a) = 0 | Q_{d_j}(a) \equiv Q^{i}_{d_j}(a^t)}, \boldsymbol{i = 1, 2, \dots, N}\right] \quad \forall\, \boldsymbol{d_j \in D}$

2: Initialise the action-value function for the CUEs

$\left[\boldsymbol{Q_{c_i}(a) = 0 | Q_{c_i}(a) \equiv Q^{j}_{c_i}(a^t),\ j = 1, 2, \dots, M}\right] \quad \forall\, \boldsymbol{c_i \in C}$

3: for $\boldsymbol{d_j \in D}$ $\boldsymbol{1 \le j \le M}$ do

4: while not converge do

5: generate a random number $\boldsymbol{x \in \{0, 1\}}$

6: if $\boldsymbol{x < \varepsilon}$ then

7: Select action $\boldsymbol{a^t_i}$ randomly

8: else

9: Select action $\boldsymbol{a^t_i = \underset{a \in A}{\operatorname{argmax}}\, Q_{d_j}(a)}$

10: end if

11: Evaluate $\boldsymbol{\xi_{d_j}}$, $\boldsymbol{\Gamma_{d_j}}$ and $\boldsymbol{l_{d_j}}$ of $\boldsymbol{d_j \in D}$ for action $\boldsymbol{a^t}$

12: Measure the SINR $\boldsymbol{\xi_{c_i}}$, of CUE $\boldsymbol{c_i \in C}$ for the action $\boldsymbol{a^t}$ taken by $\boldsymbol{d_j \in D}$

13: Observe immediate reward of $\boldsymbol{d_j \in D}$ and $\boldsymbol{c_i \in C}$, $\boldsymbol{r_{d_j}(a^t)}$ and $\boldsymbol{r_{c_i}(a^t)}$ respectively

14: Update action-value for action of $\boldsymbol{d_j \in D}$ on the $\boldsymbol{i}$th RB

$$\boldsymbol{Q^{i}_{d_j}(a^t) = Q^{i}_{d_j}(a^t) + \sigma\left[r_{d_j}(a^t) + Q^{i}_{d_j}(a^t)\right]}$$

15: Update action-value for $\boldsymbol{c_i \in C}$ for action $\boldsymbol{a^t}$ of $\boldsymbol{j}$th DUE of

$$\boldsymbol{Q^{j}_{c_i}(a^t) = Q^{j}_{c_i}(a^t) + \sigma\left[r_{c_i}(a^t) + Q^{j}_{c_i}(a^t)\right]}$$

16: end while

17: end for

18: $\boldsymbol{Q_{d_j}(a) = Q_{d_j}(a) - \left[Q^{i}_{d_j}(a^t) = 0,\ i = 1, 2, \dots, N\right]} \quad \forall\, \boldsymbol{d_j \in D}$

19: $\boldsymbol{Q_{c_i}(a) = Q_{c_i}(a) - [Q^{j}_{c_i}(a^t) = 0,\ j = 1, 2, \dots, M]} \quad \forall\, \boldsymbol{c_i \in C}$

20: Order $\boldsymbol{Q_{d_j}(a)}$, $\boldsymbol{Q_{c_i}(a)}$ $\forall\, \boldsymbol{d_j \in D}$, $\forall\, \boldsymbol{c_i \in C}$ respectively

21: Match DUEs and CUEs using the DA algorithm and output matching

Algorithm 6.2 The BS-A Reinforcement Learning Algorithm

1: Initialise the action-value function for the DUEs
$\left[\boldsymbol{Q_{d_j}(a) = 0 | Q_{d_j}(a) \equiv Q^{i}_{d_j}(a^t)}, \boldsymbol{i = 1, 2, \dots, N}\right] \quad \forall \boldsymbol{d_j} \in \boldsymbol{D}$
2: Initialise the action-value function for the CUEs
$\left[\boldsymbol{Q_{c_i}(a) = 0 | Q_{c_i}(a) \equiv Q^{j}_{c_i}(a^t)}, \ \boldsymbol{j = 1, 2, \dots, M}\right] \quad \forall \boldsymbol{c_i} \in \boldsymbol{C}$
3: for $\boldsymbol{d_j} \in \boldsymbol{D}$ $\boldsymbol{1 \le j \le M}$ do
4: while not converge do
5: generate a random number $\boldsymbol{x} \in \{\boldsymbol{0}, \boldsymbol{1}\}$
6: if $\boldsymbol{x < \varepsilon}$ then
7: Select action $\boldsymbol{a^t_i}$ randomly
8: else
9: Select action $\boldsymbol{a^t_i}$=$\boldsymbol{\underset{a \in A}{\operatorname{argmax}} Q_{d_j}(a^t)}$
10: end
11: Evaluate $\boldsymbol{\xi_{d_j}}$, $\boldsymbol{\Gamma_{d_j}}$ and $\boldsymbol{l_{d_j}}$ of $\boldsymbol{d_j} \in \boldsymbol{D}$ for the action $\boldsymbol{a^t}$
12: Measure the SINR $\boldsymbol{\xi_{c_i}}$, of CUE $\boldsymbol{c_i} \in \boldsymbol{C}$ for the action $\boldsymbol{a^t}$ taken by $\boldsymbol{d_j} \in \boldsymbol{D}$
13: Observe immediate reward of $\boldsymbol{d_j} \in \boldsymbol{D}$ and $\boldsymbol{c_i} \in \boldsymbol{C}$, $\boldsymbol{r_{d_j}(a^t)}$ and $\boldsymbol{r_{c_i}(a^t)}$, respectively
14: Update action-value for action of $\boldsymbol{d_j} \in \boldsymbol{D}$ on the $\boldsymbol{i}$th RB
$$\boldsymbol{Q^{i}_{d_j}(a) = Q^{i}_{d_j}(a) + \sigma\left[r_{d_j}(a^t) + Q^{i}_{d_j}(a)\right]}$$
15: Update action-value for $\boldsymbol{c_i} \in \boldsymbol{C}$ for action $\boldsymbol{a^t}$ of $\boldsymbol{j}$th DUE
$$\boldsymbol{Q^{j}_{c_i}(a) = Q^{j}_{c_i}(a) + \sigma\left[r_{c_i}(a^t) + Q^{j}_{c_i}(a)\right]}$$
16: end while
17: end for
18: Load $\boldsymbol{Q_{d_j}(a)}$ to the BS $\quad \forall \boldsymbol{d_j} \in \boldsymbol{D}$
19: for $\boldsymbol{d_j} \in \boldsymbol{D}$ $\boldsymbol{1 \le j \le M}$ do
20: Obtain $\boldsymbol{Q(a) = \left\{Q^{i}_{d_j}(a), Q^{j}_{c_i}(a)\right\}}$ $\boldsymbol{i = 1, 2, \dots, N}$
21: $\boldsymbol{\overline{Q}(a) \subseteq Q(a) | \left\{Q^{i}_{d_j}(a), Q^{j}_{c_i}(a)\right\}} \in \mathbb{R}^+$, where $\mathbb{R}^+$ denotes positive real number
22: $\boldsymbol{Q_{TOT} = Q^{i}_{d_j}(a) + Q^{j}_{c_i}(a)} \quad \forall \boldsymbol{q} \in \boldsymbol{\overline{Q}(a)}$
23: end for
24: Set up a list for unmatched DUE $\boldsymbol{D_u = \left\{d_j : \forall d_j \in D_u\right\}}$
25: while $\boldsymbol{D_u \neq \emptyset}$ do
26: Rank $\boldsymbol{D_u}$ in increasing order of $|\boldsymbol{\overline{Q}(a)}|$
27: Start DUE $\boldsymbol{d_j} \in \boldsymbol{D_u}$: $\boldsymbol{\overline{Q}(a) \neq \emptyset}$ with the least $|\boldsymbol{\overline{Q}(a)}|$
28: $\boldsymbol{c^*_i = \underset{c_i \in R}{\max} Q_{TOT}}$
29: $\boldsymbol{D_u = D_u - d_j}$
30: $\boldsymbol{\overline{Q}(a) = \overline{Q}(a) \backslash c^*_i} \quad \forall \boldsymbol{d_{j'}} \in \boldsymbol{D_u} | \boldsymbol{j' \neq j}$
31: end while

Table 6.2: Main simulation parameters for the RLBM and BS-A Algorithms [147,148]

Parameter	Value
Carrier frequency, $\boldsymbol{f_c}$	$\mathbf{2GHz}$
System bandwidth	$\mathbf{10MHz}$
Number of resource blocks (RB), $\boldsymbol{K}$	$\mathbf{50}$
RB bandwidth	$\mathbf{180\ kHz}$
Maximum CUE transmit power, $\mathbf{P}_{c_i,\mathbf{max}}$	$\mathbf{23dBm}$
Maximum DUE transmit power, $\mathbf{P}_{d_j,\mathbf{max}}$	$\mathbf{13dBm}$
D2D distance, $\boldsymbol{L_{d_T,d_R}}$	$\mathbf{10m} \leq \boldsymbol{L_{d_T,d_R}} \leq \mathbf{20m}$
CUE SINR Threshold, $\boldsymbol{\Gamma_{c_i,\mathbf{min}}}$	$\mathbf{7\ dB}$
DUE SINR Threshold, $\boldsymbol{\Gamma_{d_j,\mathbf{min}}}$	$\mathbf{3\ dB}$
Noise power density	$-\mathbf{174}\frac{\mathbf{dBm}}{\mathbf{Hz}}$
Number of CUEs, $\boldsymbol{N}$	$\mathbf{50}$
Number of DUEs, $\boldsymbol{M}$	$\mathbf{50}$
Reliability for DUE, $\boldsymbol{p_{R_0}}$	$\mathbf{10^{-5}}$
Exploration rate, $\boldsymbol{\varepsilon}$	$\mathbf{0.7}$
Learning rate, $\boldsymbol{\sigma}$	$\mathbf{0.9}$
Number of iterations, $\boldsymbol{T}$	$\mathbf{200}$
DUE Maximum Latency, $\boldsymbol{l_{d_j,\mathbf{max}}}$	$\mathbf{50ms}$
DUE Message Size, $\boldsymbol{B_{d_j}}$	$\mathbf{15kB}$

Table 6.3: Channel model for RLBM and B-SA Algorithms [130,131,139]

Parameter	In-factory DUE link	UE-UE link	BS-UE link
Pathloss model	$\mathbf{36.8\log_{10}}(\boldsymbol{d}[\mathbf{m}]) + \mathbf{35.8}$ dB	$\mathbf{40\log_{10}}(\boldsymbol{d}[\mathbf{m}]) + \mathbf{28}$ dB	$\mathbf{37.6\log_{10}}(\boldsymbol{d}[\mathbf{m}]) + \mathbf{15.3}$ dB
Shadowing	4dB	6dB	8dB

6.3 Performance Evaluation and Results

The performance of the algorithms is verified by considering a single-cell network in an industrial setting. The simulation set-up and channel models are as described in Chapter 5 and summarised in Table 6.2 and Table 6.3. The network dynamics are captured by generating the channel fading effects randomly at each time slot. The throughput is the main metric used to evaluate the performances of the algorithms. The performances of the RLBM and BS-A are compared to the centralised optimisation, DA and P-DA schemes.

6.3.1 Throughput Performance

The throughput performance of matched DUEs as a function of the number of DUEs in the system $\boldsymbol{M}$, is shown in Fig. 6.1. It can be seen that the total DUE throughput increases with $\boldsymbol{M}$

for all the considered algorithms. Expectedly, the number of admitted DUEs increases with the introduction of new DUEs but remains constant if a valid cellular resource to share or match it cannot be found because the minimum QoS requirements are not met. The performances of centralised, B-SA and P-DA approaches are comparable, while DA method shows the least performance. The P-DA shows up to $\mathbf{10}\%$ and $\mathbf{15.65}\%$ increase in aggregate DUE throughput compared to RLBM and DA methods, respectively. This is because the P-DA approach is optimised such that consideration is given to players based on the length of their preference list. The RLBM algorithm shows a peak of $\mathbf{10.08}\%$ higher DUE throughput compared to DA. The BS-A algorithm outperforms the RLBM and DA algorithms by up to $\mathbf{6}\%$ and $\mathbf{9.69}\%$ increase in DUE throughput performance, respectively. However, it is semi-distributive, as the final resource allocation is implemented by the BS, whereas the RLBM, DA and P-DA approaches are decentralised (the channel selection is user-centric and no BS intervention to achieve autonomy). Players can make their resource allocations choices to maximise their individual and ultimately, achieve system stability.

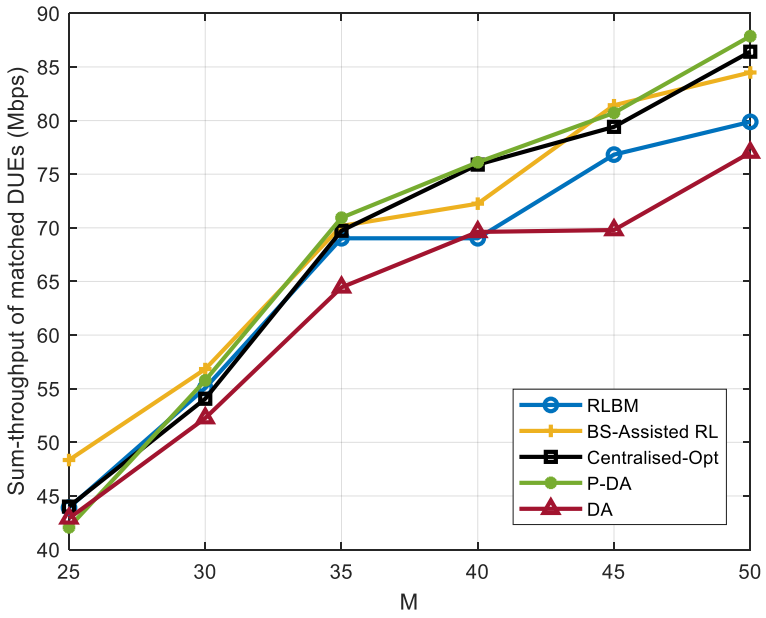

Fig. 6.1. Sum-throughput of matched DUEs with varying number of DUEs, $\boldsymbol{M}$ in the system, for $\boldsymbol{N = 50}$

The effects of increasing $\boldsymbol{M}$ on the sum throughput performance of the matched UEs (that is valid CUE-DUE pairings) is shown in Fig. 6.2. As seen in the figure, the sum throughput increases with $\boldsymbol{M}$. The performances of the P-DA and centralised optimisation are very close and hardly differentiable. The BS-A approach shows better performance at $\boldsymbol{M \leq 35}$ with up to

$\mathbf{12.05\%}$ and $\mathbf{11.3\%}$ increase in sum throughput compared to centralised and P-DA approaches, respectively. The centralised approach performed better at $\boldsymbol{M > 35}$, with up to $\mathbf{9.39\%}$ increase in throughput. The DA algorithm again shows the least performance with a $\mathbf{7.37\%}$ decrease compared to the RLBM.

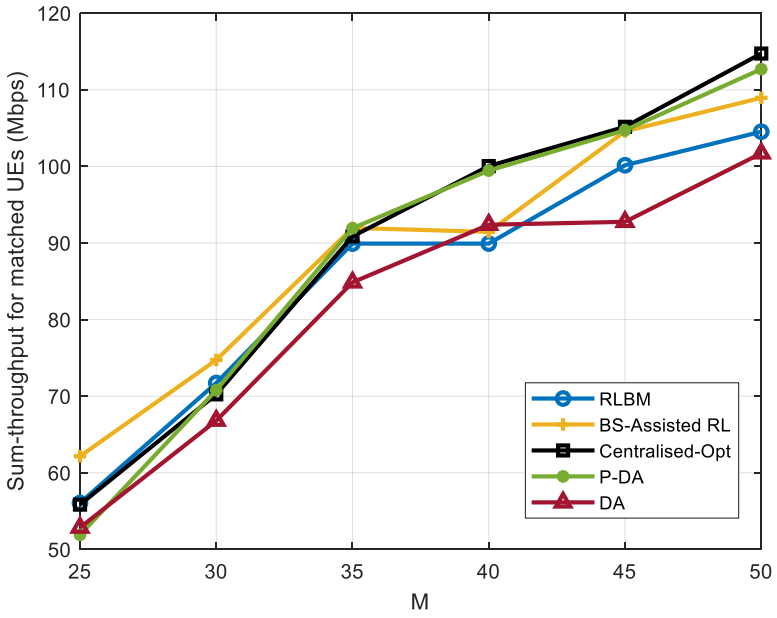

Fig. 6.2. Sum-throughput of matched UEs as a function of the number of DUEs $\boldsymbol{M}$, in the system, for $\boldsymbol{N = 50}$

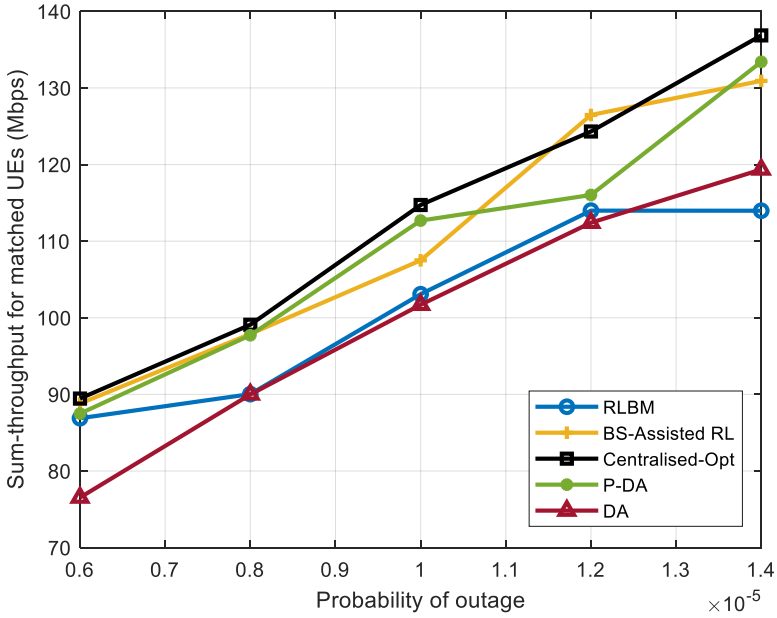

Fig. 6.3. Effect of the DUE outage ratio $\boldsymbol{p_{R_0}}$, on the sum throughput of matched CUE-DUE pair for $\boldsymbol{N = M = 50, l_{d_j,\max} = 50ms}$

The effect of the outage probability $\boldsymbol{p_{R_0}}$, and latency $\boldsymbol{l_{d_j,\max}}$ of DUEs on the sum rate of the matched UEs for all five algorithms is shown in Fig. 6.3. and Fig. 6.4. It can be concluded that the aggregate throughput increases with $\boldsymbol{p_{R_0}}$ and $\boldsymbol{l_{d_j,\max}}$. This is because higher $\boldsymbol{p_{R_0}}$ causes the interference from the CUEs to be more tolerable by the DUEs, therefore making potential CUE-DUE pairing possible. Similarly, higher $\boldsymbol{l_{d_j,\max}}$ increases the sum throughput at fixed outage probability and payload because more DUEs are able to satisfy the latency constraint since it is less stringent, therefore, increasing the DUE access rate The DUE access rate is defined as number of admitted DUEs to the number of DUEs in the system.

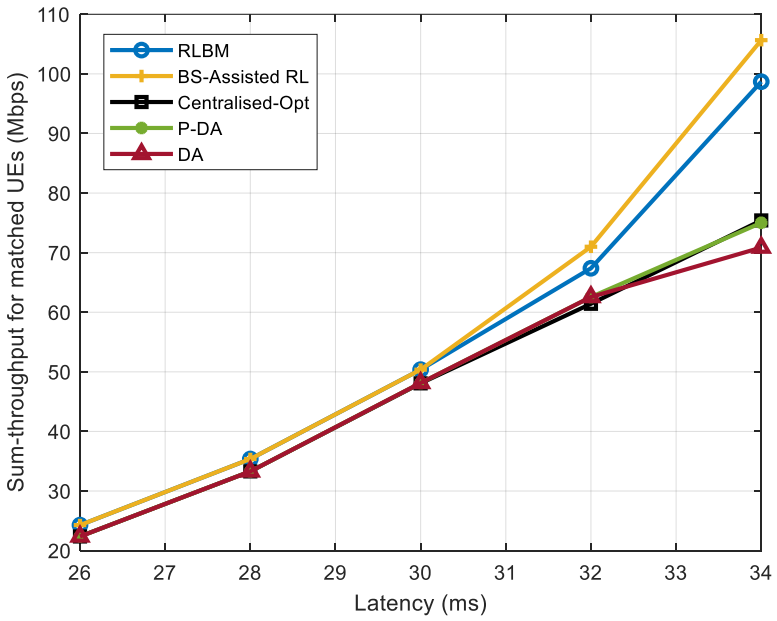

Fig. 6.4. Effect of the latency bound, $\boldsymbol{l_{d_j,\max}}$ on the sum throughput of matched CUE-DUE pair for $\boldsymbol{N = M = 50}$, $\boldsymbol{p_{R_0} = 10^{-5}}$

The impact of the size of the $\boldsymbol{Q}$-table on the aggregate throughput performance of the matched UEs for the RLBM algorithm is shown in Fig 6.5. The RLBM algorithm is distributed, however, the matching stage requires the exchange of proposals which will incur signalling overheads. The dimension of the Q-tables determines the number of accept/reject signals and invariably the message passing among the devices in the matching phase. The size of the $\boldsymbol{Q}$-table is varied to assess the trade-off between the signalling overheads and the performance. The $\boldsymbol{Q}$-table is exclusive of $\boldsymbol{Q^i_{d_j}(a), Q^j_{c_i}(a) = 0}$ for $\forall\, \boldsymbol{d_j \in D}$, $\forall\, \boldsymbol{c_i \in C}$, respectively (that is only actions that satisfy the minimum QoS are considered). For $\boldsymbol{N = M = 50}$, $\forall\, \boldsymbol{d_j \in D}$,

$\forall\, \boldsymbol{c_i} \in \boldsymbol{C}$ is varied from $\mathbf{25}\%$ to $\mathbf{100}\%$ of $|\boldsymbol{Q_{d_j}}(\boldsymbol{a})|$, $\left|\boldsymbol{Q_{c_i}}(\boldsymbol{a})\right|$. It can be seen from the figure that the throughput increases with the size of the $\boldsymbol{Q}$-table because DUE $\boldsymbol{d_j} \in \boldsymbol{D}$ has more CUEs to propose to at iteration $\boldsymbol{k}$ if it is rejected at iteration $\boldsymbol{k - l}$. Similarly, $\boldsymbol{c_i} \in \boldsymbol{C}$ will be able to receive more proposals as the size of the Q-table increases. It can be seen that by reducing $\left|\boldsymbol{Q_{d_j}}(\boldsymbol{a})\right|$ and $\left|\boldsymbol{Q_{c_i}}(\boldsymbol{a})\right|$, $\forall\, \boldsymbol{d_j} \in \boldsymbol{D}, \forall\, \boldsymbol{c_i} \in \boldsymbol{C}$, significant losses in throughput performance are apparent as reduction exceeds 70%. For example, at 55% size of the original Q-table, a 13.68%, 9.45% and 12.68% reduction can be seen in the DUE, CUE and system throughput, respectively. Reducing the Q-table dimension by less than 15% shows 0% loss in the aggregate DUE, CUE throughput and sum throughput of the matched UEs. This implies there is no change in the amount of signalling with 15% incomplete Q table for all participating UEs. This is a considerable trade-off in throughput performance for a reduced signalling overheads for the matching subroutine. It can be seen that the sum throughput of the DUE is higher than that of the CUE due to the predefined maximum outage probability, which makes it less tolerant to interference from the CUEs. This increases the SINR of the DUE, resulting in a higher throughput.

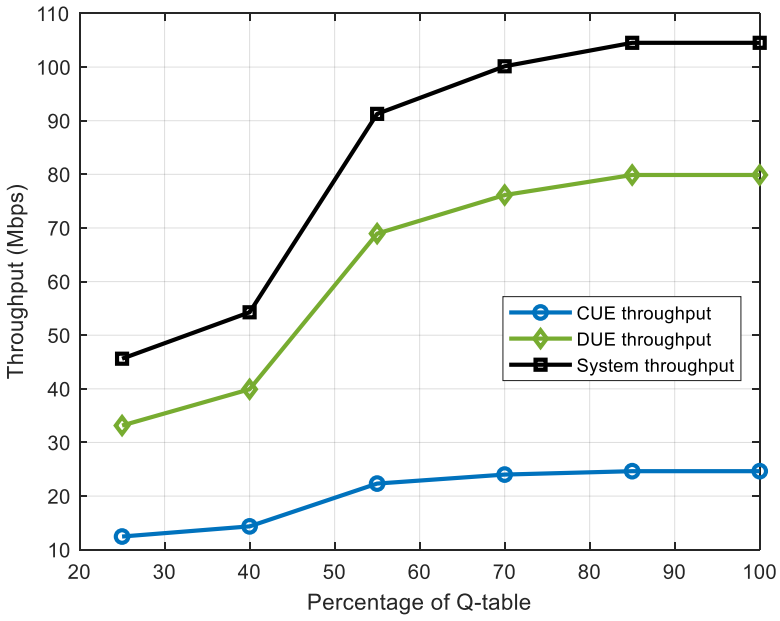

Fig. 6.5. Effect of the Q-table dimension on the throughput performance of matched UEs for the RLBM algorithm with $\boldsymbol{p_{R_0}} = \mathbf{10^{-5}}$, for $\boldsymbol{N} = \boldsymbol{M} = \mathbf{50}$

6.3.2 Signalling Overheads and Complexity Analysis

In this section, the signalling overheads and complexity of the presented algorithms are evaluated as shown in Table 6.4. The signalling overhead is evaluated in terms of the level of involvement of the BS i.e., BS-UE communication. The signalling overhead is an aggregation of channel information acquisition and information exchange by the BS-UE links. The number of iterations, $\boldsymbol{T}$ depends on the network dynamics. For the centralised optimisation method, the CSI of all links is acquired by the BS. This information includes the CUE-BS links, DUE links feedback to the BS, the interference channels information of $\boldsymbol{d_T}$-BS, CUE-$\boldsymbol{d_R}$ and the information signals to communicate the resource allocation summing up to $\boldsymbol{4MT + M}$, where $\boldsymbol{M}$ is the number of DUEs. For the P-DA and DA algorithms, the information needed by the BS includes the CUE-BS links, the interference channels information of $\boldsymbol{d_T}$-BS and information for matching subroutine which comprises $\boldsymbol{MN}$ proposals and $\boldsymbol{MN}$ accept/reject signals totalling $\boldsymbol{2MT + 2MN}$.

Table 6.4: Estimation of the signalling overhead by the BS for $\boldsymbol{M = 30}$ to $\boldsymbol{50, N = 50}$

RRM Technique	BS signalling overheads
Centralised	M(1+4T)
P-DA	2M(N+T+1)
DA	2M(N+T)
RLBM	2M(N+T)
BS-A	2M(1+T)

For the P-DA algorithm, the rate loss price has to be communicated to the DUEs by BS and acknowledged by the DUEs, making the total of $\boldsymbol{2MN + 2MT + 2M}$. For the RLBM algorithm, the BS as the receiver needs a total amount of information is $\boldsymbol{2MT}$. The information for the proposals is $\boldsymbol{MN}$ and $\boldsymbol{MN}$ accept/reject proposals from the DUEs in the matching stage. The total information for RLBM aggregates $\boldsymbol{2MT + 2MN}$. For the BS-A, the information acquired by the BS is $\boldsymbol{2MT}$. It is assumed the that the DUE Q-table is loaded to the BS as a unit (exclusive $\boldsymbol{Q^i_{d_j}(a) = 0}$), but upper-bounded by $\boldsymbol{M}$ and $\boldsymbol{M}$ information required to communicate the resource allocation to the DUEs summing to $\boldsymbol{2MT + 2M}$.

The algorithms are also evaluated in terms of their computation complexity. The run time for the algorithm also depends on the number of iterations and number of users. The average run time for different scenarios is presented in Table 6.5. It can be seen that, overall, the centralised

algorithm has the highest complexity, while the DA scheme has the least complexity, showing a $\mathbf{10.38}\%$ reduction in processing time compared to the centralised approach.

An overall comparison for the presented models using the throughput, signalling overheads and complexity metrics is shown in Table 6.6 and Fig. 6.6. Figures in red and italics are a degradation in performance compared to the centralised approach. The + and – signs are used to indicate the increment and decrement of the values used to measure the performances of considered schemes relative to the centralised approach. It can be seen that the centralised approach has the best throughput performance but shows corresponding high signalling and complexity in comparison to the other approaches. DA has the least throughput performance and shows the least complexity, while BS-A has the least signalling overhead. The BS-A shows a $\mathbf{49.81}\%$ reduction in signalling, $\mathbf{0.94}\%$ reduction in complexity at $\mathbf{8.58}\%$ lower throughput performance compared to the centralised approach, which is a good tradeoff, using the use case 2 scenario as an instance.

The P-DA approach shows $\mathbf{37.45}\%$ reduction in signalling, $\mathbf{8.14}\%$ decrease in complexity with a $\mathbf{0.588}\%$ reduction in throughput performance compared to the centralised approach, which is also a considerable trade-off; but up to $\mathbf{24.63}\%$ increase in signalling compared to the BS-A approach. The RLBM scheme performs slightly better than DA in terms of throughput with a slightly higher complexity, but $\mathbf{37.78}\%$ and $\mathbf{2}\%$ decrease in signalling overhead and complexity, respectively, with a $\mathbf{10.11}\%$ reduction in throughput relative to the centralised approach. The P-DA scheme has $\mathbf{9.32}\%$ higher throughput than RLBM with a $\mathbf{0.34}\%$ higher complexity and $\mathbf{0.2}\%$ increase in signalling.

Table 6.5: Performance of different techniques for different values of ***M***

Technique	***M***	Complexity (s)	Sum Throughput (Mbps)
Centralised	30	0.6997	70.2415
	40	0.7384	100.0366
	50	0.7696	114.7231
P-DA	30	0.6630	70.7830
	40	0.6783	99.4483
	50	0.7592	112.6872
DA	30	0.6456	66.8117
	40	0.6618	92.3800
	50	0.7304	101.7014
RLBM	30	0.6969	70.3187
	40	0.7237	88.4736
	50	0.7566	103.0787
BS-A	30	0.6748	72.7855
	40	0.7315	89.6745
	50	0.7761	107.4996

Table 6.6: Performance of Different Techniques Explored Relative to the Centralised Approach

Technique	***M***	Signalling Overheads	Complexity	Sum Throughput
P-DA	30	-37.45%	-5.23%	+0.77%
	40	-37.45%	-8.14%	*-0.59%*
	50	-37.45%	-1.34%	*-1.77%*
DA	30	-37.58%	-7.73%	*-4.88%*
	40	-37.58%	-10.38%	*-7.65%*
	50	-37.58%	-5.09%	*-11.4%*
RLBM	30	-37.58%	-0.39%	+2.11%
	40	-37.58%	-2.00%	*-10.12%*
	50	-37.58%	-1.69%	*-8.89%*
BS-A	30	-49.81%	-3.56%	+6.39%
	40	-49.81%	-0.94%	*-8.58%*
	50	-49.81%	*+0.84%*	*-5.04%*

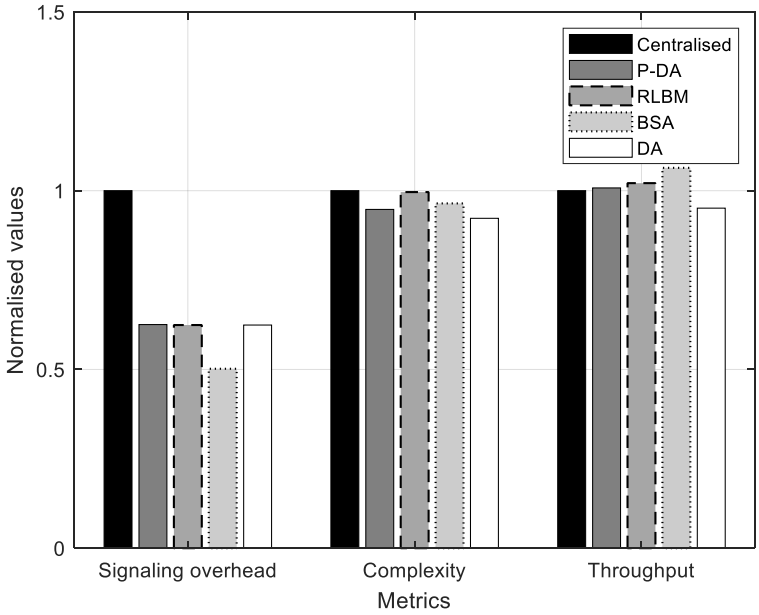

Fig. 6.6(a). Overall performance comparison with the centralised approach as a reference

Use case 1: $\boldsymbol{M = 30, N = 50}$

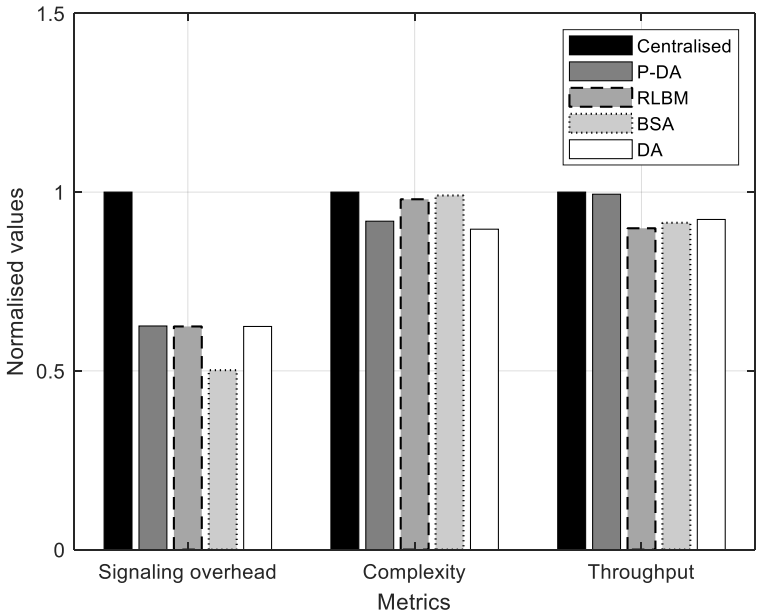

Fig. 6.6(b). Overall performance comparison with the centralised approach as a reference

Use case 2: $\boldsymbol{M = 40, N = 50}$

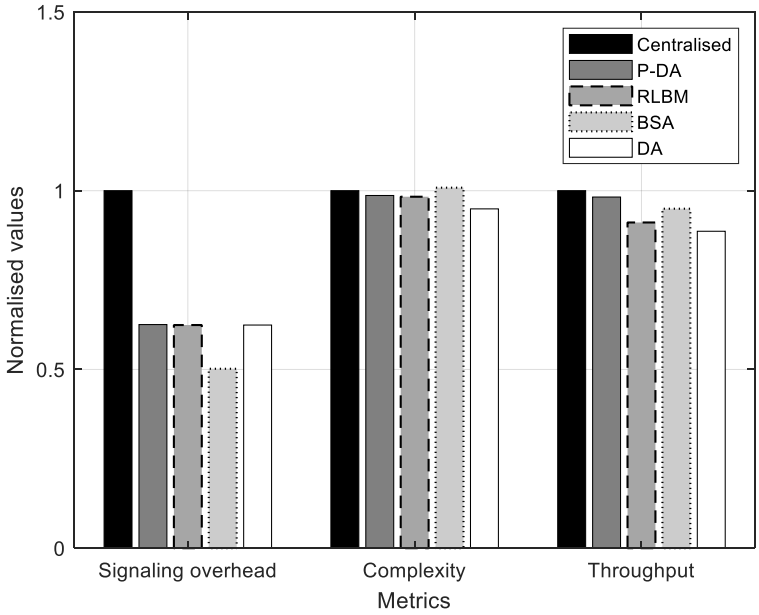

Fig. 6.6(c). Overall performance comparison with the centralised approach as a reference

Use case 3: $\boldsymbol{M = N = 50}$

6.4 Chapter Conclusions

Reinforcement learning-based RRM techniques were presented, targetting the deployment of D2D links in a URLLC industrial environment. Simulation results show that RLBM and P-DA are promising techniques to achieve better throughput performance at lower signalling overheads and complexity compared to the centralised and DA approaches. Therefore, distributed approaches are more suitable for smart manufacturing applications with massive device deployment, in which device autonomy and system stability are important. For throughput maximisation in a low-density network in which self-organisation is not crucial, the centralised scheme would be the best approach to adopt at the cost of signalling and complexity. On the other hand, BS-A is a semi-distributive approach which offers a good trade-off of throughput, complexity and signalling overheads compared to P-DA, RLBM and centralised approaches.

Chapter 7

Conclusions and Directions for Future Work

In this chapter, a summary of the main contributions of the research work developed in this thesis and directions for future work, are presented.

7.1 Conclusions and Summary of Contributions

Next-generation wireless networks (5G-and-beyond) are expected to address the challenges posed by the requirements for new applications and emerging use cases. The growth in new device types is putting pressure on the radio spectrum that is already considered a scarce and congested resource. Ultra-Reliable Low Latency Communication (URLLC) is one of the use cases for 5G-and-beyond technologies which supports real-time communications and mission-critical applications. Smart manufacturing, automation and control for FoF are considered some of the most demanding URLLC applications in terms of reliability and latency requirements. D2D communication is one of the next-generation technologies with the potential to improve spectrum efficiency and data rates, to expand network capacity and offload traffic at the BS. Integrating D2D into future industrial wireless networks and next-generation manufacturing can support the creation of mMTCs and URLLC.

The research work in this reported has addressed some of the challenges posed by the coexistence of D2D links in cellular and multi-tier HetNet and their deployment in FoF, while meeting URLLC requirements. These challenges include interference mitigation and coordination as well as spectrum and power allocation. The research process used to address the challenges entailed, a literature review of relevant related works, state-of-the-art in the field and identifying some gaps in knowledge.

Three main RRM approaches were investigated namely, centralised optimisation, matching theory and machine learning. Mathematical models were formulated to represent the network scenarios and novel algorithms were developed to address some identified RRM challenges. Numerical simulations were used to verify the performance of different techniques developed for the scenarios considered. The conclusions from the results are as follows:

- The centralised approach may provide an optimal performance for throughput maximisation in a low-density network in which self-organisation is not crucial.
- Distributed schemes such as the P-DA and RLBM can support device autonomy and system stability with a good throughput performance and low signalling overheads and complexity.
- The semi-distributed approach such as BS-A scheme can provide a good balance of throughput-complexity-signalling but does not fully support self-organisation.

7.2 Impact of Research from a Practical Perspective

The main aim of the research reported in this thesis was to investigate and develop new radio resource management (RRM) schemes achieving energy efficiency and optimised spectrum utilisation, while satisfying target performance metrics for the users and services. Regardless of the limitations of the developed techniques presented in this research work, the results from adopting these, suggest the possibility of developing a conceptual framework to assist in the selection of an appropriate scheme to meet specific priorities, as presented in Table 7.1. The table below provides a qualitative evaluation of the key techniques developed for system throughput maximisation, while minimising complexity and signaling overheads subject to predefined latency and reliability requirements.

Table 7.1 Qualitative Evaluation of the Different Schemes

	Cent-Opt	**DA**	**P-DA**	**RLBM**	**B-SA**
RRM Approach	Centralised	Distributed	Distributed	Distributed	Semi-distributed
RRM Technique	Mathematical optimisation	Matching theory	Matching theory	Reinforcement learning	Reinforcement learning
Throughput	Best	Worst	Average	Average	Average
Complexity	Worst	Best	Average	Average	Average
Signalling Overheads	Worst	Average	Average	Average	Best

7.3 Directions for Future Work

Further possible extensions of the work presented in this thesis are described below.

1. In conventional cellular networks, each area is partitioned into cells and the BSs are deployed in each cell to serve UEs within their coverage. The BSs are connected together and to the core network through a backhaul network. Cell-Free Massive Multiple-Input-

Multiple-Output (CF-mMIMO) systems comprise distributed Access Points (APs) connected to a Central Processing Unit (CPU) through the fronthaul network. In contrast to the cellular structure, there are no cells or cell boundaries in a CF-mMIMO network. The APs operate jointly and serve surrounding UEs in a wide area within the same time and frequency resources. CF-mMIMO is expected to facilitate uniform coverage, increased reliability, improved spectrum, and energy efficiency. Due to its inherent benefits, CF-mMIMO is considered an important technology for 6G systems. In theory, CF-mMIMO reduces the distance between the APs and the UEs. However, in practice, this is seldomly the case, as the APs cannot be installed arbitrarily. Therefore, in future ultra-dense networks (UDNs), there are possibilities of direct D2D communication between devices if they are in proximity compared to the surrounding APs. This densification makes interference more complex if D2D and CF-mMIMO UEs are using the same radio resources. As such, resource management algorithms for user association, power and channel allocation should be studied for such scenarios. Federated learning is an evolving ML paradigm that has been shown to improve the training time of network entities (such as UEs and APs) and could be considered for investigation for the coexistence of D2D communication and in a CF-mMIMO system and is a possible avenue for extending this work. [149,150]

2. The spectrum sharing scenarios considered in this work are based on uplink (UL) transmission. Downlink (DL) spectrum reuse is more complex because the BS generates a high interference level to the DUEs which results in performance degradation. The DL supports the demand for a higher download capacity because typically, there is more download than upload data traffic. However, recently, the user traffic patterns are becoming more dynamic, as more traffic is expected in the UL (e.g., backing up data to online or cloud storage services, video calls and conferences). It is expected that spectrum utilisation in the UL and DL will be flexible [151]. The optimisation of flexible resource allocation for uplink (UL) and downlink (DL) resources to meet diverse needs and provide the best possible user experience is, therefore, worth investigating.

3. The DUEs considered in this work were assumed to be static or semi-static. This may be applicable to factory devices with low or no mobility such as in communication between industrial controllers and process automation. Motion control use cases such as the case of 3D printing machine, machine tools and packaging machines have node mobility that is up to 20m/s, Augmented Reality (AR), up to 5m/s and inbound logistics for manufacturing,

up to 8m/s [152]. Therefore, RRM techniques taking into account device mobility is an important area of investigation and an extension to this work.

4. The P-DA technique presented in this thesis was investigated for one-to-one associations between the CUEs and DUEs. Other possible extensions of the P-DA scheme are to study its adaptability to one-to-many assignments, where a CUE can share its resources with more than one DUE simultaneously. Evaluating the trade-off between matching stability, system revenue and performance (in terms of system sum-rate and reuse gain) are important factors to be considered.
5. The spectrum sharing schemes presented in this thesis focused mainly on resource allocation. Technical challenges relating to security, trust and privacy issues, resulting from spectrum sharing between the legacy Human-Type Communication (HTC) devices and Machine-Type Communication (MTC) devices in UDNs need to be addressed. Blockchain technology uses a decentralised database that stores transaction records in a verifiable manner by providing a trusted channel for information exchange [153,154]. A possible extension of this research work is to investigate blockchain-based spectrum sharing.

References

[1] M. Weiser, R. Gold and J. S. Brown, "The origins of ubiquitous computing research at PARC in the late 1980s," IBM Systems Journal, Vol. 38, no. 4, pp. 693-696, 1999.

[2] R. Khan, S. Khan, R. Zaheer and S. Khan, "Future internet: the internet of things architecture, possible applications and key challenges," in Proc. of International Conference on Frontiers of Information Technology, pp. 257-260, Dec. 2012.

[3] S. Alraih, I. Shayea, M. Behjati, R. Nordin, N. F. Abdullah, A. Abu-Samah and D. Nandi, "Revolution or evolution? technical requirements and considerations towards 6G mobile communications," Sensors, Vol.22, no.3, pp.762, Jan. 2022.

[4] P. K. Maddikunta, Q.V. Pham, B. Prabadevi, N. Deepa, K. Dev, T. R. Gadekallu, R. Ruby and M. Liyanage, "Industry 5.0: A survey on enabling technologies and potential applications. Journal of Industrial Information Integration," Vol. 26, pp. 100257, Mar. 2022.

[5] 5G and Factories of the Future- White paper, Available online: https://5g-ppp.eu/wp-content/uploads/2014/02/5G-PPP-White-Paper-on-Factories-of-the-Future-Vertical-Sector.pdf., Last accessed 11/07/2022

[6] 3GPP Standard TS 22.368 V10.0.0, "Service requirements for machine-type communications (MTC); stage 1", Mar. 2010.

[7] N. Xia, C. Hsiao-Hwa and Y. Chu-Sing, "Radio resource management in machine-to-machine communications—a survey," IEEE Communications Surveys & Tutorials, Vol. 20, no. 1, pp. 791-828, Oct. 2017.

[8] Cisco Annual Internet Report (2018-2023) White Paper, Available online: https://www.cisco.com/c/en/us/solutions/collateral/executive-perspectives/annual-internet-report/white-paper-c11-741490.html, Last accessed 11/07/2022.

[9] S. Zahoor and R.N. Mir, "Resource management in pervasive internet of things: a survey," Journal of King Saud University-Computer and Information Sciences, Vol. 33, no. 8, pp. 921-935, Oct. 2021.

[10] M. Z. Chowdhury, M. Shahjalal, S. Ahmed and Y. M. Jang, "6G wireless communication systems: applications, requirements, technologies, challenges, and research directions," in IEEE Open Journal of the Communications Society, Vol. 1, pp. 957-975, Jul. 2020.

[11] H. Jayakumar, R. Arnab, K. Younghyun, S. Soubhagya, S. L. Woo and R. Vijay, "Energy-efficient system design for IoT devices," in Proc. of Design Automation Conference (ASP-DAC), in IEEE 21st Asia and South Pacific, pp. 298-301, Mar. 2016.

[12] IEA Report, "More data, less energy, making network standby more efficient in billions of connected devices," International Energy Agency, Vol. 2, Jun. 2014.

[13] Telecoms.com_Annual_Industry_Survey_2018_11.26.18.pdf, Last accessed 12/09/2020.

[14] M. E. Tarerefa, O. Falowo and N. Ventura, "Energy efficient user association scheme in cellular machine to machine communications," in Proc. of 2017 IEEE AFRICON, pp. 192-197, Nov. 2017.

[15] N. A. Johansson, Y. P. E. Wang, E. Eriksson and M. Hessler, "Radio access for ultra-reliable and low-latency 5G communications," in Proc. of 2015 IEEE International Conference on Communication Workshop (ICCW), pp. 1184-1189, Jun. 2015.

[16] B. Holfeld, D. Wieruch, T. Wirth, L. Thiele, S.A. Ashraf, J. Huschke, I. Aktas and J. Ansari, "Wireless communication for factory automation: An opportunity for LTE and 5G systems," IEEE Communications Magazine, Vol.54, no. 6, pp.36-43, Jun. 2016.

[17] J. Kaur, M. Arif Khan, M. Iftikhar, M. Imran and Q. E. Ul Haq, "Machine learning techniques for 5G and beyond networks," IEEE Access, Vol. 9, pp. 23472-23488, Jan. 2021.

[18] B. Chen, J. Wan, A. Celesti, D. Li, H. Abbas and Q. Zhang, "Edge computing in IoT-based manufacturing," IEEE Communications Magazine, Vol. 56, no.9, pp.103-109 Sep. 2018.

[19] W. S. Afifi, A. A. El-Moursy, M. Saad, S. M. Nassar and H. M. El-Hennawy, "A novel scheduling technique for improving cell-edge performance in 4G/5G systems," Ain Shams Engineering Journal, Vol.12, no. 1, pp. 487-495, Mar. 2021.

[20] M. Zekri, B. Jouaber and D. Zeghlache, "A review on mobility management and vertical handover solutions over heterogeneous wireless networks," Computer Communications, Vol. 35, no.17, pp. 2055-2068, Oct. 2012.

[21] P. Cheng, L. Deng, H. Yu, Y. Xu and H. Wang, "Resource allocation for cognitive networks with D2D communication: An evolutionary approach," in Proc. IEEE wireless communications and networking conference (WCNC), pp. 2671-2676, Apr. 2012.

[22] O.N. Yilmaz, Y.P.E. Wang, N.A. Johansson, N. Brahmi, S.A. Ashraf and J. Sachs, "Analysis of ultra-reliable and low-latency 5G communication for a factory automation use case,". in Proc. of 2015 IEEE International Conference on Communication Workshop (ICCW), pp. 1190-1195, Jun. 2015.

[23] T. Park, N. Abuzainab and W. Saad, "Learning how to communicate in the internet of things: finite resources and heterogeneity," IEEE Access, Vol. 4, pp. 7063-7073, Nov. 2016.

[24] L. Song, D. Niyato, Z. Han and E. Hossain, "Game-theoretic resource allocation methods for device-to-device communication," IEEE Wireless Communication, Vol. 21, no. 3, pp.136-144, Jun. 2014.

[25] P. Semasinghe, S. Maghsudi and E. Hossain, "Game theoretic mechanisms for resource management in massive wireless IoT systems," IEEE Communications Magazine, Vol. 55, no.2, pp.121-127, Feb. 2017.

[26] S. Bayat, Y. Li, L. Song and Z. Han, "Matching theory: Applications in wireless communications," IEEE Signal Processing Magazine, Vol. 33, no. 6, pp. 103-122. Nov. 2016.

[27] F. Tariq, M. R. Khandaker, K. K. Wong, M. A. Imran, M. Bennis and M. Debbah. "A speculative study on 6G," IEEE Wireless Communications, Vol. 27, no.4, pp.118-125, Aug. 2020.

[28] GSM Association. "Spectrum for the internet of things GSMA, public policy position," 2016. Available online- https://www.gsma.com/spectrum/wp-content/uploads/2018/12/Spectrum-IOT-Position-Paper.pdf, Last accessed 11/07/2022.

[29] https://clear5g.eu/ Last accessed 12/09/2020.

[30] ITU-R, "ITU-R M. (IMT-2020.TECH PERF REQ) – "Minimum Requirements Related to Technical Performance for IMT2020 Radio Interface(s)," Report ITU-R M.2410-0, 2017.

[31] 3GPP, "Study on new radio (NR) access technology physical layer aspects," TR 38.802, 2017.

[32] H. Zhang, N. Liu, X. Chu, K. Long, A. H. Aghvami and V. C. M. Leung, "Network slicing based 5G and future mobile networks: mobility, resource management, and challenges," IEEE Communication Magazine, Vol. 55, no. 8, pp. 138–145, Aug. 2017.

[33] P. Popovski, K. F. Trillingsgaard, O. Simeone and G. Durisi, "5G wireless network slicing for eMBB, URLLC, and mMTC: a communication-theoretic view," IEEE Access, Vol.28, no.6, pp. 55765-55779, Sep. 2018.

[34] 3GPP TSG RAN WG1 Meeting 87, 2016.

[35] A. Mukherjee, "Energy efficiency and delay in 5G ultra-reliable low-latency communications system architectures," IEEE Network, Vol. 32, no. 2, pp. 55-61, Apr. 2018.

[36] 5G Americas White paper, "New services and applications with ultra-reliable low-latency communication," Nov. 2018. Available online: https://www.5gamericas.org/wpcontent/uploads/2019/07/5G_Americas_URLLLC_White_Paper_Final__updateJW.pdf, Last Accessed 31/07/2022.

[37] C. Yeh, G. Do Jo, Y.J. Ko and H.K. Chung, "Perspectives on 6G wireless communications," ICT Express, Jan. 2022.

[38] A.I. Salameh and M. El Tarhuni, "From 5G to 6G—Challenges, technologies, and applications," Future Internet, Vol. 14, no.4, p.117, Apr. 2022.

[39] Huawei, "Main characteristics of 4G, 5G and 6G," Available online: https://forum.huawei.com/enterprise/fr/principales-caract%C3%A9ristiques-des-r%C3%A9seaux-sans-fil-4g-5g-et-6g/thread/886631-100363, Last accessed 16/07/2022.

[40] Theodore Rappaport, "Wireless communication: theory and practice," Prentice Hall, pp.1-576, 2002.

[41] M. N. Reza, C. A. Malarvizhi, S. Jayashree and M. Mohiuddin, "Industry 4.0–Technological Revolution and Sustainable Firm Performance," In Proc. of Emerging Trends in Industry 4.0 (ETI 4.0), pp. 1-6, May 2021.

[42] S. Gaiardelli, S. Spellini, M. Lora and F. Fummi, "Modeling in industry 5.0: what is there and what is missing: special session 1: languages for industry 5.0," in Proc. of IEEE 2021 Forum on specification and Design Languages (FDL), pp. 1-8, Sep. 2021.

[43] X. Xu, Y. Lu, B. Vogel-Heuser and L. Wang, "Industry 4.0 and Industry 5.0—Inception, conception and perception," Journal of Manufacturing Systems, Vol. 61, pp. 530-535, Oct. 2021.

[44] Smart manufacturing and smart industry in context, Available online: https://www.i-scoop.eu/industry-4-0/manufacturing-industry/, Last accessed 11/07/2022.

[45] K. Zhou, T. Liu and L. Zhou, "Industry 4.0: Towards future industrial opportunities and challenges," in Proc. of 12th IEEE International Conference on Fuzzy Systems and Knowledge Discovery (FSKD), pp. 2147-2152, Aug 2015.

[46] B. Chen, J. Wan, L. Shu, P. Li, M. Mukherjee and B. Yin, "Smart factory of industry 4.0: key technologies, application case, and challenges," IEEE Access, Vol. 6, pp. 6505-6519, Dec. 2018.

[47] I. Aktas, J. Ansari, S. Auroux, D. Parruca, M. D. Guirao and B. A. Holfeld, "A coordination architecture for wireless industrial automation," in Proc. of 23th European Wireless Conference, pp. 1-8, May 2017.

[48] https://www.nokia.com/blog/licensed-unlicensed-spectrum-cellular-iot-question/ Last accessed 11/07/2022

[49] H. Chen, R. Abbas, P. Cheng, M. Shirvanimoghaddam, W. Hardjawana, W. Bao, Y. Li and B. Vucetic, "Ultra-Reliable Low Latency Cellular Networks: Use Cases, Challenges and approaches," IEEE Communications Magazine, Vol. 56, No. 12, pp. 119-125, 2018.

[50] J. Ansari, I. Aktas, C. Brecher, C. Pallasch, N. Hoffmann, M. Obdenbusch, M. Serror, K. Wehrle and J. Gross "Demo: a realistic use-case for wireless industrial automation and control," in Proc. of IEEE International Conference on Networked Systems (NetSys), pp. 1-2, 2017.

[51] B. Chen, M. Imran, F. Tao, D. Li, C. Liu and S. Ahmad, "Toward dynamic resources management for IoT-based manufacturing," IEEE Communications Magazine, Vol. 56, no. 2, pp. 52-59, Sep. 2018.

[52] A. Asadi, Q. Wang and V. Manuso, "A survey on device-to-device communication in cellular networks," IEEE Commuincations Surveys and Tutorials, Vol. 16, no. 4, pp. 1801-1819, Apr. 2014.

[53] K. Doppler and M. Xiao, "Device-to-Device communication as an underlay to LTE-advanced networks," IEEE Communications Magazine, Vol. 47, no. 12, pp. 42-49, Dec. 2009.

[54] O. Hayat, R. Ngah, S.Z. Hashim, M.H. Dahri, R.F. Malik and Y. Rahayu, "Device discovery in D2D communication: A survey," IEEE Access, Vol. 7, pp. 131114 -34, Sep. 2019.

[55] H. Zhang, Y. Liao and L. Song, "Device-to-device communication underlaying cellular networks in unlicensed bands," in Proc. of IEEE International Conference on Communications (ICC), pp. 1-6, Mar. 2017.

[56] R. H. Tehrani, S. Vahid, D. Triantafyllopoulou, H. Lee and K. Moessner, "Licensed spectrum sharing schemes for mobile operators: a survey and outlook," IEEE Communications Surveys & Tutorials, Vol. 18, no.4, Jun. 2016.

[57] J. M. Gimenez-Guzman, I. Marsa-Maestre, D. Orden, E. de la Hoz and T. Ito, "On the Goodness of using Orthogonal Channels in WLAN IEEE 802.11 in Realistic Scenarios," Wireless Communications and Mobile Computing, Nov. 2018

[58] Y. Han, S. E. Elayoubi, A. Galindo-Serrano, V. S. Varma and M. Messai, "Periodic radio resource allocation to meet latency and reliability requirements in 5G networks," in Proc. of IEEE 87th Vehicular Technology Conference (VTC Spring), pp. 1–6, Jun. 2018.

[59] C. She, C. Yang and T.Q. Quek, "Radio resource management for ultra-reliable and low-latency communications," IEEE Communications Magazine, Vol. 55, no. 6, pp. 72-8, Jun. 2017.

[60] S.A. Ashraf, I. Aktas, E. Eriksson, K.W. Helmersson and J. Ansari, "Ultra-reliable and low-latency communication for wireless factory automation: From LTE to 5G," in Proc. of 2016 IEEE 21st International Conference on Emerging Technologies and Factory Automation (ETFA), pp. 1-8, Sep. 2016.

[61] 5G Forum, "5G Vision, Requirements, and Enabling Technologies," Available online: https://www.scribd.com/document/383830051/5G-Vision-Requirements-and-Enabling-Technologies-1, Accessed 11/07/2022

[62] D. Feng, L. Lai, J. Luo, Y. Zhong, C. Zheng and K. Ying, "Ultra-reliable and low-latency communications: applications, opportunities and challenges," Science China Information Sciences, Vol. 64, no.2, pp.1-2, Feb. 2021.

[63] B. Singh, Z. Li, O. Tirkkonen, M. A. Uusitalo and P. Mogensen, "Ultra-reliable communication in a factory environment for 5G wireless networks: link level and deployment study," in Proc. of IEEE 27th Annual International Symposium on Personal, Indoor, and Mobile Radio Communications (PIMRC), pp. 1-5, Sep. 2016.

[64] X. XiPeng, "Technical, commercial and regulatory challenges of QoS: an internet service model perspective," Morgan Kauffman, pp. 225-246, Aug. 2008.

[65] Andrea Goldsmith, "Wireless Communication," Cambridge University Press, pp 1-97, 2005.

[66] B. Singh, O. Tirkkonen, Z. Li and M.A. Uusitalo, “Resource allocation strategy for ultra- reliable communication in a factory environment,” in Proc. of GWS, Nov. 2016.

[67] N. Brahmi, O. N. Yilmaz, K. W. Helmersson, S. A. Ashraf and J. Torsner, “Deployment strategies for ultra-reliable and low-latency communication in factory automation,” in Proc. of 2015 IEEE Globecom Workshops (GC Wkshps), pp. 1-6, 2015.

[68] NGMN Alliance, “5G E2E Technology to Support Verticals URLLC Requirements,” Feb. 2020. Available online: https://ngmn.org/wp-content/uploads/200210-NGMN_Verticals_URLLC_Requirements_v16.pdf

[69] 3gpp, ZVEI, https://5g-acia.org/wp-content/uploads/5G-ACIA_WP_Key-5G-Use-Cases-and-Requirements_SinglePages.pdf , Last accessed 12/07/2022.

[70] S. Auroux, D. Parruca and H. Karl., “Joint real-time scheduling and interference coordination for wireless factory automation,” in Proc. of 2016 IEEE 27th Annual International Symposium on Personal, Indoor, and Mobile Radio Communications (PIMRC), pp. 1-6, Sep. 2016.

[71] A. A. Zulkifli, T. Huynh, K. Kuroda and K.M. Hasegawa, “Interference management under multi-channel for device-to-device underlaying cellular networks,” in Proc.19th International Symposium on Wireless Personal Multimedia Communications (WPMC), pp. 324-329, Nov. 2016.

[72] Y. Liu, R. Wang and Z. Han, “Interference-constrained pricing for D2D networks,” IEEE Transactions on Wireless Communications, Vol. 16, no. 1, pp. 475-486, Nov. 2016.

[73] D. D. Ningombam, S. S. Hwang and S. Shin, “A novel resource sharing mechanism for device-to-device communications underlaying LTE-A uplink cellular networks,” in Proc. 2018 Tenth International Conference on Ubiquitous and Future Networks (ICUFN), pp. 829-833, Jul. 2018.

[74] S. Shamaei, S. Bayat and A.M.A Hemmatyar, “Interference management in D2D-enabled heterogeneous cellular networks using matching theory,” IEEE Transactions on mobile computing, Vol. 18, no.9, pp. 2091-2102, Sep. 2018.

[75] A. J. Peterson, “A numerical method for computing interval distributions for an inhomogeneous poisson point process modified by random dead times,” Biological Cybernetics, Vol. 115, no. 2, pp.177-190, Apr. 2021.

[76] X. Liu, H. Xiao and A. T. Chronopoulos, “Joint mode selection and power control for interference management in D2D-Enabled heterogeneous cellular networks,” IEEE Transactions on Vehicular Technology, Vol. 69, no. 9, pp. 9707-9719, Jun. 2020.

[77] P. Pawar and A. Trivedi, “Power allocation approach for underlay D2D communication in cellular network,” in Proc. of 2017 Conference on Information and Communication Technology (CICT), pp. 1-4, Nov. 2017.

[78] T. Sun, W. Zhao, C. Zhang, Y. Li and Q. Man, “Efficient power allocation for device-to-device communication underlaying cellular networks,” in 2017 IEEE 9th International Conference on Communication Software and Networks (ICCSN), pp. 207-211, May 2017.

[79] M. Baniasadi, B. Maham and H. Kebriaei, “Power control for D2D underlay cellular communication: Game theory approach,” in 8th International Symposium on Telecommunications (IST), pp. 314-319, Sep. 2016.

[80] Y. Jiang, Q. Liu, F. Zheng, X. Gao and X. You, “Energy-efficient joint resource allocation and power control for D2D communications,” IEEE Transactions on Vehicular Technology, Vol.65, no.8, pp.6119-6127, Aug. 2015.

[81] S. Latif, F. Pervez, M. Usama and J. Qadir, “Artificial intelligence as an enabler for cognitive self-organizing future networks,” arXiv preprint arXiv:1702.02823, Feb. 2017.

[82] A. Asheralieva and Y. Miyanaga, “An autonomous learning-based algorithm for joint channel and power level selection by D2D pairs in heterogeneous cellular networks,” IEEE transactions on communications, Vol. 64, no. 9, pp. 3996-4012, Jul. 2016.

[83] T. Akhtar, C. Tselios and I. Politis, “Radio resource management: approaches and implementations from 4G to 5G and beyond,” Wireless Networks, Vol. 27, no. 1, pp.693-734, Jan. 2021.

[84] P. Arnold, V. Rakocevic and J. Habermann, “Hybrid radio resource management with co-scheduling for relay extended OFDMA networks,” Wireless Personal Communications, Vol.109, no.2, pp.1133-1160, Nov. 2019.

[85] Y. L. Lee, T. C. Chuah, J. Loo and A. Vinel, “Recent advances in radio resource management for heterogeneous LTE/LTE-A networks,” IEEE Communications Surveys & Tutorials, Vol. 16, no. 4, 2142-80, Jun. 2014.

[86] M. Haddad, S. E. Elayoubi, E. Altman and Z. Altman, “A hybrid approach for radio resource management in heterogeneous cognitive networks,” IEEE Journal on Selected Areas in Communications, Vol. 29, no. 4, pp. 831-42, Mar. 2011.

[87] Z. Li and C. Guo, “Multi-agent deep reinforcement learning based spectrum allocation for D2D underlay communications,” IEEE Transactions on Vehicular Technology, Vol. 69, no. 2, pp. 1828-1840, Dec. 2019.

[88] Z. Han, D. Niyato, W. Saad, T. Başa and A. Hjørungnes “Game theory in wireless and communication networks: theory, models and applications,” Cambridge University Press, Oct. 2011.

[89] H. Dun, F. Ye, S. Jiao, Y. Li and T. Jiang, “The Distributed Resource Allocation for D2D Communication with Game Theory,” in Proc. of IEEE-APS Topical Conference on Antennas and Propagation in Wireless Communications (APWC), Sep 9 pp. 104-108, Sep. 2019.

[90] W. Sun, E. Strom, F. Brannstrom, K. Sou and Y. Sui, “Radio resource management for D2D-based V2V communication,” IEEE Transactions on Vehicular Technology, Vol. 65, no. 8, pp. 6636-6650, Sep. 2016.

[91] S. Li, Q. Ni, Y. Sun, G. Min and S. Al-Rubaye, “Energy-efficient resource Allocation for industrial cyber-physical IoT systems in 5G era,” IEEE Transactions on Industrial Informatics, Vol. 14, no. 6, pp. 2618-2628, Jan. 2018.

[92] M. Ashraf, M. Bennis, C. Perfecto and W. Saad, “Dynamic proximity-aware resource allocation in vehicle-to-vehicle (V2V) communications, in Proc. of IEEE Globecom Workshops (GC Workshops), pp. 1-6, Dec. 2016.

[93] S. Yang, J. Wang, Y. Han and X. Jiang, "Dynamic spectrum allocation algorithm based on matching scheme for smart grid communication network," in Proc. of IEEE International Conference on Computer and Communications (ICCC), pp. 3015-3019, Oct. 2017.

[94] S. Aroua, I. El Korbi, Y. Ghamri-Doudane, and L. A. Saidane, "A Distributed cooperative spectrum resource allocation in smart home cognitive wireless sensor networks," in Proc. of IEEE Symposium on Computers and Communications (ISCC), pp. 754-759, Jul. 2017.

[95] F. Rothlauf, "Optimization Methods. In: Design of Modern Heuristics. Natural Computing Series," Springer, Berlin, Heidelberg, pp.45-102, 2011.

[96] B. Ma, B. Niu, Z. Wang and V. W. Wong, "Joint power and channel allocation for content delivery using millimeter wave in smart home networks," in Proc. of Global Communications Conference (GLOBECOM), pp. 4745-4750, Dec. 2014.

[97] D. Li, X. Chu and J. Zhang, "Joint optimization of power allocation and relay selection for smart grid neighborhood area networks," Smart Grid Communications (SmartGridComm), 2015 IEEE International Conference, pp. 217-222, Nov. 2015.

[98] M. Mardani, S. Mohebi, B. Maham and M. Bennis, "Delay-sensitive resource allocation for relay-aided M2M communication over LTE-advanced networks", in Proc. of 2017 IEEE Symposium on Computers and Communications (ISCC), Jul. 2017.

[99] L. Liang, G.Y. Li and W. Xu, "Resource allocation for D2D-enabled vehicular communications," IEEE Transactions on Communications, Vol. 65, no. 7, pp. 3186-3197, Apr. 2017.

[100] G. Yu, L. Xu, D. Feng, R. Yin, G. Ye Li and Y. Jiang, "Joint mode selection and resource allocation for device-to-device communications," IEEE Transactions on Communications, Vol. 62, no. 11, 3814-3824, Oct. 2014.

[101] Y. Gu, W. Saad, M. Bennis, M. Debbah and Z. Han, "Matching theory for future wireless networks: fundamentals and applications," IEEE Communication Magazine, Vol.53, no. 5, pp. 52-59, May 2015.

[102] D. Gale and L. Shapely, “College admission and stability of marriage,” The American Mathematical Monthly, Vol. 69, no.1, pp.9-15, Jan. 1962.

[103] Z. Zhou, K. Ota, M. Dong and C. Xu, 2016. “Energy-efficient matching for resource allocation in D2D enabled cellular networks,” IEEE Transactions on Vehicular Technology, Vol. 66, no. 6, pp.5256-5268, Oct. 2016.

[104] Y. Gu, Y. Zhang, M. Pan and Z. Han, “Matching and cheating in device-to-device communications underlying cellular networks,” IEEE Journal on Selected Areas in Communications, Vol. 33, no. 10, pp. 2156-2166, Jun. 2016.

[105] M. T. Islam, A. M. Taha, S. Akl and M. Abu-Elkheir, “A stable algorithm for resource allocation for underlaying device-to-device communications,” in Proc. of IEEE International Conference on Communication (ICC), Malaysia, May 2016.

[106] X. Mao, B. Zhang, Y. Chen, J. Yu and Z. Han, “Matching game-based resource allocation for 5G H-CRAN networks with device-to-device communication,” in Proc. of IEEE Personal Indoor and Mobile Radio Communication (PIMRC), Montreal Canada, Oct. 2017.

[107] J. Zhang, X. Wang, B. Zhang, X. Bi, B. Guo and Y. Wu, “Resource allocation for D2D communication underlying 5G heterogeneous cloud radio access networks,” in Proc. of 2019 IEEE 19th International Conference on Communication Technology (ICCT), pp. 854-859, Oct. 2019.

[108] S. M. Ahsan Kazmi, N. H. Tran, T. M. Ho, D. K. Lee and C. S. Hong, “Decentralised spectrum allocation in D2D underlying cellular networks,” in Proc. of IEEE Asia-Pacific Network Operations and Management Symposium (APNOMS), Kanasawa, Japan, pp. 1-6, Oct. 2016.

[109] P. V. Klaine, M. A. Imran, O. Onireti and R. D. Souza, “A survey of machine learning techniques applied to self-organizing cellular networks,” IEEE Communications Surveys & Tutorials, Vol. 19, no. 4, pp. 2392-431, Jul. 2017.

[110] C. Jiang, H. Zhang, Y. Ren, Z. Han, K. C. Chen and L. Hanzo, "Machine learning paradigms for next-generation wireless networks," IEEE Wireless Communications, Vol. 24, no. 2, pp. 98-105, Dec. 2016.

[111] P. Simon, "Too big to ignore: the business case for big data," John Wiley & Sons, Vol. 72, Mar. 2013.

[112] W. Saad, M. Bennis and M. Chen, "A vision of 6G wireless systems: applications, trends, technologies, and open research problems." IEEE network, Vol. 34, no. 3, pp. 134-142, Oct. 2019.

[113] M. Bkassiny, Y. Li and S.K. Jayaweera, A survey on machine-learning techniques in cognitive radios. IEEE Communications Surveys & Tutorials,Vol. 5, no.3, pp.1136-1159, Oct. 2012.

[114] J. Alzubi, A. Nayyar and A. Kumar, "Machine learning from theory to algorithms: an overview," in Journal of Physics: Conference series, IOP Publishing, Vol. 1142, No. 1, pp. 012012, Nov. 2018.

[115] M. Najla, D. Gesbert, Z. Becvar and P. Mach, "Machine learning for power control in D2D communication based on cellular channel gains," in Proc. of 2019 IEEE GLOBECOM Workshops (GC Wkshps), pp. 1-6, Dec. 2019.

[116] K. Zia, N. Javed, M. N, Sial, S. Ahmed, A. A. Pirzada and F. Pervez, "A distributed multi-agent RL-based autonomous spectrum allocation scheme in D2D enabled multi-tier HetNets," IEEE Access, no.7, pp. 6733-6745, Jan. 2019.

[117] D. P. Bertsakas, "Dynamic programming and optimal control," Belmont, MA, USA: Athena Scientific, Vol. 1, no. 2, Nov. 1995.

[118] B. Fernandez-Gauna, I. Etxeberria-Agiriano and M. Graña, "Learning multirobot hose transportation and deployment by distributed round-robin Q-learning," PloS one. Vol.10, no.7, Jul. 2015.

[119] K.K. Nguyen, T.Q. Duong, N.A. Vien, N.A. Le-Khac and M.N. Nguyen, "Non-cooperative Energy Efficient Power Allocation Game in D2D Communication: A

Multi-Agent Deep Reinforcement Learning Approach," IEEE Access, Vol. 7, pp. 100480-100490, Jul. 2019.

[120] S. De Bast, R. Torrea-Duran, A. Chiumento, S. Pollin and H. Gacanin, "Deep Reinforcement Learning for Dynamic Network Slicing in IEEE 802.11 networks," in Proc. of IEEE Conference on Computer Communications Workshops (INFOCOM WKSHPS), pp. 264-269, Apr. 2019.

[121] H. Wu, X. Li and Y. Deng, "Deep learning-driven wireless communication for edge-cloud computing: opportunities and challenges," Springer, Journal of Cloud Computing, Vol. 9, no. 21, pp.1-4, Dec. 2020.

[122] S. Nie, Z. Fan, M. Zhao, X. Gu and L. Zhang, "Q-learning based power control algorithm for D2D communication," in Proc. of IEEE 27th Annual International Symposium on Personal, Indoor, and Mobile Radio Communications (PIMRC), pp.1-6, Sep. 2016.

[123] A. S. Strekalovsky, "On non-convex optimization problems with DC equality and inequality constraints," IFAC-PapersOnLine, Vol. 51, no. 32, pp.895-900, Jun. 2018.

[124] M. Rasti, A. R. Sharafat and J. Zander, "A distributed dynamic target-SIR tracking power control algorithm for wireless cellular networks," IEEE Transactions on Vehicular Technology, Vol. 59, issue 2, pp. 906-916, Nov. 2010.

[125] S. K. Sharma and X. Wang, "Towards massive machine type communications in ultra-dense cellular IoT networks: current issues and machine learning-assisted solutions," IEEE Communications Surveys & Tutorials, Vol. 22, no.1, pp. 426-471, May 2019.

[126] G. J. Foschini and Z. Milijanic, "A simple distributed autonomous power control algorithm and its convergence," IEEE Transactions on Vehicular Technology, vol 42, issue 4, pp. 641-646, Nov. 1993.

[127] A. Abedin and M. Rasti, "A distributed joint power control and mode selection scheme for D2D-enabled cellular systems," in Proc. of IEEE Symposium on Computer and Communication (ISCC), pp. 1284-1289, Jun. 2016.

[128] B. Gu, X. Zhang, Z. Lin and M. Alazab, "Deep multiagent reinforcement-learning-based resource allocation for internet of controllable things," IEEE Internet of Things Journal, Vol. 8, no.5, pp.3066-3074, Sep. 2020.

[129] T.D. Hoang, L.B. Le and T. Le-Ngoc, "Radio resource management for optimizing energy efficiency of D2D communications in cellular networks," IEEE 26th Annual International Symposium on Personal, Indoor, and Mobile Radio Communications (PIMRC), pp. 1190-1194, Aug. 2015.

[130] H. Xing and S. Hakola, "The investigation of power control schemes for a device-to-device communication integrated into OFDMA cellular system," in Proc. of IEEE Personal Indoor and Mobile Radio Communication (PIMRC), pp. 1775-1780, Sep. 2010.

[131] Evolved Universal Terrestrial radio Access (E-UTRA); Further advancements for E-UTRA physical layer aspects (release 9), 3GPP, document 36.814, v9.0.0, 2010.

[132] C. Liu, "Data Transformation: Standardization vs Normalization" https://www.kdnuggets.com/2020/04/data-transformation-standardization-normalization.html. Last accessed: 06/05/2023.

[133] J. Ma, "Modified Shannon's capacity for wireless communication," IEEE Microwave Magazine, Vol.22, no.9, pp.97-100, Aug. 2021.

[134] M.M. Elmesalawy, "D2D communications for enabling Internet of things underlaying LTE cellular networks," Journal of Wireless networking and Communications, Vol.6, no.1, pp.1-9, 2016.

[135] I. Sanusi, K. Nasr and K. Moessner, "A device to device spectrum sharing scheme for wireless industrial applications", in Proc. of IEEE, European Conference on Network and Communication (EuCNC), pp.353-357, Jun. 2019.

[136] D. Feng, L. Lu, Y. Yuan-Wu, G. Ye Li, G. Feng and S. Li, "Device-to-Device communications underlaying cellular networks," IEEE Transactions on Communications, Vol. 61, no. 8, pp. 3541-3551, Jul. 2014.

[137] L. Wang, H. Tang, H. Wu and G.L. Stüber, "Resource allocation for D2D communications underlay in Rayleigh fading channels," IEEE Transactions on Vehicular Technology, Vol. 66, no.2, pp.1159-1170, Apr. 2016.

[138] H. Wang and X. Chu, "Distance-constrained resource-sharing criteria for device-to-device communications underlaying cellular networks," Electronics letters, Vol. 48, no. 9, pp. 528-530, Apr. 2012.

[139] Y. Xiao, K. Chen, C. Yuen and L. A. DaSilva, "Spectrum sharing device-to-device communications in cellular networks: a game theoretic approach," in Proc. of IEEE International Symposium on Dynamic Spectrum Access Networks (DYSAN), Apr. 2014.

[140] WINNER II Channel Models, Standard IST-4-027756 WINNER II D1.1.2 V1.2, 2007.

[141] B. Tian, L. Wang, Y. Ai and A. Fei, "Reinforcement learning based matching for computation offloading in D2D communications," in Proc. of 2019 IEEE/CIC International Conference on Communications in China (ICCC), IEEE, pp. 984-988, Aug. 2011.

[142] L. Liang, H. Ye and G. Y. Li, "Spectrum sharing in vehicular networks based on multi-agent reinforcement learning," IEEE Journal on Selected Areas in Communications, Vol. 37, no. 10, pp. 2282-92, Aug. 2019.

[143] A.T. Kasgari and W. Saad, "Model-free ultra-reliable low latency communication (URLLC): a deep reinforcement learning framework," in Proc. IEEE International Conference on Communications (ICC), pp. 1-6, May 2019.

[144] H. Yang, X. Xie and M. Kadoch, "Intelligent resource management based on reinforcement learning for ultra-reliable and low-latency IoV communication networks," IEEE Transactions on Vehicular Technology, Vol.68, no. 5, pp.4157-4169, Jan. 2019.

[145] F.E. Souhir, A. Belghith and F. Zarai, "A reinforcement learning-based radio resource management algorithm for D2D-based V2V communication," in Proc.15th International Wireless Communications & Mobile Computing Conference (IWCMC), pp. 1367-1372, Jan. 2019.

[146] Y. Wei, Y. Qu, M. Zhao, L. Zhang and F. R. Yu, "Resource allocation and power control policy for device-to-device communication using multi-agent reinforcement learning," Computers, Materials & Continua, Vol. 63, no. 3, pp.1515-1532, May 2020.

[147] I.O. Sanusi, K.M. Nasr and K. Moessner, "Radio resource management approaches for reliable device-to-device (D2D) communication in wireless industrial applications," IEEE Transactions of Cognitive Communication and Networking, Vol. 7, no. 3, pp.905-916, Sept. 2021.

[148] Gabriel Brown, "Ultra-reliable low-latency communication for 5G industrial automation," White Paper, Qualcomm, Available online: https://www.qualcomm.com/media/documents/files/read-the-white-paper-by-heavy-reading.pdf. Last accessed 12/07/2021.

[154] H. Masoumi, M.J. Emadi and S. Buzzi, "Coexistence of D2D communications and cell-free massive MIMO systems with low resolution ADC for improved throughput in beyond-5G networks, IEEE Transactions on Communications, Vol.70, no. 2, pp.999-1013, Nov. 2021.

[155] H. He, X. Yu, J. Zhang, S. Song and K. B. Letaief, "Cell-free massive MIMO for 6G wireless communication networks," Journal of Communications and Information Networks, Vol.6, no.4, pp.321-35, Dec. 2021.

[156] GSMA, "5G TDD Synchronisation Q & A", Available online: https://www.gsma.com/spectrum/wp-content/uploads/2021/03/5G-TDD-Synchronisation-QA.pdf Last accessed 12/07/2022.

[157] 5G Alliance for Connected Industry and Automation, "5G for automation in industry: primary use cases, functions and service requirements," White paper, 2019. Available online:https://5g-acia.org/wp-content/uploads/2021/04/5G-ACIA_5G-for-Automation-in-Industry-.pdf Last accessed 12/07/2022.

[158] Z. Zhou, X. Chen, Y. Zhang and S. Mumtaz, "Blockchain-empowered secure spectrum sharing for 5G heterogeneous networks," IEEE Network, Vol. 34, no.1, pp.24-31, Jan. 2020.

[159] S. Han and X. Zhu, “Blockchain based spectrum sharing algorithm,” in Proc. of IEEE 19th International Conference on Communication Technology (ICCT), pp. 936-940, Oct. 2019.